INFORMATION TO USERS

This manuscript has been reproduced from the microfilm master. UMI films the text directly from the original or copy submitted. Thus, some thesis and dissertation copies are in typewriter face, while others may be from any type of computer printer.

The quality of this reproduction is dependent upon the quality of the copy submitted. Broken or indistinct print, colored or poor quality illustrations and photographs, print bleedthrough, substandard margins, and improper alignment can adversely affect reproduction.

In the unlikely event that the author did not send UMI a complete manuscript and there are missing pages, these will be noted. Also, if unauthorized copyright material had to be removed, a note will indicate the deletion.

Oversize materials (e.g., maps, drawings, charts) are reproduced by sectioning the original, beginning at the upper left-hand corner and continuing from left to right in equal sections with small overlaps.

Photographs included in the original manuscript have been reproduced xerographically in this copy. Higher quality 6" x 9" black and white photographic prints are available for any photographs or illustrations appearing in this copy for an additional charge. Contact UMI directly to order.

Bell & Howell Information and Learning
300 North Zeeb Road, Ann Arbor, MI 48106-1346 USA

UMI®
800-521-0600

Adaptive Control of Nonlinear Discrete-Time Systems and its Application to Control of a Flexible-Link Manipulator

Mohammad Reza Rokui

A Thesis

in

The Department

of

Electrical and Computer Engineering

Presented in Partial Fulfillment of the Requirements

for the Degree of Doctor of Philosophy at

Concordia University

Montréal, Québec, Canada

August 1997

ABSTRACT

Adaptive Control of Nonlinear Discrete-Time Systems and its Application to Control of a Flexible-Link Manipulator

Mohammad Reza Rokui, Ph.D.
Concordia University, 1997

The objectives of this research work are to develop direct and indirect adaptive control strategies for discrete-time nonlinear systems and to investigate the applicability of the proposed schemes to adaptive tracking control of a flexible-link manipulator. The first problem considered is *indirect adaptive control* of a fully as well as a partially input-output feedback linearizable n*th* order affine SISO nonlinear system represented in the state-space form. The objective is to make the output $y(k)$ track a reference trajectory $y_m(k)$ despite the fact that the parameters of the system are unknown. Towards this end, a local diffeomorphism for the change of coordinates and a nonlinear feedback control law are obtained so that the nonlinear system is rendered input to output equivalent into a linear system. The resulting linear system is then used to solve the output tracking control problem using conventional linear control theory. A *multi-output recursive-least-square (RLS)* algorithm is employed to identify the unknown parameters. Using the Lyapunov technique it is shown that provided the zero dynamics is exponentially stable the adaptively controlled closed-loop system is stable .

The second problem addressed is the *direct adaptive tracking control* problem of a class of SISO discrete-time nonlinear systems represented in the input-output form. To solve the problem, the state-space model is first derived and the appropriate control input is obtained. By employing the *projection algorithm* as a parameter estimator, the closed-loop stability of the adaptively controlled system is addressed using Lyapunov technique.

As an application, the indirect adaptive control strategy is employed to control a single link flexible manipulator. Towards this end, the discrete-time model of the manipulator and its zero dynamics are derived first. By using the output re-definition technique, the adaptive input-output linearization scheme is then applied. The regressor form of the link's dynamic equations is also developed for the multi-output RLS identification algorithm. The performance of the adaptively controlled closed-loop system is investigated through numerical simulations to show the advantages and the main features of the proposed strategy.

Finally to evaluate the performance of the proposed controller, an experimental test-bed of a single-link flexible manipulator is used for implementation. The real-time controller and estimator are implemented on a TMS system board which uses a TMS320C30 Digital Signal Processing (DSP) chip. The actual results are then compared with the simulation results to verify and validate the theoretical findings.

To my wife Katayoun, and my sons Kiarash and Sorush

ACKNOWLEDGMENTS

I would like to express my profound and sincere appreciation to my supervisor Professor Khashayar Khorasani for his constant encouragement and invaluable guidance and significant support throughout the course of this dissertation.

I also thanks the members of my Ph.D. qualifying examination committee who has given me the confidence and support through their suggestions and advice.

Thanks are also due to all my friends and my colleagues for their support and technical help especially to my friend Ali who was a great help in the experimental phase of the research and Mehrdad whom I have had several discussions on the second part of the thesis.

Last but not the least, I am greatly indebted to my parents, my wife, and my sons who have always been a source of strength to me and always stood behind me with great patience and encouragement without whom the present work would not have been possible.

CONTENTS

LIST OF FIGURES

LIST OF SYBMOLES

$F(x_k, u_k)$ Vector field $f(x_k) + g(x_k)u_k$

f_o Vector field $F(x_k, u_k)$ when $u_k = 0$

f_o^i i-times composition of f_o, i.e., $\underbrace{f_o \circ f_o \cdots \circ f_o}_{i-times}$

n Degree of nonlinear system

γ Relative degree

M_L Payload mass $[kg]$

$\hat{M}_L$ Estimate of payload mass $[kg]$

$(M_L)_{controller}$ Payload mass used in non-adaptive feedback linearization $[kg]$

m Number of flexible modes

A Beam cross-section area$[m^2]$

ρ Mass density $[\frac{kg}{m^3}]$

I_0 Hub inertia $[kgm^2]$

I Beam area moment of inertia about the neutral axis $[kgm^2]$

J_0 Beam inertia with respect to hub $[kgm^2]$

J_p Payload inertia $[kgm^2]$

θ Unknown parameter vector $[\theta_1\ \theta_2\ \ldots\ \theta_p]^T$

$\hat{\theta}$ Estimate of unknown parameter vector

$\tilde{\theta}$ Estimation error $\theta - \hat{\theta}$

Θ Upperbound of θ

$\boldsymbol{\Phi}(x_k)$ Local diffeomorphism

$\Phi(x)$ Mode shapes vector $[\phi_1(x)\ \phi_2(x)\ \cdots\ \phi_m(x)]^T$

$\phi_i(x)$ i^{th} mode shape (eigenfunction)

ξ_k Observable coordinates $[z_{1,k}\ z_{2,k}\ \ldots\ z_{\gamma,k}]^T$

η_k Unobservable coordinates $[\eta_{1,k}\ \eta_{2,k}\ \ldots\ \eta_{n-\gamma,k}]^T$

$\eta(k)$ Unobservable coordinates of Flexible link $[\boldsymbol{\eta}_1^T(k)\ \ \boldsymbol{\eta}_2^T(k)]^T$ or $[\boldsymbol{\eta}_{n1}^T(k)\ \ \boldsymbol{\eta}_{n2}^T(k)]^T$

$\boldsymbol{\beta}_1$ Row vector $[\beta_1\ \cdots\ \beta_m]$ with $\beta_i(L) \triangleq \frac{\alpha_i \phi_i(L)}{L}$

$\boldsymbol{\beta}_2$ A constant scalar

β Row vector $[1\ \boldsymbol{\beta}_1]$

$\boldsymbol{a}_1$ Row vector $[\boldsymbol{\beta}_2\ \ \boldsymbol{\beta}_1]$

α_i A constant scalar between ± 1

E Young's modulus $[Nm^2]$

L Beam length $[m]$

q Joint (hub) angle

$\boldsymbol{\delta}$ Vector of flexible modes $[\delta_1\ \ \delta_2\ \ \ldots\ \ \delta_m]^T$

$M(\boldsymbol{\delta})$ Inertia matrix

h Coriolis and centrifugal forces $[h_1\ \ \mathbf{h}_2^T]^T$

$Fri(\dot{q})$ Coulomb friction $[Nm]$

D Viscous and structural damping matrix $\begin{bmatrix} D_1 & 0 \\ 0 & \mathbf{D}_2 \end{bmatrix}$

$\mathbf{k}$ Stiffness matrix $\begin{bmatrix} 0 & 0 \\ 0 & \mathbf{k}_2 \end{bmatrix}$

$\tau(t)$ Input torque applied by DC motor to flexible link manipulator

$\Upsilon(x_k, v_k)$ Nonlinear control law

Ψ Regressor vector

ym_k Reference trajectory

$y_m(k)$ Reference trajectory

$e_{i,k}$ i-th tracking error signal, i.e., $y_{k+i-1} - ym_{k+i-1}$

$w(x,t)$ Beam deflection, i.e., $\sum_{i=1}^{m} \phi_i(x)\delta_i(t)$

T Sampling period

$e(k)$ Normalized re-defined output tracking error $y(k) - y_m(k)$

$e_t(k)$ Normalized tip position tracking error $y_t(k) - y_m(k)$

Chapter 1

Introduction

In this chapter several issues related to the adaptive tracking control of discrete-time nonlinear systems and their applications to control of a flexible-link manipulator are investigated. In Section 1.1 a general overview on control design of a physical system is outlined. The main features of nonlinear feedback linearization technique are then compared to the local linearization technique that is commonly used in practice. In Section 1.2 the main objectives of the proposed research are described. In Section 1.2.1 existing methods in the literature that deal with adaptive control problem of continuous-time as well as discrete-time systems represented in both state-space and input-output forms are reviewed. Section 1.2.2 covers a literature review on modeling, non-adaptive and adaptive control of flexible-link manipulator. The contributions and accomplishments of this dissertation are stated in Section 1.3.

1.1 General overview

The objective of control design can basically be stated as follows. Given a physical system to be controlled and the desired specifications, construct a feedback control law so to make the closed-loop system display the desired behavior. For example if

the desired task involves large and high speed motions, then nonlinear effects of the plant will be significant and therefore, it may be necessary to consider the nonlinearities in order to achieve the desired performance.

Generally the task of the control system can be divided into two categories: stabilization (or regulation) and tracking (or servo). In stabilization problem, a control system, called a *stabilizer* or a regulator, is to be designed so that the states of the closed-loop system will be stabilized around an equilibrium point. Examples of stabilization tasks are temperature control, altitude control of a aircraft and position control of robot arms. In tracking control problem, the design objective is to construct a controller, called a *tracker*, so that the system output tracks a given predefined trajectory. Problems such as making an aircraft fly along a specified path or making the end effector of a robot manipulator following some desired trajectories are typical tracking examples.

As in the analysis of nonlinear control systems, there are only a few methods available for designing a nonlinear controller. The first step in designing a control system for a given physical plant is to derive a meaningful *model* of the plant, i.e., a model that captures the key dynamics of the plant in the operational range of interest. Models of physical systems come in various forms, depending on the adopted methodology and given assumptions. Some forms, however, lend themselves more easily to control design. Specifically feedback linearization technique deals with transforming an original nonlinear system model into an equivalent model of a simpler linear form.

Feedback linearization techniques for nonlinear control design have attracted a great deal of research interest in the past few years. The central idea is to transform the nonlinear system dynamics into a fully or partially linearized form. Once this is

accomplished, feedback linearization strategy opens the door for applying linear design methodology to nonlinear systems. This design methodology differs entirely from conventional linearization (i.e., local Jacobian linearization) technique in that feedback linearization is achieved by exact state transformation and nonlinear feedback rather than by linear Taylor series approximations of the dynamics.

The idea of simplifying a system's dynamics form by choosing a different state representation is not totally novel. In mechanics, for instance, it is well known that the form and complexity of a system model depend considerably on the choice of reference frames or coordinates system. Feedback linearization techniques can be viewed as a way of *transforming original system models into an equivalent model of a simple form.* Feedback linearization techniques have been used successfully to address some practical control problems. These include the control of helicopter, high performance aircraft, spacecraft attitude control [64], industrial robots and biomedical devices. More applications of this control methodology are currently being developed in industry. However, feedback linearization approach has also a number of shortcomings and limitations that are still very much topics of current research.

1.1.1 Local Linearization

Lyapunov's linearization method is concerned with the local stability of a nonlinear system. It is a formalization of the intuition that a nonlinear system should behave very close to its linearized approximation for small range of motions. Since virtually all physical systems are inherently nonlinear to a certain extent, Lyapunov's linearization method serves as the fundamental justification for using linear control techniques in practice. Consider the nonlinear discrete-time system

$$x(k+1) = f(x(k), u(k)) \tag{1.1}$$

where function $f(x(k), u(k))$ is continuously differentiable. To linearize system (1.1) around some operating point $x = x_0$ and $u = u_0$, we have

$$x_0(k+1) + \triangle x(k+1) = f(x_0, u_0) + \left(\frac{\partial f}{\partial x}\right)_{x_0,u_0} \triangle x(k) + \left(\frac{\partial f}{\partial u}\right)_{x_0,u_0} \triangle u(k) + f_{h.o.t.} \quad (1.2)$$

where $\triangle x(k) \triangleq x(k) - x_0$, $\triangle u(k) \triangleq u(k) - u_0$ and $f_{h.o.t.}$ stands for the higher-order-terms. However, since at operation point $x_0(k+1) = f(x_0, u_0)$, equation (1.2) yields the following linear approximation of the original nonlinear system at the equilibrium point $x = x_0, u = u_0$ as

$$\triangle x(k+1) = A \triangle x(k) + B \triangle u(k)$$

where constant matrix $A = \left(\frac{\partial f}{\partial x}\right)_{x_0,u_0}$ denotes the Jacobian matrix of vector field f with respect to x at $x = x_0, u = u_0$ and matrix $B = \left(\frac{\partial f}{\partial u}\right)_{x_0,u_0}$ denotes the Jacobian matrix of vector field f with respect to u at the same operating point.

1.1.2 Feedback Linearization

Since in this thesis we are concerned with the adaptive control of nonlinear discrete-time systems with application to a single-link flexible manipulator, some concepts such as normal forms, internal dynamics, zero dynamics and non-minimum phase characteristics in the nonlinear framework are reviewed next for convenience. Toward this ends, consider the following nonlinear discrete-time system which is affine in input u_k

$$\begin{aligned} x_{k+1} &= f(x_k) + g(x_k)u_k \\ y_k &= h(x_k) \end{aligned} \quad (1.3)$$

where $x_k \in \Re^n$, $y_k \in \Re$ and $u_k \in \Re$. It is further assumed that f, g and h are analytic functions and origin is the equilibrium of the system. The objective is to have the output y_k track a reference trajectory ym_k using a change of coordinate and a bounded nonlinear feedback. But first let us introduce the notion of the relative

degree of a system.

Definition 1.1 *The system (1.3) is said to have relative degree $\gamma \leq n$ if for all $x_k \in \Re^n$ and $u_k \in \Re$,*

$$\frac{\partial y_{k+i}}{\partial u_k} = 0\,, \quad i = 0, ..., \gamma - 1$$
$$\frac{\partial y_{k+\gamma}}{\partial u_k} \neq 0.$$

Through state-dependent coordinate transformation $z_k = \boldsymbol{\Phi}(x_k) \triangleq [\xi_k^T \;\; \eta_k^T]^T$ and input transformation (nonlinear feedback control), one may linearize the whole system from input to output so that in new coordinates it takes the following equivalence representation called normal form (Isidori [26], Nijmeijer & Van der Shaft [59])

$$\begin{aligned} z_{i,k+1} &= z_{i+1,k},\ i = 1, 2, \cdots \gamma - 1 \\ z_{\gamma,k+1} &= \alpha(\xi_k, \eta_k, u_k) = v_k \\ \eta_{k+1} &= q(\xi_k, \eta_k) \\ y_k &= z_{1,k} \end{aligned} \tag{1.4}$$

where $\xi_k \triangleq [z_{1,k} \;\; z_{2,k} \;\; \cdots \;\; z_{\gamma,k}]^T = [y_k \;\; y_{k+1} \;\; \cdots \;\; y_{k+\gamma-1}]^T$ characterizes the observable states, v_k is the new input to the system and the unobservable states $\eta_k \triangleq [\eta_{1,k} \;\; \cdots \;\; \eta_{n-\gamma,k}]^T$ is to be specified such that the Jacobian matrix of the state transformation $z_k = \boldsymbol{\Phi}(x_k)$ is locally full rank, i.e., $\boldsymbol{\Phi}(x_k)$ is a local diffeomorphism at the origin. The structure of the above equations is best illustrated in the block diagram form depicted in Figure (1.1). This system clearly appears decomposed into a *linear subsystem* of dimension γ called *external dynamics*, that is responsible for the input-output behavior, and a possibly *nonlinear system* of dimension $n - \gamma$ called *internal dynamics*, that its dynamics however does not affect the output.

Note that if $\gamma = n$, the nonlinear system (1.3) is said to be input to state (or fully) linearizable where the nonlinear system does not have any internal dynamics. We can define an intrinsic property of a nonlinear system by considering the system's

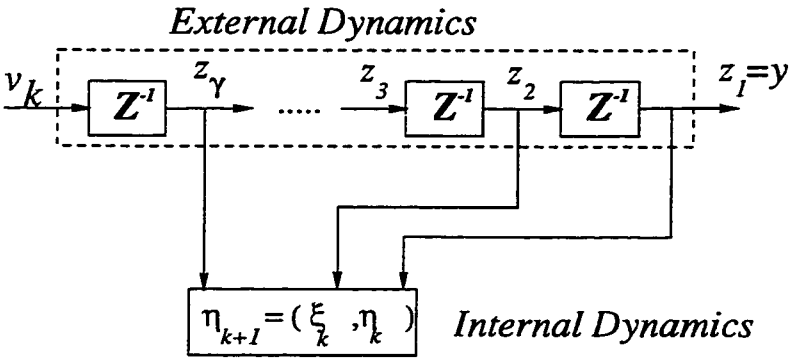

Figure 1.1: External and internal dynamics of a nonlinear system

internal dynamics when the control input is such that the output y_k is maintained at zero for all time. Studying this so-called *zero dynamics* will allow us to make some conclusions about the stability of the internal dynamics. Therefore, based on the normal form (1.4), the zero dynamics will be

$$\eta_{k+1} = q(0, \eta_k)$$

Note that $y_k \equiv 0$ implies $\xi_k \equiv 0$ for all time. The nonlinear system (1.3) is said to be *minimum phase* if its zero dynamics is asymptotically stable and otherwise it is called *nonminimum phase*. The above terminology is adopted from linear system theory where a transfer function, which has a zero in the right half of the complex plane, is called nonminimum phase.

This dissertation aims to address two major issues: (i) Adaptive control of nonlinear discrete-time systems and (ii) Application of the proposed method to tracking control of a single-link flexible manipulator. For the first part, the plant to be considered is a discrete-time system represented in the state-space form. It is assumed that the system could be either fully or partially linearizable with parametric uncertainties. The *certainty equivalence principle* will be invoked so that the estimates of the unknown parameters may be used in designing the feedback linearizing controller. The aim of the second part is to apply the nonlinear adaptive scheme

proposed in the first part to a single-link flexible manipulator and to compare the simulation results with performance results obtained for an actual flexible-link manipulator. In this part after deriving the discrete-time model of the flexible-link, the output re-definition scheme is used so that the resulting zero dynamics is exponentially stable. Finally, the indirect adaptive feedback linearization and tracking control problem proposed in first part are utilized by assuming that the *payload mass* is unknown. The performance of the adaptively controlled closed-loop system is examined through numerical simulations. Experiments are also performed to demonstrate the main features of the proposed strategies. To gain more insight into the nature of the problem, the existing literature is reviewed in the following .

1.2 Literature Review

1.2.1 Adaptive Control of Nonlinear Systems

Adaptive control of different classes of feedback linearizable continuous-time nonlinear systems has been studied extensively over the past few years. Few examples, Kanellakopoulos *et al.* [31, 33] developed a direct adaptive regulator and tracking scheme for a class of feedback linearizable nonlinear system that is transformable into a so-called *parametric-pure-feedback form.* In [56], Nam & Arapostathis presented a model reference adaptive control scheme for a class of nonlinear systems when the relative degree is equal to degree of system. Sastry & Isidori in [73] introduced adaptive control of minimum phase nonlinear systems using input-output linearization method. Krstic *et al.* [39] proposed a design procedure for adaptive nonlinear control in which the number of parameter estimates is minimal, that is, without overparametrization. Teel *et al.* in [80, 81] and Lin & Kanellakopoulos [46] utilized indirect techniques for adaptive input-output linearization. There has been also research on employing the output feedback instead of the full-state feedback in Kanellakopoulos *et al.* [32, 34] and by utilizing observer-based identifier along with

output feedback in Krstic *et al.* [41] and Kanellakopoulos *et al.* [35].

Unfortunately the above adaptive schemes for continuous-time systems cannot be directly extended to nonlinear discrete-time systems, a topic to which so far only a few papers have been devoted. This is partly due to the fact that one is faced with considerable technical difficulties in generalizing the continuous-time results to discrete-time systems. The most important difficulty has to do with the lack of applicability of Lyapunov techniques to design adaptive control for discrete-time systems. This is due to the fact that in the continuous-time domain the derivative of a Lyapunov function is linearly parameterized with respect to the unknown parameters (provided that the continuous-time system is linear with respect to its parameters) whereas in the discrete-time domain the difference of a Lyapunov function is not linear with respect to the unknown parameters (Kanellakopoulos *et al.* [30], Song & Grizzle [77]). The other difficulty is due to the fact that in continuous-time domain differentiation is a linear operation whereas in discrete-time domain the composition is a nonlinear operation and this often results in loss of linear parameterization even when the plant is linearly parameterized. Finally, the problem of state stabilization is less understood in the discrete-time domain than in the continuous-time domain (Byrnes *et al.* [3] & Yeh & Kokotovic [90]).

It is worth pointing out that as a first step in using any adaptive algorithm, one must find conditions under which the nonlinear discrete-time system can be represented in an equivalent controllable/observable linear system. This topic has been investigated extensively for continuous-time systems (Isidori [26], Nijmeijer & Van der Shaft [59]) and the necessary and sufficient conditions for feedback linearizability of a continuous-time system using the differential geometry have been obtained. To construct the local coordinate transformation and feedback control law, one needs to solve a set of partial differential equations dependent on the vector fields of the

system model. The equivalent necessary and sufficient conditions for transforming a nonlinear discrete-time system into an equivalent linear system were developed by Grizzle [21] and Jakubczyk [27]. These conditions are given in terms of distributions that are defined using the system map. However, these conditions are fairly tedious to check for a given system. Lee *et al.* [43] presented a constructive proof of necessary and sufficient conditions for linearization of single-input single-output discrete-time system by a state-coordinate transformation and a state-coordinate change and nonlinear feedback. Once the Lee *et al.* [43] conditions are satisfied, the linearizing transformation can be obtained as the inverse of a diffeomorphism, that is an n-times composition of the system map with respect to the input arguments. In another work Nam [55] has obtained necessary and sufficient conditions for a nonlinear system that can be put in the form $x_{k+1} = G_{u_k} \circ F(x_k)$. Also Jayaraman & Chizeck in [28] has formulated the feedback linearization problem for discrete-time systems in terms of a set of partial differential equations that are similar in structure to their continuous-time counterparts. Finally, the necessary and sufficient conditions for approximate linearizability are given by Lee & Marcus [45], and input-output linearization using Volterra series expansion is given by Lee & Marcus [44].

Although a great deal of progress has been made in the area of control of continuous-time nonlinear systems in recent years, in contrast, adaptive control of discrete-time nonlinear systems remains a largely unsolved problem. In what follows the most significant results for discrete-time nonlinear systems that are available in the literature to date are reviewed. Recently Yeh & Kokotovic [90] designed a state feedback controller to achieve tracking of a reference signal for a class of SISO nonlinear discrete-time systems in the so-called *parametric-strict-feedback form* given by

$$
\begin{aligned}
x_1(k+1) &= x_2(k) + \theta^T \phi_1(x_1(k)) \\
&\vdots \\
x_{n-1}(k+1) &= x_n(k) + \theta^T \phi_{n-1}(x_1(k), \cdots, x_{n-1}(k)) \\
x_n(k+1) &= u(k) + \theta^T \phi_n(x_1(k), \cdots, x_n(k)) \\
y(k) &= x_1(k)
\end{aligned} \tag{1.5}
$$

where $\theta \in \Re^p$ is the unknown parameter vector and $\phi_1(x_1, \cdots, x_n) : \Re^i \rightarrow \Re^p$ $i = 1, \cdots, n$ are known nonlinear functions. Depending on the growth conditions of the nonlinearities, global boundedness and convergence are achieved with various update laws. Indeed, the above work is the discrete-time version of the results given in Kanellakopoulos *et al.* [31]. Zhao & Kanellakopoulos in [94] proposed another approach for system (1.5) to yield global stability and tracking without imposing any growth conditions on the nonlinearities. They replaced the traditional parameter estimator with an uncertainty identifier scheme which in a finite number of time steps collects all the information necessary to completely identify the uncertain part of the system. Beyond this interval, the control law becomes a straightforward "look ahead" design which utilizes the information at the identification phase.

The adaptive output feedback design is developed by Yeh & Kokotovic [89] for the following class of systems that may be viewed as a discrete-time version of the continuous-time systems considered in Kanellakopoulos *et al.* [34], namely

$$
\begin{aligned}
x(k+1) &= Ax(k) + \alpha_0(y(k)) + \sum_{j=1}^{p} a_j \alpha_j(y(k)) + b\beta(y(k))u(k) \\
y(k) &= cx(k)
\end{aligned} \tag{1.6}
$$

where $x \in \Re^n$, $y \in \Re$, $u \in \Re$, $A = \begin{bmatrix} 0 & I_{(n-1)\times(n-1)} \\ 0 & 0 \end{bmatrix}$, $b = [0, \cdots, 0, b_m, \cdots, b_0]^T$, $c = [1, \cdots, 0]^T$ and $a_j (j = 1, \cdots, p)$ and $b_i (i = 0, \cdots, m)$ are the unknown parameters. Also $\alpha_l \in C^\infty(\Re, \Re^n)$ with $\alpha_l(y) = [\alpha_{l1}(k), \cdots, \alpha_{ln}(k)]^T, l = 0, \cdots, p$ and

$\beta \in C^{\infty}(\Re, \Re)$. A systematic design procedure was developed for the deterministic case and dependent on the characteristics of the nonlinearities, global convergence can be ensured. A new Least-Square estimator with nonlinear data weighting was developed by Kanellakopoulos [30] for a simple discrete-time nonlinear system $x(k+1) = u(k) + \theta\phi(x(k))$ where $x \in \Re$ is both the state and the output, $\theta \in \Re$ is a constant unknown parameter and $\phi(x(k))$ is a known nonlinear function which is bounded for a bounded $x(k)$. It was shown that global stability is achievable through Lyapunov analysis without imposing any growth conditions. Also for a class of MISO systems, Stubbs & Svoronos [79] proposed a simple feedback linearization scheme and used it in developing an adaptive control strategy.

In Kung & Womack [42] stability and convergence for the adaptive control of a cascade connection of a finite odd order polynomial followed by a linear system were addressed. Recker & Kokotovic [63] considered the indirect adaptive control of the same class when the nonlinearity is a deadzone and Lin & Yong in [47] has generalized these methods to MIMO systems with more general nonlinear input. By using output feedback, the model reference adaptive control for a class of discrete-time systems consisting of a linear system followed by a nonlinear element and other nonlinearities dependent on the delayed outputs were developed by Song and Grizzle [77]. In this paper they have tried to extend the existing conventional method for model reference adaptive control of discrete-time linear systems to their nonlinear models. Using a different viewpoint, Yu & Muller [91] and Ossman [60] have examined indirect adaptive control of interconnected systems where each subsystem is subjected to bounded disturbances and to possibly unbounded interconnections with the other subsystems. For such a system an adaptive feedback law is described that stabilizes the interconnected system and result in bounded subsystem input and output signals. Furthermore, Cook [10] has considered the effect of plant nonlinearities on the operation of an adaptive control system designed with the assumption

of a linear structure and Guillaume *et al.* in [22, 23] have addressed the sampled-data adaptive regulation control of a class of continuous-time nonlinear systems that are *state linearly stabilizable*, namely, a nonlinear continuous-time system which can be linearized using a static feedback control strategy. Finally, Chen & Khalil in [8, 6, 7] have addressed the adaptive control of the following discrete-time system using neural networks

$$y(k+1) = f_o(., W_1) + g_o(., V_1)u(k-d+1) \tag{1.7}$$

where d is the relative degree, $f_o(., W_1)$ and $g_o(., V_1)$ are smooth functions of unknown parameter vectors W_1 and V_1 and known functions $[y(k-n+1), \ \ldots \ , y(k), u(k-d-m+1), \ldots, u(k-d)]^T$ where $m \leq n$. Also, Chen & Tsao [9] have considered the adaptive control of (1.7) when $d = 1$.

1.2.2 Control of Flexible-Link Manipulators

In recent years the study of flexible-link manipulators has received a great deal of attention because the flexible-link robots have a few advantages over the rigid-link robots. For instance, flexible robots can be driven at higher speeds and have lighter weight and therefore use lower energy. These properties are of significant importance for some applications such as light weight space robots. Despite these advantages, the major drawback of flexibility arises during the control of the tip position. It is well-known that the model of a flexible-link manipulator when the output is taken as the tip position exhibits, in general, a non-minimum phase behavior [83], namely, its zero dynamics is unstable. The zero dynamics may be viewed as the evolution of the internal dynamics subject to a particular input that causes the output to be kept identically equal to zero for all time. The source of this behavior may be traced to the non-colocated nature of the sensor and actuator used for controlling the tip position. This property hinders perfect tracking of the desired tip position when a bounded and a causal input is used with output feedback. The other aspect of the

problem deals with the use of an appropriate model for designing control schemes. Clearly, a dynamic model that describes the system behavior in an accurate way is highly desirable. Theoretically, the dynamic equations of a flexible-link manipulator is of infinite dimension since it is described by a set of partial differential equations (PDE). In other words, an infinite number of coordinates are required to kinematically describe each link. However, an infinite dimensional model may not suitable for control system design due to factors such as the complexity of the dynamic model and the band-limited nature of the sensors and actuators. In modeling of flexible manipulators commonly one truncates the number of flexible modes. The dynamic equations are still highly nonlinear and form a coupled set of ordinary differential equations that possess a two-time-scale nature, namely, a slow time-scale associated with the rigid modes and a fast time-scale associated with the flexible modes. Another major question in controller design is the number and type of sensors. An important information that should be provided to the controller is an accurate estimate of the tip position which can be provided by using a camera or strain gauge measurements, although tip rate measurements are not directly obtainable.

To model a flexible-link manipulator Cannon & Schmitz [4] used the assumed modes method. They have assumed zero payload and pinned-free eigenfunctions for mode shapes. With this approximation, the mode shapes form a complete set of orthogonal functions. Finally using the Lagrangian formulation and taking into account the structural damping of the beam, a set of decoupled differential equations were obtained. Wang & Vidyasagar [83] have used clamped-free mode shapes and have shown that the transfer function from torque input to tip position output does not have a well-defined relative degree even if the number of modes is increased to obtain a more accurate model of the flexible-link arm.

The problem of control of flexible-link manipulators have received considerable attention in the past several years. Although most of the research results have been applied to single-link flexible manipulators, the experiments conducted for a single-link robot provide a basis for further investigations to multi-link arms. The nonminimum phase property is always present when the output is taken as the tip position [49]. In this case any attempt to achieve exact tracking through inverse dynamics results in an unstable closed-loop system. Note that the tracking of joint angles can always be obtained in a stable fashion since the system with this output is always minimum phase. However, this control may of course yield unacceptable tip deflections.

Of the early experimental work in this area, the work of Cannon & Schmitz [4] aimed at the end-point regulation problem. Also, De Luca & Siciliano [14] considered the trajectory tracking control problem of a single-link flexible manipulator when output is joint angle and a suitable point along the link using inverse dynamics. Since output re-definition is key to achieving smaller tip error in a stable fashion, Wang & Vidyasagar [83] introduced the reflected-tip position as a new output for a single-link flexible arm. De Luca & Lanari in [13] studied the regions of sensor-actuator locations to achieve minimum phase property for a single-link arm. Based on the concept of transmission zero assignment introduced in Patel & Misra [61], Geniele *et al.* [19] have applied it to a single-link flexible manipulator. The basic idea is to add a feedforward block to the plant so that the zeros of the new system are at prescribed locations in the left half-plane. The nonlinear approach to design a joint controller based on the singular perturbation theory was introduced by Siciliano & Book [75]. A singularly perturbed model for a multi-link manipulators was derived based on a modeling approach that was developed for flexible-joint manipulator introduced by Khorasani & Spong [38]. To overcome the limitation associated

with the above joint control strategies, several researchers used integral manifold approach introduced in Khorasani [37] and Spong *et at.* [78] to control the flexible-link manipulator [24, 25, 51, 52, 74]. The work of Hashtrudi-Zaad & Khorasani [24, 25] which is based on an integral manifold approach may also be interpreted as a form of output re-definition. In this work, new *fast* and *slow* outputs are defined and the original tracking problem is reduced to tracking the *slow* output and stabilizing the *fast* dynamics. A nonlinear model of a two-link flexible manipulator is used in Moallem *et at.* [51]. Also the inverse dynamics control strategy for tip position tracking of multi-link flexible manipulators was introduced in Moallem *et at.* [53].

The majority of the proposed control schemes require knowledge about the system's parameters including payload. However, during robot operation change of payload may occur and therefore, adaptive control techniques should be employed. Adaptive control of a single-link flexible manipulator with the linearized model of the link has been investigated in [16] by Feliu *et al.* and in [76] by Siciliano *et al.* using the continuous-time model and in [92] and [93] using the discrete-time model of the link by Yuh and Yurkovich & Pacheco, respectively. Also, Koivo & Lee [40] and Yang & Gibson [88] have considered the problem of discrete-time adaptive control of the linearized dynamics of a two-link flexible manipulator. The problem of controlling the tip position trajectory of a two-link flexible manipulator using a continuous-time self-tuning scheme and a least-square identification scheme was considered by Lucibello & Bellezza [48] where the payload variations are allowed. Also, a neural network based adaptive control of a flexible-link manipulator was presented in Donne & Özgüner [15] and Mahmood & Walcott [50]. The former considered the control of a single-link flexible manipulator whose dynamics are only partially unknown; in a sense that the rigid body dynamics are assumed to be known and the flexible dynamics are learned by neural networks, while the latter considered the on-line learning of a neural networks for both system identification and control

stages. Also, the non-adaptive feedback linearization of a rigid robot based on a discrete-time model was studied in Ganguly *et al.* [17] where the relative degree of the system is equal to the degree of the system.

Warshaw & Schwartz in [84, 85] have investigated the performance and stability of sampled-data version of Slotine & Li's direct adaptive controller for a rigid robot because Slotine & Li's method is relatively simple computationally, does not require measurement of accelerations and furthermore has good stability and convergence properties. The continuous-time reference adaptive control scheme was extended to discrete-time domain by Yang *et al.* [87] and sufficient conditions for stability of the resulting controlled system were also obtained. A predictive adaptive control algorithm for tip position based on the ZOH equivalent of the dynamic model of a flexible link was developed by Centinkunt & Wu [5] where a lattice filter was used for purpose of parameter identification. The proposed control algorithm together with the lattice filter form a special self-tuning regulator. Finally Qian & Ma [62] designed a discontinuous control law for a single-link flexible manipulator based on the variable structure theory.

1.3 Contributions of this Dissertation

This thesis focuses on three main steps in engineering practice and problem solving, namely, theoretical development, numerical simulations and experimental implementation. In the first part of the thesis, we are specifically dealing with indirect and direct adaptive control of discrete-time nonlinear systems. In the second part, after addressing the discretization problem of a single-link flexible manipulator dynamic equations, the application of the proposed adaptive feedback linearization and tracking control strategies were investigated. In the last part, experimental results are included to confirm both the numerical simulations and theoretical findings. The contributions and achievements of this research are now summarized as follows.

1. Indirect Adaptive Control of Fully Linearizable Discrete-Time Nonlinear Systems

The first problem addressed in this thesis is the *indirect adaptive control* of the following n*th* order affine SISO nonlinear system represented in the state-space form

$$\begin{aligned} x_{k+1} &= f(x_k, \theta) + g(x_k, \theta)u_k \\ y_k &= h(x_k, \theta) \end{aligned} \tag{1.8}$$

where $x_k \in M$ is the state vector, $u_k \in U$ is the control input, $\theta \in \Re^p$ is the vector of unknown parameters, $y(k) \in \Re$ is the output and M and U are submanifolds of $\Re^n$ and $\Re$, respectively. It is also assumed that f, g and h are analytic nonlinear functions that are linearly parameterized. Since it is assumed that the system (1.8) is fully input-output linearizable, it has no internal and zero dynamics. The objective is to have the output $y(k)$ track a reference trajectory $y_m(k)$ as k goes to infinity despite the fact that the parameters vector θ is unknown. Towards this end, we first assume that θ is known and try to find a local diffeomorphism for the change of coordinates and a nonlinear feedback control law such that system (1.8) is rendered

input to output equivalent into a linear system. The resulting linear system is then used to solve the output tracking control problem using conventional linear control theory. Next the *multi-output Recursive-Least-Square (RLS)* algorithm is employed to identify the unknown vector θ. Based upon a certainty equivalence principle the estimated parameters are then utilized in the controller. Finally, by using the Lyapunov technique the adaptively controlled closed-loop system is shown to be stable. The main contributions of this chapter are the proof of stability of the closed-loop system and application of the multi-output RLS identification algorithm to indirect feedback linearization problem. This work can be considered as the discrete-time version of the results developed by Teel *et al.* in [81] for continuous-time nonlinear systems. This topic is considered in Chapter 2 and has appeared in Rokui & Khorasani [65, 70].

2. Adaptive Tracking Control of Partially Linearizable Discrete-Time Nonlinear Systems

Since most of the practical systems are not fully feedback linearizable, this part of the thesis is essentially concerned with generalizing the approach introduced in Chapter 2 to partially input-output linearizable discrete-time nonlinear systems. The system considered has internal and zero dynamics in addition to external dynamics. The main steps to design the controller and identifier are the same as those steps considered in Chapter 2 but the proof of stability is considerably more different since the effects of internal and zero dynamics have to be taken into account. This topic is addressed in Chapter 3 and has appeared in Rokui & Khorasani [68, 69].

3. Discrete-Time Nonlinear Adaptive Tracking Control of a Flexible-Link Manipulator

Although in recent years the output re-definition method of a flexible-link manipulator based on the *continuous model* has received a great deal of attention currently there is no work in the literature on the applicability of this method to *discrete-time* model of flexible link manipulators. Therefore, the aim of this part is to apply the nonlinear adaptive control scheme proposed in Chapter 3 to a single-link flexible manipulator. The discrete-time model of the flexible-link manipulator is derived using two methods: forward difference method (Euler approximation) and a new method that enjoys the properties of both the forward difference and the step-invariance schemes. It is shown that both methods result in a similar discrete-time model with only a slight difference in forward dynamics and zero dynamics. The output re-definition scheme is used so that the resulting zero dynamics is exponentially stable. Finally, the indirect adaptive feedback linearization and tracking control problem proposed in Chapter 3 is utilized where it is assumed that the "payload mass" is unknown. The performance of the adaptively controlled closed-loop system is examined through numerical simulations to illustrate the main features of the proposed strategy. This topic is covered in Chapter 4 and has appeared in Rokui & Khorasani [66, 67].

4. Input-Output Model Based Adaptive Control for a Class of Discrete-Time Nonlinear Systems

The *direct adaptive tracking control* problem for SISO nonlinear systems represented in the input-output form

$$y(k+d) = F^T(z(k))W + G^T(z(k))Vu(k) \tag{1.9}$$

is investigated where $F(z(k))$ and $G^T(z(k))$ are smooth functions of known functions $[y(k-n+d),\ \ldots\ , y(k+d-1), u(k-m), \ldots, u(k-1)]^T$ with $m \leq n$. Note that the constant d is the relative degree of the system and the unknown vectors $W \in \Re^{p1}$ and $V \in \Re^{p2}$. This class of systems are also considered in [6, 7, 8, 9]. To solve the

direct adaptive tracking control of system (1.9), a state-space model is first obtained and the input that renders the system input-output equivalent into a linear system is derived. Note that the internal and zero dynamics are also taken into consideration. Finally, by employing the *Projection Algorithm* (or Normalized Least-Mean-Square) as a parameter estimator, the closed-loop stability of the adaptively controlled system is addressed, where it is shown that under certain conditions the tracking error is l_∞-bounded. This topic is addressed in Chapter 5 and was presented in Rokui & Khorasani [71].

5. Experimental Results

To evaluate and demonstrate the performance of the proposed adaptive feedback linearization controller to a single-link flexible manipulator, experiments on a test bed are conducted. The setup has two significant features that highlight the main characteristics of flexible manipulators: nonlinear dynamics and nonminimum phase behavior. The control and identification algorithms were coded in TMS320C30 C-language and tailored for execution in a real-time environment to the PC TURBO C-language program which acts as a monitor program for downloading the DSP program into the TMS system board and transferring the real-time data from board memory to the hard disk. The experimental results are given in Chapter 6.

Chapter 2

Indirect Adaptive Control of Fully Linearizable Discrete-Time Nonlinear Systems

In this chapter an indirect adaptive control for a class of discrete-time nonlinear systems shown in Figure 2.1 is developed. Since it is assumed that the system is fully input-output linearizable, the system has no zero dynamics. The unknown parameters of the system are first identified by using a multi-output *Recursive Least-Square (RLS)* algorithm. Certainty equivalence principle is then used to design an adaptive controller using the feedback linearization strategy. The stability properties of the closed-loop system are investigated by invoking the Lyapunov theory where it is shown that the closed-loop system consisting of the identifier and the nonlinear controller is stable. Finally, numerical simulations are included to illustrate the performance of the proposed controller [65, 70].

2.1 Introduction

In recent years the study of nonlinear adaptive control of continuous-time systems has received a great deal of attention in the literature (cf. Kanellakopoulos *et al.* [33], Nam & Arapostathis [56], Sastry & Isidori [73] and the references therein). However, adaptive control of discrete-time nonlinear systems has been emphasized to a much lesser extent. This is partly due to the fact that Lyapunov techniques are not conveniently applicable to discrete-time systems. Specifically for discrete-time systems the unknown parameters do not appear linearly in the time difference of the Lyapunov function candidate, whereas for the continuous-time systems the unknown parameters do indeed appear linearly in the time derivative of the Lyapunov function candidate. Therefore, a different approach has to employed for discrete-time systems.

In the following the most relevant results that are available in the literature for adaptive control of discrete-time nonlinear systems are reviewed. In [86] an indirect adaptive control strategy for a bilinear system is introduced by Wen & Hill. A direct adaptive control approach with a very simple nonlinearity is developed in [10] by Cook. Datta in [12], Ossman in [60] and Yu & Miller in [91] examined different

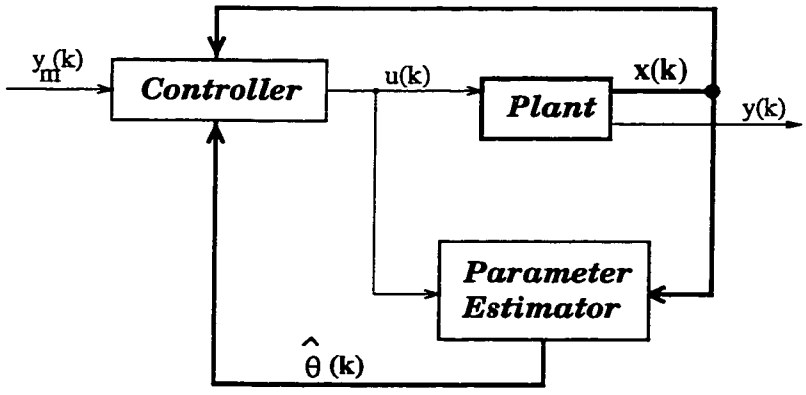

Figure 2.1: Block diagram of an indirect adaptive controller

aspects of adaptive control of interconnected systems and Song & Grizzle investigated in [77] an adaptive output feedback control for a class of nonlinear systems. Recently Kanellakopoulos in [30] developed a direct adaptive control scheme for a first order nonlinear system. It is important to point out that all the above work have considered an input-output model of a discrete-time system for designing the controller. In [90] a state feedback controller is designed to achieve tracking of a reference signal for a class of SISO nonlinear discrete-time systems by Yeh & Kokotovic. The adaptive output feedback design developed by Yeh & Kokotovic in [89] may be viewed as a discrete-time version of the continuous-time scheme considered in [34] by Kanellakopoulos *et al.*.

This chapter is organized as follows. In Section 2.1, the non-adaptive feedback linearization and tracking controller for a discrete-time nonlinear system is considered. In Section 2.2, the adaptive version of the results in Section 2.1 are developed. The stability analysis motivated by the Lyapunov technique is included in Section 2.3. Numerical simulations are included in Section 2.4 to illustrate the advantages of the proposed controller.

2.2 Non-Adaptive Feedback Linearization of Discrete-Time Nonlinear Systems

In this section, the non-adaptive input-output feedback linearization for a discrete-time nonlinear SISO system is first examined. Consider the following system

$$\begin{aligned} x_{k+1} &= f(x_k) + g(x_k)u_k \\ y_k &= h(x_k) \end{aligned} \tag{2.1}$$

where $x_k \in M$ is the state vector, $u_k \in U$ is the control input and $y_k \in \Re$ is the output with M and U are submanifolds of $\Re^n$ and $\Re$, respectively. It is also assumed

that $f : M \to M$, $g : M \to M$ and $h : M \to \Re$ are analytic functions and the origin is the equilibrium of the system. Let us denote the function $f(x_k) + g(x_k)u_k$ by $F(x_k, u_k)$ and $F(x_k, 0) = f(x_k)$ by f_o. Then, f_o^i denotes the i-times composition of f_o, that is, $\underbrace{f_o \circ f_o \cdots \circ f_o}_{i-times}$. We first need to introduce the following definition:

Definition 2.1 *The system (2.1) is said to have relative degree $\gamma \leq n$ if for all states $x_k \in M \in \Re^n$ and all inputs $u_k \in U_u \in \Re$*

$$\frac{\partial y_{k+i}}{\partial u_k} = \frac{\partial h \circ f_o^i}{\partial u_k} = 0\,, \quad i = 0, ..., \gamma - 1$$
$$\frac{\partial y_{k+\gamma}}{\partial u_k} = \frac{\partial h \circ f_o^{\gamma-1} \circ F(x_k, u_k)}{\partial u_k} \neq 0.$$

According to the above definition $y_{k+i} = h \circ f_o^i\,, \quad i = 0, ..., \gamma - 1$ are all independent of u_k and $y_{k+\gamma} = h \circ f_o^{\gamma-1} \circ F(x_k, u_k)$ is the first output affected by the input u_k. By using the above definition, a new appropriate coordinate system may be defined to transform the nonlinear system into a controllable linear system. Towards this end, by assuming that the relative degree γ is equal to order of system n, then $y_{k+i} = h \circ f_o^i(x_k)\,, \quad i = 0, ..., n - 1$ are independent of u_k but y_{k+n} depends explicitly on u_k. Consequently, the change of coordinates given locally for all $x_k \in U_x \subset M$ by

$$\begin{aligned} z_k &= [z_{1,k} \;\; z_{2,k} \;\; \cdots \;\; z_{n,k}]^T \\ &\triangleq [y_k \;\; y_{k+1} \;\; \cdots \;\; y_{k+n-1}]^T \\ &= [h(x_k) \;\; h \circ f_o(x_k) \;\; \cdots \;\; h \circ f_o^{n-1}(x_k)]^T \end{aligned} \tag{2.2}$$

defines a local diffeomorphism $z_k = \Phi(x_k)$ that should transform the nonlinear system (2.1) into a linear equivalent system. Note that by construction the Jacobian matrix of the change of coordinates $z_k = \Phi(x_k)$ is full rank for all $x_k \in U_x \subset M$.

Using these new coordinates the dynamical system (2.1) becomes

$$\begin{aligned} z_{1,k+1} &= h \circ f_o(x_k) = z_{2,k} \\ &\vdots \\ z_{n-1,k+1} &= h \circ f_o^{n-1}(x_k) = z_{n,k} \\ z_{n,k+1} &= h \circ f_o^{n-1} \circ F(x_k, u_k) \end{aligned}$$

At this stage by treating $h \circ f_o^{n-1} \circ F(x_k, u_k)$ as a new input v_k to the system, an explicit nonlinear feedback control law $u_k = \Upsilon(x_k, v_k)$ may be obtained where it is assumed that the feedback law is non-singular, that is, $\frac{\partial \Upsilon}{\partial v_k} \neq 0$. To find the feedback control law, we need the following theorem:

Theorem 2.1 (Implicit Function Theorem) *(Khalil [36])*
Assume that $F : \Re^n \times \Re^m \to \Re^n$ is a continuously differentiable function at each point (x, y) of an open set $s \subset \Re^n \times \Re^m$. Let (x_0, y_0) be a point in s for which $F(x_0, y_0) = 0$ and $\frac{\partial F}{\partial x}|_{(x_0,y_0)}$ is nonsingular. Then, there exist neighborhoods $V_x \subset \Re^n$ for x_0 and $V_y \subset \Re^m$ for y_0 such that for each $y \in V_y$ the equation $F(x, y) = 0$ has a unique solution $x = g(y)$ where $g(y)$ is continuously differentiable at $y = y_0$. In other words, x can be parameterized in term of y near (x_0, y_0).

Assuming now that zero belongs to image of $h \circ f_0^{n-1} F(x_k, .)$, it is then evident that around the point $(u_k, v_k) = (u_k, 0)$ the conditions of above Theorem 2.1 for the function $G(u_k, v_k, x_k) \triangleq h \circ f_0^{n-1} F(x_k, u_k) - v_k$ are met since $\frac{\partial G}{\partial u}|_{(u_0,0,x_k)} \neq 0$ due to the "relative degree definition". As a result, there exists a function $\Upsilon : \Re^{n+1} \to \Re$ as an explicit nonlinear control law $u_k = \Upsilon(x_k, v_k)$ which linearizes the whole dynamics. To find such a nonlinear feedback let us rewrite the feedback law as

$$v_k = h \circ f_o^{n-1} \circ F(x_k, u_k) = h \circ f_o^n(x_k) + S(x_k, u_k) \triangleq y_{k+n}$$

where $S(x_k, u_k) = h \circ f_o^{n-1} \circ F(x_k, u_k) - h \circ f_o^n(x_k)$. From the definition of the relative degree it follows that $\frac{\partial S(x_k,u_k)}{\partial u_k} = \frac{\partial y_{k+n}}{\partial u_k} \neq 0$. Therefore, there exists a feedback law

$\Upsilon : \Re^n \times \Re \to \Re$ such that

$$y_{k+n} = h \circ f_o^{n-1} \circ F(x_k, \Upsilon(x_k, v_k)) = v_k$$

or $v_k - h \circ f_o^n(x_k) = S(x_k, \Upsilon(x_k, v_k))$. Therefore, the function $\Upsilon(x_k, v_k)$ is nothing but the inverse of the function $S(x_k, .)$ or

$$u_k = \Upsilon(x_k, v_k) = S^{-1}(x_k, v_k - h \circ f_o^n) \tag{2.3}$$

To summarize, by using the state transformation $z_k = \Phi(x_k)$ given by (2.2) and the nonlinear feedback control law $u_k = \Upsilon(x_k, v_k)$ given by (2.3), the system (2.1) may now be described locally in the normal form (Isidori [26], Nijmeijer & Van der Shaft [59])

$$\begin{bmatrix} z_{1,k+1} \\ z_{2,k+1} \\ \vdots \\ z_{n-1,k+1} \\ z_{n,k+1} \end{bmatrix} = \begin{bmatrix} 0 & 1 & 0 & \cdots & 0 \\ 0 & 0 & 1 & \cdots & 0 \\ \vdots & \vdots & \vdots & \vdots & \vdots \\ 0 & 0 & 0 & \cdots & 1 \\ 0 & 0 & 0 & \cdots & 0 \end{bmatrix} \begin{bmatrix} z_{1,k} \\ z_{2,k} \\ \vdots \\ z_{n-1,k} \\ z_{n,k} \end{bmatrix} + \begin{bmatrix} 0 \\ 0 \\ \vdots \\ 0 \\ 1 \end{bmatrix} v_k$$

$$y_k = z_{1,k} \tag{2.4}$$

We are now in a position to introduce the tracking control problem for the linearized system (2.4). The objective of the controller is to guarantee that the output y_k tracks asymptotically a reference trajectory ym_k as $k \to \infty$. Towards this end, the input v_k is chosen according to

$$v_k = ym_{k+n} + \alpha_1(ym_{k+n-1} - y_{k+n-1}) + \cdots + \alpha_n(ym_k - y_k)$$

where α_i's $i = 1, \cdots, n$ are selected such that $\mathcal{Z}^n + \alpha_1 \mathcal{Z}^{n-1} + \cdots + \alpha_n$ is a Hurwitz polynomial. Since $y_{k+n-i} = z_{n-i+1,k}$, $i = 1, \cdots, n$ and $z_{n,k+1} = y_{k+n} = v_k$, therefore by substituting v_k in (2.4) it yields

$$y_{k+n} = ym_{k+n} - \alpha_1 e_{1,k+n-1} - \alpha_2 e_{1,k+n-2} - \cdots - \alpha_n e_{1,k}$$

or equivalently, $e_{1,k+n} + \alpha_1 e_{1,k+n-1} + \cdots + \alpha_n e_{1,k} = 0$, where the tracking error is defined by $e_{1,k} \triangleq y_k - ym_k$. Consequently, the error signal $e_{1,k}$ goes to zero asymptotically as time k goes to infinity.

In the next section an indirect adaptive version of the above feedback linearization scheme and the nonlinear tracking controller is developed.

Remark 2.1 *Because the relative degree γ is equal to the degree of the nonlinear system n, the input-output linearization method discussed is identical to the input-state linearization.*

2.3 Indirect Adaptive Feedback Linearization

The proposed adaptive control approach introduced in this section is developed based on the fact that there exist a state space coordinate transformation and a nonlinear state feedback control law that renders the *known* nonlinear system (2.1) into a linear controllable system (2.4). Since parametric uncertainties are present, the "certainty equivalence principle" will be invoked so that the estimates of the unknown parameters may be used in designing the controller. It is worthwhile to note that such a technique was employed by Teel *et. al* [81] for *continuous-time nonlinear* systems. The details of the identifier structure and the adaptive tracking controller are elaborated in the following subsections.

2.3.1 Identification Part

Let us consider the system of the form

$$\begin{aligned} x_{k+1} &= f(x_k, \theta) + g(x_k, \theta) u_k \\ y_k &= h(x_k, \theta) \end{aligned} \tag{2.5}$$

where $x_k \in \Re^n$ is the state vector, $y_k \in \Re$ is the output, $u_k \in \Re$ is the control input and $\theta \in \Re^p$ is the vector of unknown parameters. It is further assumed that f, g and h are linear with respect to θ, i.e., we have

$$\begin{aligned} f(x_k, \theta) &= \sum_{i=1}^{p} \theta_i f_i(x_k) \\ g(x_k, \theta) &= \sum_{i=1}^{p} \theta_i g_i(x_k) \\ h(x_k, \theta) &= \sum_{i=1}^{p} \theta_i h_i(x_k) \end{aligned} \tag{2.6}$$

where $\theta = [\theta_1 \ \theta_2 \ ... \ \theta_p]^T$ is the vector of unknown parameters and the functions f_i, g_i and h_i, $i = 1, \cdots, p$ are assumed to be known *a priori*. To identify the vector θ, the multi-output RLS algorithm discussed in Goodwin & Sin [20] is used. Towards this end, let's rearrange system (2.1) into the following nonlinear regressor form

$$Y_{k+1} = \Psi_k^T \theta \tag{2.7}$$

where $Y_{k+1} \in \Re^n$ is the observation vector, $\theta \in \Re^p$ is the unknown parameters vector and $\Psi_k^T \in \Re^n \times \Re^p$ is the regressor matrix. Equation (2.7) is derived by observing that $x_{k+1} = Y_{k+1}$ and the regressor Ψ_k^T contains all the known nonlinear functions

$$\Psi_k^T = [f_1(x_k) + g_1(x_k)u_k \quad \cdots \quad f_p(x_k) + g_p(x_k)u_k]$$

We are now in a position to use the RLS algorithm to estimate θ. In the case of a single output RLS algorithm, the objective is to estimate θ in $y_{k+1} = \psi_k^T \theta$ where $y_{k+1} \in \Re$, $\theta \in \Re^p$ and $\psi_k \in \Re^p$ such that the following cost function is minimized

$$J_N(\theta) = \frac{1}{2}(\theta - \hat{\theta}_0)^T P_0^{-1}(\theta - \hat{\theta}_0) + \frac{1}{2}\sum_{k=1}^{N}(y_k - \psi_{k-1}^T \theta)^2$$

where $\hat{\theta}_k = [\hat{\theta}_{1,k} \ ... \ \hat{\theta}_{p,k}]^T$ is the estimate of the unknown parameters at time k, $\hat{\theta}_0$ is its initial estimate and $P_0 = P_0^T > 0$ is a positive definite matrix. Similarly, for the multi-output RLS algorithm, the cost function to minimize is chosen as

$$J_N(\theta) = \frac{1}{2}(\theta - \hat{\theta}_0)^T P_0^{-1}(\theta - \hat{\theta}_0) + \frac{1}{2}\sum_{k=1}^{N}(Y_k - \Psi_{k-1}^T \theta)^T R^{-1}(Y_k - \Psi_{k-1}^T \theta)$$

where $R = R^T > 0$. It is shown in Goodwin & Sin [20] that the value of θ minimizing $J_N(\theta)$ can be computed using the following update law

$$\hat{\theta}_k = \hat{\theta}_{k-1} + P_{k-2}\Psi_{k-1}[\Psi_{k-1}^T P_{k-2}\Psi_{k-1} + R]^{-1}[Y_k - \Psi_{k-1}^T\hat{\theta}_{k-1}] \quad (2.8)$$

$$P_{k-1} = P_{k-2} - P_{k-2}\Psi_{k-1}[\Psi_{k-1}^T P_{k-2}\Psi_{k-1} + R]^{-1}\Psi_{k-1}^T P_{k-2} \quad (2.9)$$

where $P_{-1} = P_0 > 0$. The stability property of this algorithm may be studied by using the Lyapunov function candidate $V(\tilde{\theta}_k) \triangleq \tilde{\theta}_k^T P_{k-1}^{-1}\tilde{\theta}_k$, where the estimation error is $\tilde{\theta}_k \triangleq \hat{\theta}_k - \theta$. Subtracting θ from both sides of (2.8) yields

$$\tilde{\theta}_k = \tilde{\theta}_{k-1} - P_{k-2}\Psi_{k-1}[\Psi_{k-1}^T P_{k-2}\Psi_{k-1} + R]^{-1}\Psi_{k-1}^T\tilde{\theta}_{k-1} \quad (2.10)$$

and in view of (2.9) and the matrix inversion lemma, it may be shown that

$$\tilde{\theta}_k = P_{k-1}P_{k-2}^{-1}\tilde{\theta}_{k-1} \quad (2.11)$$

Therefore, using (2.10) and (2.11) $\triangle V_{k+1}^{\tilde{\theta}} \triangleq V(\tilde{\theta}_{k+1}) - V(\tilde{\theta}_k)$ satisfies

$$\begin{aligned}\triangle V_{k+1}^{\tilde{\theta}} &= \tilde{\theta}_{k+1}^T P_k^{-1}\tilde{\theta}_{k+1} - \tilde{\theta}_k^T P_{k-1}^{-1}\tilde{\theta}_k \\ &= \tilde{\theta}_{k+1}^T P_k^{-1} P_k P_{k-1}^{-1}\tilde{\theta}_k - \tilde{\theta}_k^T P_{k-1}^{-1}\tilde{\theta}_k = (\tilde{\theta}_{k+1}^T - \tilde{\theta}_k^T)P_{k-1}^{-1}\tilde{\theta}_k \\ &= -\tilde{\theta}_k^T\Psi_k[\Psi_k^T P_{k-1}\Psi_k + R]^{-1}\Psi_k^T\tilde{\theta}_k \leq 0 \end{aligned} \quad (2.12)$$

Consequently, the dynamical process (2.8)-(2.9) is stable and in particular the prediction error $\tilde{\theta}_k$ and parameter estimates $\hat{\theta}$ are bounded (belong to l_∞). The boundedness of the parameter estimates will be used subsequently in the proof of stability of the closed-loop adaptively controlled system.

2.3.2 Control Part

Motivated by the results of previous section, system (2.5) may be transformed into a normal form by using a coordinate transformation and a nonlinear state feedback control law that depend on the unknown parameter θ. By substituting θ with its

estimate $\hat{\theta}_k$, the coordinate transformation becomes $\hat{z}_k = [\hat{z}_{1,k} \quad \hat{z}_{2,k} \quad \cdots \quad \hat{z}_{n,k}]^T$ where

$$\hat{z}_{i,k} = \hat{y}_{k+i-1} = \hat{h} \circ \hat{f}_o^{i-1} \ , \quad i = 1, ..., n \tag{2.13}$$

with $\hat{h} \triangleq h(x_k, \hat{\theta}_k)$ and $\hat{f}_0 \triangleq f(x_k, \hat{\theta}_k)$. Furthermore, the feedback control law (2.3) becomes

$$u_k = \Upsilon(x_k, \hat{v}_k) = S^{-1}(x_k, \hat{v}_k - h \circ \hat{f}_o^n) \tag{2.14}$$

where $\hat{v}_k = ym_{k+n} + \sum_{i=1}^{n} \alpha_i (ym_{k+n-i} - \hat{y}_{k+n-i})$ and $\hat{y}_{k+n-i} = \hat{z}_{n-i+1,k}$, $i = 1, \cdots, n$. Now define the tracking error signals as

$$e_{i,k} \triangleq y_{k+i-1} - ym_{k+i-1} = z_{i,k} - ym_{k+i-1}, \ i = 1, \cdots, n \tag{2.15}$$

Note that, $\hat{z}_{n,k+1}$ which is equal to $\hat{v}_k$ may be written as

$$\hat{z}_{n,k+1} = ym_{k+n} + \sum_{i=1}^{n} \alpha_i (ym_{k+n-i} - \hat{z}_{n-i+1,k}) \tag{2.16}$$

If $\sum_{i=1}^{n} \alpha_i z_{n-i+1,k}$ and $z_{n,k+1}$ are now added to and subtracted from the right hand side of (2.16), it yields

$$e_{n,k+1} + (\hat{z}_{n,k+1} - z_{n,k+1}) = -\sum_{i=1}^{n} \alpha_i e_{n-i+1,k} + \sum_{i=1}^{n} \alpha_i (z_{n-i+1,k} - \hat{z}_{n-i+1,k})$$

In other words, we get $e_{n,k+1} = -\sum_{i=1}^{n} \alpha_i e_{n-i+1,k} + \tau_k$ where

$$\tau_k \triangleq \tau(x_k, u_k, \theta, \hat{\theta}_k) = (z_{n,k+1} - \hat{z}_{n,k+1}) + \sum_{i=1}^{n} \alpha_i (z_{n-i+1,k} - \hat{z}_{n-i+1,k}) \tag{2.17}$$

The above results characterize the dynamics of the tracking error system, namely

$$e_{i,k+1} = z_{i+1,k} - ym_{k+i} = e_{i+1,k} \ , \quad i = 1, ..., n-1$$

$$e_{n,k+1} = -\alpha_n e_{1,k} - \alpha_{n-1} e_{2,k} - \ \cdots \ - \alpha_1 e_{n,k} + \tau_k$$

or in the matrix form

$$\begin{bmatrix} e_{1,k+1} \\ e_{2,k+1} \\ \vdots \\ e_{n-1,k+1} \\ e_{n,k+1} \end{bmatrix} = \begin{bmatrix} 0 & 1 & 0 & \cdots & 0 \\ 0 & 0 & 1 & \cdots & 0 \\ \vdots & \vdots & \vdots & \vdots & \vdots \\ 0 & 0 & 0 & \cdots & 1 \\ -\alpha_n & -\alpha_{n-1} & -\alpha_{n-2} & \cdots & -\alpha_1 \end{bmatrix} \begin{bmatrix} e_{1,k} \\ e_{2,k} \\ \vdots \\ e_{n-1,k} \\ e_{n,k} \end{bmatrix} + \begin{bmatrix} 0 \\ 0 \\ \vdots \\ 0 \\ \tau_k \end{bmatrix} \tag{2.18}$$

Equivalently, the closed-loop system becomes

$$e_{k+1} = A_n e_k + B_n(x_k, u_k, \theta, \hat{\theta}_k) \tag{2.19}$$

where A_n is the Hurwitz matrix in (2.18) and $B_n(x_k, u_k, \theta, \hat{\theta}_k) \triangleq B_{n,k} = [0\ 0\ \cdots\ \tau_k]^T$. In the next section the stability properties of the closed-loop system consisting of (2.8)-(2.9) and (2.19) are investigated.

2.4 Stability Analysis of the Adaptively Controlled Closed-Loop System

In order to prove the stability of the closed-loop system the vector $B_{n,k}$ is first expressed as a product of two terms Γ_k and $\mathcal{X}_k$ where $\Gamma_k \triangleq \Gamma(x_k, u_k)$ is a matrix and $\mathcal{X}_k \triangleq \mathcal{X}(\theta, \hat{\theta}_k)$ is a vector. Towards this end, two cases are considered next.

2.4.1 Case I: Linear Output

Suppose $h(x_k, \theta)$ in (2.5) is linear with respect to x_k, i.e., $h(x_k, \theta) = \sum_i \theta_i x_{i,k}$. Using the results from the previous section, the function τ_k in (2.17) may be expressed as

$$\tau_k = \alpha_1(z_{n,k} - \hat{z}_{n,k}) + \alpha_2(z_{n-1,k} - \hat{z}_{n-1,k}) + \cdots + \alpha_n(z_{1,k} - \hat{z}_{1,k}) + (z_{n,k+1} - \hat{z}_{n,k+1}) \tag{2.20}$$

The term $z_{1,k} - \hat{z}_{1,k}$ may be written as

$$h(x_k, \theta) - h(x_k, \hat{\theta}_k) = \sum_i \theta_i x_{i,k} - \sum_i \hat{\theta}_{i,k} x_{i,k} = \sum_i \tilde{\theta}_{i,k} x_{i,k}$$

where $\tilde{\theta}_{i,k} \triangleq \theta_i - \hat{\theta}_{i,k}$. The next term $z_{2,k} - \hat{z}_{2,k}$ has the form

$$h(x_k, \theta) \circ f_o - h(x_k, \hat{\theta}_k) \circ \hat{f}_o = (\sum_i \theta_i x_{i,k}) \circ (\sum_j \theta_j f_j) - (\sum_i \hat{\theta}_{i,k} x_{i,k}) \circ (\sum_j \hat{\theta}_{j,k} f_j)$$

which after simplification becomes

$$z_{2,k} - \hat{z}_{2,k} = \sum_i \sum_j \tilde{\beta}_{ij}^2(\theta, \hat{\theta}_k) H_{ij}^2(x_k, u_k)$$

where $\tilde{\beta}_{ij}^2(\theta,\hat{\theta}_k) \triangleq \theta_i\theta_j - \hat{\theta}_{i,k}\hat{\theta}_{j,k}$ and $H_{ij}^2(x_k,u_k) \triangleq x_{i,k} \circ f_j \in \Re$. It now follows that by overparameterizing and by using additional functions, $z_{2,k}-\hat{z}_{2,k}$ and $z_{1,k}-\hat{z}_{1,k}$ may be expressed as a product of Γ_k and $\mathcal{X}_k$. By proceeding along this line it is easy to show that $f_o^l \triangleq (\sum_j \theta_j f_j)^l$ may be expressed as $f_o^l = \sum_j r_j^l(\theta) G_j^l(x_k,u_k)$ for some known functions $r_j^l(\theta)$ and $G_j^l(x_k,u_k)$. Consequently, $z_{l,k} - \hat{z}_{l,k} = h \circ f_o^l - \hat{h} \circ \hat{f}_o^l$, $l = 3,\cdots,n$ may be expressed as

$$\begin{aligned} z_{l,k} - \hat{z}_{l,k} &= (\sum_i \theta_i x_{i,k}) \circ (\sum_j r_j^l G_j^l) - (\sum_i \hat{\theta}_{i,k} x_{i,k}) \circ (\sum_j \hat{r}_{j,k}^l G_j^l) \\ &= \sum_i \sum_j \tilde{\beta}_{ij}^l(\theta,\hat{\theta}_k) H_{ij}^l(x_k,u_k) \ , \ l = 3,\cdots,n \end{aligned}$$

where $\tilde{\beta}_{ij}^l(\theta,\hat{\theta}_k) \triangleq \theta_i r_j^{l-1} - \hat{\theta}_i \hat{r}_{j,k}^{l-1}$ and $H_{ij}^l(x_k,u_k) \triangleq x_{i,k} \circ G_j^{l-1}$. Finally by using the above procedure the last term in (2.20), namely, $z_{n,k+1} - \hat{z}_{n,k+1}$ may be expressed as $z_{n,k+1} - \hat{z}_{n,k+1} = \sum_i \sum_j \tilde{\pi}_{ij}(\theta,\hat{\theta}_k) N_{ij}(x_k,u_k)$, where $\tilde{\pi}_{ij} \triangleq \theta_i\omega_j - \hat{\theta}_{i,k}\hat{\omega}_j$. To summarize, the function τ_k may be written as

$$\tau_k = \alpha_n \sum_i \tilde{\theta}_{i,k} x_{i,k} + \alpha_{n-1} \sum_{i,j} \tilde{\beta}_{ij}^2 H_{ij}^2 + \alpha_{n-2} \sum_{i,j} \tilde{\beta}_{ij}^3 H_{ij}^3 + \cdots + \alpha_1 \sum_{i,j} \tilde{\beta}_{ij}^n H_{ij}^n + \sum_{i,j} \tilde{\pi}_{ij} N_{ij}$$

or in general τ_k has the form $\tau_k = \sum_{i=1}^q \mu_i(x_k,u_k) A_i(\theta,\hat{\theta}_k)$ with q a positive integer. Consequently, the vector $B_{n,k}$ may now be expressed in the form

$$B_{n,k} = [0 \ 0 \ \cdots \ \tau_{n,k}]^T = \Gamma(x_k,u_k)\mathcal{X}(\theta,\hat{\theta}_k) \tag{2.21}$$

where Γ_k and $\mathcal{X}_k$ are given by

$$\Gamma_k = \begin{bmatrix} 0 & 0 & \cdots & 0 \\ 0 & 0 & \cdots & 0 \\ \vdots & \vdots & \vdots & \vdots \\ \mu_1 & \mu_2 & \cdots & \mu_q \end{bmatrix} \ , \ \mathcal{X}_k = \begin{bmatrix} A_1 \\ A_2 \\ \vdots \\ A_q \end{bmatrix}$$

Remark 2.2 *It is important to emphasize that the overparametrization and over-representation in $\mathcal{X}_k$ and Γ_k are only introduced to facilitate the proof of stability of the closed-loop system. For the purpose of control design and parameter estimation*

only the minimal number of parameters and functions are used as in (2.8)-(2.9) and (2.13)-(2.14).

2.4.2 Case II: Nonlinear Output

When $h(x_k, \theta) = \sum_{i=1}^{p} \theta_i h_i(x_k)$ is nonlinear with respect to x_k, then the procedure developed for **Case I** to separate τ_k into functions $\Gamma(x_k, u_k)$ and $\mathcal{X}(\theta, \hat{\theta}_k)$ becomes more complicated. To overcome this problem observe that the function τ_k consists of a sum of $n+1$ terms where each term may be represented in the general form

$$h(x_k, \theta) \circ f_o^l(x_k, u_k, \theta) - h(x_k, \hat{\theta}_k) \circ \hat{f}_o^l(x_k, u_k, \hat{\theta}_k) \tag{2.22}$$

Therefore, we have

$$h(x_k, \theta) \circ f_o^l(x_k, u_k, \theta) - h(x_k, \hat{\theta}_k) \circ \hat{f}_o^l(x_k, u_k, \hat{\theta}_k) = \sum_j \tilde{\zeta}_j(\theta, \hat{\theta}_k) L_j(x_k, u_k) \tag{2.23}$$

Consequently, (2.23) is partitioned into a function of (x_k, u_k) and a function of $(\theta, \hat{\theta}_k)$. We may now proceed along the lines that were used for **Case I** without loss of generality to separate τ_k into Γ_k and $\mathcal{X}_k$. To summarize, in both **Cases I** and **II** we have shown that the vector $B_{n,k} = [0\ 0\ \cdots\ \tau_k]^T$ may be expressed as in (2.21). Therefore, the equations of the adaptively controlled closed-loop system becomes

$$e_{k+1} = A_n e_k + \Gamma(x_k, u_k) \mathcal{X}(\theta, \hat{\theta}_k) \tag{2.24}$$

In the next section, stability properties of the above closed-loop system with the estimator dynamics given by (2.8)-(2.9) will be investigated.

2.4.3 Proof of Stability

The following discussion is partially inspired from the results in Johansson [29] which was developed for direct adaptive control of linear systems. However, we are going to use them to investigate the stability conditions of our proposed indirect adaptive

controller. There are several essential differences between proposed results and those in Johansson [29] that would make the following derivations completely different. Let Λ be the positive definite solution of

$$A_n^T \Lambda A_n - \Lambda + I = -Q \tag{2.25}$$

where Q is an arbitrary positive definite matrix. Apply the Cholesky factorization to Λ, i.e., $\Lambda = L^T L$. Also let $\mathcal{K}^2 \triangleq \lambda_{max}(A_n^T \Lambda A_n)$, $F \triangleq \frac{1}{\mathcal{K}} L A_n$, $G_k \triangleq \mathcal{K} L \Gamma_k$, $c^2 \triangleq \mathcal{K}^2 + 1$. By using (2.24) it then follows that

$$\begin{aligned} e_{k+1}^T \Lambda e_{k+1} - e_k^T \Lambda e_k &= (A_n e_k + \Gamma_k \mathcal{X}_k)^T \Lambda (A_n e_k + \Gamma_k \mathcal{X}_k) - e_k^T \Lambda e_k \\ &= e_k^T A_n^T \Lambda A_n e_k - e_k^T \Lambda e_k + e_k^T A_n^T \Lambda \Gamma_k \mathcal{X}_k \\ &+ \mathcal{X}_k^T \Gamma_k^T \Lambda A_n e_k + \mathcal{X}_k^T \Gamma_k^T \Lambda \Gamma_k \mathcal{X}_k \end{aligned} \tag{2.26}$$

Adding and subtracting $e_k^T F^T F e_k + \mathcal{X}_k^T G_k^T G_k \mathcal{X}_k$ to and from the right hand side of (2.26) gives

$$\begin{aligned} e_{k+1}^T \Lambda e_{k+1} - e_k^T \Lambda e_k &= e_k^T (A_n^T \Lambda A_n - \Lambda + F^T F) e_k \\ &+ \mathcal{X}_k^T (G_k^T G_k + \Gamma_k^T \Lambda \Gamma_k) \mathcal{X}_k \\ &- (F e_k - G_k \mathcal{X}_k)^T (F e_k - G_k \mathcal{X}_k) \end{aligned} \tag{2.27}$$

The first term in (2.27) satisfies $e_k^T (A_n^T \Lambda A_n - \Lambda + F^T F) e_k \leq -e_k^T Q e_k$ in view of the above choice of $\mathcal{K}$, and the third term is always non-positive. Hence,

$$e_{k+1}^T \Lambda e_{k+1} - e_k^T \Lambda e_k \leq -e_k^T Q e_k + c^2 \mathcal{X}_k^T \Gamma_k^T \Lambda \Gamma_k \mathcal{X}_k \tag{2.28}$$

A partial Lyapunov function candidate $V_2(e_k) \triangleq \ln(1 + \mu e_k^T \Lambda e_k)$, $\mu > 0$ is now selected for the error dynamics (2.24). The time difference of $V_2(e_k)$ along the trajectory (2.24), that is, $\Delta V_{k+1}^e \triangleq V_2(e_{k+1}) - V_2(e_k)$ satisfies the following inequality

$$\begin{aligned} \Delta V_{k+1}^e &= \ln(1 + \mu e_{k+1}^T \Lambda e_{k+1}) - \ln(1 + \mu e_k^T \Lambda e_k) \\ &= \ln(\frac{1 + \mu e_{k+1}^T \Lambda e_{k+1}}{1 + \mu e_k^T \Lambda e_k}) = \ln(1 + \mu \frac{e_{k+1}^T \Lambda e_{k+1} - e_k^T \Lambda e_k}{1 + \mu e_k^T \Lambda e_k}) \\ &\leq \mu(\frac{e_{k+1}^T \Lambda e_{k+1} - e_k^T \Lambda e_k}{1 + \mu e_k^T \Lambda e_k}) \end{aligned} \tag{2.29}$$

We now need to formally state our assumptions:

Assumption 2.1 *The reference output trajectory ym_k and its next $n-1$ samples are all bounded by a constant b.*

Assumption 2.2 *$\Gamma(x_k, u_k)$ is cone-bounded in x_k and uniform in u_k.*

Assumption 2.3 *The unknown parameter vector θ is upperbounded by Θ, i.e.* $\| \theta \| \leq \Theta$.

Using Assumption 2.1 and (2.15) one gets

$$\| z_k \| \leq \| e_k \| + b \tag{2.30}$$

Since x_k is a local diffeomorphism in z_k, it follows that

$$\| x_k \| \leq l_x \| z_k \|, \; x_k \in U_x \tag{2.31}$$

with $l_x > 0$. Furthermore, from Assumption 2.2 we have

$$\| \Gamma(x_k, u_k) \| \leq l_z \| x_k \|, \; \forall \, u_k \in U_u \tag{2.32}$$

with $l_z > 0$. Defining the total Lyapunov function candidate as $V(e_k, \tilde{\theta}_k) \triangleq V_2(e_k) + V_1(\tilde{\theta}_k)$ for the closed-loop system (2.8)-(2.9) and (2.24) it may be shown that

$$\begin{aligned} \triangle V_{k+1} &= \triangle V^e_{k+1} + \triangle V^{\tilde{\theta}}_{k+1} \\ &\leq \mu\left(\frac{-e_k^T Q e_k + c^2 \mathcal{X}_k^T \Gamma_k^T \Lambda \Gamma_k \mathcal{X}_k}{1 + \mu e_k^T \Lambda e_k}\right) - \tilde{\theta}_k^T \Psi_k [\Psi_k^T P_{k-1} \Psi_k + R]^{-1} \Psi_k^T \tilde{\theta}_k \\ &\leq \mu\left(\frac{-e_k^T Q e_k + c^2 \mathcal{X}_k^T \Gamma_k^T \Lambda \Gamma_k \mathcal{X}_k}{1 + \mu e_k^T \Lambda e_k}\right) \end{aligned} \tag{2.33}$$

where $\triangle V^{\tilde{\theta}}_{k+1}$ is defined in section 3.1. By taking the l^∞ norm from both sides of (2.33) and using (2.30)-(2.32) and the fact that $1 \leq |1 + \mu e_k^T \Lambda e_k| \leq 1 + \mu \| \Lambda \| \| e_k \|^2$, one obtains

$$\begin{aligned} \triangle V_{k+1} &\leq \frac{-\mu \lambda_{min}(Q) \| e_k \|^2}{1 + \mu \| \Lambda \| \| e_k \|^2} + \mu c^2 \| \Lambda \| \| \Gamma_k \|^2 \| \mathcal{X}_k \|^2 \\ &\leq \frac{-\mu \lambda_{min}(Q) \| e_k \|^2}{1 + \mu \| \Lambda \| \| e_k \|^2} + \mu \| \Lambda \| (c l_x l_z)^2 (\| e_k \| + b)^2 \| \mathcal{X}_k \|^2 \end{aligned} \tag{2.34}$$

Since $\mathcal{X}_k$ in general may be expressed as $T(\theta) - T(\hat{\theta}_k)$ where T is a known vector function, we can conclude that

$$\begin{aligned} \| \mathcal{X}_k \| &\leq \| T(\theta) \| + \| T(\hat{\theta}_k) \| \\ &\leq \delta + \| T(\hat{\theta}_k) \| \end{aligned} \tag{2.35}$$

where $\delta \triangleq \| T(\theta) \|$ is known with $\| \theta \| \leq \Theta$ in view of Assumption 2.3. Substituting (2.35) in (2.34) one gets

$$\triangle V_{k+1} \leq \frac{-\mu \lambda_{min}(Q) \| e_k \|^2}{1 + \mu \| \Lambda \| \| e_k \|^2} + \mu \| \Lambda \| (c l_x l_z)^2 (\| e_k \| + b)^2 (\delta + \| T(\hat{\theta}_k) \|)^2 \tag{2.36}$$

Provided that $\triangle V_{k+1} \leq 0$, then the closed-loop system is stable in the sense of Lyapunov. Therefore, using (2.36) it is sufficient that $T(\hat{\theta}_k)$ satisfies the following inequality

$$(\delta + \| T(\hat{\theta}_k) \|)^2 \leq \frac{\lambda_{min}(Q) \| e_k \|^2}{\| \Lambda \| (c l_x l_z)^2 (\| e_k \| + b)^2 (1 + \mu \| \Lambda \| \| e_k \|^2)} \tag{2.37}$$

Consequently, a bounded region $U_{\hat{\theta}}$ for the parameter estimates $\hat{\theta}_k$ may be constructed so that $U_{\hat{\theta}} = \{(\hat{\theta}_k, e_k) | \triangle V_{k+1} \leq 0\}$. Note that by selecting a sufficiently small $\| \Lambda \|$ from the Lyapunov equation the right hand side of (2.37) may be made larger given the fact that the matrix A_n and therefore, matrix Λ is at our disposal. Provided that the bound (2.37) holds, it then follows that $\triangle V_{k+1} \leq 0$. Hence, e_k and $\tilde{\theta}_k$ remain locally bounded. This implies that x_k is also locally bounded. Furthermore, if the parameter estimation error approaches to zero, then the tracking error e_k also converges to zero, since $\mathcal{X}_k \to 0$ and A_n is a Hurwitz matrix in (2.24). On the other hand, if the parameter estimation error does not approach to zero, then the bound for the tracking error may be obtained as follows. From (2.24) one gets

$$e_k = \psi(k, 0) e_0 + \sum_{i=0}^{k-1} \psi(k, i+1) B_{n,i} \tag{2.38}$$

where $B_{n,i} \triangleq B_{n,k}|_{k=i} = [0 \;\; 0 \;\; \cdots \;\; \Gamma(x_i, u_i) \mathcal{X}(\theta, \hat{\theta}_i)]$ and $\psi(k, j)$ is the state transition matrix associated with A_n, that is, $\psi(k, j) = A_n^{k-j}$. Since A_n is a Hurwitz matrix,

therefore the state transition matrix satisfies $|\psi(k,j)| \leq \alpha_1(\alpha_2)^{k-j}$ for $0 < \alpha_2 < 1$ and $0 < \alpha_1 < \infty$. Thus, from (2.38) it follows that

$$\| e_k \| \leq \| \alpha_1(\alpha_2)^k e_0 \| + \| \sum_{i=0}^{k-1} \alpha_1(\alpha_2)^{k-i-1} B_{n,i} \| \tag{2.39}$$

When $k \to \infty$, the first term in the right hand side of (2.39) vanishes to zero, therefore

$$\| e_k \| \leq \sum_{j=0}^{\infty} \alpha_1(\alpha_2)^j \| B_{n,j} \| \leq \| B_{n,k} \| \frac{\alpha_1}{1-\alpha_2}$$

Now from previous discussion we have $\| B_{n,k} \|^2 \leq \frac{1}{c^2\|\Lambda\|} \frac{\mu\lambda_{min}(Q)\|e_k\|^2}{1+\mu\|\Lambda\|\|e_k\|^2}$. Hence, it follows that in steady state $\| e_k \|$ satisfies the following inequality

$$\| e_k \|^2 \leq \frac{\beta^2 - 1}{\mu \| \Lambda \|} \tag{2.40}$$

where $\beta \triangleq \frac{\alpha_1}{c(1-\alpha_2)} \sqrt{\frac{\mu\lambda_{min}(Q)}{\|\Lambda\|}}$. Given the fact that V_k is a function of $\tilde{\theta}_k$ we need to express it as a function of $\hat{\theta}_k$ in order to characterize the region of stability. Observe that $V(e_k, \tilde{\theta}_k) = V_2(e_k) + V_1(\tilde{\theta}_k)$ with $V_1 = \| P_{k-1}^{-1} \| \| \tilde{\theta}_k \|^2 \leq \| P_{k-1}^{-1} \| (\| \hat{\theta}_k \|^2 + 2\Theta \| \hat{\theta}_k \| + \Theta^2)$ where Θ represents the upper bound of the parameter θ as in Assumption 2.3. Therefore, defining V_n as a new function of $\hat{\theta}_k$ instead of $\tilde{\theta}_k$, we get $V_n(e_k, \hat{\theta}_k) \triangleq V_2(e_k) + \| P_{k-1}^{-1} \| (\| \hat{\theta}_k \|^2 + 2\Theta \| \hat{\theta}_k \| + \Theta^2)$ so that $V \leq V_n \leq c$, $c > 0$ and $V_n = c$ is the largest level set contained in $\triangle V_{k+1} \leq 0$. Consequently, for all $(e_k, \hat{\theta}_k) \in \Omega_c$ the closed-loop system is stable, where $\Omega_c \triangleq \{(e_k, \hat{\theta}_k) | V_n(e_k, \hat{\theta}_k) \leq c\}$, $c > 0$ and $V_n(e_k, \hat{\theta}_k) = c$ is the largest level set contained in $\triangle V_{k+1} \leq 0$. The following theorem summarizes the results of this section.

Theorem *Consider the nonlinear discrete-time system (2.5) with unknown parameter vector θ. The closed-loop system consisting of an identifier (2.8)-(2.9), a state space coordinate transformation (2.13) and a nonlinear feedback control law (2.14) is*

locally stable for all states $(e_k, \hat{\theta}_k) \in \Omega_c$, *if the Assumptions 2.1-2.3 and the inequality (2.37) are satisfied. In other words, in steady state the closed-loop adaptively controlled system has a bounded tracking error given by (2.40).*

Remark 2.3 *If the input of the identifier is "persistently exciting " (this needs to be specified formally and precisely for discrete-time systems), the estimation error approaches to zero (i.e. if* $\hat{\theta}_k \to \theta$, *then* $\mathcal{X}_k \to 0$*). Consequently, the error dynamics (2.24) is driven by an input that is approaching to zero and is therefore asymptotically stable. In other words,* e_k *converges to zero as* $k \to \infty$.

2.5 Numerical Simulations

In this section the main features and the advantages of the proposed adaptive control algorithm over a non-adaptive strategy are illustrated through a numerical example. Consider the following discrete-time nonlinear system

$$\begin{aligned} x_{1,k+1} &= \theta_1 x_{2,k} \\ x_{2,k+1} &= \theta_1 x_{3,k} + \theta_2 x_{1,k} x_{2,k} \\ x_{3,k+1} &= \theta_2 x_{2,k} + \theta_3 (1 + x_{2,k}) u_k \\ y_k &= \theta_1 x_{1,k} \end{aligned}$$

where it is assumed that the parameters θ_1, θ_2 and θ_3 are unknown. It is easy to verify that the relative degree of the above system is $\gamma = 3$. Therefore, the method proposed in this chapter may be used to find an input signal u_k such that the output y_k tracks a reference trajectory ym_k with bounded error despite uncertainty in the parameters of the system. Towards this end, define the new coordinates as $z_k = [z_{1,k} \;\; z_{2,k} \;\; z_{3,k}]^T \triangleq [h \;\; h \circ f_o \;\; h \circ f_o^2]^T$, where

$$f_0 \triangleq f(x_k) = \begin{bmatrix} \theta_1 x_{2,k} \\ \theta_1 x_{3,k} + \theta_2 x_{1,k} x_{2,k} \\ \theta_2 x_{2,k} \end{bmatrix}$$

and

$$z_{1,k} = \theta_1 x_{1,k}$$

$$z_{2,k} = z_{1,k+1} = \theta_1^2 x_{2,k}$$

$$z_{3,k} = z_{2,k+1} = \theta_1^2(\theta_1 x_{3,k} + \theta_2 x_{1,k} x_{2,k})$$

Therefore, in the new coordinate system we have

$$\begin{bmatrix} z_{1,k+1} \\ z_{2,k+1} \\ z_{3,k+1} \end{bmatrix} = \begin{bmatrix} 0 & 1 & 0 \\ 0 & 0 & 1 \\ 0 & 0 & 0 \end{bmatrix} \begin{bmatrix} z_{1,k} \\ z_{2,k} \\ z_{3,k} \end{bmatrix} + \begin{bmatrix} 0 \\ 0 \\ 1 \end{bmatrix} v_k$$

$$y_k = z_{1,k} \tag{2.41}$$

where $v_k \triangleq a_k + b_k u_k$ and

$$b_k = \theta_1^3 \theta_3 (1 + x_{2,k}) \ , \quad a_k = \theta_1^3 \theta_2 x_{2,k} (\theta_1 x_{3,k} + \theta_2 x_{1,k} x_{2,k}) + \theta_1^3 \theta_2 x_{2,k} \tag{2.42}$$

The feedback linearizing control is given by $u_k = \frac{v_k - a_k}{b_k}$, where the external input v_k is selected as $v_k = ym_{k+3} + \alpha_1(ym_{k+2} - z_{3,k}) + \alpha_2(ym_{k+1} - z_{2,k}) + \alpha_3(ym_k - z_{1,k})$ and α_1, α_2 and α_3 are chosen so that $\mathcal{Z}^3 + \alpha_1 \mathcal{Z}^2 + \alpha_2 \mathcal{Z} + \alpha_3$ is a Hurwitz polynomial.

For the adaptive case, we have to substitute θ, z and v with $\hat{\theta}$, $\hat{z}$ and $\hat{v}$, respectively. To identify the unknown parameters the open-loop system is written in a regressor form $Y_{k+1} = \Psi_k^T \theta$, where $Y_k = [x_{1,k}\ x_{2,k}\ x_{3,k}]^T$. In other words,

$$\begin{bmatrix} x_{1,k+1} \\ x_{2,k+1} \\ x_{3,k+1} \end{bmatrix} = \begin{bmatrix} x_{2,k} & 0 & 0 \\ x_{3,k} & x_{1,k} x_{2,k} & 0 \\ 0 & x_{2,k} & (1 + x_{2,k}) u_k \end{bmatrix} \begin{bmatrix} \theta_1 \\ \theta_2 \\ \theta_3 \end{bmatrix} \triangleq \Psi_k^T \theta$$

may now be used to identify the unknown parameters using the multi-output RLS algorithm given in (2.8)-(2.9). Application of the parameter dependent coordinate transformation $\hat{z}_{1,k} = \hat{\theta}_{1,k} x_{1,k}$, $\hat{z}_{2,k} = \hat{\theta}_{1,k}^2 x_{2,k}$ and $\hat{z}_{3,k} = \hat{\theta}_{1,k}^2 (\hat{\theta}_{1,k} x_{3,k} + \hat{\theta}_{2,k} x_{1,k} x_{2,k})$ results in an equivalent linearized system (2.41). The new input is given by $\hat{v}_k =$

$\hat{a}_k + \hat{b}_k u_k$, where $\hat{a}_k$ and $\hat{b}_k$ are obtained from (2.42) with θ replaced with $\hat{\theta}_k$.

The simulations are performed for a plant with $\theta_1 = 1$, $\theta_2 = 2$, and $\theta_3 = 3$. Also, the reference trajectory is chosen as $ym_k = 0.1 * [\sin(\frac{2\pi k}{50}) + \sin(\frac{2\pi k}{30})]$. The constants α_i's are designed such that the roots of $\mathcal{Z}^3 + \alpha_1 \mathcal{Z}^2 + \alpha_2 \mathcal{Z} + \alpha_3$ are located at -0.1, -0.15, and -0.33. The results are shown in Figure 2.2. It follows that after the transient response dies out, the tracking error converges to zero. This is due to the fact that the estimation error ($\| \theta_k - \hat{\theta}_k \|$) approaches to zero asymptotically. For the sake of comparison the non-adaptive tracking results (using the true system parameters in the controller) are shown in Figure 2.3.

The advantage of the proposed adaptive scheme is now illustrated by considering the situation in which the actual values of θ_1, θ_2, and θ_3 are 1.2, 2.4, and 3.6 (representing a 20% parametric uncertainty from the nominal values). Figure 2.4 shows the performance of the non-adaptive controller designed based on the nominal parameter values $\theta_1 = 1$, $\theta_2 = 2$, and $\theta_3 = 3$. It can be seen that the closed-loop system is **unstable**. For comparison, Figure 2.5 depicts the simulation results for the proposed indirect adaptive controller. The results clearly illustrate that the closed-loop system is asymptotically stable. The adaptive and non-adaptive feedback linearization are compared in Table (2.1). These results reveal that the maximum tracking error and maximum input of adaptive tracking control are higher than those of non-adaptive case when there is no uncertainty on parameters. However when there is 20% parameter uncertainty, the adaptive controller behaves in the same fashion as before but the non-adaptive controller is unstable.

	Max. Tracking Error	Steady State Error	Maximum Input	Steady state Estimation Error
Adaptive Control (No Uncertainty)	3.9	0	6.25	0
Non-Adaptive Control (No Uncertainty)	1.44	0	4.6	–
Adaptive Control (20% Uncertainty)	12.3	0	10	0
Non-Adaptive Control (20% Uncertainty)	unstable	unstable	unstable	–

Table 2.1: Comparison between adaptive and non-adaptive tracking control problem

2.6 Conclusions

In this chapter an indirect adaptive control scheme for a discrete-time nonlinear system that is fully input-output linearizable is developed. The identifier is constructed based on the multi-output RLS algorithm that uses full state and input of the system. The controller is designed by utilizing the feedback linearization technique and the certainty equivalence principle. The main contribution of this chapter is the proof of stability of the closed-loop adaptive system. In contradistinction to continuous-time systems where the Lie derivatives are linear operators in the unknown parameters, for discrete-time systems this linear parameterization is not preserved by the composition operators. Consequently, the control problem is considerably more complicated. This problem is resolved by overparametrization and overrepresentation of the error dynamics in the proof of the stability. Based on Lyapunov analysis it is shown that all the signals of the closed-loop system remain bounded (belong to l_∞) and furthermore, if the parameter estimation error approaches to zero, then the output tracking error does also approach to zero and consequently, asymptotic tracking is achieved.

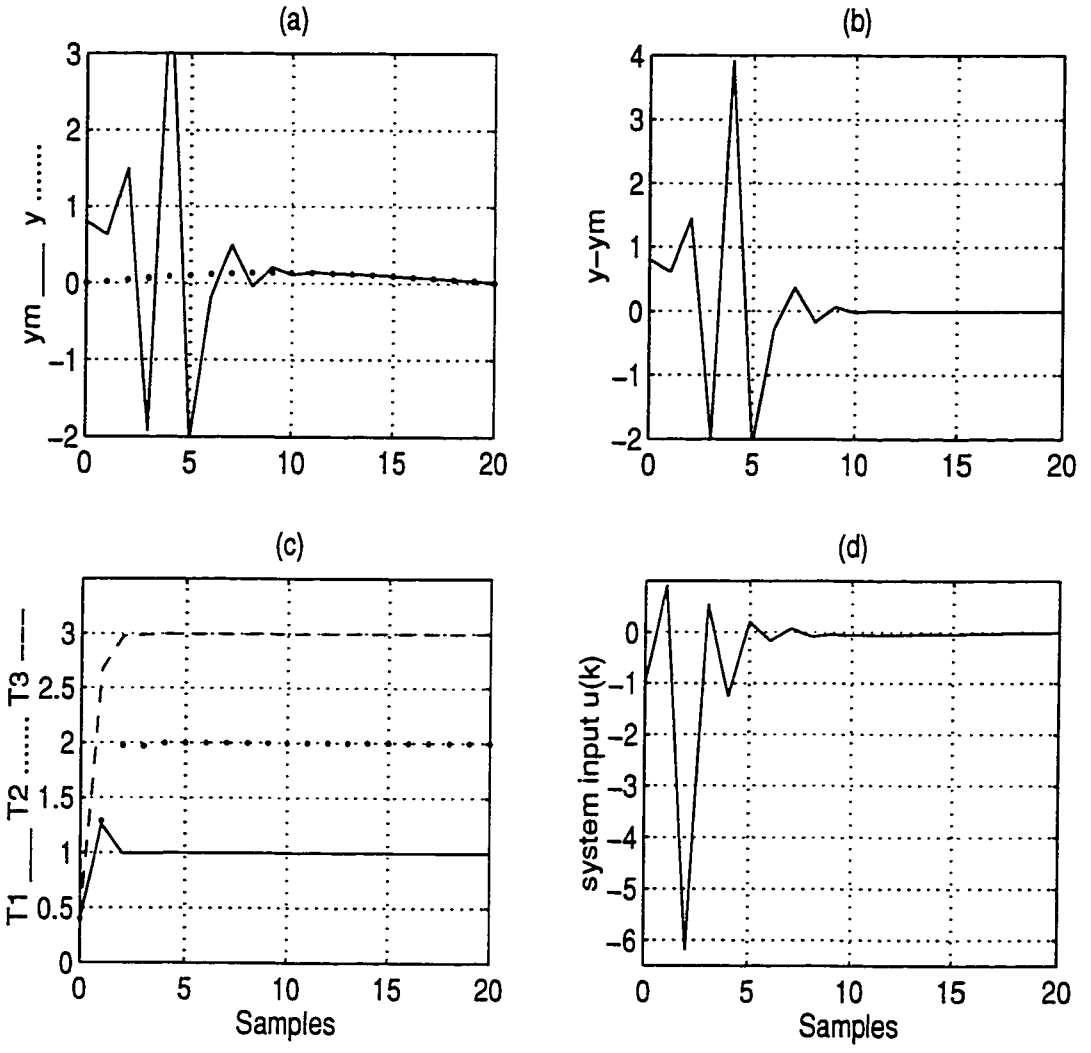

Figure 2.2: Indirect adaptive tracking control. (a) the actual output y_k ___ and the desired output ym_k ..., (b) the tracking error, (c) estimation of unknown parameters $T_1 = \hat{\theta}_{1,k}$ ___, $T_2 = \hat{\theta}_{2,k}$ ..., $T_3 = \hat{\theta}_{3,k}$ — — (d) the control input u_k.

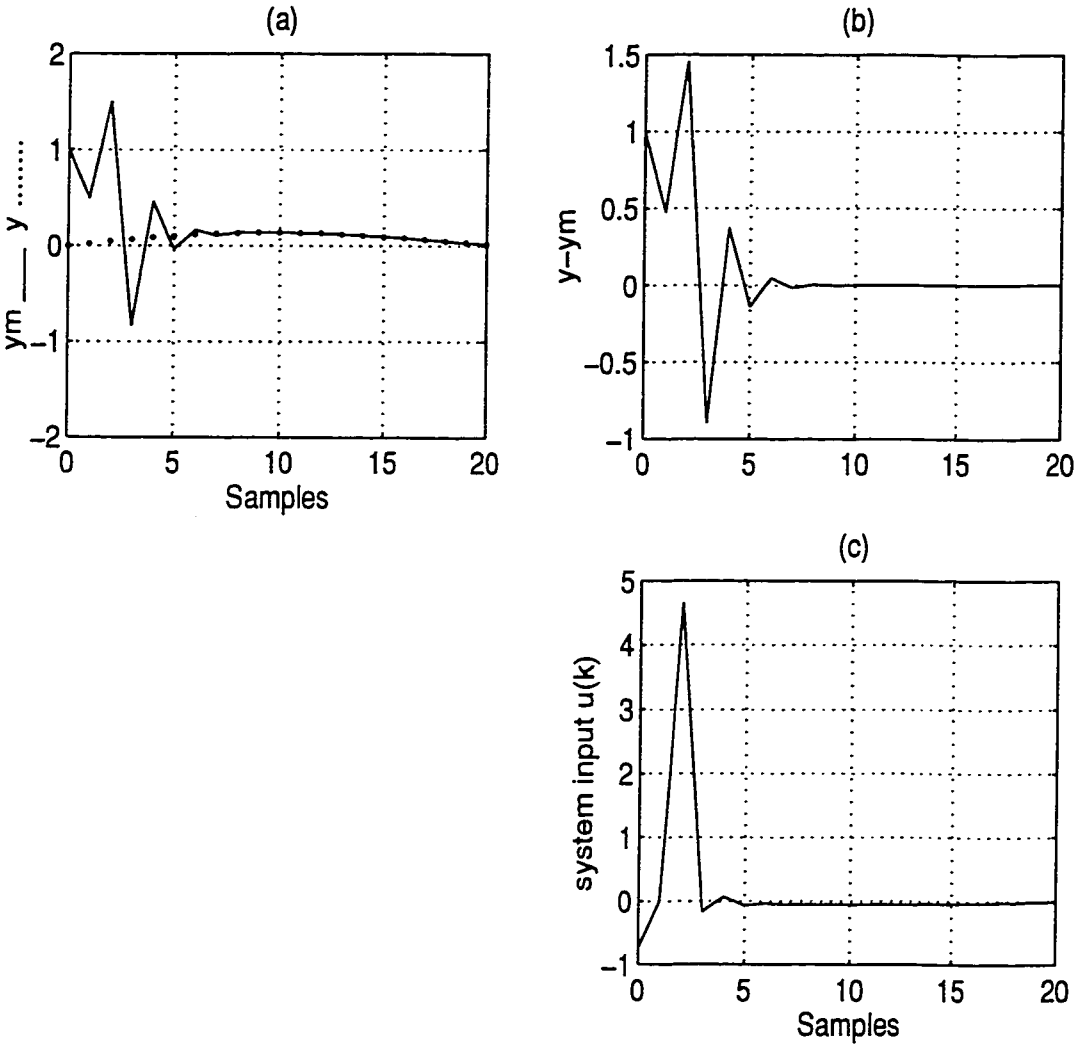

Figure 2.3: Indirect non-adaptive tracking control. (a) the actual output y_k — and the desired output ym_k ..., (b) the tracking error, (c) the control input u_k.

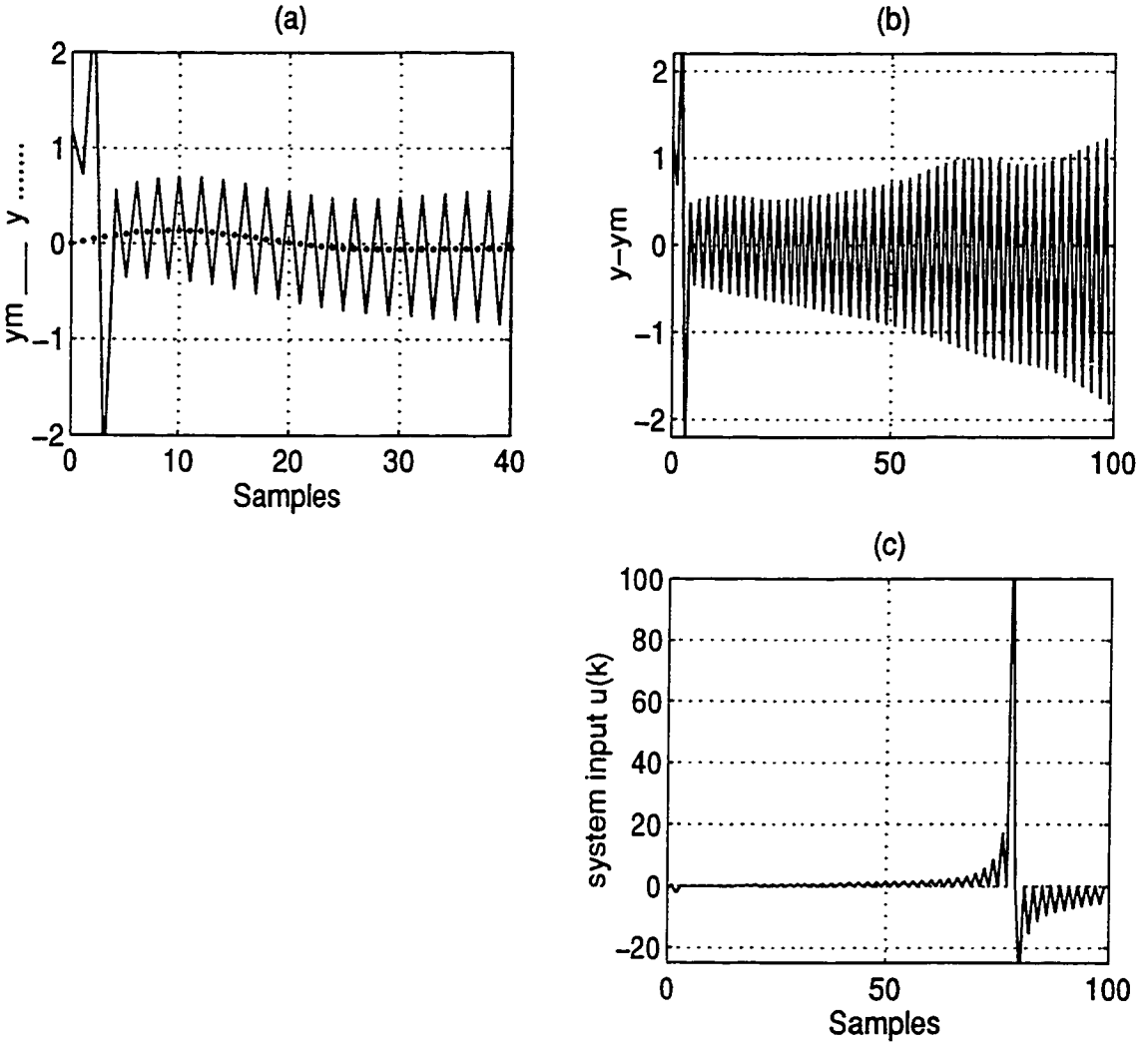

Figure 2.4: *Instability* of the non-adaptive tracking control subject to 20% parametric uncertainty. (a) the actual output y_k ___ and the desired output ym_k ..., (b) the tracking error, (c) the control input u_k.

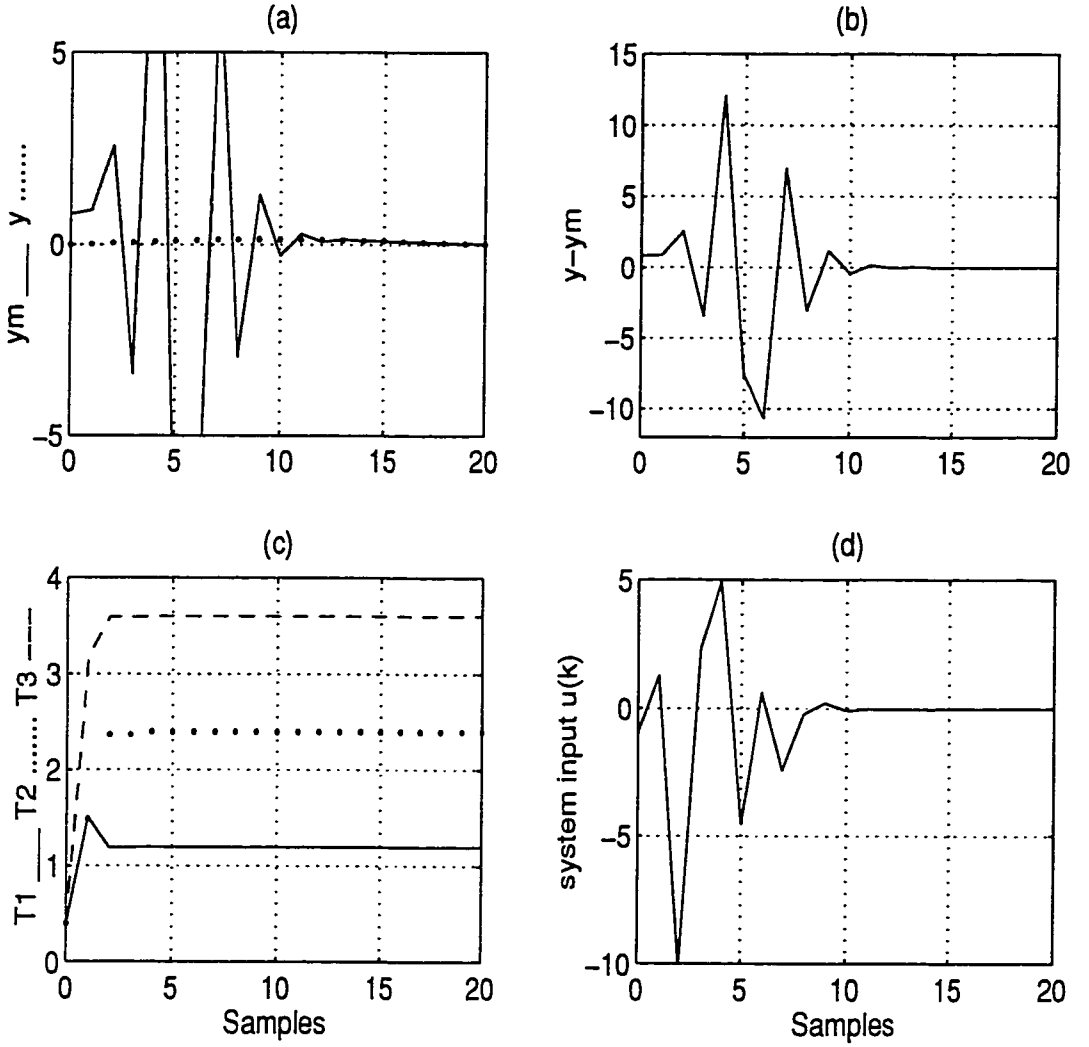

Figure 2.5: Robustness of the Indirect adaptive tracking control subject to 20% parametric uncertainty. (a) the actual output y_k ___ and the desired output ym_k ..., (b) the tracking error, (c) estimation of unknown parameters $T_1 = \hat{\theta}_{1,k}$ ___, $T_2 = \hat{\theta}_{2,k}$ ..., $T_3 = \hat{\theta}_{3,k}$ – – (d) the control input u_k.

Chapter 3

Adaptive Tracking Control of Partially Linearizable Discrete-Time Nonlinear Systems

This chapter is concerned with the tracking control problem of a discrete-time nonlinear systems that is partially input-output linearizable. The objective here is to generalize the approach introduced in Chapter 2 to partially input-output linearizable discrete-time systems with zero dynamics. Towards this end, similar to the procedure in Chapter 2, a multi-output RLS algorithm is utilized as a discrete-time parameter estimator whose output is used in the feedback linearization process. The linearized system is then used for the output tracking control problem. It is shown that by using the Lyapunov stability technique and provided that the zero dynamics are exponentially stable, all signals in the closed-loop system remain bounded. Moreover, if the estimation error goes to zero asymptotically, the tracking error approaches to zero as well [68, 69].

3.1 Introduction

Adaptive control of feedback linearizable continuous-time nonlinear systems has been studied extensively over the past few years by Kanellakopoulos *et al.*[34], Nam & Arapostathis [56], Sastry & Isidori [73] and Teel *et al.* [81]. However, only recently adaptive control of linearizable discrete-time systems is investigated by Chen & Khalil [6, 7], Chen & Tsao [9], Lin & Yong [47] and Yeh & Kokotovic [90, 89]. Also sampled-data control of continuous-time nonlinear systems is investigated by Guillaume *et al.* [22, 23] . Unfortunately, adaptive schemes developed for continuous-time systems cannot be directly extended to discrete-time systems due to some technical difficulties. The most important one in our opinion is the lack of direct applicability of Lyapunov techniques for designing the adaptive laws. This is due to the fact that for linearly parameterizable continuous-time systems the derivative of a Lyapunov function is linear with respect to the unknown parameters, whereas for discrete-time systems the difference of a Lyapunov function is nonlinear with respect to the unknown parameters. Another difference is that for continuous-time systems differentiation is a linear operation while for discrete-time systems the composition is a nonlinear operation.

In this chapter the approach proposed in Chapter 2 and in [65, 70] is generalized to discrete-time systems that are not fully input-output linearizable. The internal and zero dynamics of the system are taken into consideration in both the definition of the state-space coordinate transformation as well as the proof of the closed-loop stability. A state-space representation of the system where the nonlinearities are linear with respect to the unknown parameters is considered. The unknown parameters of the system are estimated using a multi-output RLS algorithm. The certainty equivalence principle is then invoked to design an adaptive control system. Using Lyapunov stability theory, it is shown that provided the zero dynamics are exponentially stable, then the adaptively controlled closed-loop system will be also

stable [69]. Moreover, if the parameter estimation error goes to zero asymptotically, then the tracking error will approach to zero as well. Numerical simulations are included to illustrate and validate the performance of the proposed strategy.

3.2 Input-Output Linearization and Tracking Control Problem

Consider the SISO affine discrete-time nonlinear system

$$\begin{aligned} x_{k+1} &= f(x_k, \theta) + g(x_k, \theta)u_k \\ y_k &= h(x_k, \theta) \end{aligned} \tag{3.1}$$

where $x_k \in M$ is the state vector, $u_k \in U_u$ is the control input, $\theta \in \Re^p$ is the vector of unknown parameters and M and U_u are submanifolds of $\Re^n$ and $\Re$, respectively. It is also assumed that $f : M \to M$, $g : M \to M$ and $h : M \to \Re$ are analytic functions and origin is the equilibrium of the system. It is further assumed that f and g are linearly parameterized with respect to the unknown parameters vector θ, that is, (2.6) is valid for system (3.1) as well. The objective is to have the output y_k track asymptotically a reference trajectory ym_k as k goes to infinity despite the fact that the parameters vector θ is unknown.

Following the method proposed in Chapter 2, it is first assumed that θ is known and a local diffeomorphism is obtained for the change of coordinates and the nonlinear feedback control such that system (3.1) is rendered input to output equivalent into a linear system. The resulting linear system is then used to solve the output tracking control problem using conventional linear control theory. Finally, based upon a certainty equivalence principle the estimated parameters are utilized in the controller. In the following the local diffeomorphism, the nonlinear feedback control and the internal dynamics are obtained. It is then shown how to integrate these concepts in

order to develop the proposed adaptive scheme.

To find out the new coordinates for system (3.1), according to the Definition 2.1, $y_{k+i} = h \circ f_o^{i-1} \circ F = h \circ f_o^i$, $i = 1, ..., \gamma - 1$ are all independent of u_k and $y_{k+\gamma} = h \circ f_o^{\gamma-1} \circ F$ is the first output affected by input u_k. This implies that the nonlinear system (3.1) is partially input to output linearizable. In this case the transformation $z_k = \Phi(x_k) \triangleq [\xi_k^T \ \ \eta_k^T]^T$ consists of two coordinates ξ_k and η_k. The first coordinate $\xi_k \in \Re^\gamma$ which characterizes the observable states, and is defined for all $x_k \in U_x \in M$, is specified by

$$\begin{aligned} \xi_k &\triangleq [z_{1,k} \ \ z_{2,k} \ \ \cdots \ \ z_{\gamma,k}]^T \\ &= [y_k \ \ y_{k+1} \ \ \cdots \ \ y_{k+\gamma-1}]^T \\ &= [h(x_k) \ \ h \circ f_o(x_k) \ \ \cdots \ \ h \circ f_o^{\gamma-1}(x_k)]^T \end{aligned} \tag{3.2}$$

The second coordinate $\eta_k \in \Re^{n-\gamma}$, where $\eta_k \triangleq [\eta_{1,k} \ \ \cdots \ \ \eta_{n-\gamma,k}]^T$, is to be specified to characterize the unobservable states. The choice of the coordinate η_k is at our disposal as long as the Jacobian matrix of the transformation $z_k = \Phi(x_k) = [\xi_k^T \ \ \eta_k^T]^T$ is locally full rank. Proceeding along the same lines as in Chapter 2, it may be shown that in the new coordinate system $\Phi(x_k)$ with the feedback control law $u_k = \Upsilon(x_k, v_k)$, system (3.1) may be described locally in the normal form

$$\begin{cases} z_{1,k+1} = z_{2,k} \\ \quad \vdots \\ z_{\gamma-1,k+1} = z_{\gamma,k} \\ z_{\gamma,k+1} = h \circ f_o^{\gamma-1} \circ F(x_k, u_k, \theta) \end{cases}$$
$$\begin{cases} \eta_{1,k+1} = \eta_{1,k} \circ F(x_k, u_k, \theta) \\ \quad \vdots \\ \eta_{n-\gamma,k+1} = \eta_{n-\gamma,k} \circ F(x_k, u_k, \theta) \\ y_k = z_{1,k} \end{cases} \tag{3.3}$$

where $v_k = h \circ f_o^{\gamma-1} \circ F(x_k, u_k, \theta)$ is a new control input to be selected. Observe

that the dynamics of (3.3) is partitioned into a *linear subsystem* of dimension γ that characterizes the input-output behavior of the system (a chain of γ delays from input to output) and a possibly *nonlinear subsystem* of dimension $n-\gamma$ whose dynamics does not affect the output.

To have the output y_k track a reference trajectory ym_k, the input v_k is chosen as

$$v_k = ym_{k+\gamma} + \alpha_1(ym_{k+\gamma-1} - y_{k+\gamma-1}) + \cdots + \alpha_\gamma(ym_k - y_k) \tag{3.4}$$

where $\alpha_i,\ i = 1, ..., \gamma$ are selected such that the polynomial $\mathcal{Z}^\gamma + \alpha_1\mathcal{Z}^{\gamma-1} + \cdots + \alpha_\gamma$ is Hurwitz. Using (3.3) and (3.4) and defining the output tracking error as $e_{1,k} \triangleq y_k - ym_k$, it may be shown that the governing dynamics for $e_{1,k}$ is given by, $e_{1,k+\gamma} + \alpha_1 e_{1,k+\gamma-1} + \cdots + \alpha_\gamma e_{1,k} = 0$.

When the parameter vector θ is considered to be unknown, the multi-output RLS identifier (2.8)-(2.8) is employed to give an estimate of θ which in turn is used to define the change of coordinates as $\hat{z}_k = [\hat{\xi}_k^T \ \ \eta_k^T]^T$, where $\hat{\xi}_k = [\hat{z}_{1,k} \ \cdots \ \hat{z}_{\gamma,k}]^T$ and

$$\hat{z}_{i,k} = \hat{y}_{k+i-1} = \hat{h} \circ f_0^{i-1},\ i = 1, \ldots, \gamma \tag{3.5}$$

Therefore, the nonlinear feedback controller becomes

$$u_k = \Upsilon(x_k, \hat{v}_k) = S^{-1}(x_k, \hat{v}_k - h \circ \hat{f}_o^\gamma) \tag{3.6}$$

with $\hat{v}_k = ym_{k+\gamma} + \sum_{i=1}^{\gamma} \alpha_i(ym_{k+\gamma-i} - \hat{y}_{k+\gamma-i})$. Now defining the tracking error signals as $e_{i,k} \triangleq y_{k+i-1} - ym_{k+i-1} = z_{i,k} - ym_{k+i-1},\ i = 1, \ldots, \gamma$ and proceeding along the same lines as Section 2, the dynamics of the tracking error system becomes

$$\begin{aligned}
e_{1,k+1} &= z_{2,k} - ym_{k+1} = e_{2,k} \\
e_{2,k+1} &= z_{3,k} - ym_{k+2} = e_{3,k} \\
&\vdots \\
e_{\gamma-1,k+1} &= z_{\gamma,k} - ym_{k+\gamma-1} = e_{\gamma,k} \\
e_{\gamma,k+1} &= -\alpha_\gamma e_{1,k} - \alpha_{\gamma-1} e_{2,k} - \cdots - \alpha_1 e_{\gamma,k} + \tau_\gamma(x_k, u_k, \theta, \hat{\theta}_k)
\end{aligned}$$

or in the compact form

$$e_{k+1} = A_\gamma e_k + B_\gamma(x_k, u_k, \theta, \hat{\theta}_k) \tag{3.7}$$

where $e_k \triangleq [e_{1,k} \quad e_{2,k} \quad \dots \quad e_{\gamma,k}]^T$ is the tracking error state vector and Hurwitz matrix A_γ and vector $B_\gamma(x_k, u_k, \theta, \hat{\theta}_k) \triangleq B_{\gamma,k}$ are given by

$$A_\gamma = \begin{bmatrix} 0 & 1 & \cdots & 0 \\ \vdots & \vdots & \vdots & \vdots \\ 0 & 0 & \cdots & 1 \\ -\alpha_\gamma & -\alpha_{\gamma-1} & \cdots & -\alpha_1 \end{bmatrix}, \quad B_{\gamma,k} = \begin{bmatrix} 0 \\ \vdots \\ 0 \\ \tau_{\gamma,k} \end{bmatrix}$$

with $\tau_{\gamma,k} \triangleq \tau_\gamma(x_k, u_k, \theta, \hat{\theta}_k) = (z_{\gamma,k+1} - \hat{z}_{\gamma,k+1}) + \sum_{i=1}^{\gamma} \alpha_i (z_{\gamma-i+1,k} - \hat{z}_{\gamma-i+1,k})$. Note that $\tau_{\gamma,k}$ consists of $n+1$ terms $z_{i,k} - \hat{z}_{i,k}$, therefore, (i) by substituting for $z_{i,k}$ in terms of the functions $h(x_k, \theta)$ and f_o, (ii) by substituting for $\hat{z}_{i,k}$ in terms of functions $h(x_k, \hat{\theta}_k)$ and $\hat{f}_o$ and (iii) by defining additional unknown parameters and known functions (that is by overparameterization and overrepresentation), one gets $B_{\gamma,k} = \Gamma_\gamma(x_k, u_k)\mathcal{X}_\gamma(\theta, \hat{\theta}_k)$ (cf. Chapter 2).

3.3 Internal and Zero Dynamics

Let us now examine the internal dynamics of (3.1) that are governed by $\eta_{i,k+1} = \eta_{i,k} \circ F(x_k, u_k, \theta)$, $i = 1, \dots, n-\gamma$. To simplify the proof of the stability of the adaptively controlled closed-loop system, which is presented in Section 4, the functions $\eta_{i,k} \circ F(x_k, u_k, \theta)$ should be made independent of u_k. Specifically, if the functions $\eta_{i,k} \circ F$, $i = 1, \cdots, n-\gamma$ are considered as $n-\gamma$ fictitious new outputs, then the relative degree of system (3.1) with respect to each new output must be at least two. Provided that the coordinate η_k is defined (a constructive procedure for finding these fictitious outputs is given in Appendix A), then the internal dynamics which are now independent of u_k may be written as

$$\eta_{i,k+1} = \eta_{i,k} \circ F(x_k, u_k, \theta) \triangleq q_i(\xi_k, \eta_k), \quad i = 1, \dots, n-\gamma \tag{3.8}$$

or in the compact form $\eta_{k+1} = q(\xi_k, \eta_k)$, where $q \triangleq [q_1 \ \cdots \ q_{n-\gamma}]^T$. Note that θ is an unknown but constant vector, therefore for notational simplicity we have dropped it from the above equation. Consequently, the equations of the adaptively controlled closed-loop system are given by

$$e_{k+1} = A_\gamma e_k + \Gamma_\gamma(x_k, u_k)\mathcal{X}_\gamma(\theta, \hat{\theta}_k) \tag{3.9}$$

$$\eta_{k+1} = q(\xi_k, \eta_k) \tag{3.10}$$

Given the above internal dynamics, the notion of zero dynamics are now given by the following. If system (3.1) starts from an initial condition $z_{1,0} \triangleq z_{1,k}|_{k=0} = 0$ with $v_k = 0$, then $\xi_k = 0$ for all time and the output stays at zero. In other words, the solutions starting from $z_{1,0} = 0$ with $v_k = 0$ are contained in $\mathcal{H}_0 = \{z_k | z_{1,k} = 0\}$. Hence for system (3.1) any solution starting from $x_0 \in H_0 = \{x \in U_x | z_{i+1,k} = h \circ f_o^i(x_k) = 0, \ i = 0, \ldots, \gamma - 1\}$ with $u(x_k) = \Upsilon(x_k, 0)$ is contained into $\mathcal{H}_0$. These solutions, which are characterized by the dynamics of η_k, give rise to the concept of "zero dynamics" for discrete-time systems (Chen & Khalil [7], Monaco & Normand-Cyrot [54]). The following definition characterizes formally the notion of zero dynamics.

Definition 3.1 *[Chen & Khalil [7], Monaco & Normand-Cyrot [54]] The zero dynamics of system (3.1) are governed by*

$$\eta_{k+1} = q(0, \eta_k) \triangleq q_0(\eta_k) \tag{3.11}$$

Furthermore system (3.1) is said to be minimum phase if the zero dynamics (3.11) are asymptotically stable at origin and strongly minimum phase if the zero dynamics are exponentially stable at origin.

In the next section the stability properties of the adaptively controlled closed-loop system are investigated.

3.4 Stability Analysis of the Closed-Loop System

The proof of stability of the closed-loop system consisting of the error dynamics (3.7) and the internal dynamics (3.8) is outlined in this section. Towards this end, we need to make the following assumptions regarding the zero and the internal dynamics of system (3.1).

Assumption 3.1 *The zero dynamics (3.11) are exponentially stable at origin.*

Assumption 3.2 *The internal dynamics (3.8) are locally Lipschitz in both ξ_k and η_k for all $\xi_k \in U_\xi$ and $\eta_k \in U_\eta$ with known regions U_ξ and U_η and $\xi_k \triangleq [z_{1,k} \cdots z_{\gamma,k}]^T$.*

Using Assumption 3.1, it was shown in Chen & Khalil [7] that the *Converse Lyapunov Theorem* is applicable to discrete-time systems and in particular there exists a Lyapunov function $W(\eta_k)$ such that on any compact set we have

$$\begin{aligned} k_1 \parallel \eta_k \parallel^2 &\leq W(\eta_k) \leq k_2 \parallel \eta_k \parallel^2 \\ \triangle W^{\eta}_{k+1} &\triangleq W(\eta_{k+1}) - W(\eta_k) = W \circ q_0(\eta_k) - W(\eta_k) \leq -k_3 \parallel \eta_k \parallel^2 \\ \parallel \frac{\partial W(\eta_k)}{\partial \eta_k} \parallel &\leq k_4 \parallel \eta_k \parallel \end{aligned} \tag{3.12}$$

where $k_1 - k_4$ are positive constants. According to Assumption 3.2 it now follows that for all $(\xi_{1k}, \xi_{2k}) \in U_\xi$ and $(\eta_{1k}, \eta_{2k}) \in U_\eta$, we have

$$\parallel q(\xi_{2k}, \eta_{2k}) - q(\xi_{1k}, \eta_{1,k}) \parallel \leq L_2(\parallel \xi_{2k} - \xi_{1k} \parallel + \parallel \eta_{2k} - \eta_{1k} \parallel) \tag{3.13}$$

with Lipschitz constant $L_2 > 0$. To prove the stability of system (3.7)-(3.8) and (2.8)-(2.9) , the Lyapunov function candidates $V_1(\tilde{\theta}_k)$ for the identification process and $V_2(e_k)$ for the error dynamics are selected as before according to $V_1(\tilde{\theta}_k) \triangleq \tilde{\theta}_k^T P_{k-1}^{-1} \tilde{\theta}_k$ and $V_2(e_k) \triangleq \ln(1 + \mu e_k^T \Lambda e_k)$, where $\mu > 0$ and Λ is the positive definite solution of

$A_\gamma^T \Lambda A_\gamma - \Lambda + I = -Q$ for an arbitrary positive definite symmetric matrix Q. Also, the Lyapunov function candidate $W(\eta_k)$ for the zero dynamics (3.11) are selected to satisfy conditions in (3.12). Therefore, the total Lyapunov function candidate for the closed-loop system becomes

$$\begin{aligned} V(e_k, \eta_k, \tilde{\theta}_k) &\triangleq V_1(\tilde{\theta}_k) + V_2(e_k) + W(\eta_k) \\ &= \ln(1 + \mu e_k^T \Lambda e_k) + V_1(\tilde{\theta}_k) + W(\eta_k) \end{aligned} \tag{3.14}$$

Following along the the lines as in [65] and Chapter 2, it can be shown that $\triangle V_{k+1}^e + \triangle V_{k+1}^{\tilde{\theta}} \triangleq V_2(e_{k+1}) - V_2(e_k) + V_1(\tilde{\theta}_{k+1}) - V_1(\tilde{\theta}_k)$ satisfies the following inequality

$$\triangle V_{k+1}^e + \triangle V_{k+1}^{\tilde{\theta}} \leq \mu \left(\frac{-e_k^T Q e_k + c^2 \mathcal{X}_{\gamma,k}^T \Gamma_{\gamma,k}^T \Lambda \Gamma_{\gamma,k} \mathcal{X}_{\gamma,k}}{1 + \mu e_k^T \Lambda e_k} \right) \tag{3.15}$$

where $c^2 \triangleq 1 + \lambda_{max}(A_\gamma^T \Lambda A_\gamma)$. To compute $\triangle W_{k+1}^\eta$, we substitute for η_{k+1} from (3.8) and add and subtract $W \circ q_0(\eta_k)$ to and from $\triangle W_{k+1}^\eta$, to get

$$\begin{aligned} \triangle W_{k+1}^\eta &\triangleq W \circ q(\xi_k, \eta_k) - W(\eta_k) \\ &= [W \circ q_0(\eta_k) - W(\eta_k)] + [W \circ q(\xi_k, \eta_k) - W \circ q_0(\eta_k)] \end{aligned} \tag{3.16}$$

According to (3.12), the first term in the right hand side of (3.16) is less than $-k_3 \parallel \eta_k \parallel^2$. Thus,

$$\triangle W_{k+1}^\eta \leq -k_3 \parallel \eta_k \parallel^2 + W \circ q(\xi_k, \eta_k) - W \circ q_0(\eta_k) \tag{3.17}$$

Also, from (3.12) we know that the Lyapunov function $W(\eta_k)$ is decrescent, i.e. $W(\eta_k) \leq k_2 \parallel \eta_k \parallel^2$. Therefore, the function $W \circ q(\xi_k, \eta_k)$ satisfies

$$W \circ q(\xi_k, \eta_k) \leq c_1 \parallel q(\xi_k, \eta_k) \parallel^2, \quad \xi_k \in U_\xi, \quad \eta_k \in U_\eta \tag{3.18}$$

for some constant c_1. Using the above argument, it follows that the function $W \circ q_0(\eta_k)$ satisfies

$$W \circ q_0(\eta_k) \leq c_2 \parallel q_o(\eta_k) \parallel^2, \quad \eta_k \in U_\eta \tag{3.19}$$

for some constant c_2. Substituting (3.18) and (3.19) into (3.17) gives

$$\triangle W_{k+1}^{\eta} \leq -k_3 \parallel \eta_k \parallel^2 + c_1 \parallel q(\xi_k, \eta_k) \parallel^2 - c_2 \parallel q_o(\eta_k) \parallel^2 \tag{3.20}$$

On the other hand, according to Assumption 3.2, $q(\xi_k, \eta_k)$ is Lipschitz in both ξ_k and η_k. Hence, using (B.2) and the fact that $q(0,0) = 0$, then $q(\xi_k, \eta_k)$ and $q_0(\eta_k)$ may be expressed as

$$\parallel q(\xi_k, \eta_k) \parallel = \parallel q(\xi_k, \eta_k) - q(0,0) \parallel \leq L_2(\parallel \xi_k \parallel + \parallel \eta_k \parallel) \tag{3.21}$$

$$\parallel q_0(\eta_k) \parallel = \parallel q(0, \eta_k) - q(0,0) \parallel \leq L_2(\parallel \eta_k \parallel) \tag{3.22}$$

for $\xi_k \in U_\xi$, $\eta_k \in U_\eta$. Therefore, by substituting (3.21) and (3.22) into (3.20) we obtain

$$\triangle W_{k+1}^{\eta} \leq -k_3 \parallel \eta_k \parallel^2 + c_1 L_2^2(\parallel \xi_k \parallel + \parallel \eta_k \parallel)^2 - c_2 L_2^2 \parallel \eta_k \parallel^2 \tag{3.23}$$

To summarize, using (3.14), (3.15) and (3.23) and the fact that $1 \leq |1 + \mu e_k^T \Lambda e_k| \leq 1 + \mu \parallel \Lambda \parallel \parallel e_k \parallel^2$ we get

$$\begin{aligned}
\triangle V_{k+1} &\triangleq V(e_{k+1}, \eta_{k+1}, \tilde{\theta}_{k+1}) - V(e_k, \eta_k, \tilde{\theta}_k) = \triangle V_{k+1}^{e} + \triangle V_{k+1}^{\tilde{\theta}} + \triangle W_{k+1}^{\eta} \\
&\leq -\mu\left(\frac{e_k^T Q e_k + c^2 \mathcal{X}_{\gamma,k}^T \Gamma_{\gamma,k}^T \Lambda \Gamma_{\gamma,k} \mathcal{X}_{\gamma,k}}{1 + \mu e_k^T \Lambda e_k}\right) \\
&- k_3 \parallel \eta_k \parallel^2 + c_1 L_2^2(\parallel \xi_k \parallel + \parallel \eta_k \parallel)^2 - c_2 L_2^2 \parallel \eta_k \parallel^2 \\
&\leq -\frac{\mu \lambda_{min}(Q) \parallel e_k \parallel^2}{1 + \mu \parallel \Lambda \parallel \parallel e_k \parallel^2} - (k_3 + c_2 L_2^2) \parallel \eta_k \parallel^2 + \mu c^2 \parallel \Lambda \parallel \parallel \Gamma_k \parallel^2 \parallel \mathcal{X}_k \parallel^2 \\
&+ c_1 L_2^2(\parallel \xi_k \parallel + \parallel \eta_k \parallel)^2
\end{aligned} \tag{3.24}$$

We now need to make the following additional assumptions:

Assumption 3.3 *The reference output trajectory ym_k and its next $n-1$ samples are all bounded by a constant b.*

Assumption 3.4 *$\Gamma_\gamma(x_k, u_k)$ is cone-bounded in x_k and uniform in u_k.*

Assumption 3.5 *The unknown parameter vector θ is upperbounded by Θ, i.e.* $\| \theta \| \leq \Theta$.

Using Assumptions 3.3 and 3.4 and the fact that x_k is a local diffeomorphism in ξ_k and η_k, we get

$$\begin{aligned} \| \xi_k \| &\leq \| e_k \| + b, \\ \| x_k \| &\leq l_x(\| \xi_k \| + \| \eta_k \|) \leq l_x(\| e_k \| + \| \eta_k \| + b) \\ \| \Gamma_\gamma(x_k, u_k) \| &\leq l_z \| x_k \| \leq l_x l_z(\| e_k \| + \| \eta_k \| + b) \end{aligned} \tag{3.25}$$

where $l_x > 0$, $l_z > 0$, $x_k \in U_x$, $\xi_k \in U_\xi$ and $\eta_k \in U_\eta$. Therefore, using (3.25) the inequality (3.24) becomes

$$\begin{aligned} \triangle V_{k+1} &\leq -\frac{\mu \lambda_{min}(Q) \| e_k \|^2}{1 + \mu \| \Lambda \| \| e_k \|^2} - (k_3 + c_2 L_2^2) \| \eta_k \|^2 \\ &+ d_1(\| e_k \| + \| \eta_k \| + b)^2 \| \mathcal{X}_{\gamma,k} \|^2 + c_1 L_2^2(\| e_k \| + \| \eta_k \| + b)^2 \end{aligned} \tag{3.26}$$

Since $\mathcal{X}_{\gamma,k}$ in general may be expressed as $T(\theta) - T(\hat{\theta}_k)$ with T a known vector function, we can conclude that

$$\| \mathcal{X}_{\gamma,k} \| \leq \| T(\theta) \| + \| T(\hat{\theta}_k) \| \leq \delta + \| T(\hat{\theta}_k) \| \tag{3.27}$$

where $\delta \triangleq \| T(\theta) \|$ is known using $\| \theta \| \leq \Theta$ (in view of Assumption 3.5). Substituting (4.2) in (3.26) one gets

$$\begin{aligned} \triangle V_{k+1} &\leq -\frac{\mu \lambda_{min}(Q) \| e_k \|^2}{1 + \mu \| \Lambda \| \| e_k \|^2} - (k_3 + c_2 L_2^2) \| \eta_k \|^2 \\ &+ d_1(\| e_k \| + \| \eta_k \| + b)^2 (\delta + \| T(\hat{\theta}_k) \|)^2 + c_1 L_2^2(\| e_k \| + \| \eta_k \| + b)^2 \end{aligned} \tag{3.28}$$

where $d_1 \triangleq \mu \| \Lambda \| (c l_x l_z)^2$. To guarantee the stability of the closed-loop system (3.7) and (3.8) it is sufficient to have $\triangle V_{k+1} \leq 0$. Therefore, we need to guarantee that

$$\begin{aligned} (\| e_k \| + \| \eta_k \| + b)^2 \Big[d_1(\delta + \| T(\hat{\theta}_k) \|)^2 + c_1 L_2^2 \Big] \\ \leq \frac{\mu \lambda_{min}(Q) \| e_k \|^2}{1 + \mu \| \Lambda \| \| e_k \|^2} + (k_3 + c_2 L_2^2) \| \eta_k \|^2 \end{aligned}$$

The above inequality gives rise to the following bound for $\| T(\hat{\theta}_k) \|$ in terms of $\| \eta_k \|$ and $\| e_k \|$, namely

$$(\delta + \| T(\hat{\theta}_k) \|)^2 \leq \frac{1}{d_1(\| e_k \| + \| \eta_k \| + b)^2} \left[\frac{\mu \lambda_{min}(Q) \| e_k \|^2}{1+\mu \| A \| \| e_k \|^2} + (k_3 + c_2 L_2^2) \| \eta_k \|^2 \right] - \frac{c_1 L_2^2}{d_1} \tag{3.29}$$

Since $T(\hat{\theta}_k)$ is a function of $\hat{\theta}_k$, inequality (3.29) in principle characterizes a bounded region $U_{\hat{\theta}}$ for $\hat{\theta}_k$ such that the adaptively controlled closed-loop system (3.7) and (3.8) remains locally stable. Furthermore, if the parameter estimation error approaches to zero, then $\mathcal{X}_\gamma(\theta, \hat{\theta}_k) \to 0$ and therefore, the output tracking error converges to zero. This follows from (3.7) and the fact that A_γ is a Hurwitz matrix.

In conclusion, provided that (3.29) is satisfied for all $x_k \in U_x$, $\eta_k \in U_\eta$ and $\hat{\theta}_k \in U_{\hat{\theta}}$, we get $\Delta V_{k+1} \leq 0$. Now given the fact that V_k is a function of $\tilde{\theta}_k$ we need to express it as a function of $\hat{\theta}_k$ in order to characterize the region of attraction. We have $V(e_k, \tilde{\theta}_k, \eta_k) = V_1(\tilde{\theta}_k) + V_2(e_k) + W(\eta_k)$ with $V_1 = \| P_{k-1}^{-1} \| \| \tilde{\theta}_k \|^2 \leq \| P_{k-1}^{-1} \| (\| \hat{\theta}_k \|^2 + 2\Theta \| \hat{\theta}_k \| + \Theta^2)$. Therefore, defining V_n as a new Lyapunov function that is expressed in $\hat{\theta}_k$ instead of $\tilde{\theta}_k$, we get $V_n(e_k, \hat{\theta}_k, \eta_k) \triangleq \| P_{k-1}^{-1} \| (\| \hat{\theta}_k \|^2 + 2\Theta \| \hat{\theta}_k \| + \Theta^2) + V_2(e_k) + W(\eta_k)$ so that $V \leq V_n \leq c$, $c > 0$ and $V_n = c$ is the largest level set contained in $\Delta V_{k+1} \leq 0$. Consequently, for all $(e_k, \hat{\theta}_k, \eta_k) \in \Omega_c$ the closed-loop system remains stable ($e_k \in l_\infty$, $\hat{\theta}_k \in l_\infty$, and $\eta_k \in l_\infty$), where $\Omega_c \triangleq \{(e_k, \hat{\theta}_k, \eta_k) | V_n(e_k, \hat{\theta}_k, \eta_k) \leq c\}$, $c > 0$ and $V_n(e_k, \hat{\theta}_k, \eta_k) = c$ is the largest level set contained in $\Delta V_{k+1} \leq 0$. The following theorem summarizes the results of this section.

Theorem 3.1 *Consider the nonlinear discrete-time system (3.1) with unknown parameter vector θ. The adaptively controlled closed-loop system obtained by utilizing a multi-output RLS parameter estimator (2.8)-(2.9), a state-space coordinate transformation $\hat{z}_k = [\hat{\xi}_k^T \quad \eta_k^T]^T$ with $\hat{\xi}_k$ defined in (3.5) and a nonlinear feedback control law (3.6) is locally stable for all states $(e_k, \hat{\theta}_k, \eta_k) \in \Omega_c$, if the Assumptions 3.1 to*

3.5 and the inequality (3.29) are satisfied. In other words, the adaptively controlled closed-loop system has a bounded tracking error. Moreover, if the parameter estimation error approaches to zero, then the output tracking error also converges to zero.

In the next section, the main features of the proposed adaptive control algorithm will be illustrated through a numerical example.

3.5 Numerical Simulations

In this section the main features and the advantages of the proposed adaptive control strategy over a non-adaptive strategy will be demonstrated by an example. Consider the discrete-time nonlinear system

$$\begin{aligned} x_{1,k+1} &= x_{1,k} + \theta_1(1 + x_{2,k})u_k \\ x_{2,k+1} &= 0.2x_{2,k} + \theta_2 x_{1,k}x_{3,k} \\ x_{3,k+1} &= 0.5x_{3,k} + \theta_3 x_{4,k}^2 \\ x_{4,k+1} &= x_{4,k} + \theta_4 x_{1,k} \\ y_k &= x_{3,k} + x_{4,k} \end{aligned} \tag{3.30}$$

where it is assumed that the parameter vector $\theta \triangleq [\theta_{1,k} \;\; \theta_{2,k} \;\; \theta_{3,k} \;\; \theta_{4,k}]^T$ is unknown. The control objective is to find a suitable input u_k such that the output y_k tracks a reference trajectory ym_k. Assuming that θ is known, it may be shown that the relative degree of the system γ is 2, that is, we get

$$y_{k+2} = A(x_k) + B(x_k)u_k \tag{3.31}$$

where $x_k = [x_{1,k} \;\; x_{2,k} \;\; x_{3,k} \;\; x_{4,k}]^T$ and

$$\begin{aligned} A(x_k) &\triangleq 0.5(0.5x_{3,k} + \theta_3 x_{4,k}^2) + \theta_3(x_{4,k} + \theta_4 x_{1,k})^2 + x_{4,k} + \theta_4 x_{1,k} + \theta_4 x_{1,k} \\ B(x_k) &\triangleq \theta_1\theta_4(1 + x_{2,k}) \end{aligned} \tag{3.32}$$

Therefore, the first and the second new coordinates $z_{1,k}$ and $z_{2,k}$ are defined as

$$\begin{aligned} z_{1,k} &\triangleq y_k = x_{3,k} + x_{4,k} \\ z_{2,k} &\triangleq y_{k+1} = 0.5x_{3,k} + \theta_3(x_{4,k})^2 + x_{4,k} + \theta_4 x_{1,k} \end{aligned} \tag{3.33}$$

Since the dimension of the internal dynamics are also $2(n - \gamma = 4 - 2)$, therefore two more coordinates $\eta_{1,k}$ and $\eta_{2,k}$ are to be specified so that the map

$$z_k = \Phi(x_k) = [z_{1,k} \;\; z_{2,k} \;\; \eta_{1,k} \;\; \eta_{2,k}]^T = [\xi_k^T \;\; \eta_k^T]^T \tag{3.34}$$

is a diffeomorphism around $x_k = 0$. Furthermore, since the internal dynamics governed by $\eta_{1,k+1}$ and $\eta_{2,k+1}$ should be independent of the input u_k, therefore $\eta_{1,k}$ and $\eta_{2,k}$ must be selected so that the relative degree of (3.30) with respect to each of these new coordinates is at least 2 (cf. Appendix A). In this example, it turns out that without using the formal procedure outlined in the Appendix the following are suitable coordinates

$$\eta_{1,k} = x_{4,k}, \quad \eta_{2,k} = x_{2,k} \tag{3.35}$$

Consequently, the internal dynamics become

$$\begin{aligned} \eta_{1,k+1} &= x_{4,k+1} = x_{4,k} + \theta_4 x_{1,k} \\ \eta_{2,k+1} &= x_{2,k+1} = 0.2x_{2,k} + \theta_2 x_{1,k} x_{3,k} \end{aligned} \tag{3.36}$$

It is easy to show that the Jacobian of the coordinate transformation (3.34) is full rank if and only if $\theta_4 \neq 0$. Therefore, system (3.30) may be expressed in the new coordinates as

$$\begin{aligned} z_{1,k+1} &= z_{2,k} \\ z_{2,k+1} &= v_k \\ \eta_{1,k+1} &= \eta_{1,k} + \theta_4 x_{1,k} \\ \eta_{2,k+1} &= 0.2\eta_{2,k} + \theta_2 x_{1,k} x_{3,k} \\ y_k &= z_{1,k} \end{aligned}$$

where the control input u_k is selected as $u_k = \frac{v_k - A(x_k)}{B(x_k)}$ and the new input v_k is defined as

$$v_k = ym_{k+2} + \alpha_1(ym_{k+1} - z_{2,k}) + \alpha_2(ym_k - z_{1,k})$$

The parameters α_1 and α_2 are selected such that $\mathcal{Z}^2 + \alpha_1\mathcal{Z} + \alpha_2$ is a Hurwitz polynomial. The zero dynamics of the system are obtained by first computing the inverse of $\Phi(x_k)$ at $z_{1,k} = z_{2,k} = 0$, that is

$$\begin{aligned} x_{1,k} &= -\frac{0.5\eta_{1,k} + \theta_3\eta_{1,k}^2}{\theta_4} \\ x_{2,k} &= \eta_{2,k} \\ x_{3,k} &= -\eta_{1,k} \\ x_{4,k} &= \eta_{1,k} \end{aligned} \tag{3.37}$$

By substituting (3.37) into (3.36), the zero dynamics are given by

$$\begin{aligned} \eta_{1,k+1} &= 0.5\eta_{1,k} - \theta_3\eta_{1,k}^2 \\ \eta_{2,k+1} &= 0.2\eta_{2,k} + \theta_2\eta_{1,k}^2\frac{0.5 + \theta_3\eta_{1,k}}{\theta_4} \end{aligned} \tag{3.38}$$

The above system must be exponentially stable around $\eta_k = 0$. We know that system (3.38) is locally exponentially stable if and only if its linearized model is exponentially stable. The linearized model of (3.38) around $\eta_k = 0$ is obtained as $\eta_{k+1} = E\eta_k$, where E is the Jacobian matrix

$$E = \begin{bmatrix} 0.5 - 2\theta_3\eta_{1,k} & 0 \\ \frac{\theta_2}{\theta_4}\eta_{1,k}(0.25 + 3\theta_3\eta_{1,k}) & 0.2 \end{bmatrix}_{|\eta_k=0} = \begin{bmatrix} 0.5 & 0 \\ 0 & 0.2 \end{bmatrix} \tag{3.39}$$

Since the linearized model of the zero dynamics is a time-invariant system and E is a Hurwitz matrix, therefore, the zero dynamics are locally exponentially stable around $\eta_k = 0$.

To design the indirect adaptive controller the unknown parameter vector θ is replaced with its estimate $\hat{\theta}$ in the above derivations. To identify θ we rewrite system (3.30) in the regressor form $Y_{k+1} = \Psi_k^T \theta$, where the observation vector Y_{k+1} and the regressor matrix Ψ_k are given by

$$Y_{k+1} = \begin{bmatrix} x_{1,k+1} - x_{1,k} \\ x_{2,k+1} - 0.2x_{2,k} \\ x_{3,k+1} - 0.5x_{3,k} \\ x_{4,k+1} - x_{4,k} \end{bmatrix}, \quad \Psi_k = \begin{bmatrix} (1 + x_{2,k})u_k & 0 & 0 & 0 \\ 0 & x_{1,k}x_{3,k} & 0 & 0 \\ 0 & 0 & x_{4,k}^2 & 0 \\ 0 & 0 & 0 & x_{1,k} \end{bmatrix}$$

The multi-output RLS algorithm (2.8)-(2.9) is used to identify the unknown parameter vector θ. The control input u_k becomes $u_k = \frac{\hat{v}_k - \hat{A}(x_k)}{\hat{B}(x_k)}$, where $\hat{A}(x_k)$ and $\hat{B}(x_k)$ are defined from (3.32) with θ replaced by $\hat{\theta}_k = [\hat{\theta}_{1,k} \;\; \hat{\theta}_{2,k} \;\; \hat{\theta}_{3,k} \;\; \hat{\theta}_{4,k}]^T$,

$$\hat{v}_k = ym_{k+2} + \alpha_1(ym_{k+1} - \hat{z}_{2,k}) + \alpha_2(ym_k - \hat{z}_{1,k})$$

and $\hat{z}_{1,k}$ and $\hat{z}_{2,k}$ are given by (3.33) with θ replaced by $\hat{\theta}_k$. For simulation purposes it is assumed that the nominal value of θ is $\theta = [0.01 \;\; 0.05 \;\; 0.1 \;\; 0.15]^T$. Also the reference trajectory ym_k is selected as $ym_k = 0.3(\sin(0.3k) + \sin(0.05k))$, and the constants α_1 and α_2 are chosen such that the roots of $\mathcal{Z}^2 + \alpha_1\mathcal{Z} + \alpha_2$ are located at 0.9 and 0.9. Figure 3.1 shows the simulation results for the proposed indirect adaptive controller. It follows that after the transients have died out the output tracking error approaches to zero. This is due to the fact that the estimator has perfectly identified the unknown parameters.

The robustness of the proposed scheme is demonstrated by assuming a 30% variation in the parameters of the system. Figure 3.2 shows the results for the adaptively controlled system and Figure 3.3 shows the results for the non-adaptive controlled system where the nominal value of θ is directly used in the controller design. Note that although the performance of the adaptive controller is unchanged, the output tracking error for the non-adaptive controller becomes larger.

	Max. Tracking Error	Steady State Error	Maximum Input	Steady state Estimation Error
Adaptive Control (No Uncertainty)	0.175	0	19.8	0
Non-Adaptive Control (No Uncertainty)	0.166	0	18.8	–
Adaptive Control (30% Uncertainty)	0.2	0	15.5	0
Non-Adaptive Control (30% Uncertainty)	0.24	0.17	19.1	–
Adaptive Control (120% Uncertainty)	0.45	0	6.5	0
Non-Adaptive Control (120% Uncertainty)	unstable	unstable	unstable	–

Table 3.1: Comparison between adaptive and non-adaptive tracking control

It is important to note that for a sufficiently large variation in the parameters the non-adaptive controller may become even unstable. To demonstrate this, Figures 3.4 and 3.5 depict the results of the adaptive and the non-adaptive controllers, respectively, subject to 120% variation in the parameters of the system. Clearly, the non-adaptive controller is *unstable* whereas the proposed adaptive controller results in a stable operation of the closed-loop system. Table (3.1) summarizes the simulation results of adaptive and non-adaptive tracking control problem. These results reveals that as the parameter uncertainty is increased, the maximum tracking error of adaptive controller increases as well but in all cases the steady state tracking error is zero. However the performance of non-adaptive controller is deteriorated as the parameter uncertainty is increased and finally it becomes unstable.

3.6 Conclusions

An indirect adaptive control scheme for a partially input-output linearizable discrete-time nonlinear system is developed. Using the Lyapunov analysis, it is shown that

provided the zero dynamics are exponentially stable, then the adaptively controlled closed-loop system consisting of a nonlinear controller, a discrete-time parameter estimator developed based on the multi-output RLS algorithm and that uses full state feedback of the system is locally stable. In addition, if the parameter estimation error approaches to zero, then the output tracking error also approaches to zero as $t \to \infty$.

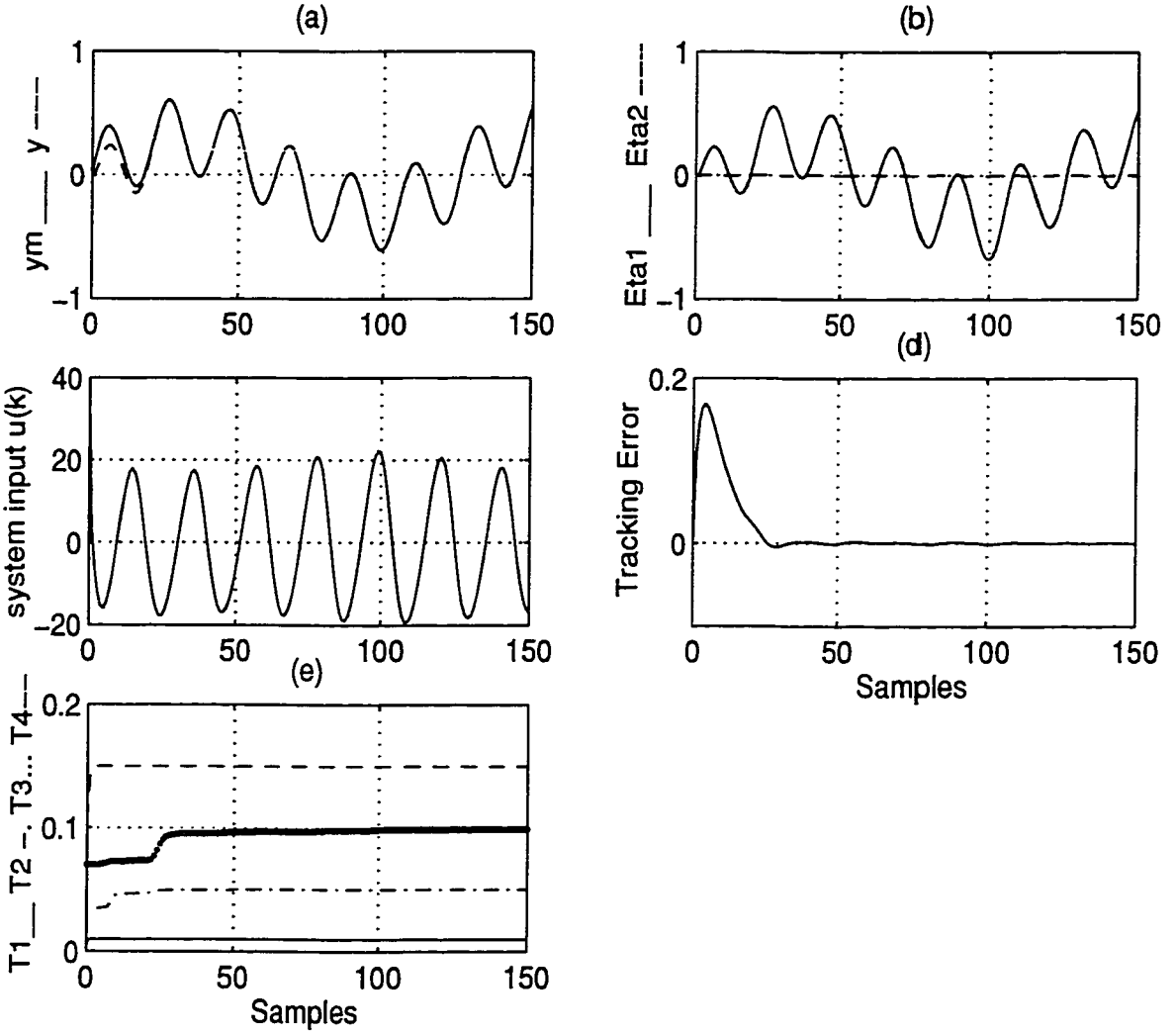

Figure 3.1: Indirect adaptive tracking control. (a) output y_k $--$ and desired trajectory ym_k ___ (b) internal dynamics $\eta_{1,k} = Eta1$ $--$ and $\eta_{2,k} = Eta2$ ___ (c) system input $u(k)$ (d) tracking error $e(k) = y_k - ym_k$ (e) estimation of unknown parameters $T_1 = \hat{\theta}_{1,k}$ ___, $T_2 = \hat{\theta}_{2,k}$ $-.$, $T_3 = \hat{\theta}_{3,k}$ ..., $T_4 = \hat{\theta}_{4,k}$ $--$

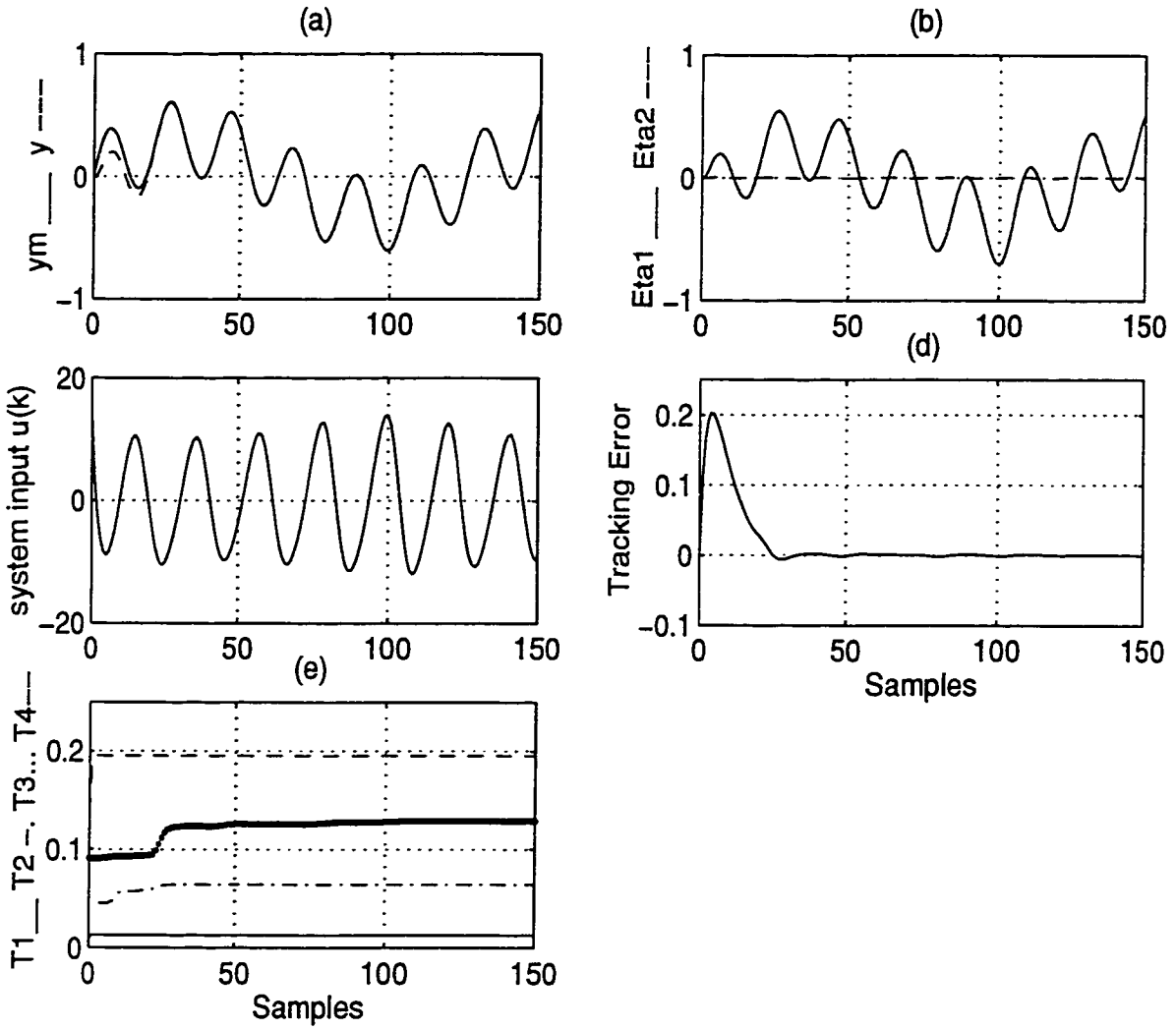

Figure 3.2: Adaptive tracking control when there is a 30% variation in parameters. (a) output y_k $--$ and desired trajectory ym_k ___ (b) internal dynamics $\eta_{1,k} = Eta1$ $--$ and $\eta_{2,k} = Eta2$ ___ (c) system input $u(k)$ (d) tracking error $e(k) = y_k - ym_k$ (e) estimation of unknown parameters $T_1 = \hat{\theta}_{1,k}$ ___, $T_2 = \hat{\theta}_{2,k}$ $-.$, $T_3 = \hat{\theta}_{3,k}$ ..., $T_4 = \hat{\theta}_{4,k}$ $--$

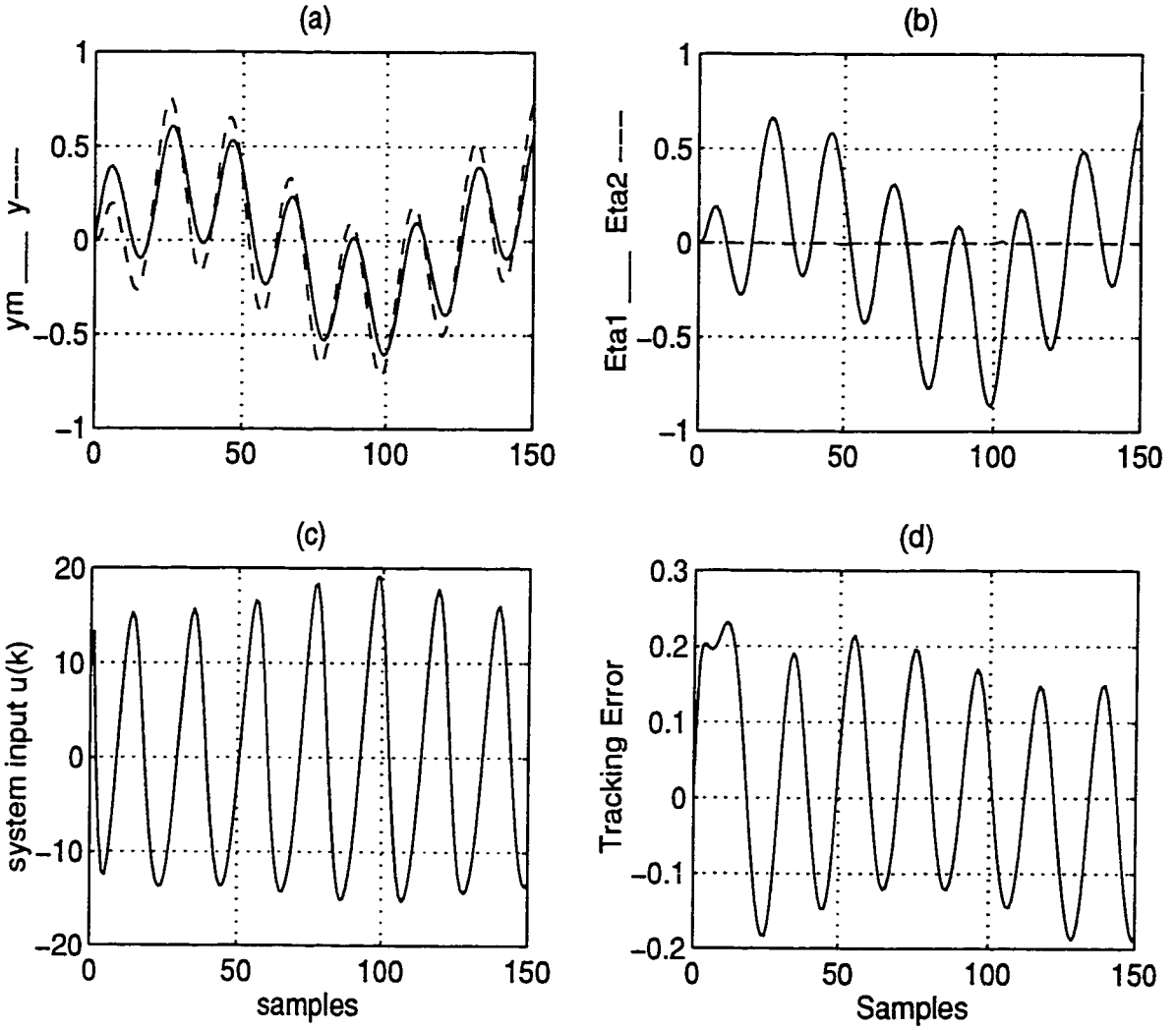

Figure 3.3: Non-adaptive tracking control when there is a 30% variation in parameters. (a) output y_k $--$ and desired trajectory ym_k ___ (b) internal dynamics $\eta_{1,k} = Eta1$ $--$ and $\eta_{2,k} = Eta2$ ___ (c) system input $u(k)$ (d) tracking error $e(k) = y_k - ym_k$

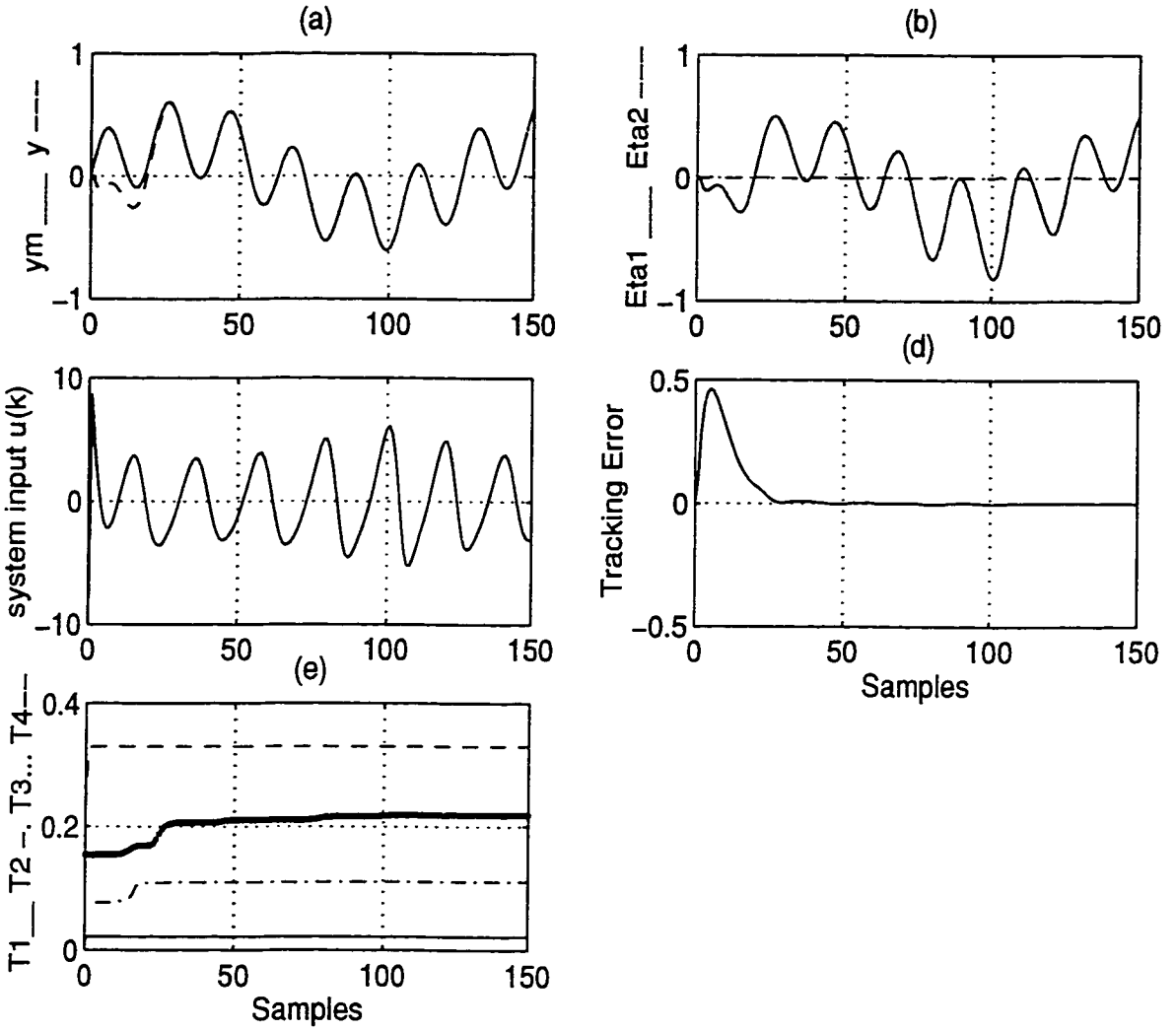

Figure 3.4: Adaptive tracking control when there is a 120% variation in parameters. (a) output y_k $--$ and desired trajectory ym_k ___ (b) internal dynamics $\eta_{1,k} = Eta1$ $--$ and $\eta_{2,k} = Eta2$ ___ (c) system input $u(k)$ (d) tracking error $e(k) = y_k - ym_k$ (e) estimation of unknown parameters $T_1 = \hat{\theta}_{1,k}$ ___, $T_2 = \hat{\theta}_{2,k}$ $-.$, $T_3 = \hat{\theta}_{3,k}$ ..., $T_4 = \hat{\theta}_{4,k}$ $--$

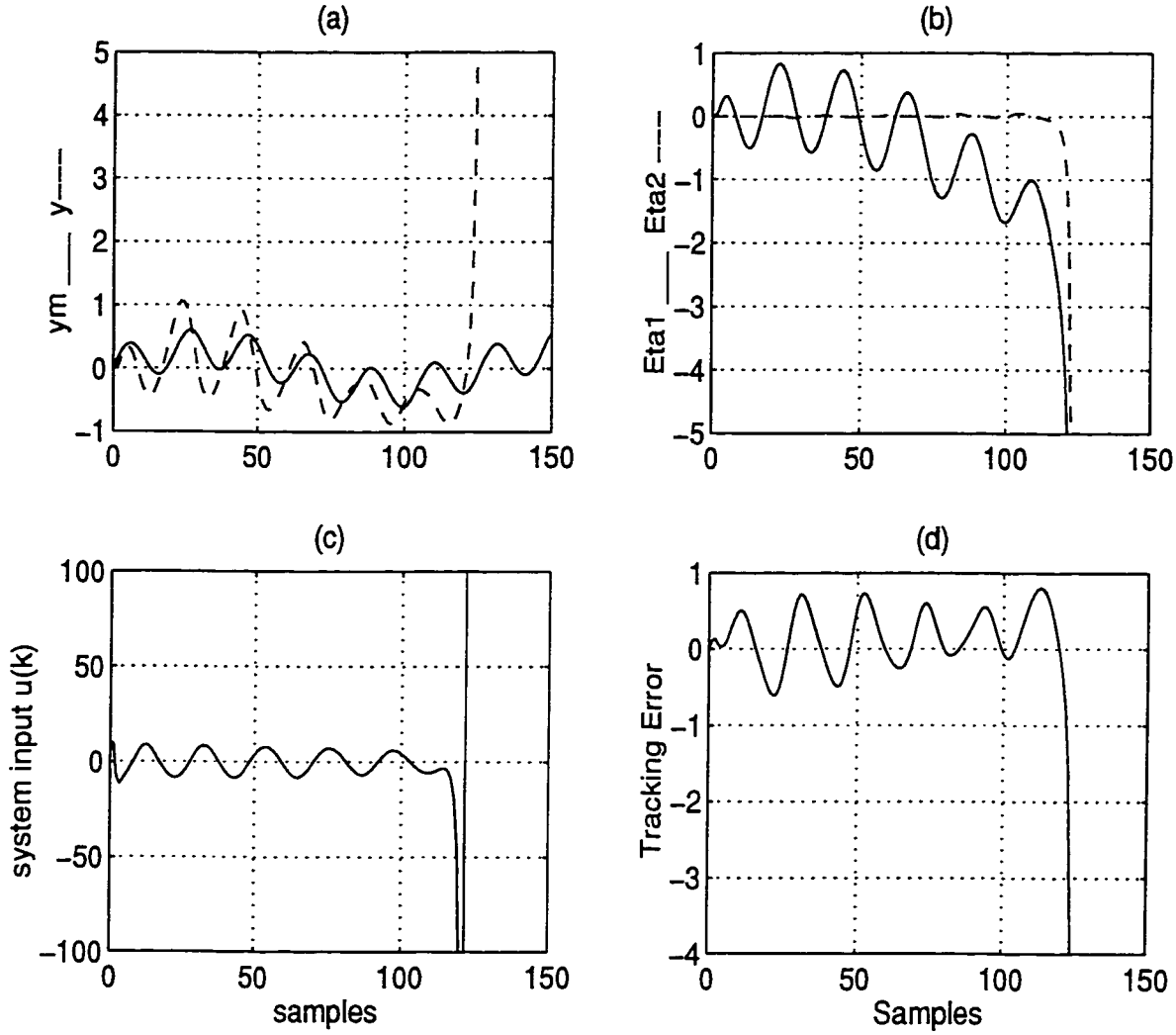

Figure 3.5: Non-adaptive tracking control when there is a 120% uncertainty in parameters. (a) output y_k $--$ and desired trajectory ym_k $\_\_$ (b) internal dynamics $\eta_{1,k} = Eta1$ $--$ and $\eta_{2,k} = Eta2$ $\_\_$ (c) system input $u(k)$ (d) tracking error $e(k) = y_k - ym_k$

Chapter 4

Discrete-Time Nonlinear Adaptive Tracking Control of a Flexible-Link Manipulator

The aim of this chapter is to apply the nonlinear adaptive control scheme proposed in Chapter 3 to a single-link flexible manipulator. The discrete-time model of the flexible-link manipulator is derived using two methods: forward difference method (Euler approximation) and a new method that enjoys the properties of both the forward difference and the step-invariance schemes. It is shown that both methods result in a similar discrete-time model with only a slight difference in forward dynamics and zero dynamics. The output re-definition scheme is used so that the resulting zero dynamics is exponentially stable. Finally, the indirect adaptive feedback linearization and tracking control problem proposed in Chapter 3 are utilized where it is assumed that the "payload mass" is unknown. The performance of the adaptively controlled closed-loop system is examined through numerical simulations to show the main features of the proposed strategy [66, 67].

4.1 Introduction

The problems of modeling and control of flexible-link manipulators have received considerable attention in the past few years (Book [2], Cannon & Schmitz [4], De Luca & Lanari [13], Geniel *et. al* [19], Madhavan & Singh [49] and Wang & Vidyasagar [83]). The majority of the proposed control schemes require knowledge about the system's parameters including payload. However, during robot operation change of payload may occur and therefore, adaptive control techniques should be employed. Adaptive control of a single-link flexible manipulator with the linearized model of the link has been investigated in [16] by Feliu *et. al* and in [76] by Siciliano *et. al* using the continuous-time model and in [92] and [93] using the discrete-time model of the link by Yuh and Yurkovich & Pacheco, respectively. Also, Koivo & Lee [40] and Yang & Gibson [88] have considered the problem of discrete-time adaptive control of the linearized dynamics of a two-link flexible manipulator. The problem of controlling the tip position trajectory of a two-link flexible manipulator using a continuous-time self-tuning scheme and a least-square identification scheme was considered by Lucibello & Bellezza [48] where the payload variations are allowed. Also, a neural network based adaptive control of a flexible-link manipulator was presented in Donne & Özgüner [15] and Mahmood & Walcott [50]. The former considered the control of a single-link flexible manipulator whose dynamics are only partially unknown; in a sense that the rigid body dynamics are assumed to be known and the flexible dynamics are learned by neural networks, while the latter considered the on-line learning of a neural networks for both system identification and control stages. Also, the non-adaptive feedback linearization of a rigid robot based on a discrete-time model with no zero dynamics were given in Ganguly *et al.* [17] (the relative degree of the system is equal to the degree of the system).

In this chapter we consider the problem of indirect adaptive control of a single-link flexible manipulator. First the discrete-time model of the manipulator is derived.

The unknown payload is identified by using a new regressor form of the system dynamics and the *multi-output recursive-least-square (RLS)* algorithm. The input-output adaptive feedback linearization scheme proposed in Chapter 3 and [69] is applied to the re-defined output so that the map between the hub and the new output is made minimum phase and stable. The stability of the adaptively controlled closed-loop system is shown by using the Lyapunov analysis and by taking into account both the internal and the zero dynamics of the system.

4.2 Continuous-Time Model of a Single-Link Flexible Manipulator

Consider the dynamic equation of a single-link flexible manipulator shown in Figure 4.1 derived by using assumed modes formulation along with the Lagrangian method (cf. Appendix C)

$$M(\boldsymbol{\delta})\begin{bmatrix} \ddot{q} \\ \ddot{\boldsymbol{\delta}} \end{bmatrix} + \begin{bmatrix} h_1(\dot{q},\boldsymbol{\delta},\dot{\boldsymbol{\delta}}) + Fri(\dot{q}) \\ \mathbf{h}_2(\dot{q},\boldsymbol{\delta}) \end{bmatrix} + \begin{bmatrix} 0 & 0 \\ 0 & \mathbf{k}_2 \end{bmatrix}\begin{bmatrix} q \\ \boldsymbol{\delta} \end{bmatrix} + \begin{bmatrix} D_1 & 0 \\ 0 & \mathbf{D}_2 \end{bmatrix}\begin{bmatrix} \dot{q} \\ \dot{\boldsymbol{\delta}} \end{bmatrix} = \begin{bmatrix} \tau(t) \\ \mathbf{0} \end{bmatrix} \tag{4.1}$$

where $q \in \Re$ is the joint (hub) angle, $\boldsymbol{\delta} = [\delta_1 \quad \delta_2 \quad \dots \quad \delta_m]^T \in \Re^m$ is the vector of flexible modes, M represents the inertia matrix, $h \triangleq [h_1 \quad \mathbf{h}_2^T]^T$ represents the Coriolis and centrifugal forces, $Fri(\dot{q})$ is the Coulomb friction, $D \triangleq \begin{bmatrix} D_1 & 0 \\ 0 & \mathbf{D}_2 \end{bmatrix} \in \Re^{(m+1)\times(m+1)}$ represents the viscous and structural damping matrix, $\mathbf{k} \triangleq \begin{bmatrix} 0 & 0 \\ 0 & \mathbf{k}_2 \end{bmatrix} \in \Re^{(m+1)\times(m+1)}$ represents the stiffness matrix and $u(t) \triangleq \tau(t)$ is the input torque. Note that integer m represents the number of flexible modes or

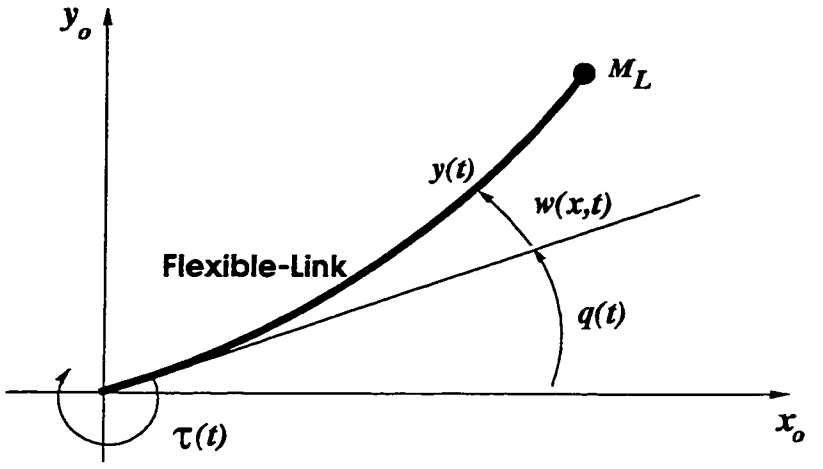

Figure 4.1: Single Link Flexible Manipulator

equivalently the number of mode shape functions considered in the model.

To obtain the state space representation of (4.1), the state vector is first defined as $x(t) \triangleq [X_1^T(t) \;\; X_2^T(t)]^T$ where

$$X_1(t) \triangleq [x_1(t) \;\; x_3(t) \;\cdots\; x_{2m+1}(t)]^T = [q \;\; \boldsymbol{\delta}^T]^T = [q \;\; \delta_1 \;\cdots\; \delta_m]^T$$
$$X_2(t) \triangleq [x_2(t) \;\; x_4(t) \;\cdots\; x_{2m+2}(t)]^T = [\dot{q} \;\; \dot{\boldsymbol{\delta}}^T]^T = [\dot{q} \;\; \dot{\delta}_1 \;\cdots\; \dot{\delta}_m]^T$$

Therefore, equation (4.1) may be written as

$$\begin{bmatrix} \dot{X}_1 \\ \dot{X}_2 \end{bmatrix} = \begin{bmatrix} X_2 \\ -M^{-1}F_1(x) + M^{-1}F_2u(t) \end{bmatrix} = \begin{bmatrix} X_2 \\ L(x,u) \end{bmatrix} \tag{4.2}$$

where $F_2 \triangleq [1 \;\; \mathbf{0}]^T$ and

$$F_1(x) \triangleq \begin{bmatrix} h_1 + Fri(\dot{q}) + D_1\dot{q} \\ \mathbf{h}_2 + \mathbf{k}_2\boldsymbol{\delta} + \mathbf{D}_2\dot{\boldsymbol{\delta}} \end{bmatrix} = [h(x) + \mathbf{k}X_1(t) + DX_2(t)]$$
$$L(x,u) \triangleq -M^{-1}F_1(x) + M^{-1}F_2u(t) \tag{4.3}$$

Following [49] and assuming that the beam deflection $w(x,t)$ is small compared to the link length L, the normalized output may be written as $q + \frac{w(L,t)}{L}$ with

$w(x,t) \triangleq \sum_{i=1}^{m} \alpha_i \phi_i(L)\delta_i$ where $\phi_i(L)$ represents the i^{th} mode shape and α_i represents a constant. Note that by changing α_i from -1 to 0 to 1, the normalized output will change from the normalized reflected tip position to the joint angle to the normalized tip position, respectively. Therefore, for the normalized tip position denoted by $y_t(t)$ it is set to $\alpha_i = 1$ and for the normalized re-defined output denoted by $y(t)$ it is set to $\alpha_i \neq 1$. Therefore, $y_t(t)$ and $y(t)$ are given by

$$\begin{aligned} y_t(t) &= q + \frac{1}{L}\sum_{i=1}^{m} \phi_i(L)\delta_i \\ y(t) &= q + \frac{1}{L}\sum_{i=1}^{m} \alpha_i\phi_i(L)\delta_i \triangleq \beta X_1(t) \end{aligned} \tag{4.4}$$

where row vectors $\beta \triangleq [1\ \beta_1]$ and $\beta_1 = [\beta_1\ \cdots\ \beta_m]$ with $\beta_i(L) \triangleq \frac{\alpha_i\phi_i(L)}{L}$. In the next section we will obtain the discrete-time model of (4.2).

4.3 Discrete-Time Model of a Single-Link Flexible Manipulator

A suitable discretization scheme for the nonlinear continuous-time system (4.2) is now developed. While there are several methods available to obtain the discrete-time equivalence of a linear continuous-time system, most of these techniques cannot be used directly for nonlinear systems. The step-invariance, impulse-invariance and pole-zero mapping methods are not applicable since $\mathcal{Z}$-transform cannot be used for nonlinear systems. Also, by using the bilinear transformation the affine structure of (4.2)-(4.3) will be lost. By using the backward difference a solution to a set of nonlinear transcendental equations is needed where, in general, the existence and uniqueness of the solution is very difficult to guarantee. As a result, the only viable choice would seem to be the forward difference method (Euler approximation). This method also was used by Nicosia *at al.* [58] but the discrete-time model is too complex and is not suitable for adaptive feedback linearization. Also it will be

shown that due to the special structure of the continuous-time model (4.2),namely due to the fact that the first $m+1$ states are linear, it is then possible to find another discretization model. Incidentally the Euler method has also been applied successfully to rigid robot manipulators Ganguly *et al.*[17]. Note that the relative degree of a rigid robot model is equal to the order of the system and the system has no internal dynamics. Therefore, results in [17] are straight forward application of feedback linearization scheme. The forward difference method approximates the derivative of $x(t)$ at instant $t = kT$ by

$$\dot{x}(kT) = \frac{1}{T}[(x(kT+T) - x(kT)]$$

where T is the sampling period of the discretization process. Using the above relationship the discrete-time equivalence of (4.2) is given by

$$\sum_1 : \quad \begin{bmatrix} X_1(k+1) \\ X_2(k+1) \end{bmatrix} = \begin{bmatrix} X_1(k) + TX_2(k) \\ X_2(k) + TL(x,u) \end{bmatrix} \tag{4.5}$$

where $X_i(k+1) \triangleq X_i(kT+T)$ and $X_i(k) \triangleq X_i(kT)$ for $i = 1, 2$.

To find the other discretization model, equation (4.3) may be first rewritten as $\dot{x} = Ax + B(x,u)$ where

$$A \triangleq \begin{bmatrix} 0 & I \\ 0 & 0 \end{bmatrix}, \quad B \triangleq \begin{bmatrix} 0 \\ L(x,u) \end{bmatrix} \tag{4.6}$$

and I is the identity matrix of dimension $m \times m$. A new method is now developed that uses both the step-invariance and the forward difference methods. Therefore, let us assume that the input $u(t)$ is constant over two consecutive sampling instants and that the input changes only at sampling instants, that is $u(t) = u(kT)$, $kT \leq t < (K+1)T$. Moreover, similar to the forward difference method it is assumed that the vector $B(x(t), u(t))$ is equal to $B(kT) \triangleq B(x(kT), u(kT))$ for $kT \leq t < (K+1)T$. Therefore, the discrete-time model of (4.3) becomes

$$x(k+1) = e^{AT}x(k) + \int_0^T e^{A(T-\tau)}d\tau B(kT) \tag{4.7}$$

Substituting now (4.6) into (4.7) and doing some algebraic manipulations give the following discrete-time model,

$$\sum_2 : \begin{bmatrix} X_1(k+1) \\ X_2(k+1) \end{bmatrix} = \begin{bmatrix} I & TI \\ 0 & I \end{bmatrix} \begin{bmatrix} X_1(k) \\ X_2(k) \end{bmatrix} + \begin{bmatrix} TI & \frac{T^2}{2}I \\ 0 & TI \end{bmatrix} \begin{bmatrix} 0 \\ L(x,u) \end{bmatrix}$$
$$= \begin{bmatrix} X_1(k) + TX_2(k) + \frac{1}{2}T^2L(x,u) \\ X_2(k) + TL(x,u) \end{bmatrix} \tag{4.8}$$

Comparing (4.5) with (4.8) reveals that both equations are almost the same except that (4.8) has an extra term in its first row. Note that the model above may be obtained directly by using the Taylors series expansion of the vector $x(t+T)$ about $t = kT$ that is

$$x(k+1) \triangleq x(kT+T) = x(kT) + \sum_{i=1}^{\infty} \frac{T^i}{i!} x^{(i)}(kT)$$

where $x^{(i)}(kT)$ stands for the i-th derivative of the state vector $x(t)$ computed at time $t = kT$. As a result, the model (4.8) can be obtained when the Taylors series expansion of $X_1(k+1)$ is truncated at $i = 2$ and that of $X_2(k+1)$ is truncated at $i = 1$. In the following section the non-adaptive and adaptive feedback linearization of (4.5) and (4.8) are considered.

4.4 Non-Adaptive Feedback Linearization and Tracking Control Problem

In this section, using the input-output linearization scheme discussed in Chapter 3 the tracking control problem for the discrete-time model (4.5) and (4.8) is considered. It is well-known that the model of a single-link flexible manipulator with a non-collocated sensor and actuator exhibits a non-minimum phase behavior (Wang & Vidyasagar [83]). This property, in general, hinders perfect tracking of the desired tip position when a bounded and a causal input is used. To achieve a minimum phase

property, namely to have an exponentially stable zero dynamics, one may utilize the output re-definition described in De Luca & Lanari [13], Madhavan & Singh [49] and Wang & Vidyasagar [83] or use the transmission zero assignment method discussed in Geniel *et al.* [19] and Patel & Misra [61] . For example, the authors in [83] proposed the reflected tip position as the new output for a single-link manipulator expressed in the continuous-time domain. However, it is not clear that this method is also applicable to discrete-time models of the flexible-link manipulator. In the following we will investigate the applicability of the reflected tip (or in general an output re-definition) strategy to the discrete-time model of a flexible-link manipulator.

4.4.1 $\sum_1$ Discrete-Time Model

Consider the discrete-time system (4.4)-(4.5) where the row vector $\beta = [1\ \beta_1\ \cdots\ \beta_m]$ is assumed to be unknown. The problem of output re-definition is to select the vector β such that the associated zero dynamics of the system are exponentially stable around $x = 0$.

Towards this end, let us first perform the input-output linearization of system (4.4)-(4.5) where one would find the successive advances of the re-defined output $y(k)$ until the input $u(k)$ appears explicitly. For our system

$$y(k+2) = A(x) + B(x)u(k) \tag{4.9}$$

is the first output affected by the input where

$$\begin{aligned} A(x(k)) &\triangleq \beta[X_1(k) + 2TX_2(k) - T^2M^{-1}F_1(x)] \\ B(x(k)) &\triangleq T^2\beta M^{-1}F_2 \end{aligned} \tag{4.10}$$

Therefore, the "relative degree"of system (4.5) with respect to output (4.4) is $\gamma = 2$. Consequently, if T and vector β are selected such that $B(x) \neq 0$, by using $u(k) = \frac{v(k)-A(x)}{B(x)}$ as the control and $v(k)$ as a new input, then the input-output linearized

model becomes $y(k+2) = v(k)$. To make the re-defined output $y(k)$ track a reference trajectory $y_m(k)$, the new input $v(k)$ is selected as

$$v(k) = y_m(k+2) + \alpha_1(y_m(k+1) - y(k+1)) + \alpha_2(y_m(k) - y(k)) \qquad (4.11)$$

where α_1 and α_2 are selected such that the polynomial $\mathcal{Z}^2 + \alpha_1\mathcal{Z} + \alpha_2$ is Hurwitz. Consequently, the re-defined output tracking error $e_1(k) \triangleq y(k) - y_m(k)$ may approach to zero as $k \to \infty$ provided that the internal dynamics are stable.

To derive the zero dynamics of system (4.4)-(4.5) observe that $y(k)$ and $y(k+1)$ are independent of input, hence the first two new coordinates $z_1(k)$ and $z_2(k)$ of the state-space coordinate transformation may be selected as

$$\begin{aligned} z_1(k) &\triangleq y(k) = \beta X_1(k) \\ z_2(k) &\triangleq y(k+1) = \beta[X_1(k) + TX_2(k)] \end{aligned} \qquad (4.12)$$

Also, since the relative degree ($\gamma = 2$) is less than the number of states ($n = 2m+2$), one may conclude that $n - \gamma = 2m$ modes are unobservable from the output. Therefore, to construct the full coordinate transformation, $2m(= n - \gamma)$ additional coordinates $\eta_i(k)$, $1 \leq i \leq 2m$ are to be found. This is to be accomplished by ensuring that the map $z = \boldsymbol{\Phi}(x) = [\xi(k) \;\; \eta(k)]^T$ is a diffeomorphism where

$$\xi(k) \triangleq [z_1(k) \;\; z_2(k)]\,, \;\; \eta(k) \triangleq [\boldsymbol{\eta}_1^T(k) \;\; \boldsymbol{\eta}_2^T(k)]^T$$

with $\boldsymbol{\eta}_1^T(k) \triangleq [\eta_1(k) \; \ldots \; \eta_m(k)]^T$ and $\boldsymbol{\eta}_2^T(k) \triangleq [\eta_{m+1}(k) \; \ldots \; \eta_{2m}(k)]^T$. The choice of the states $\eta(k)$ are at our disposal as long as the Jacobian matrix of $\boldsymbol{\Phi}(x)$ is full rank. Furthermore, to ensure that the zero dynamics of the adaptive system do not depend explicitly on the unknown parameter the states $\eta(k)$ are selected as follows

$$\boldsymbol{\eta}_1^T(k) = \Gamma X_1(k)\,, \;\; \boldsymbol{\eta}_2^T(k) = JX_2(k)$$

where $\Gamma \triangleq [0_{m\times 1}\ I_{m\times m}]$, $J \triangleq [J_{1(m\times 1)}\ J_{2(m\times m)}]$ and

$$J_1 \triangleq \begin{bmatrix} -c_1 \\ 0 \\ \vdots \\ 0 \end{bmatrix}, \quad J_2 \triangleq \begin{bmatrix} 1 & 0 & \cdots & 0 & 0 \\ -c_2 & 1 & \cdots & 0 & 0 \\ \vdots & \vdots & \vdots & \vdots & \vdots \\ 0 & 0 & \cdots & -c_m & 1 \end{bmatrix} \tag{4.13}$$

with $c_i \triangleq \frac{g_{i+1}}{g_i}$, $i = 1, 2, \cdots, m$ and g_i's are found from $M^{-1}F_2 \triangleq \frac{1}{\Delta}[g_1\ g_2\ \cdots\ g_{m+1}]^T$ (Δ is the determinant of the inertia matrix). As a result, the state transformation $\boldsymbol{\Phi}(x)$ now becomes

$$\boldsymbol{\Phi}(x) = \begin{bmatrix} z_1(k) \\ \boldsymbol{\eta}_1^T(k) \\ z_2(k) \\ \boldsymbol{\eta}_2^T(k) \end{bmatrix} = \begin{bmatrix} 1 & \boldsymbol{\beta}_1 & 0 & 0 \\ 0 & I_m & 0 & 0 \\ 1 & \boldsymbol{\beta}_1 & T & T\boldsymbol{\beta}_1 \\ 0 & 0 & J_1 & J_2 \end{bmatrix} \begin{bmatrix} X_1(k) \\ X_2(k) \end{bmatrix} \tag{4.14}$$

It can be shown that the map $\boldsymbol{\Phi}(x)$ is a diffeomorphism provided that $T \neq 0$ and $det(J_2 - J_1\boldsymbol{\beta}_1) \neq 0$ which is equivalent to $\beta\mathbf{G} \neq 0$ where $\mathbf{G} \triangleq [g_1\ g_2\ \cdots\ g_{m+1}]^T$. (Note that $X_1(k) = [q\ \ \boldsymbol{\delta}^T]^T$ and $X_2(k) = [\dot{q}\ \ \dot{\boldsymbol{\delta}}^T]^T$). Consequently, the internal dynamics are governed by

$$\begin{aligned} \boldsymbol{\eta}_1(k+1) &= \Gamma X_1(k+1) = \boldsymbol{\eta}_1(k) + T\Gamma X_2(k) \\ \boldsymbol{\eta}_1(k+1) &= JX_2(k+1) = \boldsymbol{\eta}_2(k) + TJL(x,u) \end{aligned} \tag{4.15}$$

The state transformation (4.14) will transform the discrete-time system (4.5) with the re-defined output (4.4) into

$$\begin{aligned} \begin{bmatrix} z_1(k+1) \\ z_2(k+1) \\ \boldsymbol{\eta}_1(k+1) \\ \boldsymbol{\eta}_2(k+1) \end{bmatrix} &= \begin{bmatrix} z_2(k) \\ A(x(k)) + B(x(k))u(k) \\ \boldsymbol{\eta}_1(k) + T\Gamma X_2(k) \\ \boldsymbol{\eta}_2(k) + TJL(x,u) \end{bmatrix} \\ y(k) &= z_1(k) \end{aligned} \tag{4.16}$$

To find the zero dynamics of (4.16) we need to find the inverse of the diffeomorphism, i.e. $\boldsymbol{\Phi}^{-1}(\xi,\eta)$ when the states $z_1(k)$ and $z_2(k)$ are identically set to zero for all time, namely, $\boldsymbol{\Phi}^{-1}(0,\eta)$. This results in

$$\begin{aligned} X_1(k) &= \Lambda_1 \boldsymbol{\eta}_1(k) \\ X_2(k) &= \Lambda_1 \Lambda_2 \boldsymbol{\eta}_2(k) \end{aligned} \tag{4.17}$$

where $\Lambda_1(\beta) \triangleq \begin{bmatrix} -\boldsymbol{\beta}_1 \\ I_m \end{bmatrix}$ and $\Lambda_2(\beta, M_L) \triangleq (J_2 - J_1\boldsymbol{\beta}_1)^{-1}$. Therefore, substituting (4.17) into (4.15) and using the definition of $L(x,u)$ given in (4.3) yields the zero dynamics

$$\begin{aligned} \boldsymbol{\eta}_1(k+1) &= \boldsymbol{\eta}_1(k) + T\Gamma\Lambda_1\Lambda_2\boldsymbol{\eta}_2(k) \\ \boldsymbol{\eta}_2(k+1) &= \boldsymbol{\eta}_2(k) - TJM^{-1}F_1(x) + TJM^{-1}F_2u(k) \\ &= \boldsymbol{\eta}_2(k) - TJM^{-1}F_1(x) \end{aligned} \tag{4.18}$$

Note that (4.18) does not depend on input $u(k)$ since $JM^{-1}F_2 \equiv 0$ because of selection of J. Since the zero dynamics are a nonlinear system, therefore to guarantee a locally exponentially stable zero dynamics at origin, the linearized model of (4.18) is first obtained [36]

$$\begin{aligned} \boldsymbol{\eta}_1(k+1) &= \boldsymbol{\eta}_1(k) + T\Lambda_2\boldsymbol{\eta}_2(k) \\ \boldsymbol{\eta}_2(k+1) &= \boldsymbol{\eta}_2(k) - T[Q_2\mathbf{k}_2\boldsymbol{\eta}_1(k) + (Q_2\mathbf{D}_2 - Q_1\boldsymbol{\beta}_1)\Lambda_2\boldsymbol{\eta}_2(k)] \end{aligned} \tag{4.19}$$

where scalar $Q_1(\beta, M_L) \triangleq T(J_1H_{11} + J_2H_{21})(D_1 + c_{fri})$ and matrix $Q_2(\beta, M_L) \triangleq T(J_1H_{12} + J_2H_{22})$ and matrices H_{11}, H_{12}, H_{21} and H_{22} are linearized about $x = 0$ and $c_{fri}\dot{q}$ is the linearized model of the Coulomb friction $Fri(\dot{q})$ used in (4.1). The objective is to choose the re-defined output such that the linearized zero dynamics given by (4.19), and written in the compact form $\eta(k+1) \triangleq E\eta(k)$, is locally exponentially stable. In other words, a vector β and sampling period T should be

found such that the matrix E is made Hurwitz, where

$$E(\beta, M_L) \triangleq \begin{bmatrix} I_m & T\Lambda_2 \\ -Q_2\mathbf{k}_2 & I_m + Q_0\Lambda_2 \end{bmatrix}_{2m\times 2m} \tag{4.20}$$

and $Q_0 \triangleq Q_1\boldsymbol{\beta}_1 - Q_2\mathbf{D}_2$.

4.4.2 $\sum_2$ Discrete-Time Model

The input-output linearization for system (4.8) with output (4.4) is impossible to accomplish due to the fact that the linearized model of system (4.8) associated with output (4.4) has a marginally stable zero dynamics for all values of β (the model has a pole at $\mathcal{Z} = -1$). Consequently, to get around this difficulty one should define a different output so that the minimum phase property can be ensured. To find this new output we need to use the following proposition:

Proposition 4.1 *(Bartbot et al.)[1]*
Given the following continuous-time dynamical system of relative degree γ described in normal form

$$\begin{aligned} \dot{x}_{a,i} &= x_{a,i+1}\ , \quad 1 \le i \le \gamma - 1 \\ \dot{x}_\gamma &= b(x_a, x_b) + a(x_a, x_b)u \\ \dot{x}_b &= Q(x_a, x_b) \\ y &= x_{a1} \end{aligned}$$

Then, there exists a modified output $y_n(t)$ as $y_n(t) = \sum_{i=1}^{\gamma} = c^T x_a$ with respect to which the relative degree of discrete-time system is equal to γ where $x_a \triangleq [x_{a1}\ x_{a2}\ \cdots\ x_{a\gamma}]^T$ is the vector of the observable states of the continuous-time system and $c_T \triangleq [c_1\ \ c_2\ \cdots\ c_\gamma]^T$ where $c_i \in \Re$.

Using the above proposition we will now show that the re-defined output for system (4.8) should have the form

$$y_n(k) = \sum_{i=1}^{2m+2} a_i x_i(k) \triangleq \begin{bmatrix} \boldsymbol{a}_1 & \boldsymbol{a}_2 \end{bmatrix} \begin{bmatrix} X_1(k) \\ X_2(k) \end{bmatrix} \tag{4.21}$$

where m is the number of flexible modes and $X_1(k) \triangleq [x_1(k) \;\; x_3(k) \;\cdots\; x_{2m+1}(k)]^T$ and $X_2(k) \triangleq [x_2(k) \;\; x_4(k) \;\cdots\; x_{2m+2}(k)]^T$. Also $\boldsymbol{a}_1 \triangleq [a_1 \;\; a_3 \;\ldots\; a_{2m+1}]^T \in \Re^{m+1}$ and $\boldsymbol{a}_2 \triangleq [a_2 \;\; a_4 \;\ldots\; a_{2m+2}]^T \in \Re^{m+1}$ should be obtained such that the relative degree of system (4.8) associated with output (4.4) is γ and the corresponding zero dynamics are exponentially stable.

To show that (4.21) is the suitable output note that to find the normal form of (4.2)-(4.4) one takes the successive derivatives of the output until the input $u(k)$ appears. In this case the first and second derivatives of $y(t) = \beta X_1(t)$ are $\dot{y}(t) = \beta X_2(t)$ and $\ddot{y}(t) = \beta \dot{X}_2(t) = \beta L(x,u)$, respectively. As a result, the relative degree of the continuous-time system is $\gamma = 2$ and the observable states of the continuous-time system are $x_{a1} = y(t)$ and $x_{a2} = \dot{y}(t)$. According to the proposition, the new output of the discrete-time system (4.8) should be a linear combination of $y(t)$ and $\dot{y}(t)$, or equivalently $X_1(t)$ and $X_2(t)$. This confirms the choice of the new output given by (4.21).

To find the unknown coefficients a_i, $i = 1, ..., 2m+2$, the relative degree of system (4.8) associated with the output (4.21) is matched with that of the continuous-time system (4.2) associated with the output (4.4). Therefore, calculating $y_n(k+1)$ gives

$$y_n(k+1) = \begin{bmatrix} \boldsymbol{a}_1 & \boldsymbol{a}_2 \end{bmatrix} \begin{bmatrix} X_1(k+1) \\ X_2(k+1) \end{bmatrix} = [\boldsymbol{a}_1 \;\; \boldsymbol{a}_2] \begin{bmatrix} X_1(k) + TX_2(k) + \frac{T^2}{2} L(x,u) \\ X_2(k) + TL(x,u) \end{bmatrix} \tag{4.22}$$

If we set $\boldsymbol{a}_2 = -\frac{T}{2}\boldsymbol{a}_1$, then (4.22) becomes $y_n(k+1) = \left[\begin{array}{cc} \boldsymbol{a}_1 & \frac{T}{2}\boldsymbol{a}_1 \end{array}\right] x(k)$ which becomes input independent. Thus, computing $y_n(k+2)$ gives

$$y_n(k+2) = \left[\begin{array}{cc} \boldsymbol{a}_1 & \frac{T}{2}\boldsymbol{a}_1 \end{array}\right] \left[\begin{array}{c} X_1(k) + TX_2(k) + \frac{T^2}{2}L(x,u) \\ X_2(k) + TL(x,u) \end{array}\right] \triangleq A_n(x) + B_n(x)u(k) \tag{4.23}$$

where $A_n(x)$ and $B_n(x)$ are given by

$$A_n(x) \triangleq \boldsymbol{a}_1[X_1(k) + \frac{3T}{2}X_2(k) - T^2M^{-1}F_1(x)] \quad , \quad B_n(x) \triangleq T^2\boldsymbol{a}_1M^{-1}F_2 \tag{4.24}$$

Therefore, the relative degree of system (4.8) with respect to the new output (4.21) is 2 and consequently, the dimension of the unobservable states (internal dynamics) is $2m(=n-\gamma)$. Now the first two new coordinates $z_{n1}(k)$ and $z_{n2}(k)$ may be selected as

$$\begin{aligned} z_{n1}(k) &\triangleq y_n(k) = \boldsymbol{a}_1X_1(k) - \frac{\mathrm{T}}{2}\boldsymbol{a}_1X_2(k) \\ z_{n2}(k) &\triangleq y_n(k+1) = \boldsymbol{a}_1X_1(k) + \frac{\mathrm{T}}{2}\boldsymbol{a}_1X_2(k) \end{aligned} \tag{4.25}$$

and the other $2m$ new coordinates may be chosen as before as $\boldsymbol{\eta}_{n1}(k) = \Gamma X_1(k)$ and $\boldsymbol{\eta}_{n2}(k) = JX_2(k)$ where $\Gamma \triangleq [0_{m\times 1}\ I_{m\times m}]$, $J \triangleq [J_{1(m\times 1)}\ J_{2(m\times m)}]$ and J_1 and J_2 are defined in (4.13). Therefore, the resulting internal dynamics become

$$\begin{aligned} \boldsymbol{\eta}_{n1}(k+1) &= \Gamma X_1(\boldsymbol{k}+1) = \boldsymbol{\eta}_{n1}(k) + T\Gamma X_2(k) \\ \boldsymbol{\eta}_{n2}(k+1) &= JX_2(\boldsymbol{k}+1) = \boldsymbol{\eta}_{n2}(k) + TJL(x,u) \end{aligned} \tag{4.26}$$

To summarize, if $\boldsymbol{a}_1$ is defined as $[\boldsymbol{\beta}_2\ \ \boldsymbol{\beta}_1]$, the coordinate transformation becomes

$$\left[\begin{array}{c} z_{n1}(k) \\ \boldsymbol{\eta}_{n1}(k) \\ z_{n2}(k) \\ \boldsymbol{\eta}_{n2}(k) \end{array}\right] = \left[\begin{array}{cccc} \boldsymbol{\beta}_2 & \boldsymbol{\beta}_1 & -\frac{T}{2}\boldsymbol{\beta}_2 & -\frac{T}{2}\boldsymbol{\beta}_1 \\ 0 & I & 0 & 0 \\ \boldsymbol{\beta}_2 & \boldsymbol{\beta}_1 & \frac{T}{2}\boldsymbol{\beta}_2 & \frac{T}{2}\boldsymbol{\beta}_1 \\ 0 & 0 & J_1 & J_2 \end{array}\right] \left[\begin{array}{c} X_1(k) \\ X_2(k) \end{array}\right] \tag{4.27}$$

which is a global diffeomorphism if $T \neq 0$, $\boldsymbol{\beta}_2 \neq 0$ and $det(\boldsymbol{\beta}_2 J_2 - J_1 \boldsymbol{\beta}_1) \neq 0$. Also the internal dynamics take the form

$$\begin{aligned} \boldsymbol{\eta}_{n1}(k+1) &= \Gamma X_1(k+1) = \boldsymbol{\eta}_{n1}(k) + T\Gamma X_2(k) \\ \boldsymbol{\eta}_{n2}(k+1) &= \Gamma X_2(k+1) = \boldsymbol{\eta}_{n2}(k) + TJL(x,u) \end{aligned} \tag{4.28}$$

To find the zero dynamics, first the inverse of diffeomorphism (4.28) when $z_{n1}(k) = z_{2n}(k) = 0$ should be found. After doing some algebraic manipulation one gets,

$$\begin{aligned} X_1(k) &= \Lambda_{n1}\boldsymbol{\eta}_{n1}(k) + \frac{T}{2}\boldsymbol{\beta}_2\Lambda_{n1}\Lambda_{n2}\boldsymbol{\eta}_{n2}(k) \\ X_2(k) &= \Lambda_{n1}\Lambda_{n2}\boldsymbol{\eta}_{n2}(k) \end{aligned} \tag{4.29}$$

where $\Lambda_{n1} \triangleq \begin{bmatrix} -\boldsymbol{\beta}_1 \\ \boldsymbol{\beta}_2 I_m \end{bmatrix}$ and $\Lambda_{n2} \triangleq (\boldsymbol{\beta}_2 J_2 - J_1\boldsymbol{\beta}_1)^{-1}$. Therefore, substituting (4.29) into (4.28) yields the zero dynamics as

$$\begin{aligned} \boldsymbol{\eta}_{n1}(k+1) &= \boldsymbol{\eta}_{n1}(k) + T\Gamma\Lambda_{n1}\Lambda_{n2}\boldsymbol{\eta}_{n2}(k) \\ \boldsymbol{\eta}_{n2}(k+1) &= \boldsymbol{\eta}_{n2}(k) + TJ\left[-M^{-1}F_1(x) + M^{-1}F_2u(k)\right] \\ &= \boldsymbol{\eta}_{n2}(k) - TJM^{-1}F_1(x) \end{aligned} \tag{4.30}$$

Now using $M^{-1}|x=0 \triangleq \begin{bmatrix} H_{11} & H_{12} \\ H_{21} & H_{22} \end{bmatrix}$, $Q_1 \triangleq T(J_1H_{11} + J_2H_{21})(c_{fri} + D_1)$ and $Q_2 \triangleq T(J_1H_{12} + J_2H_{22})$ where $c_{fri}\dot{q}$ is the linearized model of the Coulomb friction $Fri(\dot{q})$, the linearized model of the nonlinear zero dynamics (4.30) becomes

$$\begin{aligned} \boldsymbol{\eta}_{n1}(k+1) &= \boldsymbol{\eta}_{n1}(k) + T\boldsymbol{\beta}_2\Lambda_{n2}\boldsymbol{\eta}_{n2}(k) \\ \boldsymbol{\eta}_{n2}(k+1) &= \boldsymbol{\eta}_{n2}(k) - [Q_2\boldsymbol{k}_2\boldsymbol{\eta}_{n1}(k) + Q_0\Lambda_{n2}\boldsymbol{\eta}_{n2}(k)] \end{aligned} \tag{4.31}$$

where matrix $Q_0 \triangleq -Q_2\boldsymbol{\beta}_2(\boldsymbol{D}_2 + \frac{T}{2}\boldsymbol{k}_2) + Q_1\boldsymbol{\beta}_1$. Hence, the output should be re-defined such that the linearized model of the zero dynamics given by (4.31) and written in the compact form $\eta_n(k+1) \triangleq E_n\eta_n(k)$ is exponentially stable. In other words, a vector β should be found to make the matrix E_n Hurwitz, where

$$E_n(\beta, M_L) = \begin{bmatrix} I & T\boldsymbol{\beta}_2\Lambda_{n2} \\ -Q_2\boldsymbol{k}_2 & I - Q_0\Lambda_{n2} \end{bmatrix}_{2m\times 2m} \tag{4.32}$$

Comparing (4.32) with (4.20) reveals that both matrices have the same structure. However in this case we have more parameters to play with to make E_n a Hurwitz matrix. Since the effect of viscous and structural damping is very important to make E_n Hurwitz, in this case it is increased to $\boldsymbol{D}_2 + \frac{T}{2}\boldsymbol{k}_2$. Now suppose that the payload mass is unknown but its upper bound is known *a priori*. The objective is to find $\boldsymbol{\beta}_1$, $\boldsymbol{\beta}_2$ and T given uncertainty in M_L so that matrix E or E_n is Hurwitz. This in turn would characterize the re-defined output.

4.5 Adaptive Feedback Linearization and Tracking Control Problem

In this section, using the scheme proposed in Chapter 3, the indirect adaptive feedback linearization and tracking control problem for a single-link flexible manipulator with an unknown payload mass M_L is considered. The first step is to identify the unknown parameter M_L with expressing it in the regressor form $Y(k+1) = \Psi^T(k)\theta$ where $Y(k+1)$, $\Psi^T(k)$ and θ represent the measurement vector, the regressor vector and the unknown parameter (payload), respectively. To construct the above regressor equation note that the second row of (4.2) may be expressed as

$$M\dot{X}_2 + F_1(x) = F_2 u(k) \tag{4.33}$$

where $\dot{X}_2 = \frac{X_2(k)-X_2(k-1)}{T}$ and the inertia matrix M and vector $F_1(x)$ depend linearly on payload mass M_L. Therefore, one can rewrite inertia matrix as $M = M_1 + M_L M_2$ with known matrices M_1 and M_2 belonging to $\Re^{(m+1)\times(m+1)}$ and vector $F_1(x) = F_{11}(x) + M_L F_{12}(x)$ with known vectors $F_{11}(x)$ and $F_{12}(x)$ belonging to $\Re^{(m+1)}$. By substituting for the above M and $F_1(x)$ into (4.33), the regressor form becomes

$$\begin{aligned} Y(k+1) &\triangleq \frac{1}{T}M_1[X_2(k) - X_2(k-1)] + F_{11}(x) - F_2\hat{u}(k) \\ \Psi^T(k) &\triangleq \frac{-1}{T}M_2[X_2(k) - X_2(k-1)] - F_{12}(x) \\ \theta &\triangleq M_L \end{aligned}$$

where $Y(k+1) \in \Re^{m+1}$, $\Psi^T(k) \in \Re^{m+1}$ and $\theta \in \Re$. Note that $Y(k+1)$ contains the information about the system consisting of the states and the input up to time $k+1$. An estimate $\hat{\theta}(k)$ of the unknown vector θ may now be found so that the cost function

$$J_N(\theta) = \frac{1}{2}\sum_{k=1}^{N}[Y(k) - \Psi^T(k-1)\theta]^T R^{-1}[Y(k) - \Psi^T(k-1)\theta] + \frac{1}{2}[\theta - \hat{\theta}(0)]^T P(0)^{-1}[\theta - \hat{\theta}(0)]$$

is minimized where R and $P(0)$ are given positive definite matrices and $\hat{\theta}(0)$ is an initial estimate of θ. Following Goodwin & Sin [20], it can be shown that the $\hat{\theta}(k)$ that minimizes $J_N(\theta)$ is given by the following recursive algorithm

$$\begin{aligned}
\hat{\theta}(k) &= \hat{\theta}(k-1) + P(k-2)\Psi(k-1)X_a^{-1}(k-1)[Y(k) - \Psi^T(k-1)\hat{\theta}(k-1)] \\
P(k-1) &= P(k-2) - P(k-2)\Psi(k-1)X_a^{-1}(k)\Psi^T(k-1)P(k-2) \qquad (4.34)
\end{aligned}$$

where $X_a(k-1) \triangleq \Psi^T(k-1)P(k-2)\Psi(k-1) + R$ and $P(-1) = P(0)$. The above multi-output RLS algorithm may be shown to be stable, that is, the estimation error $\tilde{\theta}(k) \triangleq \hat{\theta}(k) - \theta$ remains bounded by using the Lyapunov function candidate of the form $V_2(\tilde{\theta}(k)) \triangleq \tilde{\theta}^T(k)P^{-1}(k-1)\tilde{\theta}(k)$. To show that the above multi-output RLS algorithm is stable and results in a bounded estimate of θ first let's substitute $Y(k) = \Psi(k-1)\theta$ into (4.34) which yields

$$\tilde{\theta}(k) = \tilde{\theta}(k-1) - P(k-2)\Psi(k-1)X_a(k-1)^{-1}\Psi(k)^T\tilde{\theta}(k-1) \qquad (4.35)$$

Our goal is to show that the algorithm above is stable, that is $\tilde{\theta}(k) \in l_\infty$. Therefore,

$$\begin{aligned}
\triangle V_2(k+1) &\triangleq V_2(\tilde{\theta}(k+1)) - V_2(\tilde{\theta}(k)) \qquad (4.36) \\
&= \tilde{\theta}^T(k+1)P^{-1}(k)\tilde{\theta}(k+1) - \tilde{\theta}^T(k)P^{-1}(k-1)\tilde{\theta}(k)
\end{aligned}$$

Using the matrix inversion lemma it can be shown that the estimation error satisfies the relationship

$$\tilde{\theta}(k) = P(k-1)P^{-1}(k-2)\tilde{\theta}(k-1) \qquad (4.37)$$

Consequently, using (4.37) in (4.36) one gets

$$\triangle V_2(k+1) = [\tilde{\theta}(k+1) - \tilde{\theta}(k)]^T P^{-1}(k-1)\tilde{\theta}^T(k) \tag{4.38}$$

Now using (4.35) in (4.38) results in

$$\triangle V_2(k+1) = -[\Psi^T(k)\tilde{\theta}(k)]^T X_a^T(k)[\Psi^T(k)\tilde{\theta}(k)] \tag{4.39}$$

Hence, given that $X_a(k) = \Psi^T(k)P(k-1)\Psi(k) + R > 0$, it then follows that $\triangle V_2(k+1)$ is negative semi-definite, and so $V_2(\tilde{\theta}(k))$ is always non-decreasing. This implies that $\tilde{\theta}(k)$ remains bounded for all time (*i.e.* $\in l_\infty$). Also, it can be shown that $\| \tilde{\theta}(k) \|^2 \leq \| \hat{\theta}(0) - \theta \|^2$.

For developing the control strategy, the certainty equivalence principle is utilized. That is, the estimate of the payload mass $\hat{\theta}(k) = \hat{M}_L(k)$ given by the multi-output RLS algorithm will be used in designing the tracking control strategy. Therefore, using (4.9)-(4.11) the adaptive control law becomes

$$\begin{aligned} \hat{u}(k) &= \frac{v(k) - \hat{A}(x)}{\hat{B}(x)} \\ v(k) &= y_m(k+2) + \alpha_1(y_m(k+1) - z_2(k)) + \alpha_2(y_m(k) - z_1(k)) \end{aligned} \tag{4.40}$$

where $\hat{A}(x) \triangleq A(x(k), \hat{M}_L(k))$ and $\hat{B}(x) \triangleq B(x(k), \hat{M}_L(k))$ are $A(x)$ and $B(x)$ defined in (4.10) with the payload replaced with its estimate, respectively. Define the re-defined error signals as

$$\begin{aligned} e_1(k) &\triangleq y(k) - y_m(k) = z_1(k) - y_m(k) \\ e_2(k) &\triangleq y(k+1) - y_m(k+1) = z_2(k) - y_m(k+1) \end{aligned} \tag{4.41}$$

By adding the term $v(k)$ -- $\hat{A}(x) - \hat{B}(x)\hat{u}(k)$ (which is zero) to $y(k+2) = A(x) + B(x)\hat{u}(k)$ one gets

$$y(k+2) = v(k) + \tau(k)$$

where by using the definitions of A and B, we have

$$\begin{aligned}\tau(k) &\triangleq [A(x) - \hat{A}(x)] + [B(x) - \hat{B}(x)]\hat{u}(k) \\ &= \beta T^2(M^{-1} - \hat{M}^{-1}(k))\Xi(x, \hat{u}(k))\end{aligned} \tag{4.42}$$

and $\Xi(x, \hat{u}(k)) \triangleq -F_1(x) + F_2\hat{u}(k)$ and $F_1(x)$ and F_2 are defined in (4.3). Therefore, by using $v(k)$ given in (4.40), the error dynamics (4.41) becomes $e_1(k+1) = e_2(k)$ and $e_2(k+1) = -\alpha_2 e_1(k) - \alpha_2 e_2(k) + \tau(k)$. Also, the internal dynamics (4.15) or (4.28) may be written in the compact form

$$\eta(k+1) = q(\xi(k), \eta(k)) \tag{4.43}$$

Consequently, the zero dynamics become

$$\eta(k+1) = q(0, \eta(k)) \triangleq q_0(\eta(k)) \tag{4.44}$$

The governing equations for the closed-loop system may now be expressed as

$$\begin{aligned}e(k+1) &= He(k) + G(x(k), \hat{u}(k), \hat{\theta}(k)) \\ \eta(k+1) &= q(\xi(k), \eta(k))\end{aligned} \tag{4.45}$$

where $e(k) \triangleq [e_1(k) \;\; e_2(k)]^T$, $H = \begin{bmatrix} 0 & 1 \\ -\alpha_2 & -\alpha_1 \end{bmatrix}$ and $G = \begin{bmatrix} 0 \\ \tau(k) \end{bmatrix}$. To complete our analysis we need the following assumptions:

Assumption 4.1 *The zero dynamics (4.44) are exponentially stable at origin by properly selecting the vector β and sampling period T so that matrix E in (4.20) is Hurwitz.*

Assumption 4.2 *The internal dynamics (4.43) are locally Lipschitz in $\xi(k) \in \Omega_1$ and $\eta(k) \in \Omega$.*

Assumption 4.3 *The reference output trajectory $y_m(k)$ and its next $n-1$ samples are all bounded by a constant b_1.*

Assumption 4.4 *$\Xi(x, \hat{u}(k))$ is locally sector bounded in $x(k)$ and $\hat{u}(k)$ for $\xi(k) \in \Omega_1$, $\eta(k) \in \Omega$ and $\hat{\theta}(k) \in \Omega_{\hat{\theta}}$.*

The following theorem summarizes the characteristics of the adaptively controlled closed-loop system:

Theorem 4.1 *Consider the nonlinear discrete-time model (4.5) of a single-link flexible manipulator (4.2) where the payload mass is assumed to be a constant parameter but unknown. The adaptively controlled closed-loop system obtained by utilizing a multi-output RLS parameter estimator (4.34), a state space coordinate transformation (4.14) or (4.27) and a nonlinear feedback control (4.40) is locally stable provided that the upper bound of payload is known a priori, Assumptions (4.1) to (4.4) are satisfied and $\hat{\theta}(k)$ is maintained in a bounded region specified in (B.18) (cf. Appendix B). Consequently, the closed-loop system has a bounded re-defined output tracking error $e_1(k)$. Moreover, the tip position tracking error $e_t(k)$ remains bounded. Also, if the parameter estimation error approaches to zero, then the re-defined output tracking error $e_1(k)$ converges locally to zero as $k \to \infty$.*

Proof : See Appendix B for the details.

4.6 Case Study

The adaptive feedback linearization and tracking control strategy developed in the previous section is now applied to a single-link flexible manipulator (which is constructed in our laboratory) using one mode shape for both modeling the flexible-link and designing the controller, i.e. $m = 1$. Referring to Appendix C the dynamic

equations of such a link are given by

$$\begin{bmatrix} \dot{x}_1 \\ \dot{x}_3 \\ \dot{x}_2 \\ \dot{x}_4 \end{bmatrix} = \begin{bmatrix} x_2 \\ x_4 \\ L_1(x,u) \\ L_2(x,u) \end{bmatrix}$$

$$\begin{aligned} y(t) &= x_1 + \beta_1 x_3 \\ y_n(t) &= a_1 x_1 + a_3 x_3 - \frac{T}{2}(a_1 x_2 + a_3 x_4) \end{aligned}$$

with $x \triangleq [x_1 \;\; x_3 \;\; x_2 \;\; x_4]^T = [q \;\; \delta \;\; \dot{q} \;\; \dot{\delta}]^T$ and

$$\begin{bmatrix} L_1(x,u) \\ L_2(x,u) \end{bmatrix} = \begin{bmatrix} m_{11} & m_{12} \\ m_{12} & m_{22} \end{bmatrix}^{-1} \begin{bmatrix} -h_1 - D_1 x_2 - Fri(x_2) + u(t) \\ -\mathbf{h}_2 - \mathbf{D}_2 x_4 - \mathbf{k}_2 x_3 \end{bmatrix}$$

where $Fri(x_2)$ is the Coulomb friction and $m_{11} = r_1 + r_2 + r_3 M_L x_3^2$, $m_{12} = p_1 + p_2 M_L$, $m_{22} = q_1 + q_2 M_L$, $h_1 = 2\phi_1^2 M_L x_2 x_3 x_4 + 2\rho A x_2 x_3 x_4$ and $\mathbf{h}_2 = -\phi_1^2 M_L x_2^2 x_3 - \rho A x_2^2 x_3$. The parameters r_1, r_2, r_3, p_1, p_2, q_1, q_2 and ϕ_1 are all assumed to be known except the payload mass M_L that is assumed to be constant but unknown. The forward difference method yields the following discrete-time model

$$\begin{bmatrix} x_1(k+1) \\ x_3(k+1) \\ x_2(k+1) \\ x_4(k+1) \end{bmatrix} = \begin{bmatrix} x_1(k) + T x_2(k) \\ x_3(k) + T x_4(k) \\ x_2(k) + T L_1(k) \\ x_4(k) + T L_2(k) \end{bmatrix}$$

$$\begin{aligned} y(k) &= x_1(k) + \beta_1 x_3(k) \\ y_n(k) &= a_1 x_1(k) + a_3 x_3(k) - \frac{T}{2}(a_1 x_2(k) + a_3 x_4(k)) \end{aligned} \qquad (4.46)$$

Due to the fact that the relative degree γ is equal to 2, the first two new coordinates $z_1(k)$ and $z_2(k)$ when $y(k)$ is taken as output are selected as

$$\begin{aligned} z_1(k) &= y(k) = x_1(k) + \beta_1 x_3(k) \\ z_2(k) &= y(k+1) = x_1(k) + \beta_1 x_3(k) + T x_2(k) + T\beta_1 x_4(k) \end{aligned}$$

Since $m = 1$, we have $\Gamma = [0 \;\; 1]$ and $J = [J_1 \;\; J_2] = [-c_1 \;\; 1]$ with $c_1 = \frac{-m_{12}}{m_{22}}$. Hence, the third and fourth new coordinates are

$$\eta_1(k) = \Gamma X_1(k) = [0 \;\; 1] \begin{bmatrix} x_1(k) \\ x_3(k) \end{bmatrix} = x_3(k)$$

$$\eta_2(k) = J X_2(k) = [-c_1 \;\; 1] \begin{bmatrix} x_2(k) \\ x_4(k) \end{bmatrix} = -c_1 x_2(k) + x_4(k)$$

The linearizing input is given by (4.40) where $\hat{A}(x)$ and $\hat{B}(x)$ are $A(x, M_L)$ and $B(x, M_L)$ with M_L replaced with $\hat{M}_L$, respectively and

$$\begin{aligned} A(x, M_L) &= x_1(k) + \beta_1 x_3(k) + 2T x_2(k) + 2T\beta_1 x_4(k) \\ &\quad -\frac{T^2}{\Delta}(m_{22} - \beta_1 m_{12})(h_1 + D_1 x_2(k) + Fri(x_2)) \\ &\quad +\frac{T^2}{\Delta}(m_{12} - \beta_1 m_{11})(\mathbf{h}_2 + \mathbf{D}_2 x_4(k) + \mathbf{k}_2 x_3(k)) \\ B(x, M_L) &= \frac{T^2}{\Delta}(m_{22} - \beta_1 m_{12}) \end{aligned}$$

where Δ is the determinant of the inertia matrix M. Using the above new coordinates and the linearizing input, the linearized model of the zero dynamics become

$$\begin{bmatrix} \eta_1(k+1) \\ \eta_2(k+1) \end{bmatrix} = \begin{bmatrix} 1 & \frac{T}{1-\frac{m_{12}}{m_{22}}\beta_1} \\ -\frac{T\mathbf{k}_2}{m_{22}} & 1 - \frac{T\mathbf{D}_2}{(1-\frac{m_{12}}{m_{22}}\beta_1)m_{22}} \end{bmatrix} \begin{bmatrix} \eta_1(k) \\ \eta_2(k) \end{bmatrix} = E\eta(k) \qquad (4.47)$$

In order to have an exponentially stable zero dynamics the linear system (4.47) should have a Hurwitz matrix E. Therefore, using the Jury's stability test the following conditions for the sampling period T and parameter β_1 are found

$$\sum_1 \;\; T < \frac{\mathbf{D}_2}{\mathbf{k}_2} \;\; , \;\; \beta_1 < \frac{m_{22}}{m_{12}} - \frac{T\mathbf{D}_2}{2m_{12}} + \frac{T^2\mathbf{k}_2}{4m_{12}} \qquad (4.48)$$

Following the same procedure, It can be shown that if $y_n(k)$ is taken as the normalized re-defined output, the linearized model of the zero dynamics become

$$\begin{bmatrix} \eta_{n1}(k+1) \\ \eta_{n2}(k+1) \end{bmatrix} = \begin{bmatrix} 1 & \frac{Ta_1}{a_1-\frac{m_{12}}{m_{22}}a_3} \\ -\frac{T\mathbf{k}_2}{m_{22}} & 1 - \frac{Ta_1(\mathbf{D}_2+\frac{T}{2}\mathbf{k}_2)}{(a_1-\frac{m_{12}}{m_{22}}a_3)m_{22}} \end{bmatrix} \begin{bmatrix} \eta_{n1}(k) \\ \eta_{n2}(k) \end{bmatrix} = E_n\eta_n(k) \qquad (4.49)$$

which by means of Jury's test, the following conditions will be found

$$\sum_2 T < \frac{2\mathbf{D_2}}{\mathbf{k_2}} \ , \ a_3 < a_1(\frac{m_{22}}{m_{12}} - \frac{T\mathbf{D_2}}{2m_{12}}) \tag{4.50}$$

To specify β_1 we first select the sampling period T such that $T < \frac{\mathbf{D_2}}{\mathbf{k_2}}$. Since $m_{12} = p_1 + p_2 M_L$ and $m_{22} = q_1 + q_2 M_L$, then (4.48) gives the proper bound for β_1 provided that a bounded interval for payload M_L is initially specified. We are now in a position to consider the adaptive tracking control problem for system (4.46) by re-writing it in the regressor form $Y(k+1) = \Psi^T(k)\theta$ where $\theta = M_L$ and

$$Y(k+1) = \begin{bmatrix} r_1 \triangle x_2(k) + p_1 \triangle x_4(k) + D_1 x_2(k) + Fri(x_2) - \hat{u}(k) \\ p_1 \triangle x_2(k) + q_1 \triangle x_4(k) + \mathbf{D_2} x_4(k) + \mathbf{k_2} x_3(k) \end{bmatrix}$$

$$\Psi^T(k) = -\begin{bmatrix} (r_2 + r_3 x_3^2(k)) \triangle x_2(k) + p_2 \triangle x_4(k) + 2\phi_1^2 x_2(k) x_3(k) x_4(k) \\ p_2 \triangle x_2(k) + q_2 \triangle x_4(k) - \phi_1^2 x_2^2(k) x_3(k) \end{bmatrix}$$

where $\triangle x_2(k) \triangleq \frac{x_2(k) - x_2(k-1)}{T} \simeq \dot{x}_2(kT)$ and $\triangle x_4(k) \triangleq \frac{x_4(k) - x_4(k-1)}{T} \simeq \dot{x}_4(kT)$. For the purpose of numerical simulations the reference output $y_m(k)$ consists of three quintic functions whose fundamental frequency is around $\frac{2\pi}{6} \simeq 1 \frac{rad}{s}$. Also the constants α_1 and α_2 are chosen such that the poles of the closed-loop feedback linearized system are located at $\lambda_1 = .45$ and $\lambda_2 = .5$.

The numerical values used in the simulations are taken from the single-flexible manipulator in our lab and are given by: link's length $L = 1.2\ m$, link's mass $m_m = 1.42\ kg$, the flexural rigidity $EI = 2.44\ Nm^2$, stiffness $\mathbf{k_2} = 17.45$, damping $D_1 = 0.59$ and $\mathbf{D_2} = 0.4$, link moment of inertia $J_0 = \frac{1}{3} m_m l^2 = 0.6797\ kgm^2$, payload moment of inertia $I_0 = 0.27\ kgm^2$ and payload mass $M_L = 0.5\ kg$. In addition, the Coulomb friction is modeled as a sigmoidal function $Fri(x_2) = 4.77[\frac{2}{1+e^{-100x_2}} - 1]$. The natural frequency of the flexible mode is at $w_1 = 3.511 \frac{rad}{s}$ and we have $r_1 = 0.9497$, $r_2 = 1.44$, $r_3 = 4.00$, $p_1 = 0.9983$, $p_2 = 2.00$, $q_1 = 1.5035$, $q_2 = 4.00$ and finally $\phi_1(L) = 2.00$.

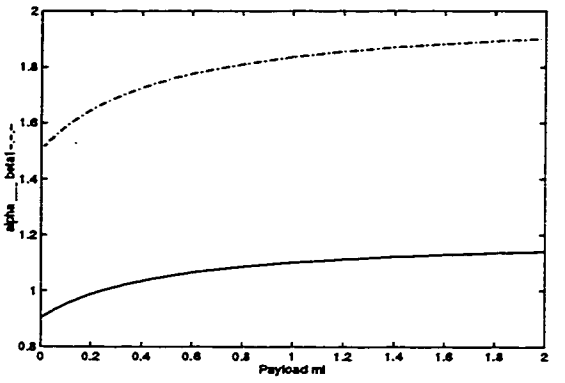

Figure 4.2: Variation of β_1, $\frac{a_3}{a_1}$ $-.-.$ and α_1 ___ with respect to payload M_L

Using the above numerical values, the conditions for the sampling period and β_1 for $\sum_1$ model yields $T < 0.0229$ and $\beta_1 < \frac{1.5035+4M_L}{0.9983+2M_L} - \frac{0.2T}{0.9983+2M_L} + \frac{4.363T^2}{0.9983+2M_L}$, respectively and for the sampling period and a_3 for $\sum_2$ model yields $T < 0.0458$ and $a_3 < a_1(\frac{1.5035+4M_L}{0.9983+2M_L} - \frac{0.2T}{0.9983+2M_L})$, respectively. The variation of β_1 and $\frac{a_3}{a_1}$ with respect to payload M_L is depicted in Figure (4.2). As this figure shows $\beta_1 < 1.51$ and $\frac{a_3}{a_1} < 1.51$ should be selected to ensure that the system is minimum-phase for all payloads. Since in this example there is no difference between $\sum_1$ and $\sum_2$, therefore $\sum_1$ is considered in the sequel.

Note that since $\beta_1 = \frac{\alpha_1\phi_1}{L}$, we get $\alpha_1 < \frac{1.51L}{\phi_1}$ or $\alpha_1 < 0.906$. Therefore, for numerical simulations we take $T = 0.01$ and $\beta_1 = 1$. Given that $L = 1.2$ and $\phi_1(L) = 2$, the constant α_1 becomes $\alpha_1 = \frac{1.2}{2} = 0.6$. Simulations are performed using the *SIMULINK* environment and Figure (4.3) shows the block diagram of the simulated system.

Figure (4.4) shows the results for the normalized value of the reference trajectory $ym = y_m(k)$, the normalized re-defined output $y = y(k)$ and the normalized tip position $yt = y_t(k)$, the tracking errors for the normalized re-defined output $e = y(k) - y_m(k)$ and for the normalized tip position $et = y_t(k) - y_m(k)$, the internal

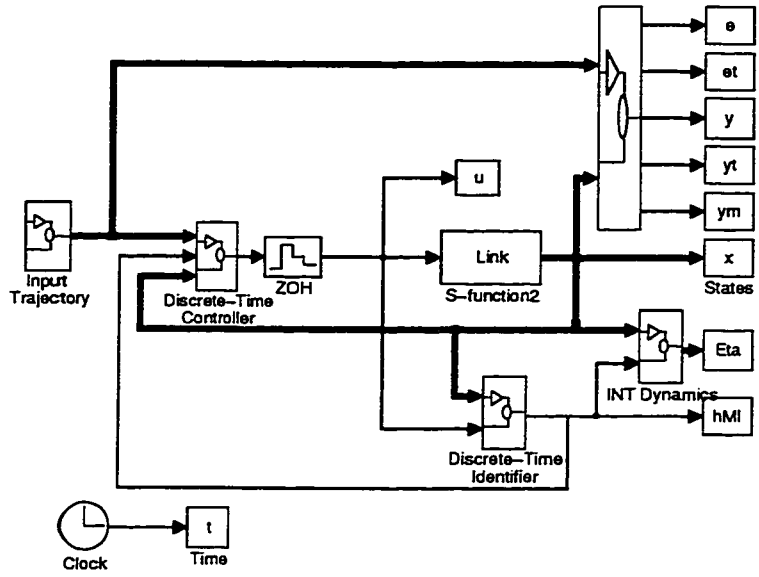

Figure 4.3: Block diagram of an adaptive tracking control of a single-link flexible manipulator using SIMULINK when the discrete-time controller is applied to a ZOH followed by the continuous-time model

dynamics $Eta1 = \eta_1(k)$ and $Eta2 = \eta_2(k)$, the estimate of the unknown parameter $Teta = \hat{M}_L$ and finally the input torque $u(k)$.

For real implementation, the designed discrete-time controller will be applied to a continuous-time system preceded by a ZOH. Therefore, simulations are also performed when the discrete-time controller is used in the continuous-time system with a ZOH. Figure (4.5) depicts the results. Note the closeness of the tracking errors obtained in Figure (4.4) to those shown in Figure (4.5).

Since we are more concerned with the tracking of the tip position (and not much the re-defined output), it is preferable to select β_1 as close as possible to its maximum value, namely, 1.51 (or equivalently to select α close to 0.906). Figure (4.6) shows the results with $T = \frac{1}{200}$ and $\beta_1 = 1.35$ (or $\alpha = 0.81$) and Figure (4.7) shows the results for $T = 0.01$ and $\beta_1 = \frac{-2}{1.2} = -1.667$ (or $\alpha = -1$). Comparing the results of

Figures (4.5), (4.6) and (4.7) reveals the impact that β_1 has as a trade-off between a lower tracking error of tip position and a higher control effort. Specifically when β_1 is far from 1.51 the good tracking of the tip position is sacrificed for a relatively low control effort (Figure (4.7)). On the other hand, in order to achieve good tracking of tip position a higher control effort is needed (Figure (4.6)).

Finally two more simulations are included to illustrate the effect of the ZOH on the minimum phase property conditions of the zero dynamics, namely $\beta_1 < 1.51$ and $T < 0.0229$. Figure (4.8) shows the results with $\beta_1 = 1.4$ and $T = \frac{1}{200}$ resulting in an unstable closed-loop system. At first, one may interpret instability result as a contradiction to the previous minimum phase conditions. But after a closer look one notes that the above minimum phase conditions are obtained without having a ZOH in the closed-loop system. In other words, the delay associated with the ZOH does now tightened our bound (e.g. from 1.51 to 1.4). Figure (4.9) shows the simulation results with $\beta_1 = 1.1$ and $T = 0.02$ where the instability is now due to the improper choice of T (compared to Figure (4.6)). In this case we would have expected that the closed-loop system without the ZOH would be unstable for $T > 0.0229$, however instability has occurred for T less than 0.0229 due to the presence of the ZOH in the closed-loop system.

In addition, simulations are performed when the desired trajectory consists of quintic and step functions. Figures (4.10) to (4.13) show the results. Figure (4.10) shows the result when both sampling period T and parameter β_1 are selected to satisfy the stability conditions $T < 0.0229$ and $\beta_1 < 1.51$. As expected, the adaptively controlled system is stable and the performance of the closed-loop is satisfactory. To observe the effect of T and β_1 on stability of the closed-loop system, β_1 is increased to 1.4 while keeping $T = \frac{1}{200}$. As Figure (4.11) shows the system is unstable since $\beta_1 \geq 1.4$. Conversely when the sampling period is increased to $T = 0.02$ with

$\beta_1 = 1$ the closed-loop system is also unstable. Figure (4.12) depicts the results and the instability should be attributed to improper value of T. When both T and β_1 are decreased to 0.01 and 1, respectively the system behaves in a stable fashion as shown in Figure (4.13).

Finally Figures (4.14) and (4.15) illustrate the performance of the closed-loop system when the conventional PD controller is applied with $K_p = 150, K_d = 50$ and $K_p = 200, K_d = 100$, respectively. As it clear the PD controller results in the steady state error and therefore, its performance is unsatisfactory. It is possible to reduce the steady state error by increasing K_p and K_d but the closed-loop becomes unstable.

Remark : The formal robustness analysis of the proposed adaptive control scheme to unmodeled dynamics is not considered in this thesis. This important issue should be investigated in future. It is expected that the bounds for β_1 and T would be further tightened as unmodeled dynamics are incorporated into the analysis. This is postulated based on the following observations reached when the ZOH is included in the closed-loop system. To illustrate the robustness of the adaptive controller which is designed with $m = 1$ to a manipulator model with $m = 1$, $m = 2$ and $m = 3$, the simulations results with $\beta_1 = 1$ and $T = 0.005$ are summarized in Table (4.1). It follows that the controller that is designed using $m = 1$ is robust with respect to the unmodeled dynamics of the link (flexible modes). As expected the maximum errors for e_1 and e_t and the input u for $m = 2$ is higher than those for $m = 1$. Although, the maximum tip position tracking error e_t is higher for $m = 3$ than that for $m = 1$, however the maximum input u is lower than that for $m = 1$. The last row of Table (4.1) shows that the closed-loop system stability conditions occur for lower values of β_1 and T when m is increased.

Number of Modes	1	2	3
Max Re-defined output tracking error($\| e_1 \|$)	4.98×10^{-4}	4.723×10^{-4}	2.557×10^{-4}
Max Tip position tracking error($\| e_t \|$)	0.5645	0.6437	0.5916
Max Input($\| u \|$)	18.2609	19.163	16.2616
$\| \eta_1 \|$	0.847	0.938	0.8417
$\| \eta_2 \|$	4.0247	4.3316	3.3882
$\| x_1 \|$	1.4058	1.4386	1.2081
$\| x_3 \|$	0.7764	0.938	0.8417
Conditions for closed-loop instability	$T \geq 0.02$ $\beta_1 \geq 1.4$	$T \geq 0.02$ $\beta_1 \geq 1.3$	$T \geq 0.01$ $\beta_1 \geq 1.2$

Table 4.1: The performance of the adaptively closed-loop system when controller which is designed with $m = 1$ is applied to a manipulator model with $m = 1, 2$ and 3.

4.7 Conclusions

In this chapter an indirect adaptive feedback linearized controller for a single-link flexible manipulator represented in the discrete-time domain has been developed. Using the discrete-time model the associated internal and the zero dynamics of the system have been obtained. The output re-definition strategy is employed so that the resulting map between the hub and the new output is guaranteed to be minimum phase. The discrete-time model is then expressed in a new regressor form and a multi-output RLS algorithm is used to identify the unknown payload parameter. Stability of the adaptively controlled closed-loop system is guaranteed by applying Lyapunov analysis. The simulation results show that the output re-definition and the proposed feedback linearization method may be successfully applied to adaptive control of single-link flexible manipulators.

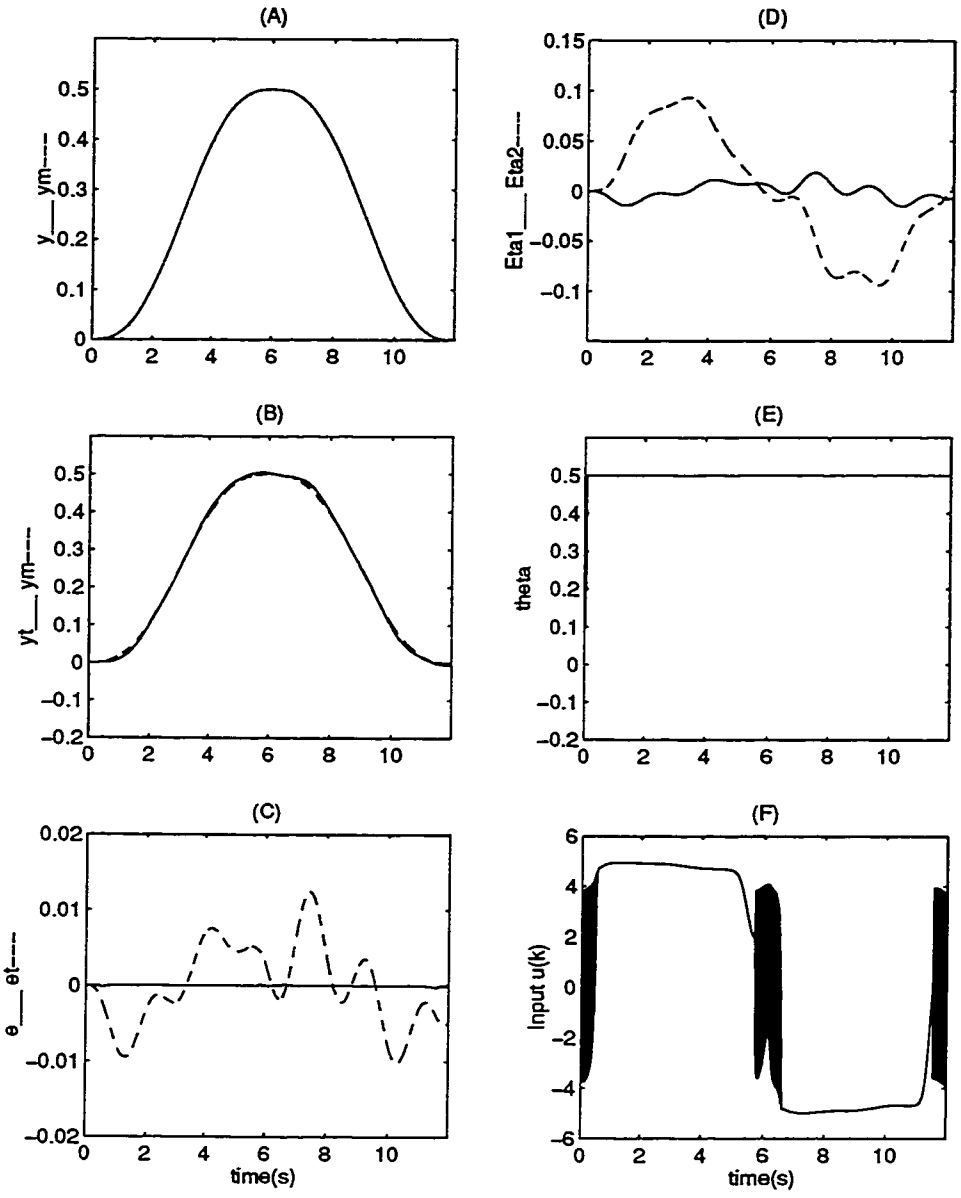

Figure 4.4: Adaptive tracking control of a single-link flexible manipulator when both controller and system model are represented in discrete-time. (A) re-defined output $y(k)$ ___ and desired trajectory $y_m(k)$ – –, (B) tip position $y_t(k)$ ___ and desired trajectory $y_m(k)$ – –, (C) tracking errors $e(k) = y(k) - y_m(k)$ ___ and $e_t(k) = y_t(k) - y_m(k)$ – –, (D) internal dynamics $\eta_1(k)$ ___ and $\eta_2(k)$ – –, (E) estimate of the payload $theta = \hat{M}_L$, (F) input torque $\tau(k) = u(k)$ for $M_L = 0.5$, $T = 0.01$, $\beta_1 = 1$ and $\hat{M}_L(0) = 0.1$.

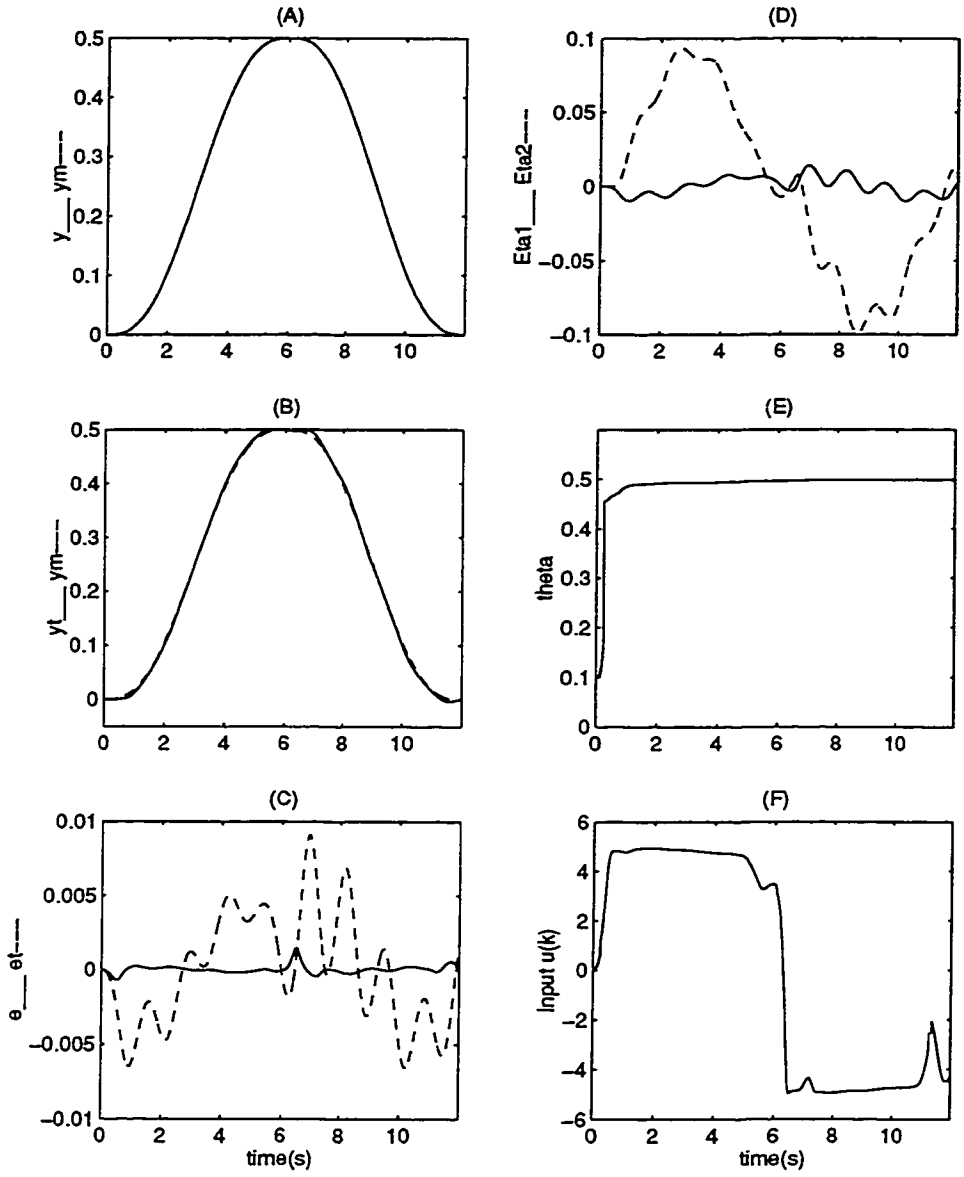

Figure 4.5: Adaptive tracking control of a single-link flexible manipulator when the discrete-time controller is applied to a ZOH followed by the continuous-time model. (A) re-defined output $y(k)$ ___ and desired trajectory $y_m(k)$ − −, (B) tip position $y_t(k)$ ___ and desired trajectory $y_m(k)$ − −, (C) tracking errors $e(k) = y(k) - y_m(k)$ ___ and $e_t(k) = y_t(k) - y_m(k)$ − −, (D) internal dynamics $\eta_1(k)$ ___ and $\eta_2(k)$ − −, (E) estimate of the payload $theta = \hat{M}_L$, (F) input torque $\tau(k) = u(k)$ for $M_L = 0.5$, $T = 0.01$, $\beta_1 = 1$ and $\hat{M}_L(0) = 0.1$.

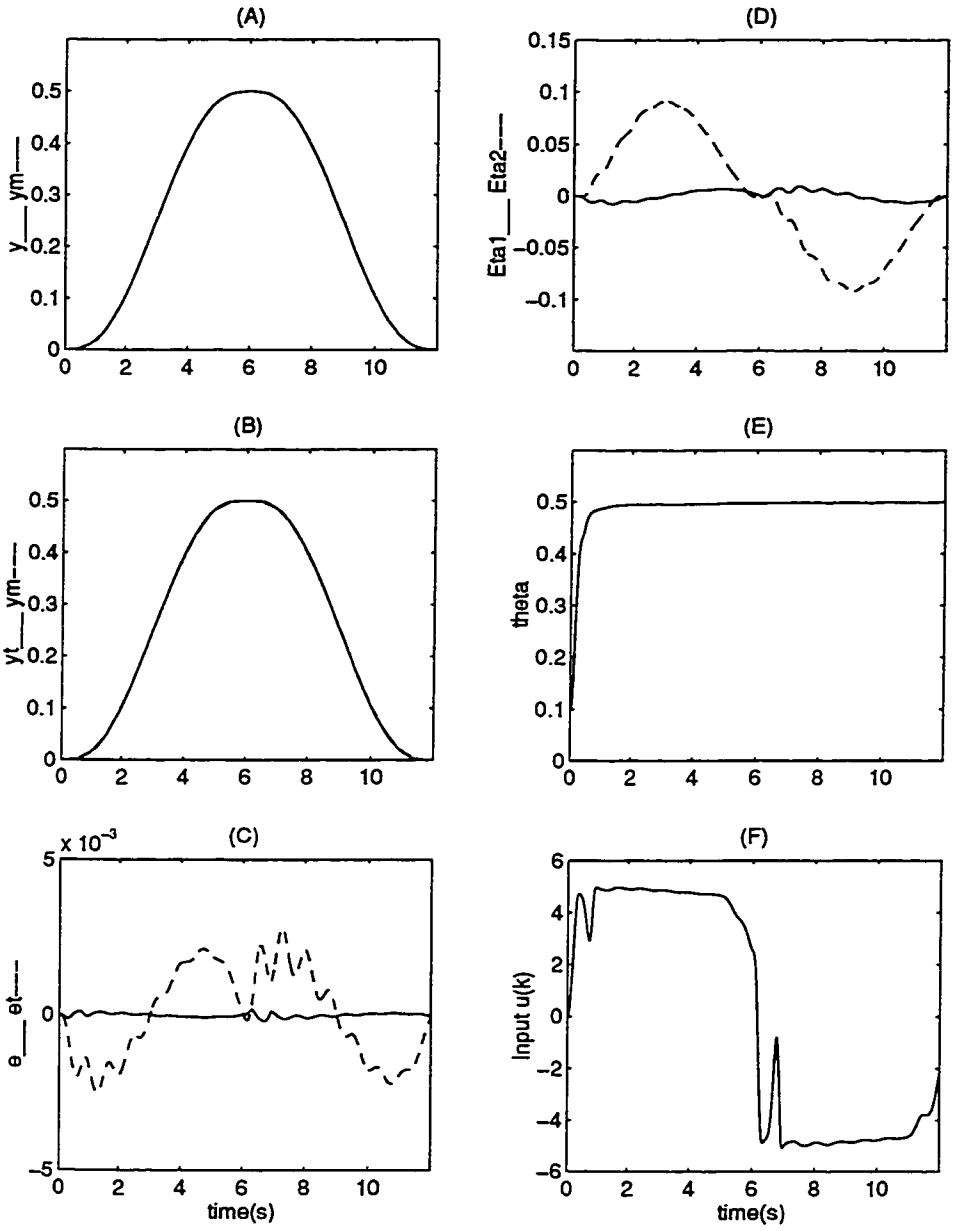

Figure 4.6: Adaptive tracking control of a single-link flexible manipulator when the discrete-time controller is applied to a ZOH followed by the continuous-time model. (A) re-defined output $y(k)$ __ and desired trajectory $y_m(k)$ − −, (B) tip position $y_t(k)$ __ and desired trajectory $y_m(k)$ − −, (C) tracking errors $e(k) = y(k) - y_m(k)$ __ and $e_t(k) = y_t(k) - y_m(k)$ − −, (D) internal dynamics $\eta_1(k)$ __ and $\eta_2(k)$ − −, (E) estimate of the payload *theta* $= \hat{M}_L$, (F) input torque $\tau(k) = u(k)$ for $M_L = 0.5$, $T = \frac{1}{200}$, $\beta_1 = 1.35$ (*or* $\alpha = 0.81$) and $\hat{M}_L(0) = 0.1$.

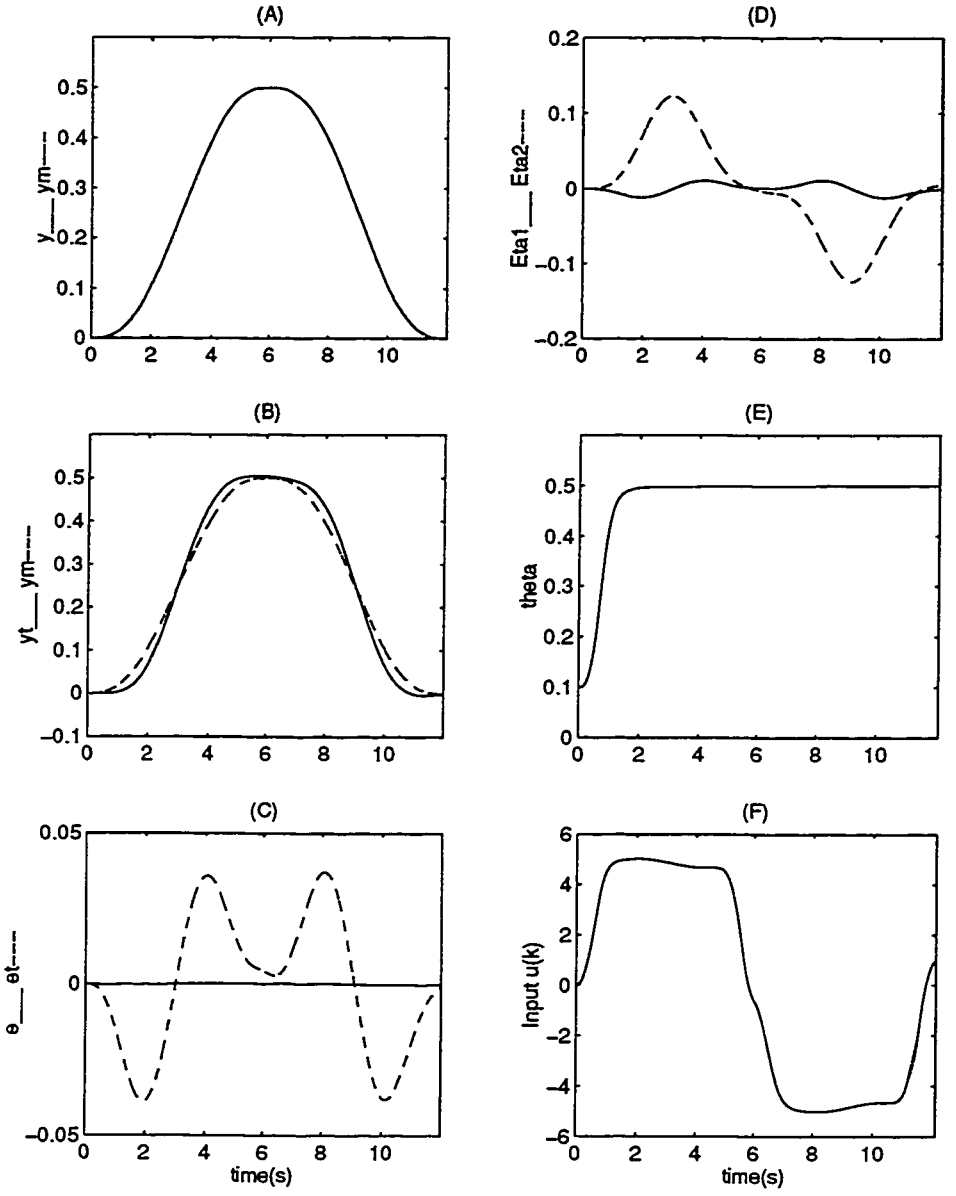

Figure 4.7: Adaptive tracking control of a single-link flexible manipulator when the discrete-time controller is applied to a ZOH followed by the continuous-time model. (A) re-defined output $y(k)$ __ and desired trajectory $y_m(k)$ − −, (B) tip position $y_t(k)$ __ and desired trajectory $y_m(k)$ − −, (C) tracking errors $e(k) = y(k) - y_m(k)$ __ and $e_t(k) = y_t(k) - y_m(k)$ − −, (D) internal dynamics $\eta_1(k)$ __ and $\eta_2(k)$ − −, (E) estimate of the payload $theta = \hat{M}_L$, (F) input torque $\tau(k) = u(k)$ for $M_L = 0.5$, $T = \frac{1}{200}$, $\beta_1 = -1.667$ $(or\ \alpha = -1)$ and $\hat{M}_L(0) = 0.1$.

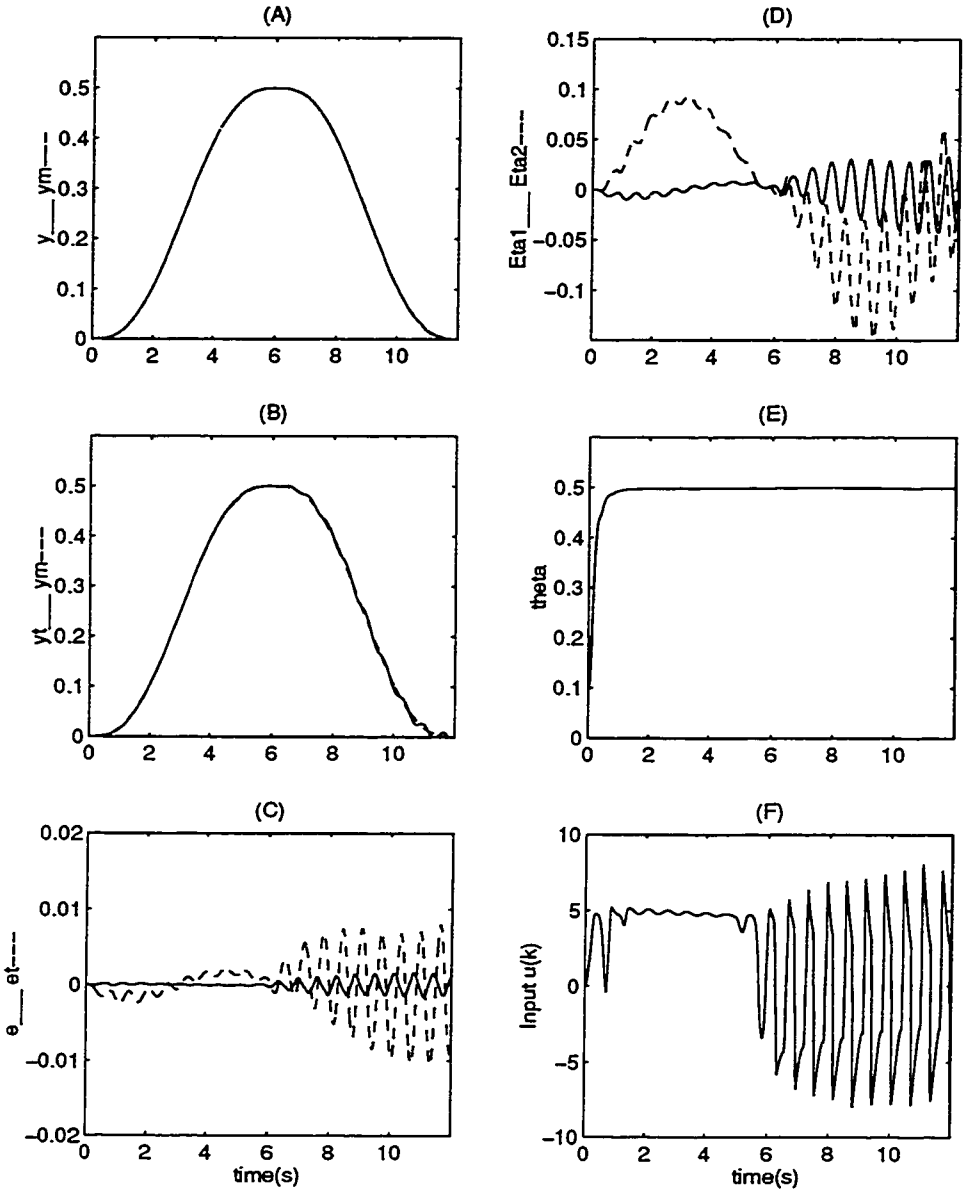

Figure 4.8: Adaptive tracking control of a single-link flexible manipulator when the discrete-time controller is applied to a ZOH followed by the continuous-time model. The system is *unstable* due to the β_1. (A) re-defined output $y(k)$ __ and desired trajectory $y_m(k)$ − −, (B) tip position $y_t(k)$ __ and desired trajectory $y_m(k)$ − −, (C) tracking errors $e(k) = y(k) - y_m(k)$ __ and $e_t(k) = y_t(k) - y_m(k)$ − −, (D) internal dynamics $\eta_1(k)$ __ and $\eta_2(k)$ − −, (E) estimate of the payload $theta = \hat{M}_L$, (F) input torque $\tau(k) = u(k)$ for $M_L = 0.5$, $T = \frac{1}{200}$, $\beta_1 = 1.4$ (*or* $\alpha = 0.84$) and $\hat{M}_L(0) = 0.1$.

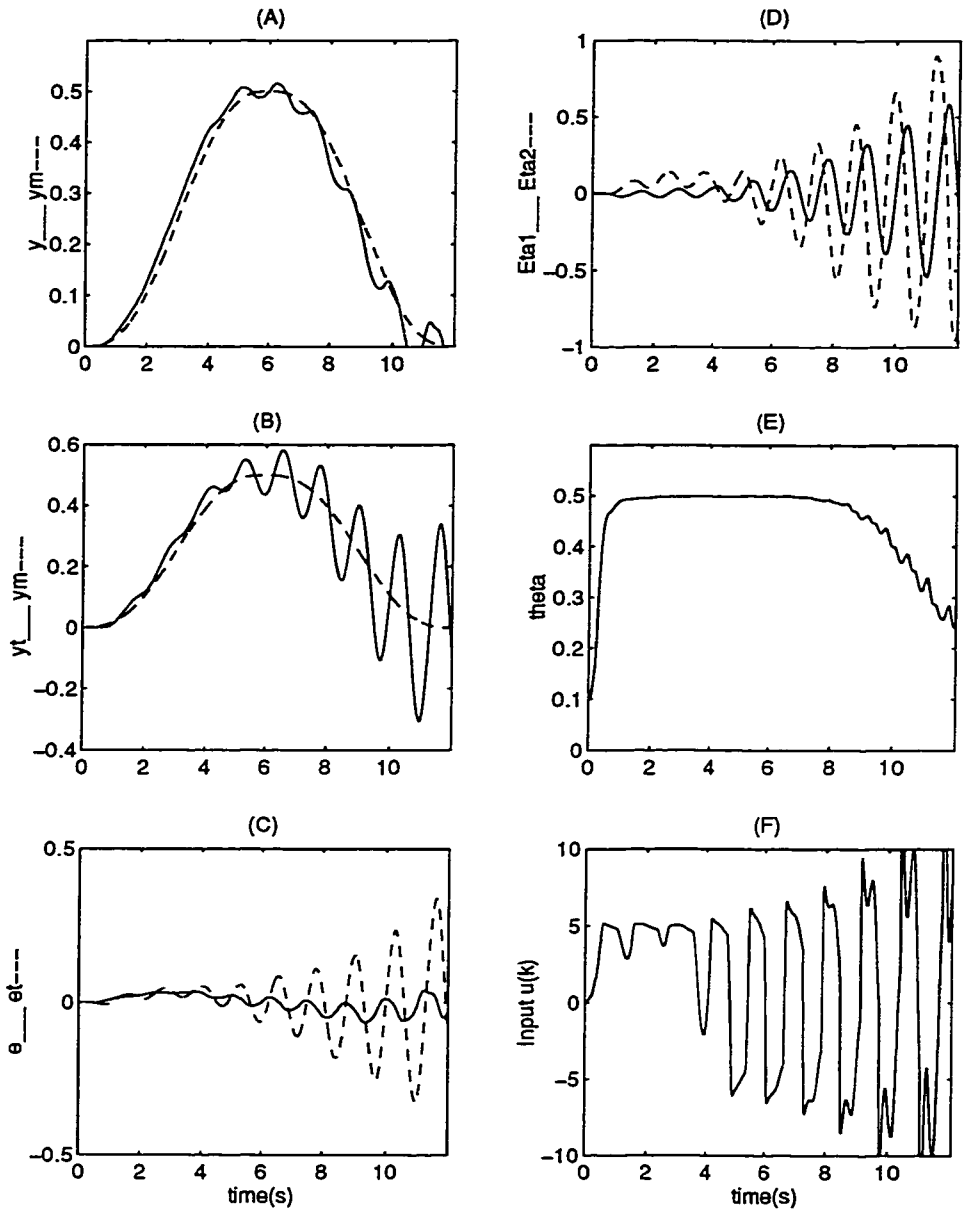

Figure 4.9: Adaptive tracking control of a single-link flexible manipulator when the discrete-time controller is applied to a ZOH followed by the continuous-time model. The system is *unstable* due to the sampling period T. (A) re-defined output $y(k)$ ___ and desired trajectory $y_m(k)$ $-\,-$, (B) tip position $y_t(k)$ ___ and desired trajectory $y_m(k)$ $-\,-$, (C) tracking errors $e(k) = y(k) - y_m(k)$ ___ and $e_t(k) = y_t(k) - y_m(k)$ $-\,-$, (D) internal dynamics $\eta_1(k)$ ___ and $\eta_2(k)$ $-\,-$, (E) estimate of the payload $theta = \hat{M}_L$, (F) input torque $\tau(k) = u(k)$ for $M_L = 0.5$, $T = 0.02$, $\beta_1 = 1.1$ (*or* $\alpha = 0.66$) and $\hat{M}_L(0) = 0.1$.

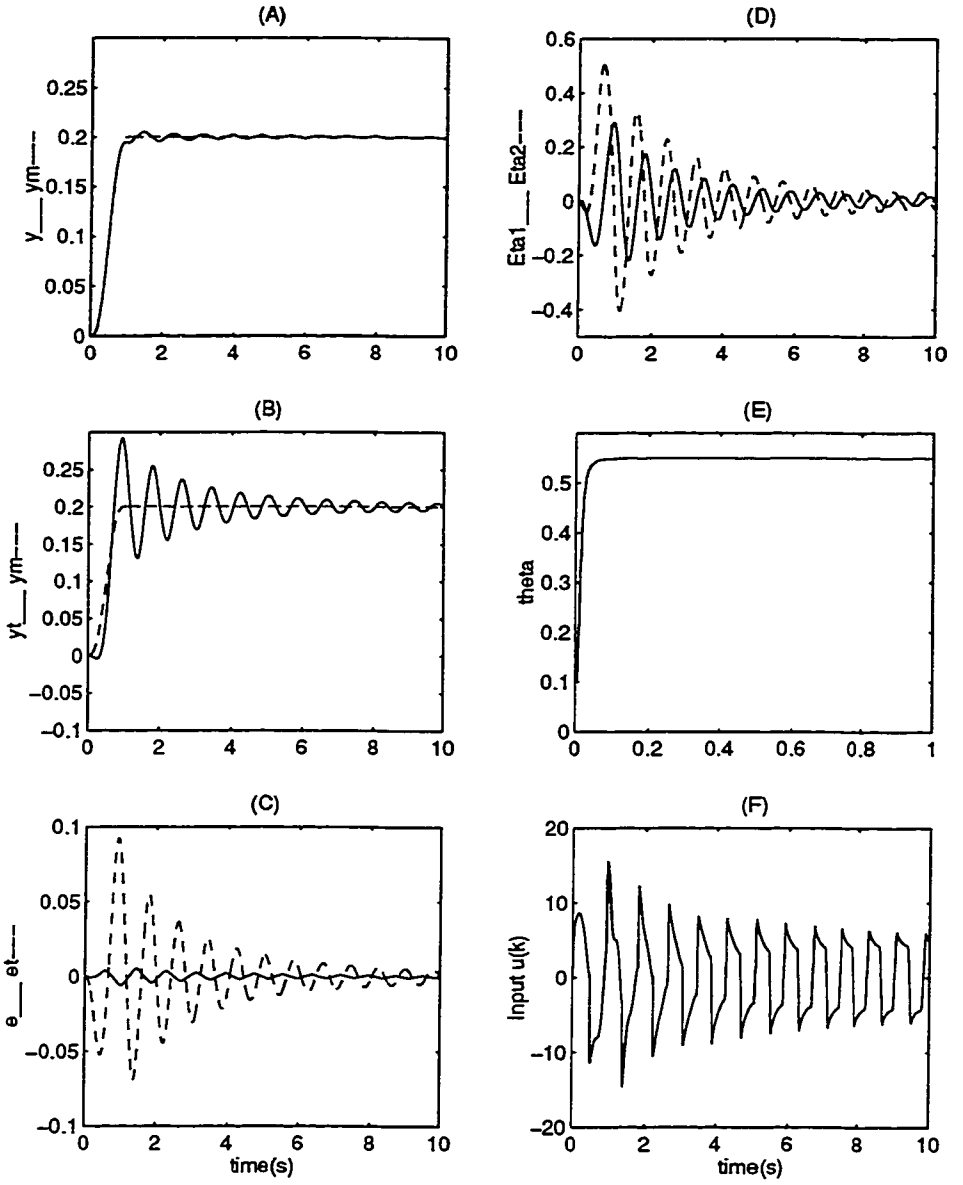

Figure 4.10: Adaptive tracking control of a single-link flexible manipulator when the discrete-time controller is applied to a ZOH followed by the continuous-time model. The desired trajectory consists of quintic and step functions. (A) redefined output $y(k)$ ___ and desired trajectory $y_m(k)$ – –, (B) tip position $y_t(k)$ ___ and desired trajectory $y_m(k)$ – –, (C) tracking errors $e(k) = y(k) - y_m(k)$ ___ and $e_t(k) = y_t(k) - y_m(k)$ – –, (D) internal dynamics $\eta_1(k)$ ___ and $\eta_2(k)$ – –, (E) estimate of the payload $theta = \hat{M}_L$, (F) input torque $\tau(k) = u(k)$ for $M_L = 0.55$, $T = \frac{1}{200}$, $\beta_1 = 1.333$ $(or\ \alpha = 0.8)$ and $\hat{M}_L(0) = 0.1$.

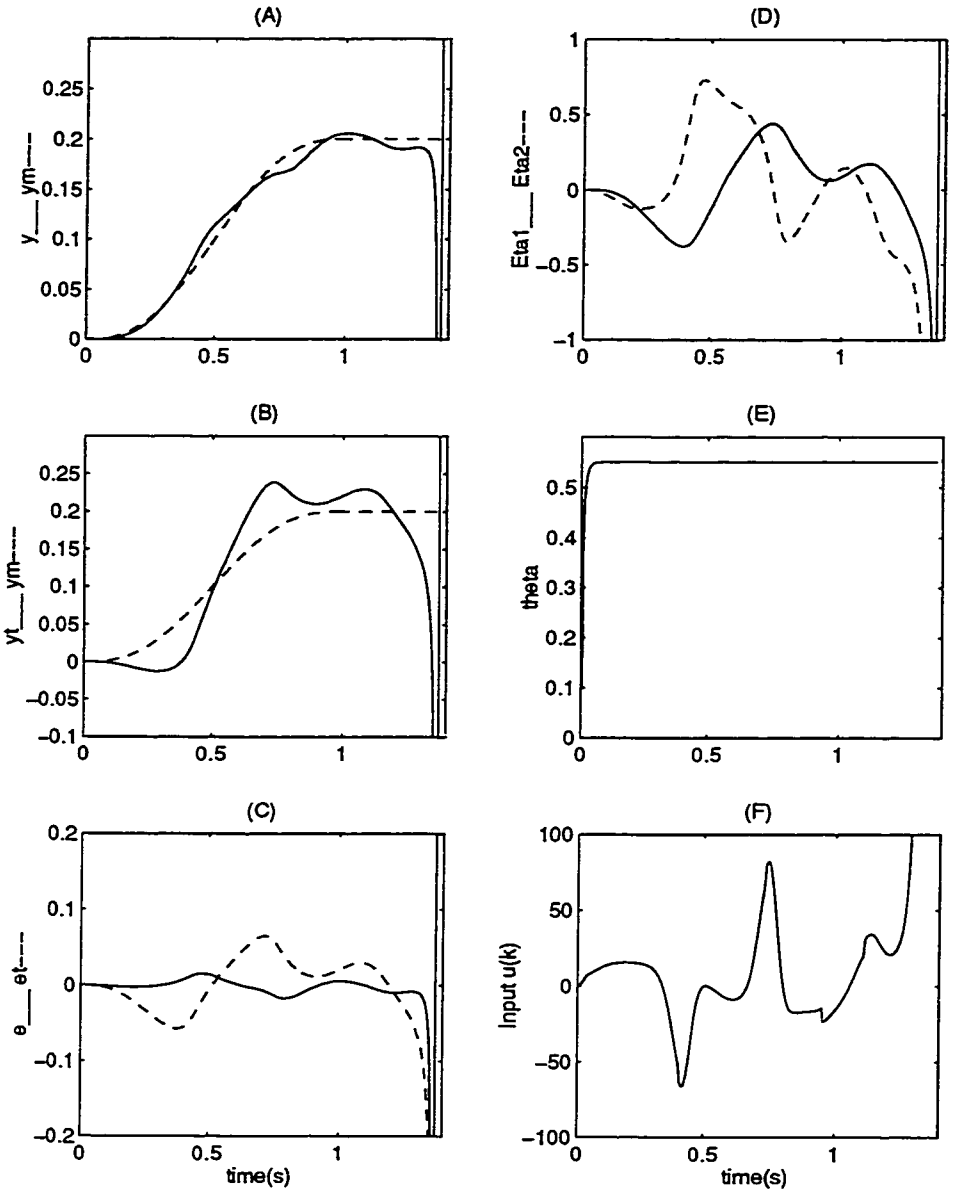

Figure 4.11: Adaptive tracking control of a single-link flexible manipulator when the discrete-time controller is applied to a ZOH followed by the continuous-time model. The desired trajectory consists of quintic and step functions. The system is *unstable* due to the β_1. (A) re-defined output $y(k)$ __ and desired trajectory $y_m(k)$ $--$, (B) tip position $y_t(k)$ __ and desired trajectory $y_m(k)$ $--$, (C) tracking errors $e(k) = y(k) - y_m(k)$ __ and $e_t(k) = y_t(k) - y_m(k)$ $--$, (D) internal dynamics $\eta_1(k)$ __ and $\eta_2(k)$ $--$, (E) estimate of the payload $theta = \hat{M}_L$, (F) input torque $\tau(k) = u(k)$ for $M_L = 0.55$, $T = \frac{1}{200}$, $\beta_1 = 1.4$ $(or\ \alpha = 0.84)$ and $\hat{M}_L(0) = 0.1$.

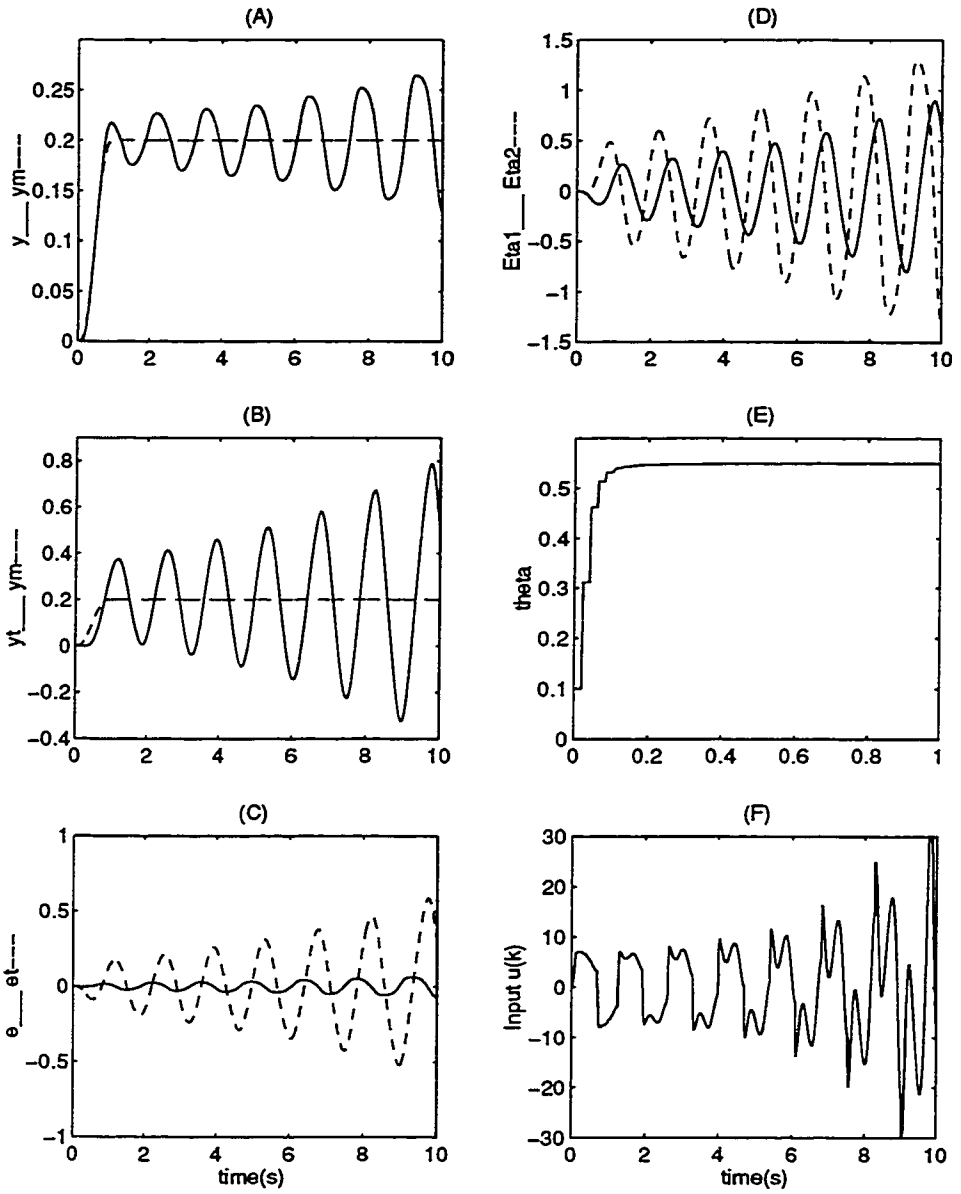

Figure 4.12: Adaptive tracking control of a single-link flexible manipulator when the discrete-time controller is applied to a ZOH followed by the continuous-time model. The desired trajectory consists of quintic and step functions. The system is *unstable* due to the sampling period T. (A) re-defined output $y(k)$ __ and desired trajectory $y_m(k)$ $--$, (B) tip position $y_t(k)$ __ and desired trajectory $y_m(k)$ $--$, (C) tracking errors $e(k) = y(k) - y_m(k)$ __ and $e_t(k) = y_t(k) - y_m(k)$ $--$, (D) internal dynamics $\eta_1(k)$ __ and $\eta_2(k)$ $--$, (E) estimate of the payload $theta = \hat{M}_L$, (F) input torque $\tau(k) = u(k)$ for $M_L = 0.55$, $T = 0.02$, $\beta_1 = 1$ $(or\ \alpha = 0.6)$ and $\hat{M}_L(0) = 0.1$.

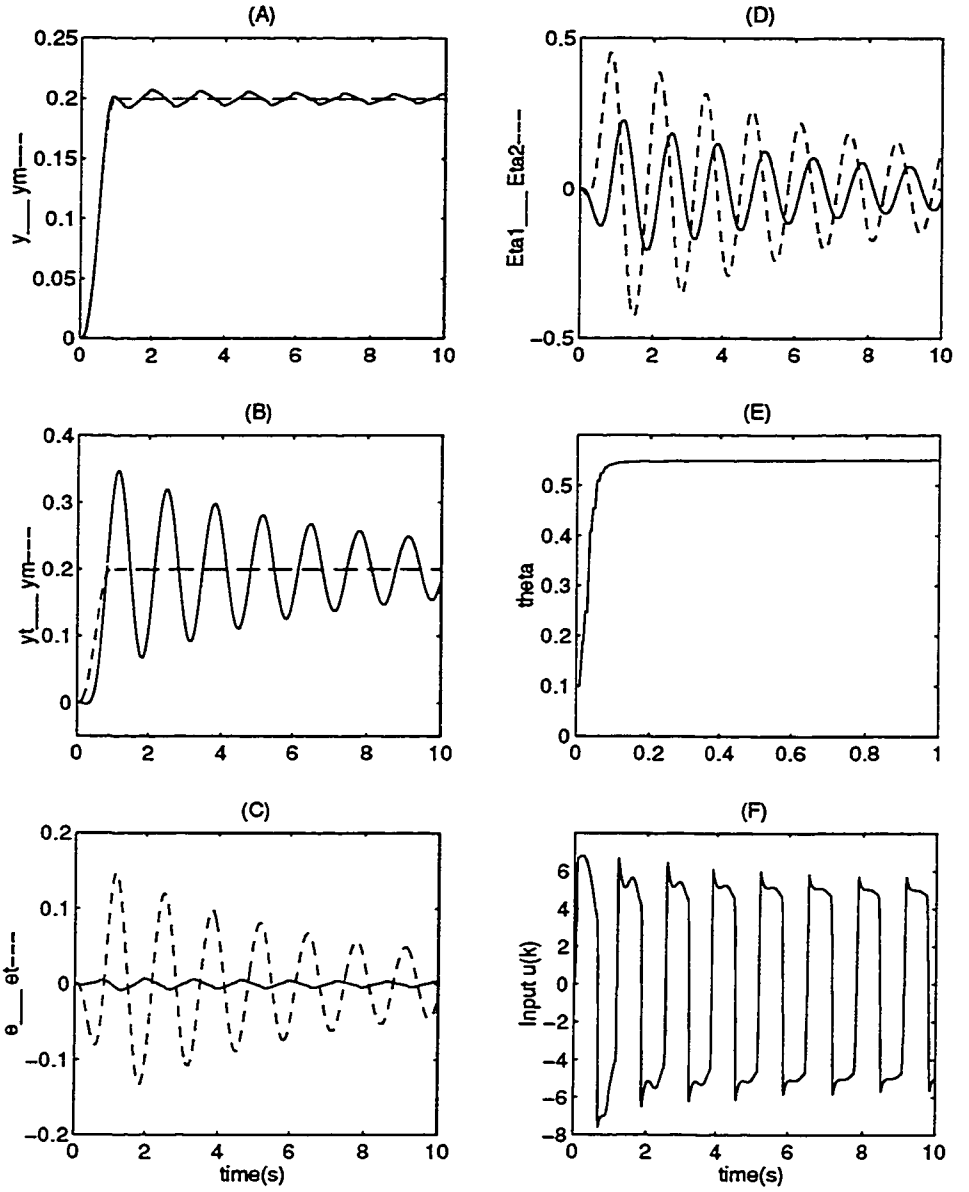

Figure 4.13: Adaptive tracking control of a single-link flexible manipulator when the discrete-time controller is applied to a ZOH followed by the continuous-time model. The desired trajectory consists of quintic and step functions. (A) redefined output $y(k)$ __ and desired trajectory $y_m(k)$ − −, (B) tip position $y_t(k)$ __ and desired trajectory $y_m(k)$ − −, (C) tracking errors $e(k) = y(k) - y_m(k)$ __ and $e_t(k) = y_t(k) - y_m(k)$ − −, (D) internal dynamics $\eta_1(k)$ __ and $\eta_2(k)$ − −, (E) estimate of the payload $theta = \hat{M}_L$, (F) input torque $\tau(k) = u(k)$ for $M_L = 0.55$, $T = 0.01$, $\beta_1 = 1$ $(or\ \alpha = 0.6)$ and $\hat{M}_L(0) = 0.1$.

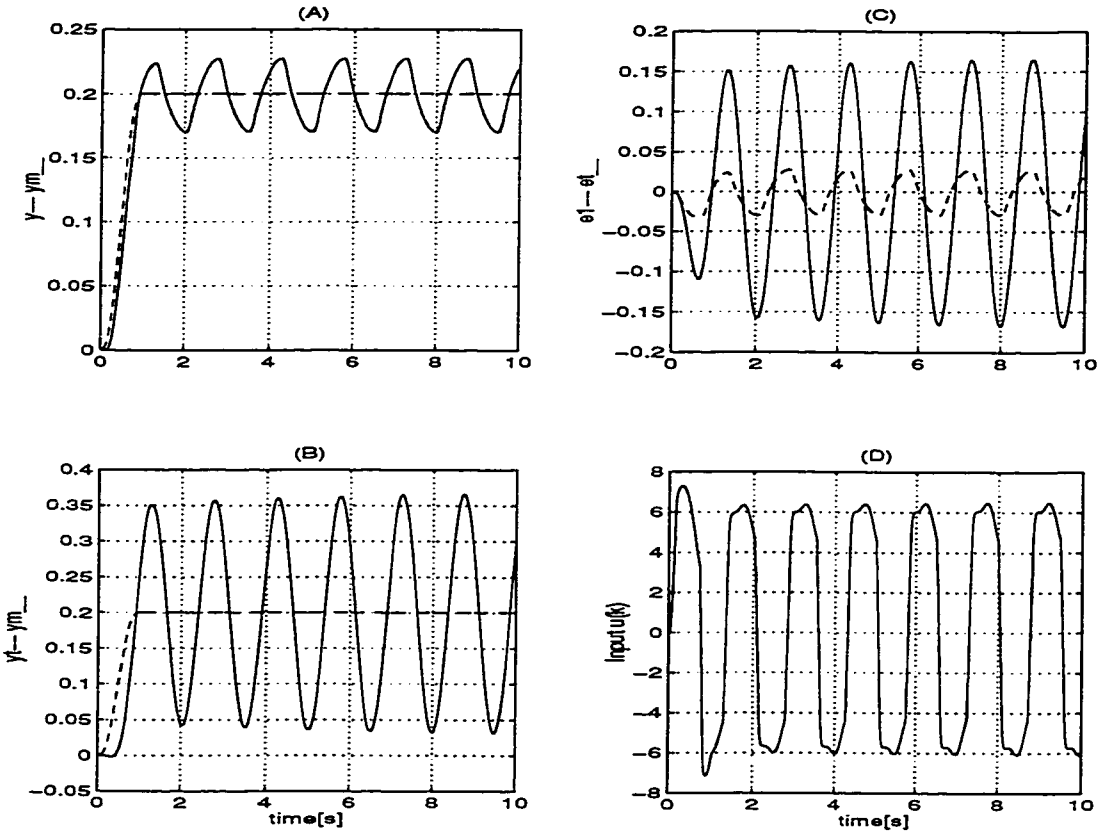

Figure 4.14: PD tracking control of a single-link flexible manipulator when the discrete-time controller is applied to a ZOH followed by the continuous-time model. (A) re-defined output $y(k)$ ___ and desired trajectory $y_m(k)$ $--$, (B) tip position $y_t(k)$ ___ and desired trajectory $y_m(k)$ $--$, (C) tracking errors $e(k) = y(k) - y_m(k)$ ___ and $e_t(k) = y_t(k) - y_m(k)$ $--$, (D) input torque $\tau(k) = u(k)$ for $K_p = 150$, $Kd = 50$, $M_L = 0.55$, $T = 0.01$, $\beta_1 = 1$ and $\hat{M}_L(0) = 0.1$.

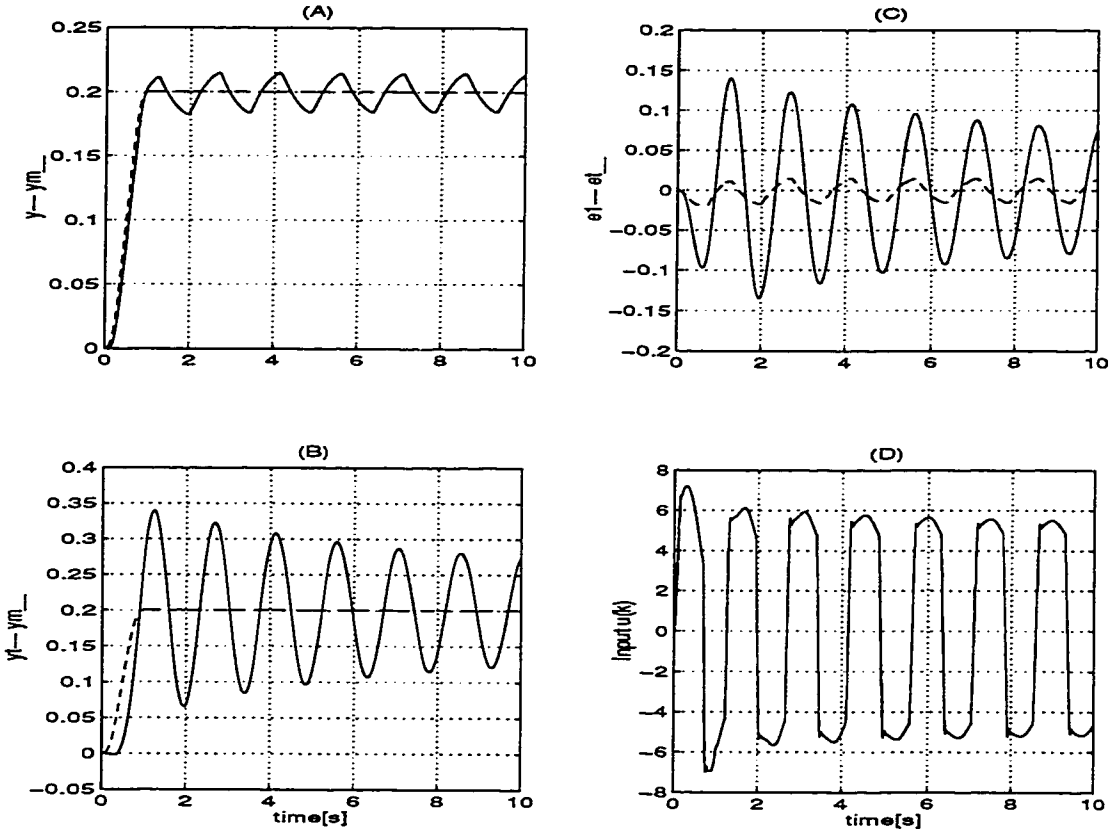

Figure 4.15: PD tracking control of a single-link flexible manipulator when the discrete-time controller is applied to a ZOH followed by the continuous-time model. Input consists of quintic and step functions. (A) re-defined output $y(k)$ ___ and desired trajectory $y_m(k)$ $-\,-$, (B) tip position $y_t(k)$ ___ and desired trajectory $y_m(k)$ $-\,-$, (C) tracking errors $e(k) = y(k) - y_m(k)$ ___ and $e_t(k) = y_t(k) - y_m(k)$ $-\,-$, (D) input torque $\tau(k) = u(k)$ for $K_p = 200$, $Kd = 100$, $M_L = 0.55$, $T = 0.01$, $\beta_1 = 0.4167$ $(or\ \alpha = 0.25)$ and $\hat{M}_L(0) = 0.1$

Chapter 5

Input-Output Model Based Direct Adaptive Control for a Class of Discrete-Time Nonlinear Systems

A direct adaptive tracking controller for a class of nonlinear discrete-time systems expressed in input-output form is developed. Using a state space representation, the linearizing input and the internal dynamics are obtained. By employing the projection algorithm the estimate of the unknown parameters are utilized in the linearization process. A Lyapunov analysis is used to show that under certain conditions (a priori lower and upper bound of the unknown parameters), the closed-loop adaptively controlled system is stable and moreover the tracking error converges to zero asymptotically. Finally, the simulation results are presented to illustrate the features of the proposed method.

5.1 Introduction

Adaptive control of different classes of feedback linearizable continuous-time nonlinear systems has been studied extensively over the past few years. Unfortunately, these adaptive schemes cannot be directly generalized to discrete-time systems due to certain technical difficulties. Among them one could mention the lack of applicability of Lyapunov techniques (Song & Grizzle [77], Kanellakopoulos [30]) and loss of linear parameterizability during the linearization process even when the original discrete-time system is linearly parameterized.

To overcome these difficulties, Yeh & Kokotovic [90] have designed a state feedback controller to achieve tracking of a reference signal for a class of SISO nonlinear discrete-time systems in the so-called *parametric-strict-feedback form.* Also, an adaptive output feedback design is developed by Yeh & Kokotovic [89] for a class of nonlinear discrete-time systems. Song & Grizzle [77] attempted to extend the existing conventional linear model reference adaptive control methods to discrete-time nonlinear systems and Kanellakopoulos [30] developed a new least-square estimator with nonlinear data weighting.

This chapter is concerned with the direct adaptive control of a class of nonlinear discrete-time systems represented by an input-output model. The model was also considered in Chen & Khalil [6, 7, 8] to control nonlinear systems using neural networks as well as in Chen & Tsao [9]. We start by using the state space representation of the system to find the linearizing controller, where the estimate of the unknown parameters are employed in the linearization process. We use a *projection algorithm* to identify the unknown parameters. Subsequently, by using the Lyapunov analysis, it is shown that under certain assumptions, the adaptively controlled closed-loop system is stable and furthermore the tracking error approaches to zero as time tends to infinity.

The aim is to consider the adaptive control of the following nonlinear discrete-time system [71]

$$\begin{cases} z_{11}(k+1) = z_{12}(k) \\ \quad \vdots \\ z_{1,n-1}(k+1) = z_{1n}(k) \end{cases}$$
$$\begin{cases} z_{1n}(k+1) = z_{1,n+1}(k) \\ \quad \vdots \\ z_{1,n+d-1}(k+1) = F^T(z(k))W + G^T(z(k))Vu(k) \end{cases}$$
$$\begin{cases} z_{21}(k+1) = z_{22}(k) \\ \quad \vdots \\ z_{2m}(k+1) = u(k-d+1) \end{cases}$$
$$y(k) = z_{1n}(k) \tag{5.1}$$

It is shown in Khalil & Chen [8, 6] that the above set of equations is a state space representation of the following input-output system

$$y(k+d) = F^T(z(k))W + G^T(z(k))Vu(k) \tag{5.2}$$

where $F(z(k))$ and $G^T(z(k))$ are smooth functions of known functions $[y(k-n+d), \ \ldots \ , y(k+d-1), u(k-m), \ldots, u(k-1)]^T$ where $m \leq n$. Note that the constant d is the relative degree of the system and the unknown vectors $W \in \Re^{p1}$ and $V \in \Re^{p2}$. Let's define the following vectors,

$$z_1^1(k) \triangleq [z_{11}(k) \ \ldots \ z_{1,n-1}(k)]^T$$
$$z_1^2(k) \triangleq [z_{1n}(k) \ \ldots \ z_{1,n+d-1}(k)]^T$$
$$z_2(k) \triangleq [z_{21}(k) \ \ldots \ z_{2m}(k)]^T$$

with $z(k) \triangleq [z_1^{1T}(k) \quad z_1^{2T}(k) \quad z_2^T(k)]^T$. Note that system (5.1) consists of two subsystems. The first subsystem comprising of $z_1^T(k) \triangleq [z_1^{1T}(k) \ \ z_1^{2T}(k)]$ states yields

the given input-output dynamics (5.2) and has the relative degree d. The second subsystem consisting of $z_2(k)$ states is unobservable from output and therefore does not affect the output. In other words, $z_2(k)$ states define the internal dynamics of system (5.2). Using the observable subsystem, and provided that the functions $F^T(z_k)W$ and $G^T(z_k)V$ are known, then the input which renders the system input-output equivalent into a linear system may be found as

$$u(k) = \frac{1}{G^T(z(k))V}[-F^T(z(k))W + v(k)] \tag{5.3}$$

where $v(k)$ is an external input that will be defined subsequently. Substituting (5.3) into (5.1) gives, $z_{1,n+d-1}(k+1) = v(k)$. Also from system equation (5.1) it is evident that

$$y(k) = z_{1n}(k)$$
$$y(k+i) = z_{1,n+i-1}(k+1) = z_{1,n+i}(k)\ ,\quad 1 \leq i \leq d-1$$

Therefore, the closed-loop equivalent subsystem after applying (5.3) into (5.1) becomes,

$$y(k+d) = v(k) \tag{5.4}$$

Now by defining the tracking error as $e_n(k) \triangleq y(k) - y_m(k)$ where $y_m(k)$ is the desired output trajectory and by taking

$$v(k) = y_m(k+d) + \sum_{i=1}^{d} \alpha_i[y_m(k+d-i) - y(k+d-i)] \tag{5.5}$$

the tracking control problem of the output $y(k)$ may now be introduced. Substituting (5.4) into (5.5) gives

$$y(k+d) = y_m(k+d) + \sum_{i=1}^{d} \alpha_i e_n(k+d-i)$$

or $e_n(k+d) + \alpha_1 e_n(k+d-1) + \cdots + \alpha_d e_n(k) = 0$ where $\alpha_i\ ,\ \ i = 1, \cdots, d$ are selected such that $\mathcal{Z}^d + \alpha_1 \mathcal{Z}^{d-1} + \cdots + \alpha_d$ is a Hurwitz polynomial.

5.2 Presence of Parametric Uncertainty

When vectors W and V are unknown, their estimates $\hat{W}(k)$ and $\hat{V}(k)$ should be used in control (5.3), that is

$$\hat{u}(k) = \frac{1}{G^T(z(k))\hat{V}(k)}[-F^T(z(k))\hat{W}(k) + v(k)] \tag{5.6}$$

Consequently, using (5.6) in (5.4) yields the following input-output representation

$$y(k+d) = F^T(z(k))W + G^T(z(k))V\hat{u}(k) \tag{5.7}$$

Now by adding the term $v(k) - F^T(z(k))\hat{W}(k) - G^T(z(k))\hat{V}(k)\hat{u}(k)$ (which is zero) to the right hand side of (5.7), and after regrouping terms one gets, $y(k+d) = v(k) + \varsigma(k)$ where

$$\varsigma(k) \triangleq F^T(z(k))(W - \hat{W}(k)) + G^T(z(k))(V - \hat{V}(k))\hat{u}(k)$$

Finally, by using (5.5) and the definition of tracking error $e_n(k)$, one gets

$$e_n(k+d) = -\alpha_1 e_n(k+d-1) - \cdots - \alpha_d e_n(k) + \varsigma(k) \tag{5.8}$$

The error equation (5.8) is represented in the state-space form by using the following error signals

$$\begin{aligned} e_i(k) &\triangleq y(k+i-n) - y_m(k+i-n) \\ &= z_{1i}(k) - y_m(k+i-n) \quad 1 \le i \le n+d-1 \end{aligned} \tag{5.9}$$

Therefore, using (5.9) one finds

$$e_i(k+1) = e_{i+1}(k)\ , \quad 1 \le i \le n+d-2$$

$$e_{n+d-1}(k+1) = e_n(k+d) = -\alpha_1 e_n(k+d-1) - \cdots - \alpha_d e_n(k) + \varsigma(k)$$

that may be written in the compact form

$$e(k+1) = Ae(k) + B\varsigma(k) \tag{5.10}$$

with $e(k) \triangleq [e_{1,k}\ e_{2,k}\ \cdots\ e_{n+d-1,k}]$, and where matrix A and vector B are equal to

$$A = \begin{bmatrix} 0 & 1 & 0 & \cdots & 0 & \cdots & 0 \\ 0 & 0 & 1 & \cdots & 0 & \cdots & 0 \\ \vdots & \vdots & \vdots & \vdots & \vdots & \vdots & \vdots \\ 0 & 0 & 0 & \cdots & 0 & \cdots & 1 \\ 0 & 0 & 0 & \cdots & -\alpha_d & \cdots & -\alpha_1 \end{bmatrix}, \quad B = \begin{bmatrix} 0 \\ 0 \\ \vdots \\ 0 \\ 1 \end{bmatrix}$$

Note that matrix A is a block upper triangular matrix; therefore, $n-1$ eigenvalues are located at 0 and the other d eigenvalues are dependent on α's.

5.3 Internal and Zero Dynamics

As mentioned before, the internal dynamics of (5.1) is characterized by $z_2(k)$ states when the input $u(k)$ is given by (5.3). This dynamics is written in a compact form

$$z_2(k+1) = q(z_1(k), z_2(k), v(k-d+1)) \tag{5.11}$$

where $q \triangleq [z_{22}(k)\ z_{23}(k)\ \cdots\ u(k-d+1)]^T$ and $u(k)$ is defined in (5.3). Now following the Definition 3.1, the zero dynamics of (5.1) is

$$z_2(k+1) = q(0, z_2(k), 0) \triangleq q_0(z_2(k)) \tag{5.12}$$

where the vector $q_0(z_2(k)) \triangleq [z_{22}(k)\ \ z_{23}(k)\ \cdots\ \frac{-F^T(0,z_2(k'))W}{G^T(0,z_2(k'))V}]^T$. In other words, equation (5.12) defines the internal dynamics when the output $y(k)$ and external input $v(k)$ are identically zero for all time.

Assumption 5.1 *The zero dynamics (5.12) is exponentially stable at origin; therefore, there exists a Lyapunov function $V_2(z_2(k)$ such that*

$$\begin{aligned} c_1 \parallel z_2(k) \parallel^2 &\leq V_2(z_2(k)) \leq c_2 \parallel z_2(k) \parallel^2 \\ \triangle V_2(k+1) &\triangleq V_2 \circ q_0(z_2(k)) - V_2(z_2(k)) \leq -\alpha \parallel z_2(k) \parallel^2 \\ \parallel \frac{\partial V_2(z_2(k))}{\partial z_2(k)} \parallel &\leq L \parallel z_2(k) \parallel \end{aligned} \tag{5.13}$$

in any compact set $z_2 \in \Omega_2 \subset \Re^m$ for some positive constants c_1, c_2 and L.

5.4 Parameter Estimation

To determine a suitable algorithm for estimating the unknown vector $\theta \triangleq [W^T\ V^T]^T$, it is well known that for a linear regressor of the form $y(k+d) = \psi^T(k)\theta$, the projection algorithm (or normalized least-mean-square) results in

$$\hat{\theta}(k+1) = \hat{\theta}(k) - \frac{a\psi(k-d+1)}{c+\psi(k-d+1)^T\psi(k-d+1)}[\hat{y}(k+1) - y(k+1)] \tag{5.14}$$

where $\hat{y}(k+d) = \psi^T(k)\hat{\theta}(k)$ and $y(k+d)$ is the observation vector. By using (5.3) and substituting $v(k)$ in (5.4) it follows that the output $y(k)$ satisfies

$$y(k+d) = F^T(z(k))W + G^T(z(k))Vu(k) \triangleq \psi^T\theta \tag{5.15}$$

where $\psi^T \triangleq [F^T(z(k))\ \ G^T(z(k))u(k)]$. Therefore, the present control algorithm can be categorized as a direct adaptive control. In the next section it will shown that algorithm (5.14) applied to system (5.15) will result in a stable closed-loop system.

5.5 Closed-Loop Stability

In this section it is shown that under certain conditions all signals of the closed-loop system comprising of the error equation (5.10) and parameter estimation (5.14) belong to l_∞ and furthermore, the tracking error $e_n(k)$ approaches to zero as $k \to \infty$.

Theorem 5.1 *Given a nonlinear discrete-time system (5.1) where W and V are unknown vectors, then the adaptively controlled closed-loop system consisting of the nonlinear feedback input (5.6) and the parameter estimator (5.14) is stable in the sense of Lyapunov for all $(e, z_2, \tilde{\theta}) \in \Omega_c$, if Assumptions 5.1-5.4 and inequality (5.29) are satisfied where $\Omega_c = \{(e, z_2, \hat{\theta}) | V_n(e, z_2, \hat{\theta}) \leq c\}$, $c > 0$ and $V_n(e, z_2, \hat{\theta}) = c$ is the largest level set contained in $\triangle V(k+1) \leq 0$. Moreover, the tracking error $e_n(k)$ goes to zero as $k \to \infty$.*

Proof :

To prove the stability of the closed-loop system, three separate Lyapunov function candidates for the error equation (5.10), the internal dynamics (5.11) and the parameter estimation (5.14) are used. Since in the error equation (5.10), A is a Hurwitz matrix, therefore for any positive definite matrix Q, there exists a positive definite matrix P such that $A^TPA - P = -Q$, and the Lyapunov function for this system may be selected as $V_1(e(k)) = e^T(k)Pe(k)$. Hence, $\triangle V_1(k+1)$ satisfies

$$\begin{aligned}\triangle V_1(k+1) &\triangleq V_1(e(k+1)) - V_1(e(k)) \\ &= -e^T(k)Qe(k) + 2e^T(k)A^TPB\varsigma(k) + \varsigma^T(k)B^TPB\varsigma(k) \\ &\leq -\lambda_{min}(Q) \parallel e \parallel^2 + c_1 \parallel e \parallel |\varsigma| + c_2|\varsigma|^2 \end{aligned} \tag{5.16}$$

where $c_1 \triangleq 2 \parallel A \parallel\parallel P \parallel$ and $c_2 \triangleq \parallel P \parallel$. The Lyapunov function candidate associated to the internal dynamics may be selected as $V_2(z_2(k))$ similar to what was defined earlier for the zero dynamics. First, the state $z_{2m}(k+1)$ of the internal dynamics (5.11) should be written as

$$\begin{aligned} z_{2m}(k+1) = u(k_1) &= \frac{-F^T(z_1(k_1), z_2(k_1))\hat{W}(k_1) + v(k_1)}{G^T(z_1(k_1), z_2(k_1))\hat{V}(k_1)} \\ &= \frac{-F^T(0, z_2(k_1))W}{G^T(0, z_2(k_1))V} + l_3 + l_2 + l_1 \end{aligned} \tag{5.17}$$

where $k_1 \triangleq k - d + 1$ and

$$\begin{aligned} l_3 &\triangleq \left[\frac{-F^T(z_1(k_1),z_2(k_1))\hat{W}(k_1)}{G^T(z_1(k_1),z_2(k_1))\hat{V}(k_1)} - \frac{-F^T(0,z_2(k_1))\hat{W}(k_1)}{G^T(0,z_2(k_1))\hat{V}(k_1)} \right] \\ l_2 &\triangleq \left[\frac{-F^T(0,z_2(k_1))\hat{W}(k_1)}{G^T(0,z_2(k_1))\hat{V}(k_1)} - \frac{-F^T(0,z_2(k_1))W}{G^T(0,z_2(k_1))V} \right] \\ l_1 &\triangleq \left[\frac{v(k_1)}{G^T(z_1(k_1),z_2(k_1))\hat{V}(k_1)} \right] \end{aligned} \tag{5.18}$$

Therefore, the internal dynamics may be written as

$$z_2(k+1) = q_0(z_2(k)) + q_1(k)$$

where the vector $q_0(z_2(k)) \triangleq [z_{22}(k) \;\; z_{23}(k) \;\cdots\; \frac{-F^T(0,z_2(k'))W}{G^T(0,z_2(k'))V}]^T$ describes the zero dynamics and $q_1(k) \triangleq [0\;0\;\cdots\; l_1+l_2+l_3]^T$. Using the above results and Assumption 5.1, the Lyapunov function candidate $V_2(z_2(k))$ satisfies the following inequality

$$\begin{aligned}\triangle V_2(k+1) &\triangleq V_2(z_2(k+1)) - V_2(z_2(k)) \\ &= [V_2(q_0(k) - V_2(z_2(k))] + [V_2(q_0(k)+q_1(k)) - V_2(q_0(k))] \quad (5.19) \\ &\leq -\alpha \parallel z_2 \parallel^2 + [V_2(q_0(k)+q_1(k)) - V_2(q_0(k))]\end{aligned}$$

Using the mean value theorem [72], the second bracket of (5.19) becomes

$$[V_2(q_0(k)+q_1(k)) - V_2(q_0(k))] = \left.\frac{\partial V_2}{\partial z_2}\right|_{z_2=q_0+\xi q_1} q_1(k) \qquad (5.20)$$

for some constant $0 \leq \xi \leq 1$. By substituting (5.20) into (5.19) and using the last inequality of (5.13) it follows that

$$\begin{aligned}\triangle V_2(k+1) &\leq -\alpha \parallel z_2 \parallel^2 + L \parallel q_0 + \xi q_1 \parallel \parallel q_1 \parallel \\ &\leq -\alpha \parallel z_2 \parallel^2 + (L \parallel q_0 \parallel + \xi L \parallel q_1 \parallel) \parallel q_1 \parallel \qquad (5.21)\end{aligned}$$

Also due to the exponential stability of the zero dynamics $\parallel q_0(z_2(k) \parallel \leq k_1 \parallel z_2 \parallel$. In addition, we have $\parallel q_1 \parallel \leq \parallel l_3 \parallel + \parallel l_2 \parallel + \parallel l_1 \parallel$. By using (5.18) and the mean value theorem, l_3 satisfies

$$|l_3| \leq \parallel \frac{\partial}{\partial z_1}[\frac{F^T(z_1(k'),z_2(k'))\hat{W}(k')}{G^T(z_1(k'),z_2(k'))\hat{V}(k')}] \parallel \parallel z_1 \parallel \leq k_2 \parallel z_1 \parallel$$

The last inequality is valid since on any compact set $(z,\theta) \in (\Re^{n+m+d-1} \times \Re^{p1+p2})$, $\frac{F^TW}{G^TV}$ is continuous; therefore, $\frac{\partial}{\partial z_1}\frac{F^TW}{G^TV}$ is also bounded [36]. Also using the same procedure it follows that l_2 satisfies $|l_2| \leq k_3 \parallel \tilde{\theta} \parallel$. Hence, q_1 satisfies

$$\parallel q_1 \parallel \leq k_2 \parallel z_2 \parallel + k_3 \parallel \tilde{\theta} \parallel + |l_1| \qquad (5.22)$$

Therefore, equation (5.21) may be written as

$$\begin{aligned}&\triangle V_2(k+1) \leq -\alpha \parallel z_2 \parallel^2 \\ &\quad + (k_2 \parallel z_2 \parallel + k_3 \parallel \tilde{\theta} \parallel + |l_1|)(Lk_2 \parallel z_2 \parallel + \xi L k_2 \parallel z_1 \parallel + \xi L k_3 \parallel \tilde{\theta} \parallel + \xi L |l_1| \quad (5.23)\end{aligned}$$

Finally, the Lyapunov function for the estimator may be chosen as $V_3(\tilde{\theta}(k)) = \tilde{\theta}(k)^T\tilde{\theta}(k)$. Thus,

$$\begin{aligned}\triangle V_3(k+1) &\triangleq V_3(\tilde{\theta}(k+1)) - V_3(\tilde{\theta}(k)) \\ &= \| \tilde{\theta}(k) - \frac{a\psi(k_1)}{c+\psi^T(k_1)\psi(k_1)}\psi(k_1)\tilde{\theta}(k) \|^2 - \tilde{\theta}(k)^T\tilde{\theta}(k) \\ &= a\frac{[\tilde{\theta}^T(k)\psi(k_1)]^2}{c+\psi^T(k_1)\psi(k_1)}\left[-2 + a\frac{\psi^T(k_1)\psi(k_1)}{c+\psi^T(k_1)\psi(k_1)} \right] \qquad (5.24)\end{aligned}$$

where $k_1 \triangleq k-d+1$. Now if $c > 0$ and $0 < a < 2$ are assumed, the bracketed term is negative and consequently $\triangle V_3(k+1) \leq 0$ or $\tilde{\theta} \in l_\infty$. Since $\| \hat{\theta}(k) - \theta \| \leq \| \hat{\theta}(0) - \theta \|$ for all $k \geq 1$, we can conclude that $\| \tilde{\theta} \| \leq \delta$ with $\| \hat{\theta}(0) \| - \delta \leq \| \theta \|$. In other words, since $\| \hat{\theta}(0) \|$ is at our disposal, by choosing δ to satisfy the previous inequality we are assuming a priori knowledge about the lower bound for θ. At this stage the Lyapunov function candidate for the whole system may be written as

$$V(e(k), z_2(k), \tilde{\theta}(k)) = V_1(e(k)) + V_2(z_2(k)) + V_3(\tilde{\theta}(k))$$

At this stage the Lyapunov function candidate for the whole system is selected as

$$V(e(k), z_2(k), \tilde{\theta}(k)) = V_1(e(k)) + V_2(z_2(k)) + V_3(\tilde{\theta}(k)) \qquad (5.25)$$

In view of (5.16), (5.23) and (5.24), $\triangle V(k+1)$ satisfies

$$\begin{aligned}\triangle V(k+1) &\triangleq \triangle V_1(k+1) + \triangle V_2(k+1) + \triangle V_3(k+1) \\ &\leq -\lambda_{min}(Q) \| e \|^2 + (c_1 \| e \| + c_2|\varsigma|)|\varsigma| - \alpha \| z_2 \|^2 \\ &+ (k_2 \| z_1 \| + k_3\delta + |l_1|).(Lk_2 \| z_2 \| + \xi Lk_2 \| z_1 \| + \xi Lk_3\delta + \xi L|l_1|) \\ &+ a\frac{[\tilde{\theta}^T(k)\psi(k_1)]^2}{c+\psi^T(k_1)\psi(k_1)}\left[-2 + a\frac{\psi^T(k_1)\psi(k_1)}{c+\psi^T(k_1)\psi(k_1)} \right] \qquad (5.26)\end{aligned}$$

Now let's make the following additional assumptions:

Assumption 5.2 *The function l_1 is locally sector bounded, namely, it satisfies $|l_1| \leq a_1 \| \hat{\theta} \| + a_2 \| e \| + a_3 \| z_2 \|$ for $e \in \Omega_e$, $z_2 \in \Omega_{z_2}$ and $\hat{\theta} \in \Omega_{\hat{\theta}}$.*

Assumption 5.3 *The vector $\psi(k)$ is locally sector bounded in $z(k)$ and $\hat{u}(k)$ for $z \in \Omega_z$ and $\| \hat{\theta} \| \in \Omega_{\hat{\theta}}$. That is, $\| \psi(k) \| \leq l_z(\| z \| + \| \hat{\theta} \|)$.*

Assumption 5.4 *The reference trajectory $y_m(k)$, its next $d-1$ samples and the last $n-1$ samples are all bounded by constant $b > 1$, so that $\| z_1 \| < \| e \| + b$.*

Since $z(k)^T = [z_1^T(k) \;\; z_2^T(k)]$, one may conclude that

$$\| z \| \leq \| z_1 \| + \| z_2 \| \leq \| e \| + \| z_2 \| + b \tag{5.27}$$

As a result, compact set Ω_z contains the union of Ω_e and Ω_{z_2} defined in Assumptions 5.2 and 5.3. Note that based on previous Assumptions $\| \varsigma \| = \delta l_z(\| z \| + \| \hat{\theta} \|)$. Using Assumptions 2-4 and the fact that $b > 1$ and $\| z_2 \| > 0$, one may rewrite (5.26) as

$$\begin{aligned} \triangle V(k+1) \;\leq\; & -\lambda_{min}(Q) \| e \|^2 - \alpha \| z_2 \|^2 \\ & + (\| e \| + \| z_2 \| + b)^2 (1 + \| \hat{\theta} \|)(c_1 l_z \delta + c_2 l_z^2 \delta^2 (1 + \| \hat{\theta} \|)) \\ & + (\| e \| + \| z_2 \| + b)^2 (d_1 + k_2 \delta + a_1 \| \hat{\theta} \|)^2 \end{aligned} \tag{5.28}$$

with suitable definitions for constant d_1. To guarantee the stability of the closed-loop system consisting of (5.10), (5.11) and (5.14), we need $\triangle V(k+1) \leq 0$. It then follows that the closed-loop system is stable in the sense of Lyapunov if $\| \hat{\theta} \|$ satisfies the following inequality

$$M(\hat{\theta}, \delta) \leq \frac{1}{(\| e \| + \| z_2 \| + b)^2} (\lambda_{min}(Q) \| e \|^2 + \alpha \| z_2 \|^2) \tag{5.29}$$

with $M(\hat{\theta}, \delta) \triangleq d_1(1 + \| \hat{\theta} \|)^2 + d_2(d_3 + \| \hat{\theta} \|)^2$. The above gives a bounded region, say $\Omega_{\hat{\theta}}$, for $\| \hat{\theta} \|$ in terms of $e \in \Omega_e$ and $z_2 \in \Omega_{z_2}$ such that inside this region, $\triangle V(k+1) \leq 0$. To make sure that $\hat{\theta}(k)$, $e(k)$ and $z_2(k)$ all belong to l_∞ one should find the largest level set $V(e, z_2, \tilde{\theta}) = c$ contained in $\triangle V(k+1) \leq 0$. Now given the fact that V is a function of $\tilde{\theta}$ we express it as a function of $\hat{\theta}$ as follows. We observe that $V(e, z_2, \tilde{\theta}) = V_1 + V_2 + V_3$ where $V_3 = \| \tilde{\theta}(k) \|^2 \leq \| \hat{\theta}(k) \|^2 + 2\delta_u \| \hat{\theta}(k) \| + \delta_u^2$

with δ_u as the upper bound of the parameter θ, i.e. $\| \theta \| \leq \delta_u$. Therefore, we get $V_n(e, z_2, \hat{\theta}) = V_1 + V_2 + \| \hat{\theta}(k) \|^2 + 2\delta_u \| \hat{\theta}(k) \| + \delta_u^2$ so that $V \leq V_n \leq c$, $c > 0$ and $V_n = c$ is the largest level set contained in $\Delta V(k+1) \leq 0$. Thus, for all $(e, z_2, \hat{\theta}) \in \Omega_c$ and $\hat{\theta} \in \Omega_{\hat{\theta}}$, $V(k+1) > 0$ and $\Delta V(k+1) \leq 0$, which in turn implies the boundedness of all the closed-loop system signals.

Next it is shown that the tracking error $e_n(k) \triangleq y(k) - y_m(k)$ goes to zero as $k \to \infty$. Since the Lyapunov function of the parameter estimator satisfies $\Delta V_3(k+1) \leq 0$, it follows that the estimation error $\tilde{\theta}(k)$ is monotonically non-increasing. Therefore, as $k \to \infty$, $\tilde{\theta}(k)$ approaches to a steady-state value and $\tilde{\theta}(k+1) \to \tilde{\theta}(k)$. As a result, $\Delta V_3(k+1) = \tilde{\theta}^T(k+1)\tilde{\theta}(k+1) - \tilde{\theta}^T(k)\tilde{\theta}(k) \to 0$, so from (5.24) one may conclude directly that

$$\frac{[\tilde{\theta}^T(k)\psi(k-d+1)]^2}{c + \psi^T(k-d+1)\psi(k-d+1)} \to 0 \tag{5.30}$$

There are two ways for which (5.30) can approach to zero. One way is for the numerator to go to zero and the other way for the denominator to go to infinity. The latter is impossible since we just showed that $\psi \in l_\infty$. Hence, as $k \to \infty$, $\psi(k) = \psi(k-d+1)$ and $\tilde{\theta}^T(k)\psi(k) \to 0$. As a result of this, $\varsigma \to 0$ and in the error equation (5.10) $B\varsigma \to 0$. Since A is a Hurwitz matrix, then one gets $e(k) \to 0$ as k goes to infinity. This implies that $e_n(k) \triangleq y(k) - y_m(k) \to 0$ as $k \to \infty$.

5.6 Numerical Simulations

In this section, we use the following unknown system which is a special case of the general system (5.1) and was considered in [9].

$$y(k+1) = w_1[y(k)y(k-1) + u(k-1)] + v_1 u(k) \tag{5.31}$$

where it is assumed that w_1 and v_1 are unknown. The objective is to compare our results with those given in [9]. Comparing (5.31) with (5.1) reveals that $n = 2$,

$m = 1$ and $d = 1$. Therefore, by taking $z_{11}(k) \triangleq y(k-1)$, $z_{12}(k) \triangleq y(k)$ and $z_{21}(k) \triangleq u(k-1)$ the state-space realization of (5.31) becomes

$$\begin{aligned} z_{11}(k+1) &= z_{12} \\ z_{12}(k+1) &= w_1[z_{12}(k)z_{11}(k) + z_{21}(k)] + v_1 u(k) \\ z_{21}(k+1) &= u(k) \end{aligned} \tag{5.32}$$

Our goal is to control this plant so that its output tracks a reference command $y_m(k)$. To use the method of this chapter the first requirement is exponential stability of the zero dynamics. Thus, the appropriate input that keeps $y(k)$, $y(k+1)$ and $y(k+2)$ identically zero becomes $u(k) = -\frac{w_1}{v_1} z_{21}(k)$ which after substituting into internal dynamics (last row in (5.32)) the zero dynamics is found as

$$z_{21}(k+1) = -\frac{w_1}{v_1} z_{21}(k)$$

which is globally exponentially stable as long as $|\frac{w_1}{v_1}| < 1$. Thus, the linearizing input becomes

$$u(k) = \frac{1}{\hat{v}_1(k)} \left[\; v(k) - \hat{w}_1(k)(z_{12}(k)z_{11}(k) + z_{21}(k)) \; \right]$$

where the new input is defined as $v(k) \triangleq y_m(k+1) + \alpha(y_m(k) - y(k))$. It is evident that to guarantee the closed-loop stability, we should have $|\alpha| < 1$. To use the projection algorithm for parameter estimation, system (5.31) should be rewritten into the regressor form $y(k+1) = \psi^T(k)\theta$ where

$$\begin{aligned} \psi^T(k) &\triangleq [y(k)y(k-1) + u(k-1) \quad u(k)] \\ \theta^T &= [w_1 \quad v_1] \end{aligned}$$

The system is adaptively controlled to track the sinusoidal reference trajectory $y_m(k) = \sin(\frac{k}{5})$. Figure 5.1 shows the result when $\hat{w}_1(0) = 4$ and $\hat{v}_1(0) = 0.8$. To compare our results with the results of [9], let $\hat{v}(0) = 1.2$ be fixed. When $y(0) = 0$, [9] showed that with $\tilde{w}_1(0) \triangleq \hat{w}_1(0) - w_1 > 3.8$ the closed-loop becomes unstable

whereas with our method we may choose $\tilde{w}_1(0) > 5.55$. Figure 5.2 shows the simulation results for this case. Also when $y(0) = 5$, they showed that if $\tilde{w}_1(0) > 1.1$ the system diverges whereas we found that $\tilde{w}_1(0) > 2.3$. For the last comparison, when $y(0) = 10$, the instability condition is given as $\tilde{w}_1(0) > 0.8$ whereas our simulation shows if $\tilde{w}_1(0) > 1.95$ the closed-loop system becomes unstable. As a result, the proposed method in this chapter gives a wider region of attraction for closed-loop system.

5.7 Conclusions

A direct adaptive tracking control approach for a discrete-time nonlinear system represented in an input-output form with relative degree equal or greater than one is developed. A *projection algorithm* is used to identify the unknown parameters that in turn are utilized in the feedback linearizing controller. It is shown that under certain assumptions (a priori lower and upper bound of the unknown parameters), the adaptively controlled closed-loop system is stable locally and moreover, the tracking error approaches to zero as k tends to infinity.

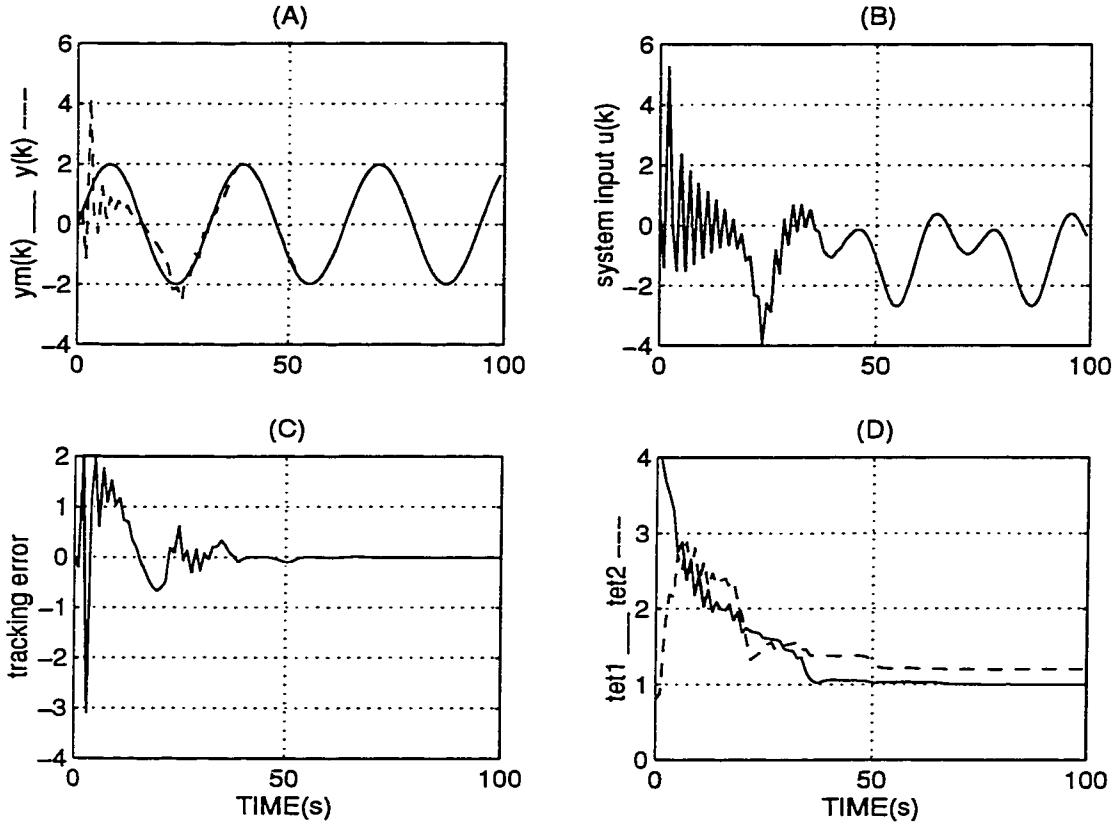

Figure 5.1: Direct adaptive tracking control. (A) output $y(k)$ ___ and the desired output $y_m(k)$ $--$, (B) control input $u(k)$, (C) tracking error $y(k) - y_m(k)$, (D) estimate of the unknown parameters θ_1 ___ and θ_2 $--$ when $\tilde{v}_1(0) = 0.8$ and $\tilde{w}_1(0) = 4$

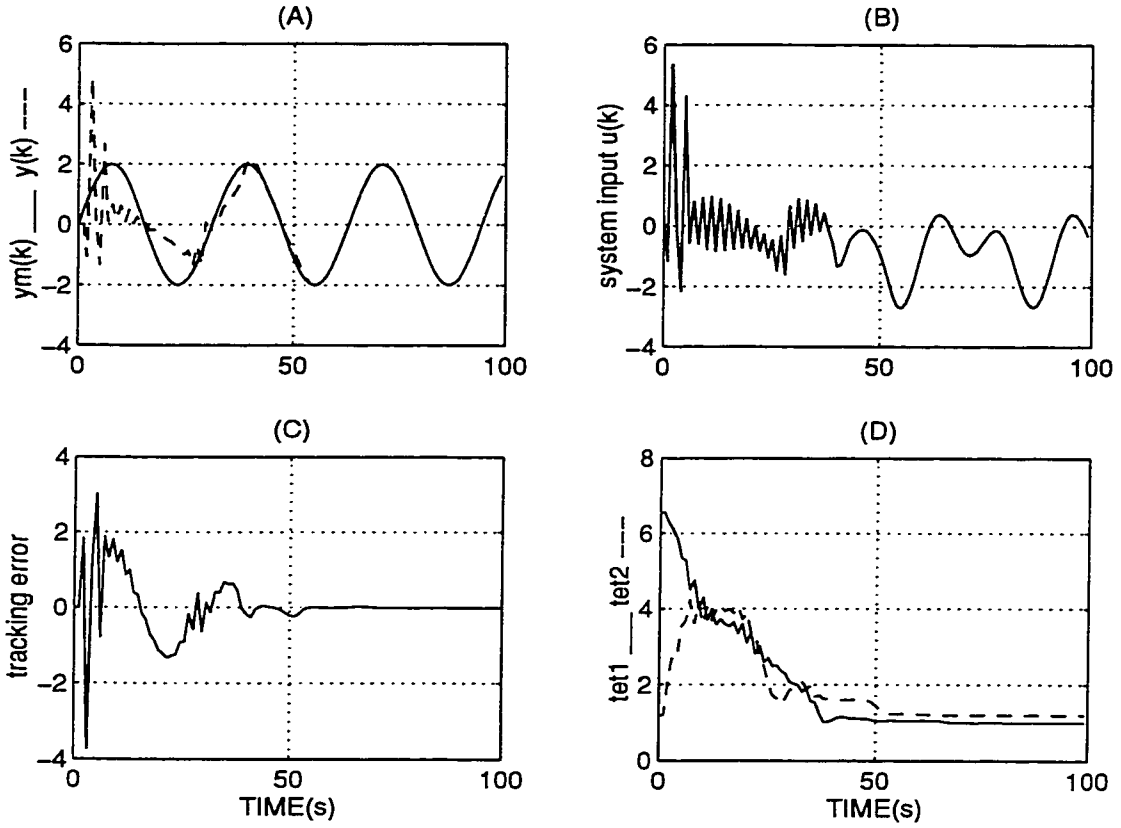

Figure 5.2: Direct adaptive tracking control. (A) output $y(k)$ ___ and the desired output $y_m(k)$ $- -$, (B) control input $u(k)$, (C) tracking error $y(k) - y_m(k)$, (D) estimate of the unknown parameters θ_1 ___ and θ_2 $- -$ when $\tilde{v}_1(0) = 1.2$ and $\tilde{w}_1(0) = 5.55$

Chapter 6

Control of a Flexible-Link Manipulator: Experimental Results

The aim of this chapter is two folds. First to show that the proposed adaptive nonlinear feedback linearization technique can be used successfully to control a single-link flexible manipulator. Second to illustrate the experimental results for the nonlinear adaptive control scheme proposed in chapter 4 and compare the results with non-adaptive feedback linearization and PD controller schemes. Figure (6.1) shows the experimental test-bed developed by Geniele [18] that consists of four principal components:

- Single flexible link manipulator along with UDT camera, camera signal conditioning amplifier, speed reducer, incremental encoder, DC servo motor and DC servo amplifier.
- Interface board.
- TMS320C30 system board.

- The host PC.

The TMS system board implements the real-time control and identification algorithms and at the beginning of each sampling period sends the control signal to the D/A converter. This signal in turn goes to DC servo amplifier which is configured as a transconductance amplifier, namely, it changes input voltage to output current in order to control the speed of the DC servo motor. The DC servo motor is connected to the flexible link through a speed reducer to decrease the speed and increase the torque since the motor has high speed and relatively low torque. To measure the hub angle, an incremental optical encoder is employed at the motor side. Also for measuring the tip deflection, a combination of an infrared emitting diode along with a camera is used. At the beginning of each sampling period the diode current is pulsed and the camera reads the tip deflection with respect to the natural position. The signal conditioning amplifier interfaces the output of the UDT camera to the A/D converter on the TMS board.

The host PC serves as a platform for TMS board and allows the user to interact with the control program and at the same time transfers the real-time data from board memory to hard disk for subsequent analysis. The functions of the interface board are to protect the DC servo motor when the system becomes unstable, to decode the incremental encoder output, to trigger the infrared diode and to provide the regulated voltage for the board. The following specifications of the test-bed components are taken from [18].

TMS320C30 System Board

The function of this board is to implement the real-time controller and identifier algorithms. It contains a Texas Instruments TMS320C30 DSP chip that operates

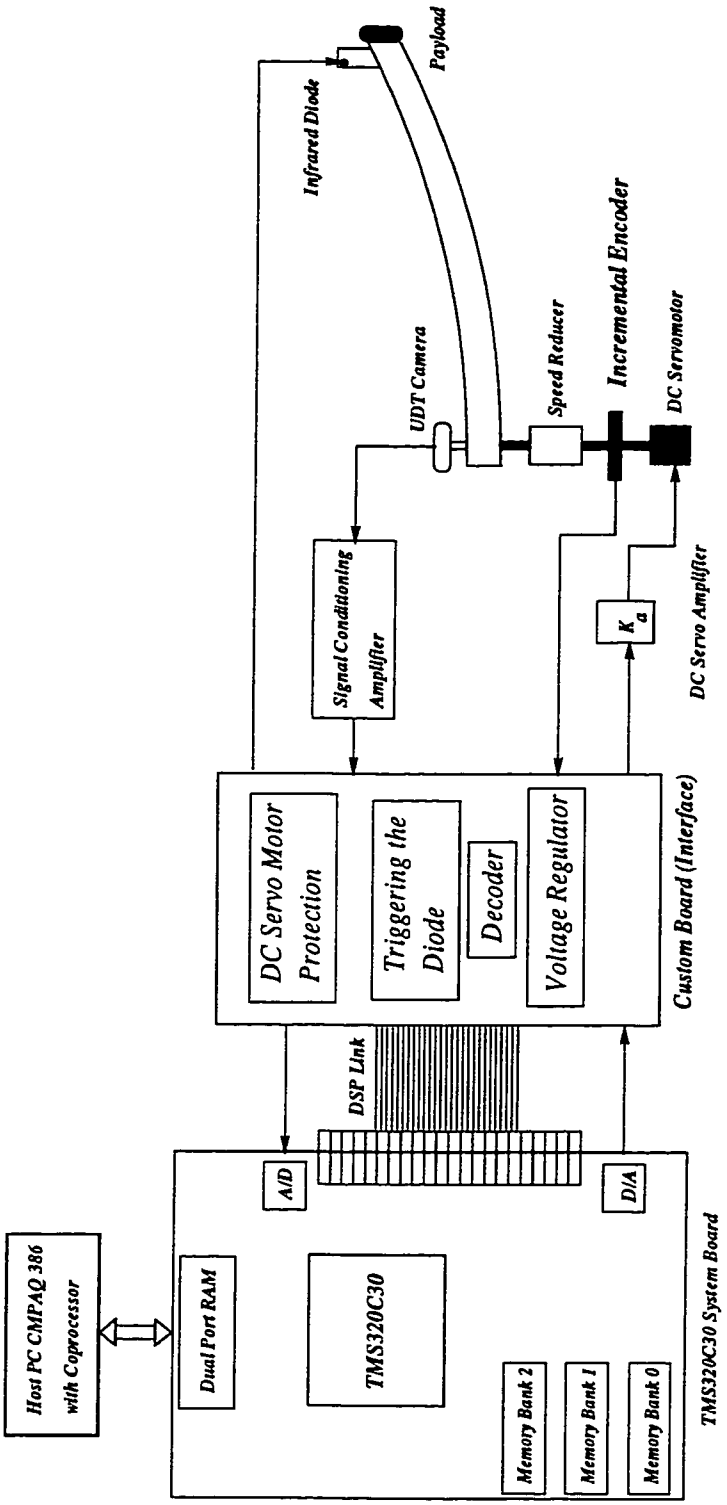

Figure 6.1: Experimental test-bed for controlling a single-link flexible manipulator

in 33.3 MHz clock and achieves a performance of 16.7 million instruction per second (MIPS) and 33.3 million floating-point operations per second (MFLOPS). Dual channel 16-bit A/D and D/A systems are included on the board. Sampling rates of up to 200 kHz are supported. The input channels include sample/hold amplifiers and both input and output channels are buffered through $4th$ order low pass filter. The full scale analog and output ranges are ± 3 *volt*. The board occupies a single 16-bit slot within a COMPAQ 386 host PC expansion bus. The board appears to the programmer as a block of eight 16-bit words within the I/O space. The board comes configured with a default I/O base address of 290 *hex*. The data is exchanged between the PC and TMS board by $64k \times 32$ bit words of Dual-Port-RAM. The TMS320C30 system board are equipped with the DSPLINK digital system expansion bus. DSPLINK is a high-speed, bi-directional bus that allows input/output directly to/from the DSP chip, thereby avoiding the PC bus bottleneck. In our system this bus is connected to a separate interface board. This board contains the programming timing circuitry which control the current through the infrared diode on tip of the flexible-link. It also incorporates the circuitry that decodes the incremental encoder since the encoder gives only relative motor position.

DC Servo Amplifier

The Copley Controls Corp. Model 215 [11] is a PWM switching amplifier designed to drive the DC servo motor. This model is configured as a transconductance amplifier which gives a linear relationship between input voltage and output current independent of the output impedance, namely, $i_{out} = 2v_{input}$. Since the full scale voltage of A/D is ± 3 *volts*, the maximum current of DC servo amplifier would be ± 6 A.

DC Servo Motor

The DC servo used is a permanent magnet DC motor from EG&G Torque Systems, Model MH3310-055G1 which develops a linear output torque, namely, $\tau_{output} = 0.1175\ i_{input}\ Nm$. Due to the fact that the maximum output current of DC servo amplifier is $\pm 6\ A$, the maximum torque range generated by motor will be $\pm 0.1175 \times 6 = \pm 0.705\ Nm$.

Incremental Encoder & Decoder

The Motion Control Devices Inc. Model M21 is an optical encoder that provides incremental resolution of 500 $\frac{cycle}{revolution}$ on each of two quadrature (A & B) signals in the motor side. The Hewlett Packard HCTL–2020 is an IC that performs quadrature decoder, counter and bus interface functions. The two incoming quadrature signals from the incremental encoder are decoded. The resolution of 500 $\frac{cycle}{revolution}$ is multiplied by a factor of four to yields a resolution of 2000 $\frac{cycle}{revolution}$. An on-chip binary counter allows to compute the absolute position.

Speed Reducer

Since the motor is a high speed and low torque actuator, it is geared down to provide sufficient torque to derive the flexible link. The HD Systems Inc. Model RH20-CC speed reducer connect the motor shaft to the link's hub. A gear ration of 1 : 50 ensures that sufficient torque is available to accelerate the link in reasonable speed. Since the maximum motor torque is $\pm 0.705\ Nm$, the amplified torque to the hub will be $\pm 0.705 \times 50 = \pm 32.25\ Nm$. Harmonic derive results in a low backlash which is essential to reduce the position error at hub. The HCTL-2020 decoder gives a resolution of 2000 $\frac{cycle}{revolution}$. Now since the counter of decoder is limited to 16 bits, the decoder can accommodate $2\pi\frac{2^{16}-1}{2000} = 65.535\pi\ rad$ of rotation in motor side or

$\frac{65.535}{50}\pi = 1.3107\pi\ rad$ in link side before overflowing.

UDT Camera

The United Detector Technology Model 274 camera [82] consists of a wide angle lens and a lateral-effect photodiode detector assembly. The 12.5 *mm* lens has a 55.5° field of view and includes a visible light blocking filter to filter out the ambient light. The lens focuses the infrared diode emitted light onto an SC-10D photodiode detector and induces currents at each of the contacts of the decoder. Since the magnitude of the current at a particular contact is proportional to the contact's proximity to the spot of the light, the relative magnitude of the currents are used to determine the absolute position of the spot.

Infrared Diode

Since the positional resolution of the tip deflection is proportional to the signal to noise ration (S/N) of the received signal at the output of camera, one way to maximizing the S/N is to use a high powered light source. The Opto Diode OD-50L Super High Power GaAlAs infrared diode supplies up to 0.6 *watts* of optical power at a wave length of 880 *nm*. Due to thermal limitations, the maximum amount of power is attainable only when the diode current is pulsed at the beginning of each sampling period with a minimized duty cycle. The current control circuitry on the interface board allows adjustment of the current level and the duty cycle.

UDT Signal Conditioning Amplifier

The United Detector Technology Model 302DIV [82] signal conditioning amplifier interfaces the position sensing photodetector to the A/D converter of the TMS board. The amplifier is configured as transimpedance which converts the incoming

low level currents to a amplified output voltage. The amplifier is adjusted so that maximum tip position of ± 25 *cm* correspond to output voltage of ± 3 *volts*. The 55° lens field of view will allow to measure the tip deflection up to ± 50 *cm*. However, as the magnitude of the tip deflection increases, the position of diode rotates viewed from the camera's frame of reference. The increasing of tip deflection along with the narrow beam width of the infrared diode results in a reduction of the optical power received at the camera. Therefore, beyond a deflection of ± 25 *cm*, the infrared diode cannot be detected accurately by the camera even though it is still within the camera's field of view. Noise and nonlinearities within the photodiode detector result in a measurement error of ± 0.25 *cm* within a deflection range of ± 10 *cm*. As the tip deflection increases to a maximum of ± 25 *cm*, the error increases to ± 1 *cm*.

6.1 Real-Time Implementation of the Controller and the Identifier

To implement the adaptive feedback linearization and tracking control strategy developed in Chapter 4, we require all states to be available. Since the number of flexible modes considered is one, we should therefore have four states available, namely, hub angle (q), its derivative ($\dot{q}$), the first flexible mode (δ_1) and its derivative ($\dot{\delta}_1$). For our given test-bed, it is clear that we can only measure q and δ_1. Therefore, $\dot{q}$ and $\dot{\delta}_1$ should be calculated numerically. Since the sampling period is $T = \frac{1}{200}$, it was observed that instead of using a simple backward difference for differentiation, a kind of first order filter gives a better response. Namely, instead of using $\dot{q}(kT) = \frac{q(kT)-q(kT-T)}{T}$, the bilinear (Tustin) discretization of the filter $D(s) = \frac{s}{s+10}$ is used where the discretized filter becomes

$$D(z) = \frac{s}{s+10}\Big|_{s=\frac{2}{T}\frac{1-z^{-1}}{1+z^{-1}}}$$

Therefore, the above filter results in the following recursions for $\dot{q}$ and $\dot{\delta}_1$, respectively

$$\dot{q}(kT) = 9.09091(q(kT) - q(kT-T)) + 0.9802\dot{q}(kT-T)$$
$$\dot{\delta}_1(kT) = 9.09091(\delta_1(kT) - \delta_1(kT-T)) + 0.9802\dot{\delta}_1(kT-T)$$

Note that the incremental encoder gives $q(kT)$ in the motor side which in the link side should be divided by the speed reducer gear ratio 50. In addition, since the UDT camera gives the tip deflection $w(L,t) = \sum_{i=1}^{m} \phi_1(L)\delta_1(t) = \phi_1(L)\delta_1(t)$ and not δ_1, one should calculate δ_1 by dividing the output signal of the camera by $\phi_1(L)$. As a result, the four states considered in both controller and identifier are as follows

$$x_1 = \frac{\theta(kT)}{50}$$
$$x_2 = 9.09091(x_1(kT) - x_1(kT-T)) + 0.9802x_2(kT-T)$$
$$x_3 = \frac{w(L,kT)}{\phi_1(L)}$$
$$x_4 = 9.09091(x_3(kT) - x_3(kT-T)) + 0.9802x_4(kT-T)$$

where $\theta(kT)$ and $w(L,kT)$ are output signal of incremental encoder and UDT camera, respectively. The real-time control and identification algorithms were coded in DSP C-language. In addition, the PC monitor program, which downloads the DSP program into the TMS system board and transfers the real-time data from board memory to the hard disk, was coded in Turbo C-language. In the following, after showing the model validation results, the real-time controller results are discussed.

6.2 Model Validation

In order to validate the accuracy of the dynamical model of a single-link flexible manipulator represented by Equation (C.11), the response of the hub (joint) angle and tip deflection to different motor torque inputs are obtained for both simulation and real test-bed applications. Simulations in Figures (6.2B) and (6.2C) compare both the joint angle and tip deflection for different values sets Coulomb friction

coefficient (c_{fri}) with those of the actual test-bed subject to the input torque $\tau_1(t)$ shown in Figure (6.2A). Looking carefully at these results reveals that the best of Coulomb frictions for this case is $c_{fri} = 4.8\ Nm$ for $\dot{\theta} > 0$ and $c_{fri} = 4.55\ Nm$ for $\dot{\theta} < 0$.

To further verify the above results, a different torque $\tau_2(t)$ shown in Figure (6.2D), is applied to both mathematical model and the test-bed. The results are shown in Figures (6.2E) and (6.2F) where one set of simulation result is compared with three different sets of experimental results. The experiments are performed with the same input torque τ_2 but with different initial joint positions. As Figures (6.2E) and (6.2F) illustrate, one can conclude that the Coulomb friction coefficient is not fixed and does depend on the initial link position.

Furthermore, it may be shown that a single set of coefficients cannot be found that yields good agreement between the responses of the model and the test-bed. To demonstrate this, a new torque τ_3 shown in Figure (6.3A) is applied to both the actual test-bed and the model and the results are shown in Figures (6.3B) and (6.3C). Based on these results one can conclude that the previous set of Coulomb friction coefficients does not necessarily result in the best agreement between the test-bed and the model responses. Specifically, the set $c_{fri} = 4.95\ Nm$ for $\dot{\theta} > 0$ and $c_{fri} = 4.6\ Nm$ for $\dot{\theta} < 0$ gives the best agreement in this case. Nevertheless, the discrepancy between the simulation and experimental results is minimal and the set of Coulomb friction coefficients mentioned earlier are considered to be the nominal values.

Finally further model simulations and test-bed experiments are performed when the open-loop system from input torque to output joint angle is closed by means of a relatively high gain PD controller. With this new design, the effects of the Coulomb

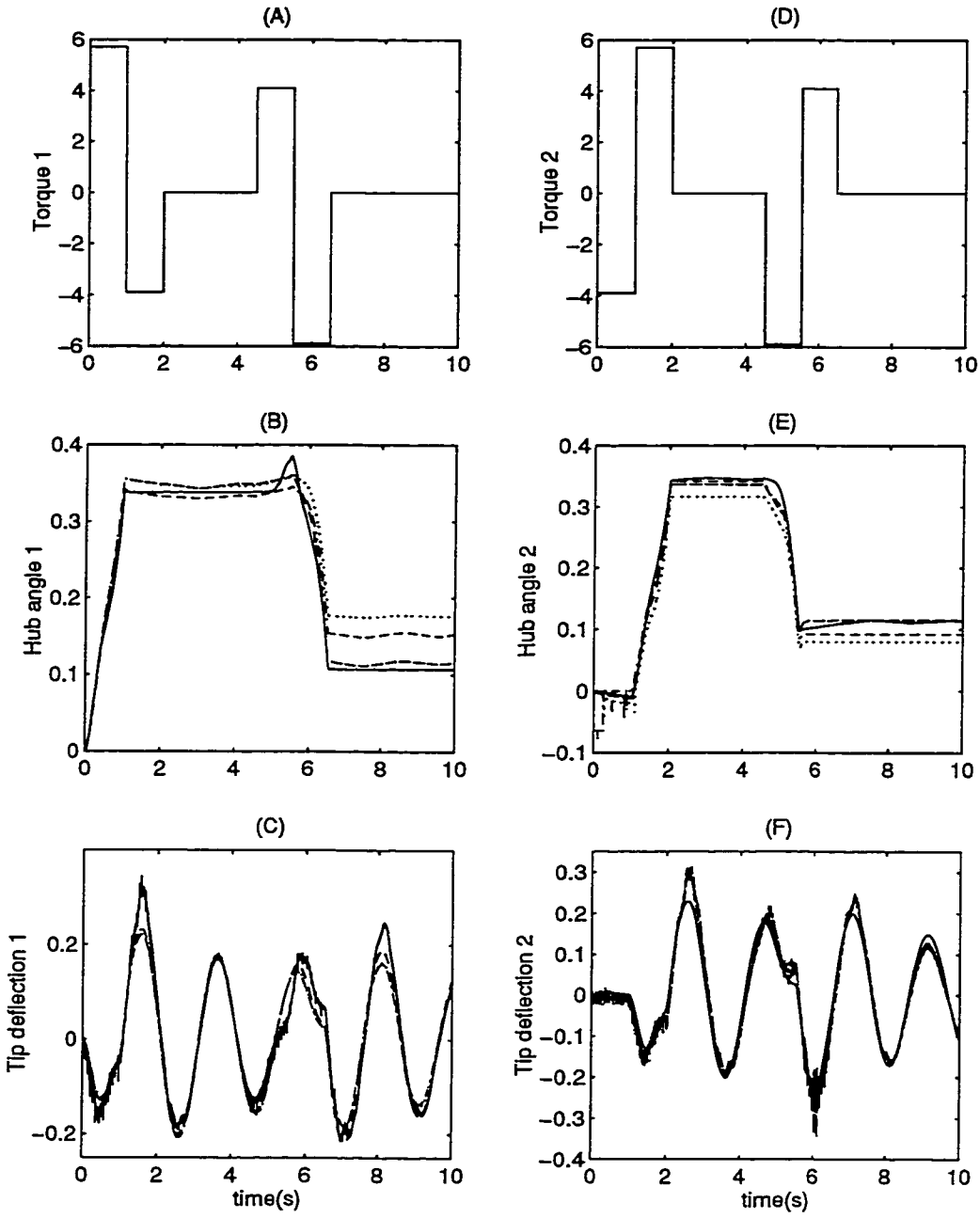

Figure 6.2: *Model Validation:* (A) applied torque $\tau_1(t)$, (B) joint angle $\theta_1(t)$, (C) tip deflection $w_1(L,t)$, where ___ represents the experimental result and the remaining curves are for model simulations with ——, —. — . and .... for $(4.8, 4.55)$, $(4.95, 4.6)$ and $(4.95, 4.55)$ Coulomb friction coefficients, respectively. (D) applied torque $\tau_2(t)$, (E) joint angle $\theta_2(t)$, (F) tip deflection $w_2(L,t)$, where ___ represents the model simulations with $(4.8, 4.55)$ Coulomb friction coefficients and the remaining curves correspond to experimental results.

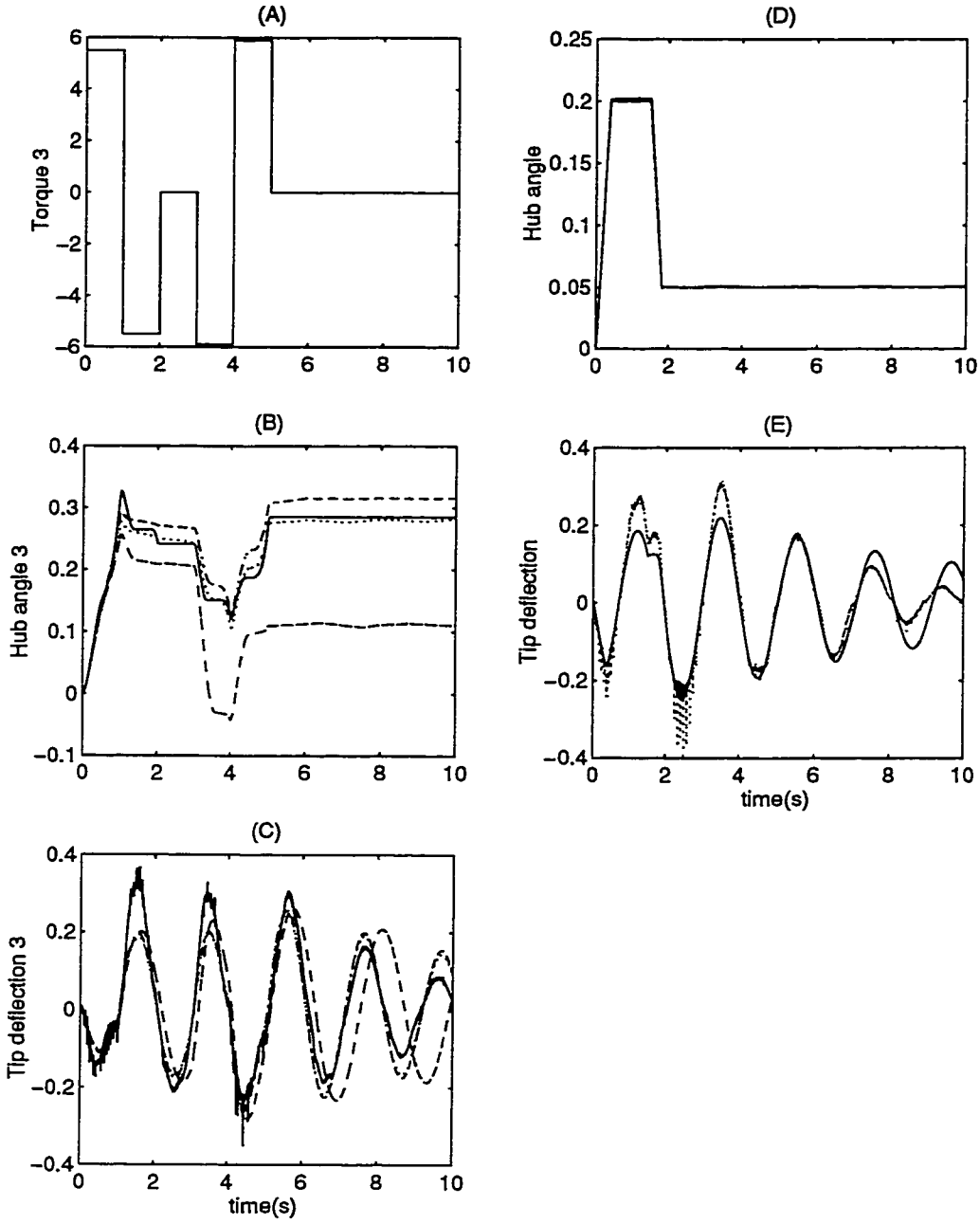

Figure 6.3: *Model Validation:* (A) applied torque $\tau_3(t)$, (B) joint angle $\theta_3(t)$, (C) tip deflection $w_3(L,t)$, where $\_\_$ represents the experimental result, and the remaining curves are for model simulations with $--$, $-.-$ and .... for $(4.8, 4.55)$, $(4.95, 4.6)$ and $(4.95, 4.55)$ Coulomb friction coefficients, respectively. (D) to (F) closed-loop responses of dynamical model and real test-bed with PD controller. (D) reference trajectory and hub angle, (F) tip deflection, where $\_\_$ represents the responses of dynamical model with $(4.8, 4.55)$ Coulomb friction coefficients and .... represents the experimental results.

friction will be reduced to a large extent and therefore the remaining dynamics of the link's model with those of real test-bed can be compared. Suppose the desired hub angle trajectory is given by Figure (6.3D). Figure (6.3D) also illustrates the joint angle of the closed-loop system when a high gain PD controller is used. Obviously there is a close agreement between the simulated and the experimental joint angles that in turn confirms the effectiveness of the PD joint controller. To get a better assessment of the results, the tip deflections are also depicted in Figure (6.3E). Again there is a good agreement between the simulated hub angle and tip deflection and those of the real test-bed. These results reveal that when the effects of the Coulomb friction are reduced significantly, the dynamical equation obtained for the single-link flexible manipulator can model the test-bed with a good accuracy and is therefore a suitable model for the design of a controller.

6.3 Experimental Results

Referring to the results of Chapter 4, we have seen that the dynamical equations of the single-link flexible manipulator is minimum phase for $\alpha < 0.906$. This condition was confirmed through several simulations provided that all the states are available for feedback and are also without measurement noise. For the real implementation, however, we cannot select α close to 0.906. On one hand, not all of the four states are available for feedback and actually we have to construct them numerically. On the other hand, the signals from the incremental encoder and particularly the camera are corrupted by noise. These corrupted signals when coupled with the saturation limit of the UDT signal conditioning amplifier result in a further limitation for the choice of α (or β_1). During real-time experiments it is observed that $\alpha = 0.25$ (or $\beta_1 = \frac{\alpha\phi_1(L)}{L} = \frac{0.25\times 2}{1.2} = 0.4167$) is quite feasible given the above constraints. Although a larger value of α could have been selected, in some cases when the noise

level becomes too high or when the amplifier saturates the closed-loop system becomes actually unstable. Consequently, all the following experimental results are obtained with $\alpha = 0.25$ and the sampling period of $T = \frac{1}{200}$.

For comparison, Figure (6.4) shows the numerical simulations for the adaptive tracking controller with $\alpha = 0.25$ when the input reference trajectory is a combination of a quintic and a step functions. The tracking error for the re-defined output ($e = y - y_m$) is practically zero however, the tracking error for the actual tip position ($e_t = y_t - y_m$) is non-zero due to the value of α (Note that $\alpha = 1$ for the normalized tip position). Also the identifier works properly and within 0.2 s it converges to the real value of the payload mass (0.55 kg).

The experimental results for the non-adaptive tracking controller are depicted in Figures (6.5) to (6.8) for different nominal values of payload used in the controller. In these experiments the actual value of payload is $M_L = 0.55\ kg$. The values of payload used in the controller $(M_L)_{controller}$ is varied from 0.1 kg to 2 kg. A Comparison of the above figures reveals that although the closed-loop system does not become unstable for the cases considered, however the re-defined tracking error is almost zero when $(M_L)_{controller}$ is equal to 0.55 kg. In other words, when the payload is exactly known *a priori*, a nonlinear feedback controller can be designed that yields acceptable performance. However, when there is an uncertainty about the payload the performance of the non-adaptive controller will be compromised.

There is also a difference between the simulation and the experimental results. Specifically there is no oscillations in the experimental tip position, the re-defined output and the input torque beyond 5 s. This is most probably due to the additional damping effects of the Coulomb friction that is inherent in the flexible link manipulator and other damping effects that are treated as unmodeled dynamics in the system.

To compare the experimental results of the non-adaptive tracking controller with those of the adaptive controller, Figure (6.9) shows the results for the adaptive controller with initial condition $\hat{M}_L(0) = 0.1$. As Figure (6.9E) illustrates the real-time identifier converges to 0.4 kg instead of actual payload mass of 0.55 kg. However, the simulation results in Chapter 4 showed that the identifier converges to the actual payload mass. The reasons for this discrepancy are two folds. First, due to the sensor noise (incremental encoder and UDT camera), the RLS algorithm will yield a biased estimate. Second, since all four states of the system $(q, \delta, \dot{q}, \dot{\delta})$ were not available for measurement, two of them $(\dot{q}, \dot{\delta})$ are constructed numerically that in turn introduce error to identifier. Figures (6.9A) and (6.9B) depict the normalized re-defined output and the normalized tip position, respectively. As expected, the results are satisfactory. In addition, Figures (6.10) and (6.11) illustrate the experimental results for the adaptive controller with different initial conditions $\hat{M}_L(0) = 1$ and $\hat{M}_L(0) = 1.5$, respectively. Comparing these results with the results of Figure (6.9) reveals that the real-time identifier suffers from the same problem, namely, it converges to a biased estimate of payload. Nevertheless, the performance of closed-loop system consisting of adaptive controller and identifier is acceptable.

Figure (6.12) shows the experimental results for the adaptive controller when the desired trajectory is chosen as four quintic functions and $\hat{M}_L(0) = 0.1$. In this case both the normalized re-defined output y and the normalized tip position y_t can track the desired output y_m since the desired trajectory is slower than the previous case. Note that there are some spikes in input $u(k)$, error and internal dynamics which are due to the incremental encoder noise.

Finally to emphasize the advantages of the adaptive and non-adaptive feedback linearization method over a conventional control technique, experimental results

are included for a PD controller in Figures (6.13) to (6.16) with different values of K_p and K_d. The closed-loop system becomes unstable for K_p greater than 200. Figure (6.13) shows the results ($K_p = 100$ and $K_d = 60$) for the experimental tip position and the re-defined output with noticeable steady state errors. The errors can be attributed to the presence of the Coulomb friction. To reduce the steady state error K_p is increased. The results are depicted in Figures (6.14) and (6.15). Although the steady state error is improved as compared to $K_p = 100$, however the system will become unstable for $K_p > 200$. To summarize, it can be concluded that the performance of a conventional PD control technique is unsatisfactory when compared to the results of an adaptive nonlinear feedback linearization technique since the closed-loop system has steady state error. Note that the selection of controller has a trade-off between the complexity of controller-identifier and the acceptable performance of closed-loop system. Although the performance of PD controller is not as good as that of the adaptive feedback linearization, the price we are paying is complexity of controller.

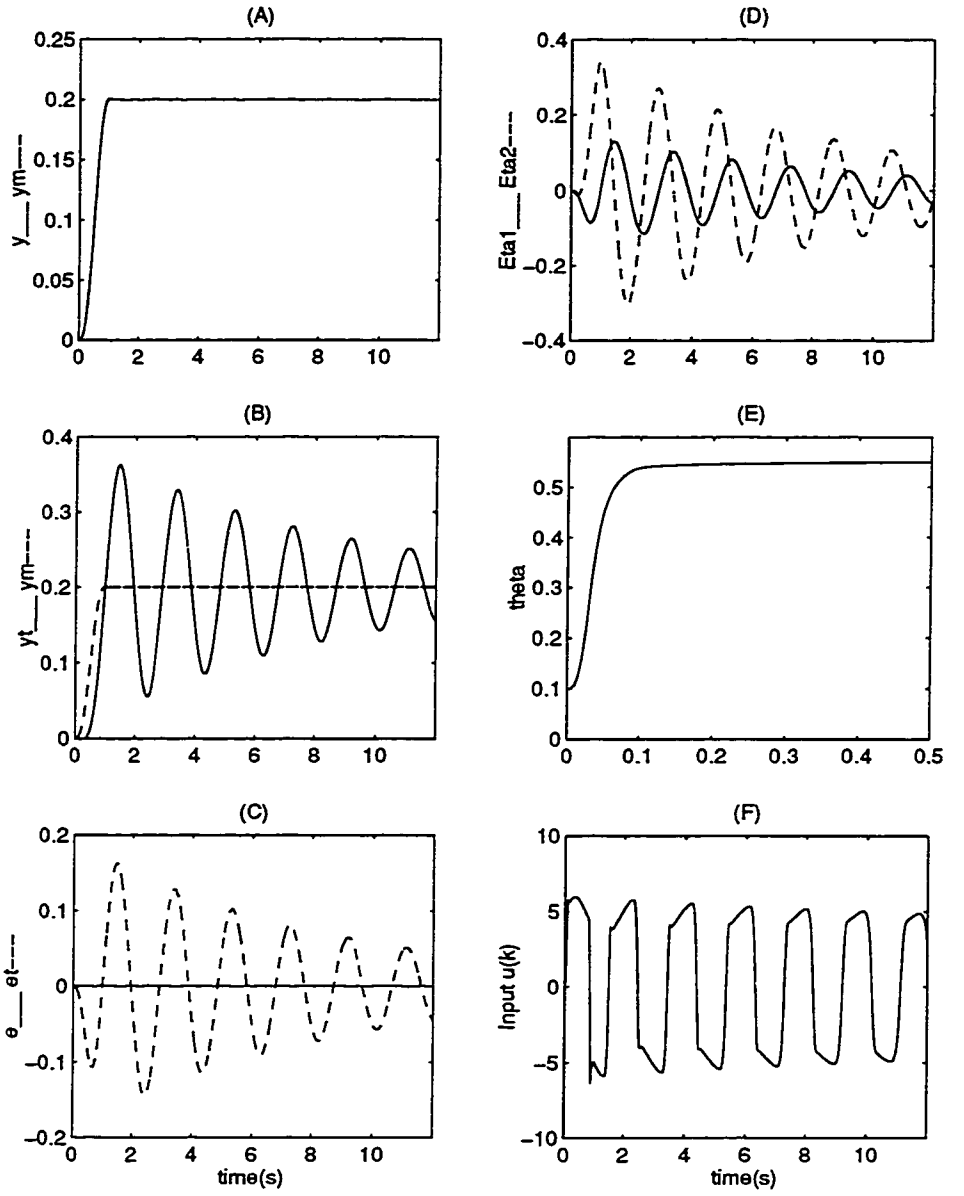

Figure 6.4: *Simulation Results:* Adaptive tracking control of a single-link flexible manipulator. (A) re-defined output $y(k)$ ___ and desired trajectory $y_m(k)$ $--$, (B) tip position $y_t(k)$ ___ and desired trajectory $y_m(k)$ $--$, (C) tracking errors $e(k) = y(k) - y_m(k)$ ___ and $e_t(k) = y_t(k) - y_m(k)$ $--$, (D) internal dynamics $\eta_1(k)$ ___ and $\eta_2(k)$ $--$, (E) estimate of the payload $\hat{M}_L$, (F) input torque $\tau(k) = u(k)$ for $M_L = 0.55$, $T = \frac{1}{200}$ and $\beta_1 = 0.4167$ (*or* $\alpha = .25$).

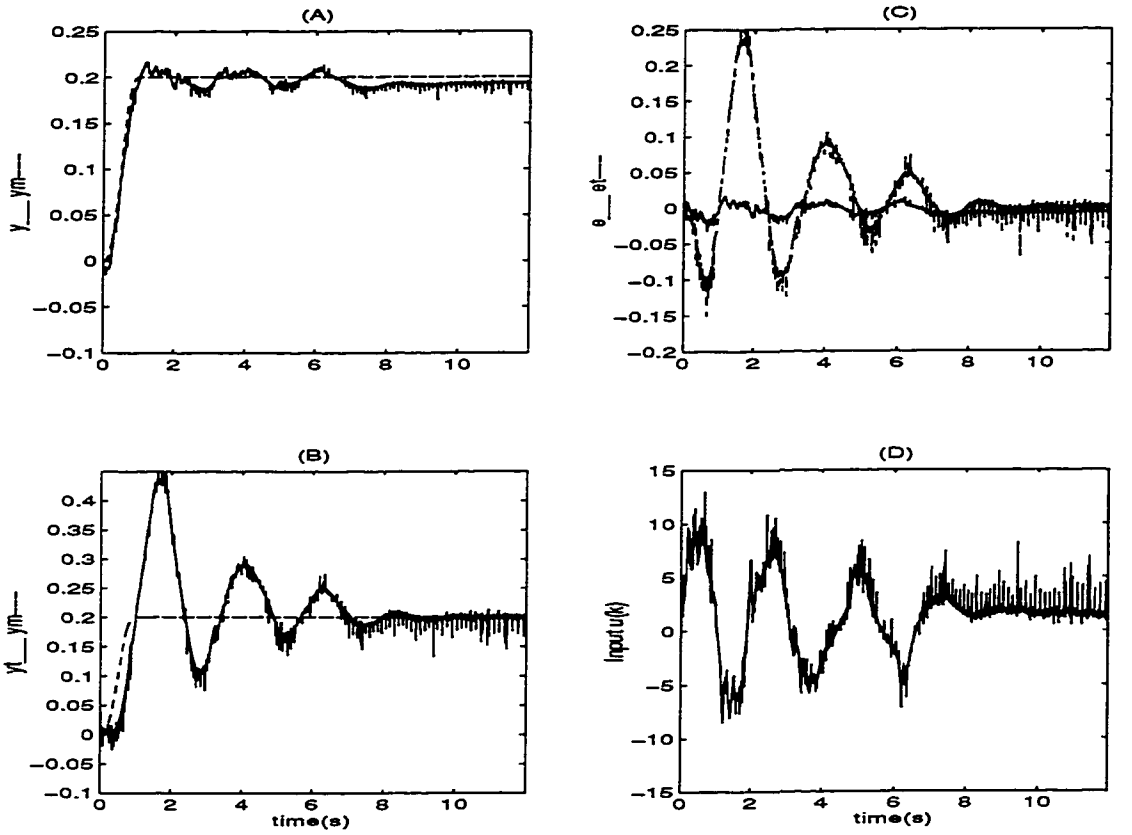

Figure 6.5: *Experimental Results:* Non-Adaptive tracking control of a single-link flexible manipulator. (A) re-defined output $y(k)$ __and desired trajectory $y_m(k)$ $--$, (B) tip position $y_t(k)$ __and desired trajectory $y_m(k)$ $--$, (C) tracking errors $e(k) = y(k) - y_m(k)$ __and $e_t(k) = y_t(k) - y_m(k)$ $--$, (F) input torque $\tau(k) = u(k)$ for $M_L = 0.55$, $(M_L)_{controller} = 0.1$, $T = \frac{1}{200}$ and $\beta_1 = 0.4167$ $(or\ \alpha = .25)$.

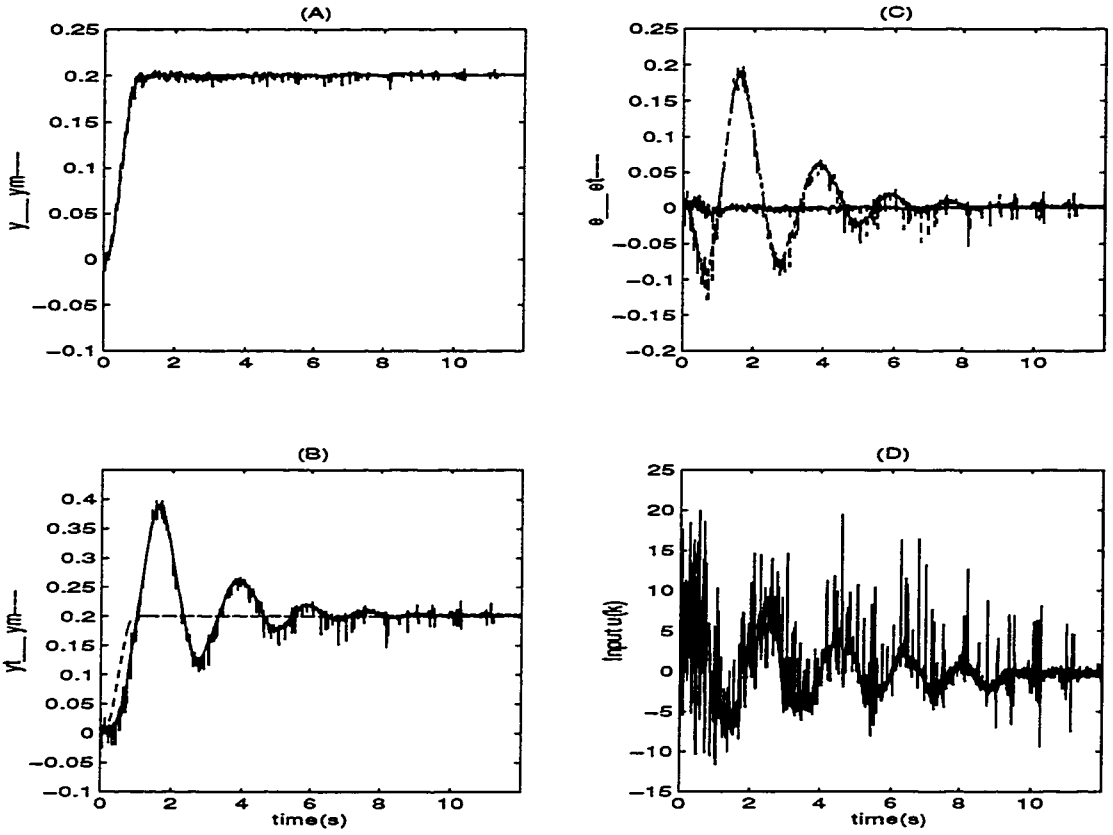

Figure 6.6: *Experimental Results*: Non-Adaptive tracking control of a single-link flexible manipulator. (A) re-defined output $y(k)$ __and desired trajectory $y_m(k)$ – –, (B) tip position $y_t(k)$ __and desired trajectory $y_m(k)$ – –, (C) tracking errors $e(k) = y(k) - y_m(k)$ __and $e_t(k) = y_t(k) - y_m(k)$ – –, (F) input torque $\tau(k) = u(k)$ for $M_L = 0.55$, $(M_L)_{controller} = 0.55$, $T = \frac{1}{200}$ and $\beta_1 = 0.4167$ (*or* $\alpha = .25$).

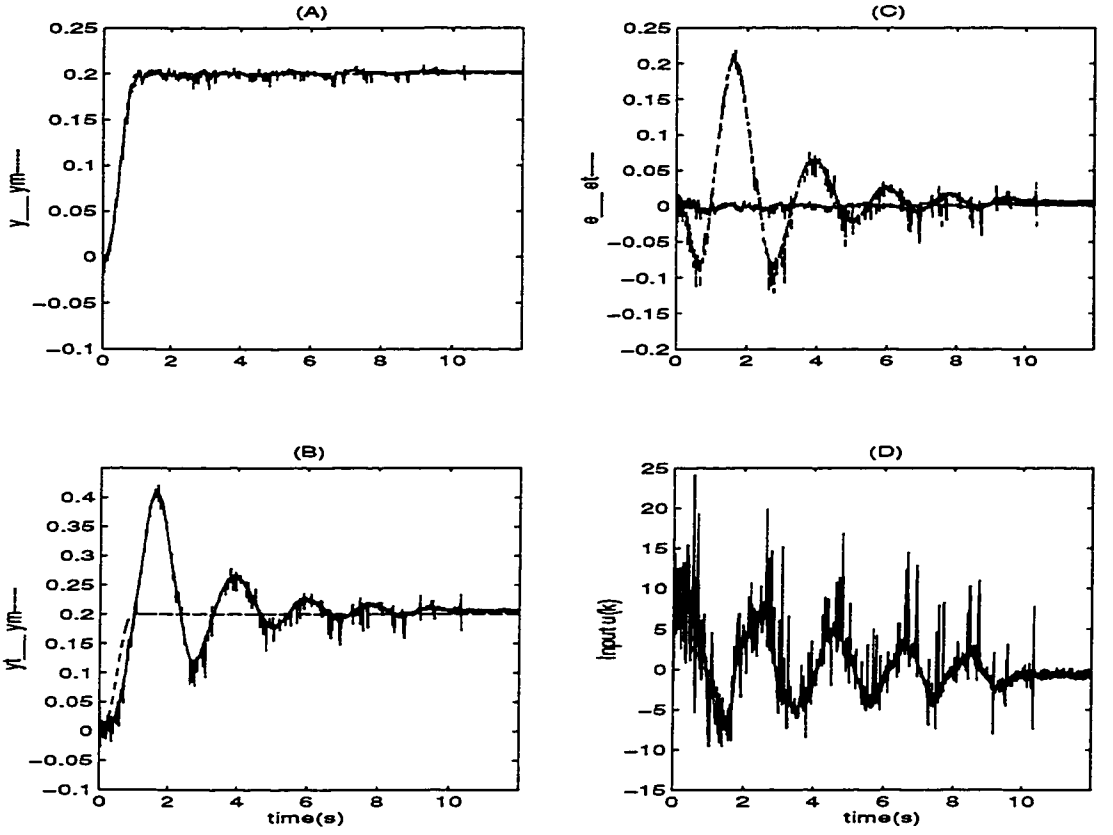

Figure 6.7: *Experimental Results:* Non-Adaptive tracking control of a single-link flexible manipulator. (A) re-defined output $y(k)$ __and desired trajectory $y_m(k)$ – –, (B) tip position $y_t(k)$ __and desired trajectory $y_m(k)$ – –, (C) tracking errors $e(k) = y(k) - y_m(k)$ __and $e_t(k) = y_t(k) - y_m(k)$ – –, (F) input torque $\tau(k) = u(k)$ for $M_L = 0.55$, $(M_L)_{controller} = 1.5$, $T = \frac{1}{200}$ and $\beta_1 = 0.4167$ (*or* $\alpha = .25$).

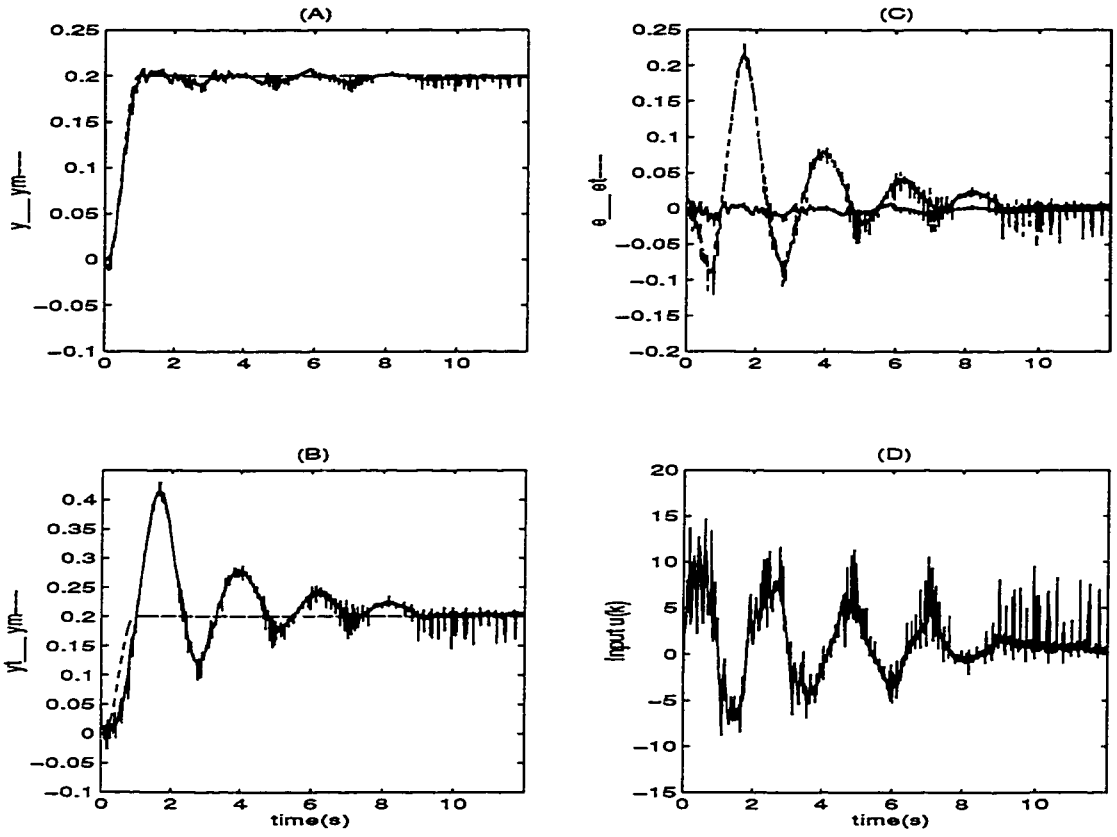

Figure 6.8: *Experimental Results:* Non-Adaptive tracking control of a single-link flexible manipulator. (A) re-defined output $y(k)$ __and desired trajectory $y_m(k)$ − −, (B) tip position $y_t(k)$ __ and desired trajectory $y_m(k)$ − −, (C) tracking errors $e(k) = y(k) - y_m(k)$ __and $e_t(k) = y_t(k) - y_m(k)$ − −, (F) input torque $\tau(k) = u(k)$ for $M_L = 0.55$, $(M_L)_{controller} = 2$, $T = \frac{1}{200}$ and $\beta_1 = 0.4167$ (*or* $\alpha = .25$).

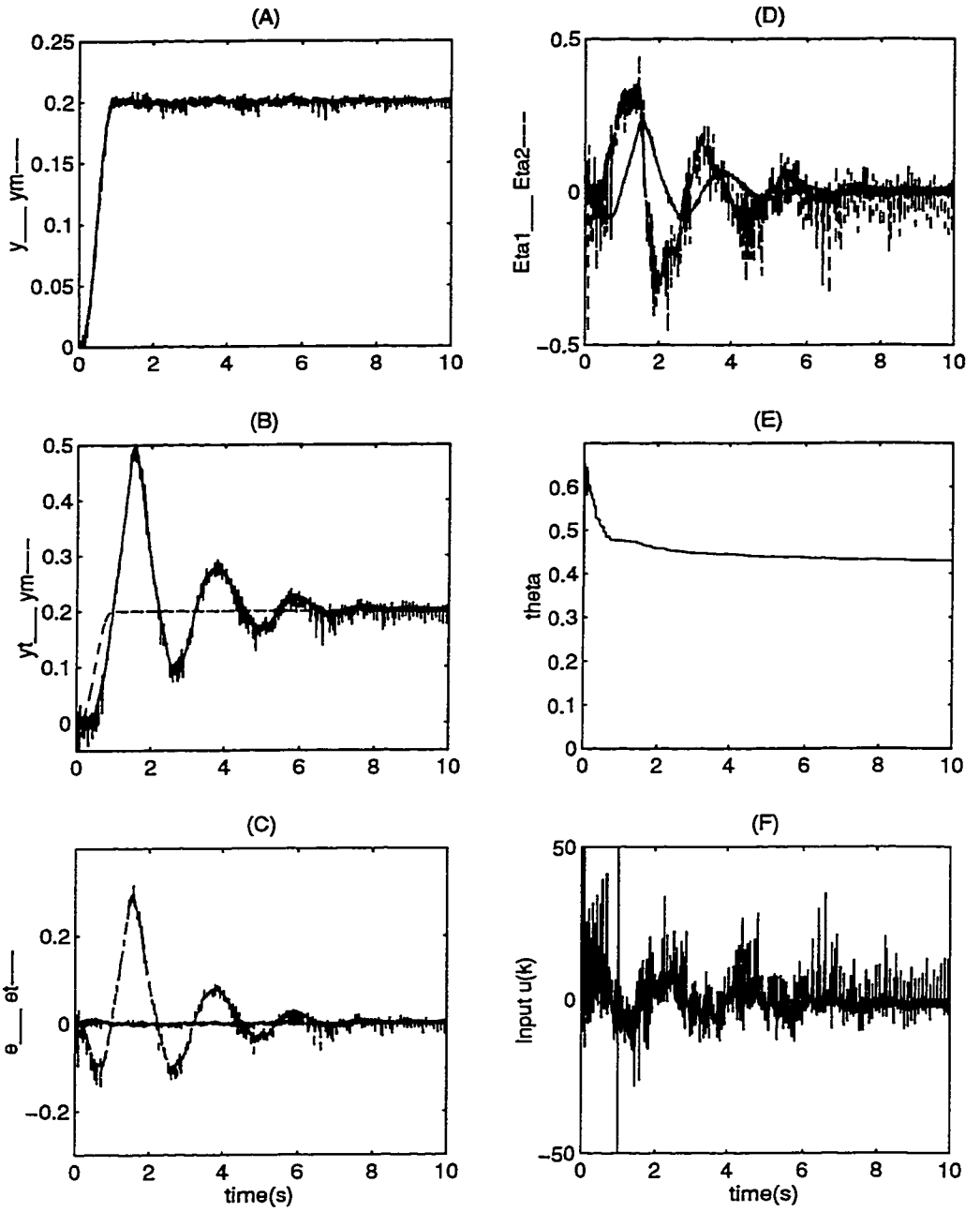

Figure 6.9: *Experimental Results:* Adaptive tracking control of a single-link flexible manipulator. (A) re-defined output $y(k)$ ___ and desired trajectory $y_m(k)$ $--$, (B) tip position $y_t(k)$ ___ and desired trajectory $y_m(k)$ $--$, (C) tracking errors $e(k) = y(k) - y_m(k)$ ___ and $e_t(k) = y_t(k) - y_m(k)$ $--$, (D) internal dynamics $\eta_1(k)$ ___ and $\eta_2(k)$ $--$, (E) estimate of the payload $\hat{M}_L$, (F) input torque $\tau(k) = u(k)$ for $M_L = 0.55$, $\hat{M}_L(0) = 0.1$, $T = \frac{1}{200}$ and $\beta_1 = 0.4167$ (*or* $\alpha = .25$).

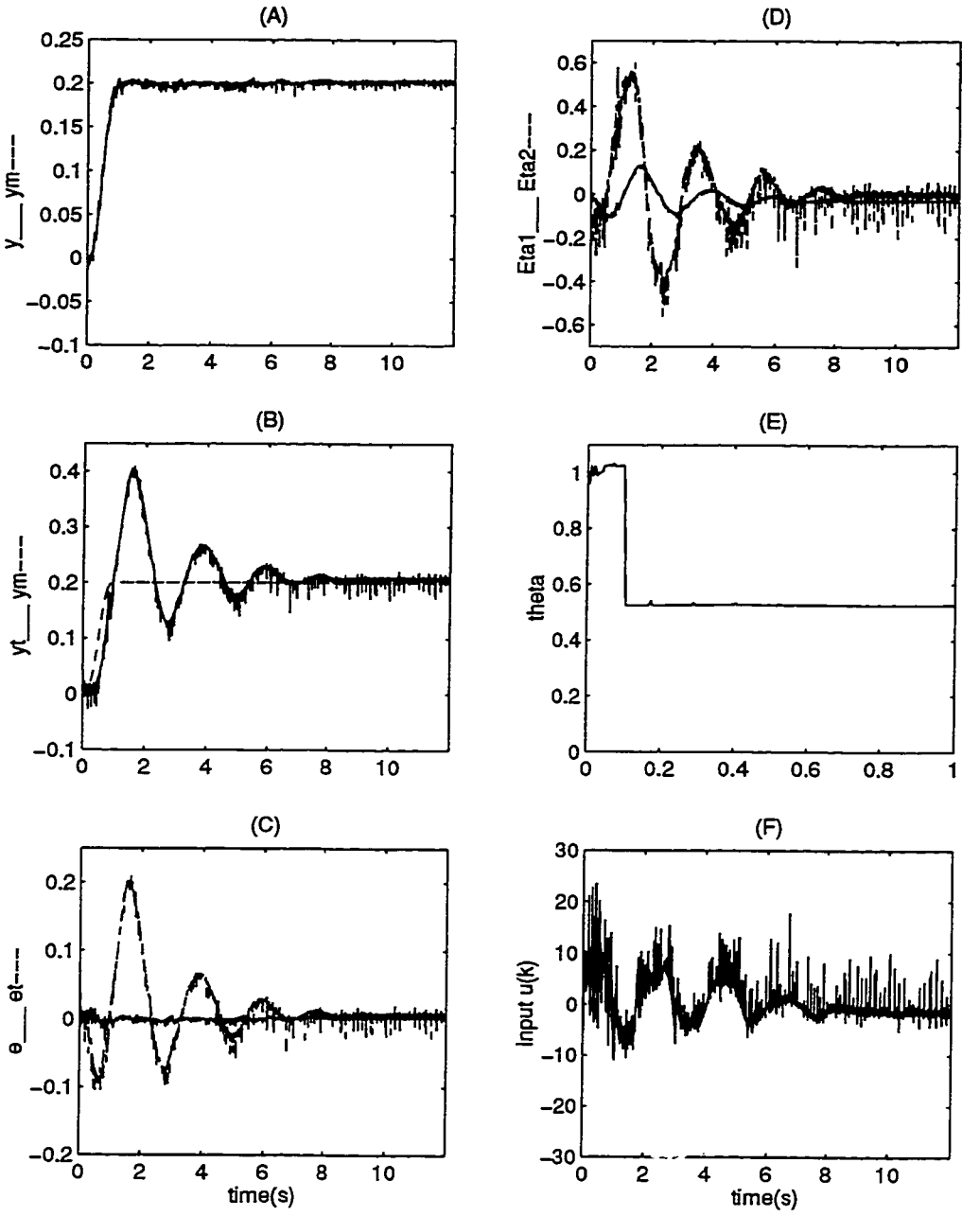

Figure 6.10: *Experimental Results:* Adaptive tracking control of a single-link flexible manipulator. (A) re-defined output $y(k)$ ___ and desired trajectory $y_m(k)$ $--$, (B) tip position $y_t(k)$ ___ and desired trajectory $y_m(k)$ $--$, (C) tracking errors $e(k) = y(k) - y_m(k)$ ___ and $e_t(k) = y_t(k) - y_m(k)$ $--$, (D) internal dynamics $\eta_1(k)$ ___ and $\eta_2(k)$ $--$, (E) estimate of the payload $\hat{M}_L$, (F) input torque $\tau(k) = u(k)$ for $M_L = 0.55$, $\hat{M}_L(0) = 1$, $T = \frac{1}{200}$ and $\beta_1 = 0.4167$ (*or* $\alpha = .25$).

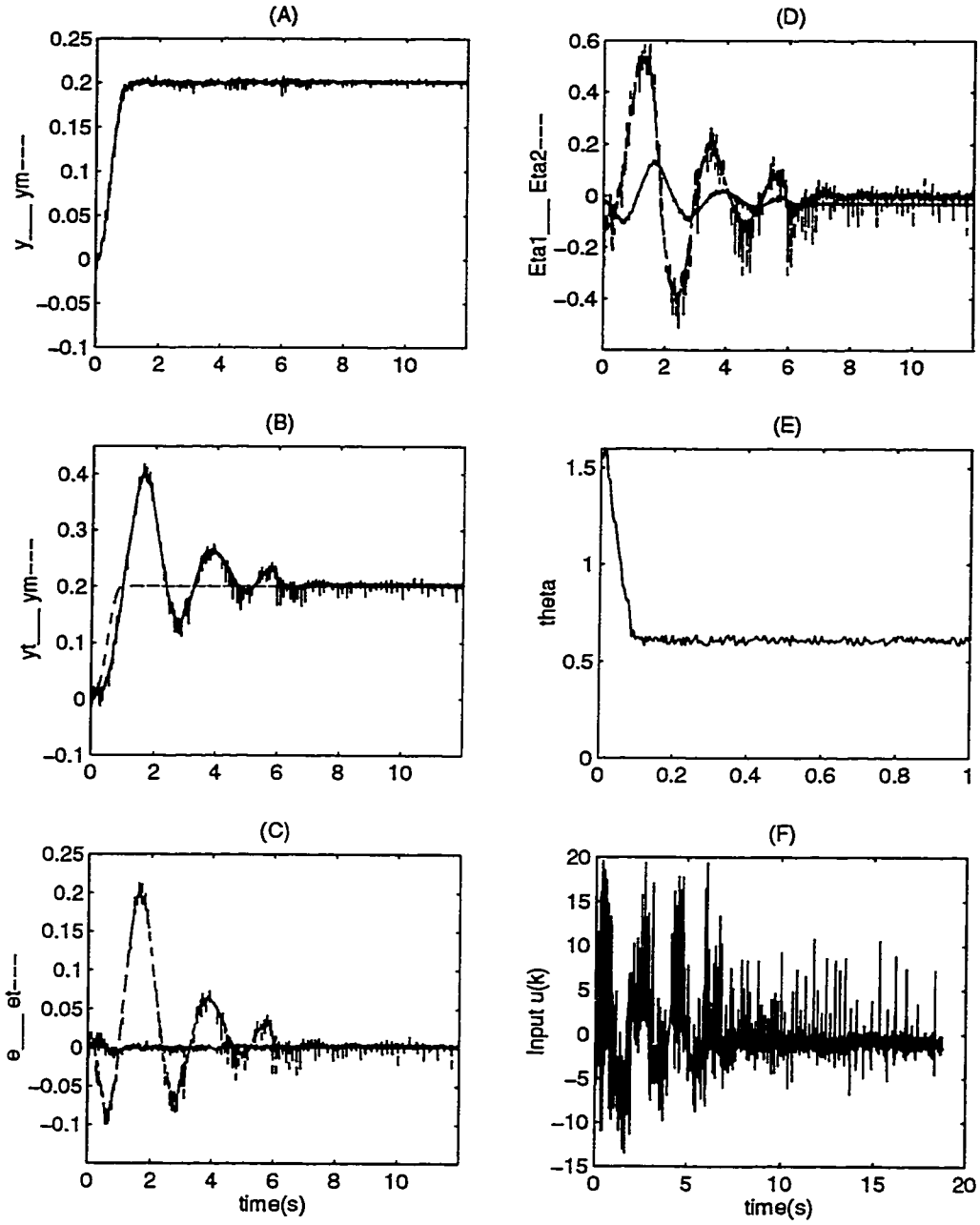

Figure 6.11: *Experimental Results:* Adaptive tracking control of a single-link flexible manipulator. (A) re-defined output $y(k)$ ___ and desired trajectory $y_m(k)$ – –, (B) tip position $y_t(k)$ ___ and desired trajectory $y_m(k)$ – –, (C) tracking errors $e(k) = y(k) - y_m(k)$ ___ and $e_t(k) = y_t(k) - y_m(k)$ – –, (D) internal dynamics $\eta_1(k)$ ___ and $\eta_2(k)$ – –, (E) estimate of the payload $\hat{M}_L$, (F) input torque $\tau(k) = u(k)$ for $M_L = 0.55$, $\hat{M}_L(0) = 1.5$, $T = \frac{1}{200}$ and $\beta_1 = 0.4167$ (*or* $\alpha = .25$).

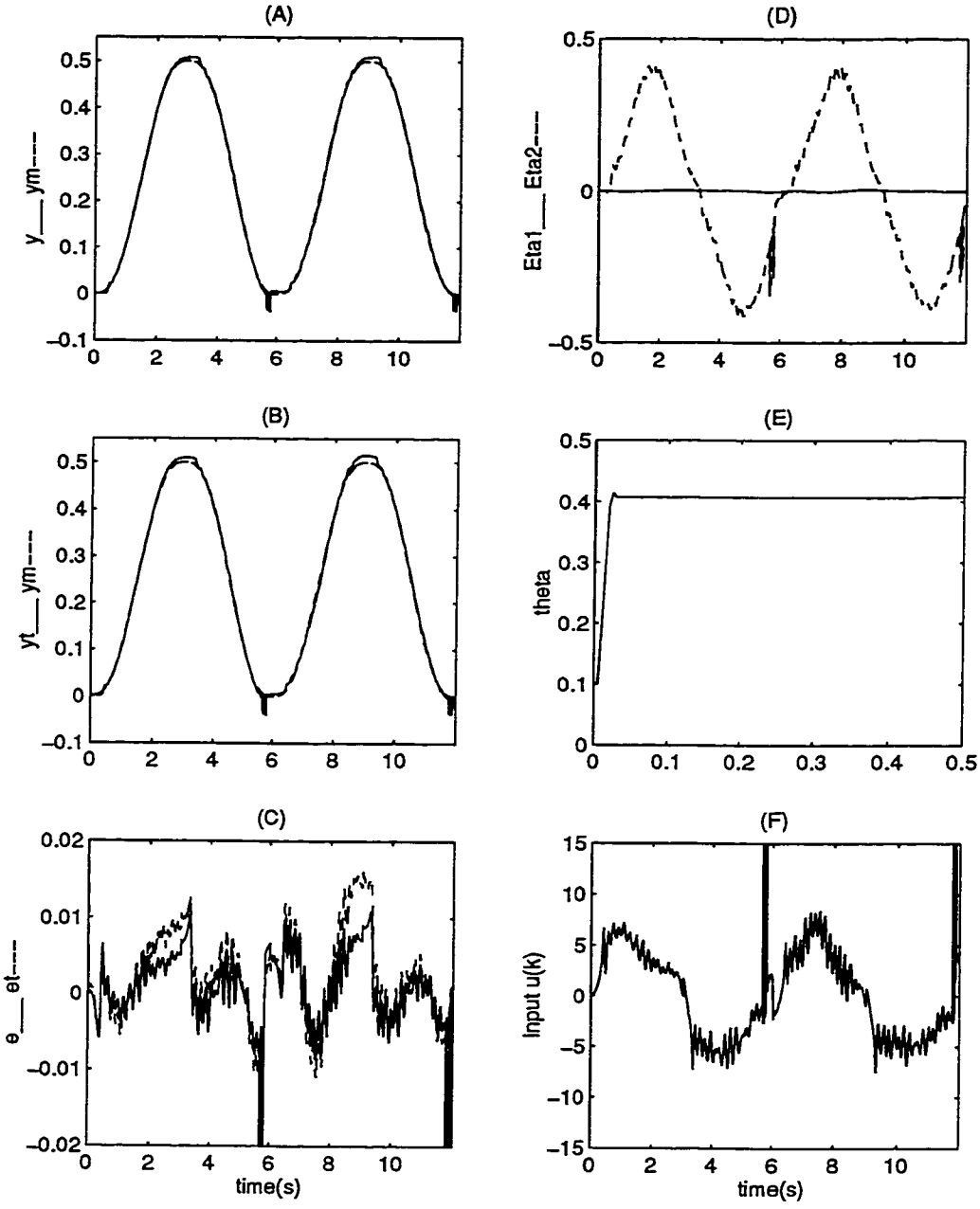

Figure 6.12: *Experimental Results:* Adaptive tracking control of a single-link flexible manipulator when the desired trajectory in four quintic functions. (A) re-defined output $y(k)$ ___ and desired trajectory $y_m(k)$ – –, (B) tip position $y_t(k)$ ___ and desired trajectory $y_m(k)$ – –, (C) tracking errors $e(k) = y(k) - y_m(k)$ ___ and $e_t(k) = y_t(k) - y_m(k)$ – –, (D) internal dynamics $\eta_1(k)$ ___ and $\eta_2(k)$ – –, (E) estimate of the payload $\hat{M}_L$, (F) input torque $\tau(k) = u(k)$ for $M_L = 0.55$, $\hat{M}_L(0) = 0.1$, $T = \frac{1}{200}$ and $\beta_1 = 0.4167$ (*or* $\alpha = .25$).

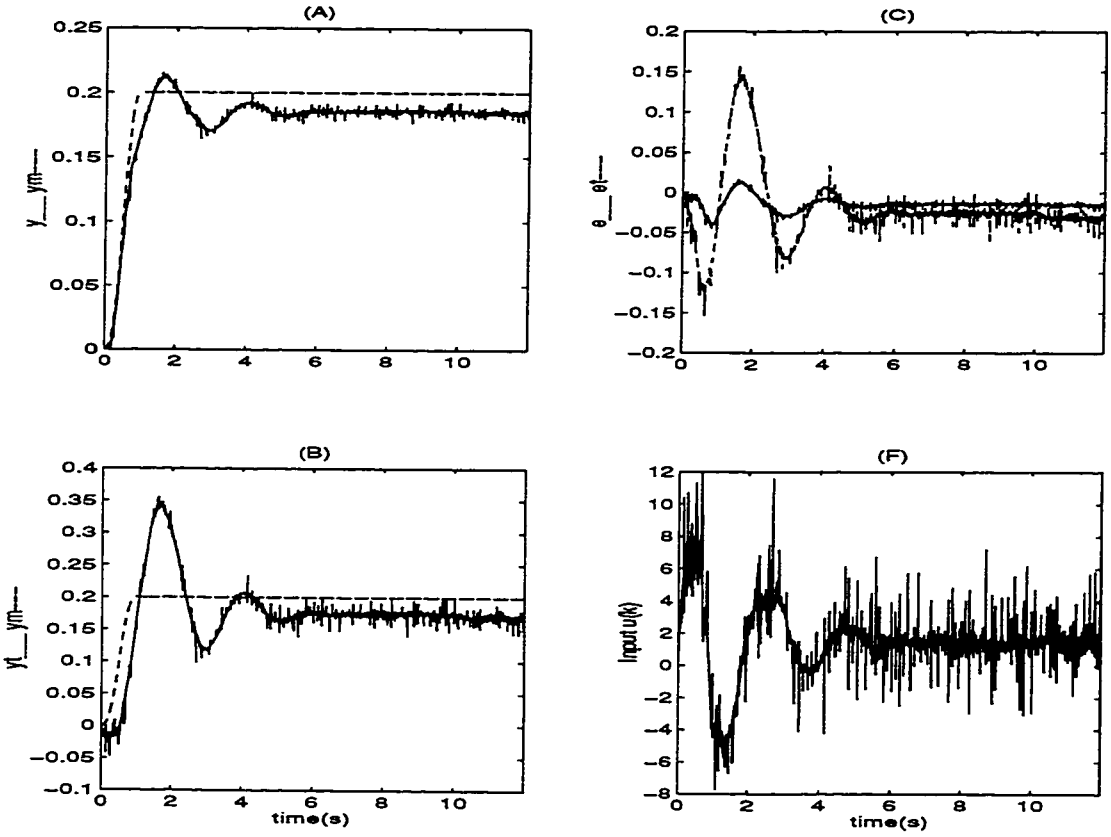

Figure 6.13: *Experimental Results:* PD controller for a single-link flexible manipulator. (A) re-defined output $y(k)$ ___ and desired trajectory $y_m(k)$ $- -$, (B) tip position $y_t(k)$ ___ and desired trajectory $y_m(k)$ $- -$, (C) tracking errors $e(k) = y(k) - y_m(k)$ ___ and $e_t(k) = y_t(k) - y_m(k)$ $- -$, (E) input torque $\tau(k) = u(k)$ $- -$, for $M_L = 0.55$, $T = \frac{1}{200}$ and $\beta_1 = 0.4167$ (*or* $\alpha = .25$), $K_p = 100$ and $K_d = 60$.

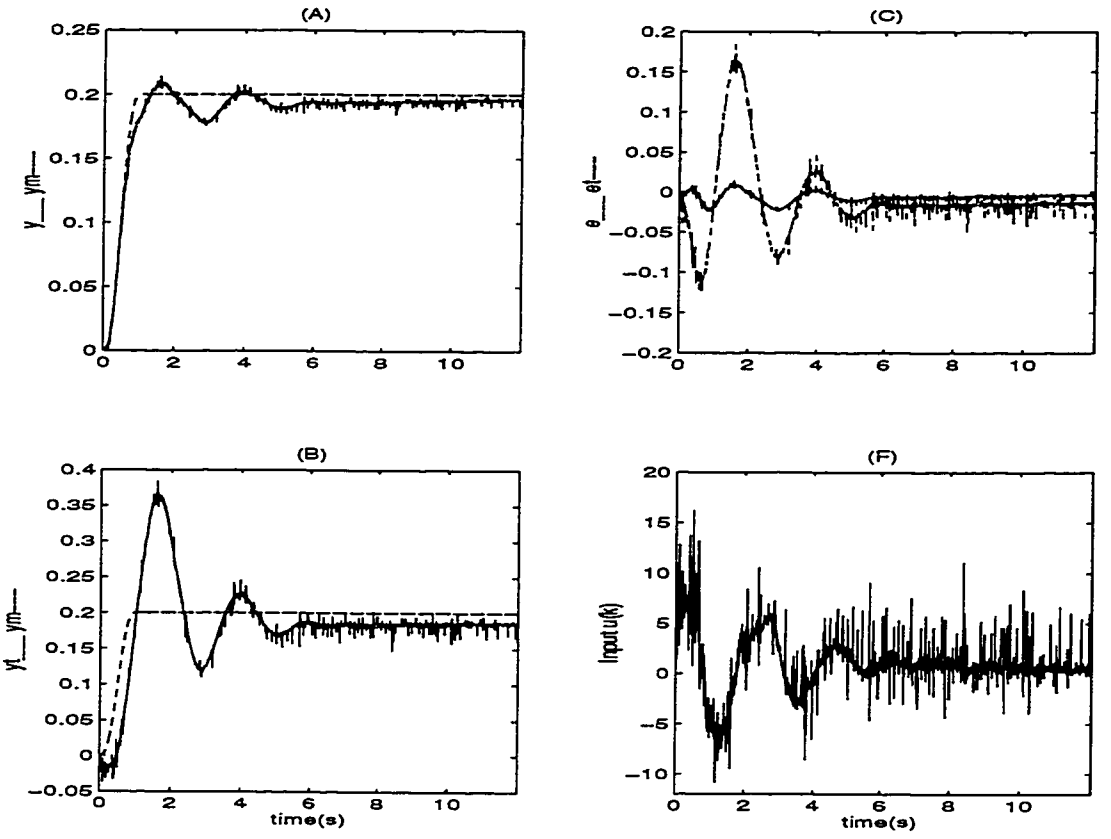

Figure 6.14: *Experimental Results:* PD controller for a single-link flexible manipulator. (A) re-defined output $y(k)$ ___ and desired trajectory $y_m(k)$ $-\,-$, (B) tip position $y_t(k)$ ___ and desired trajectory $y_m(k)$ $-\,-$, (C) tracking errors $e(k) = y(k) - y_m(k)$ ___ and $e_t(k) = y_t(k) - y_m(k)$ $-\,-$, (E) input torque $\tau(k) = u(k)$ $-\,-$, for $M_L = 0.55$, $T = \frac{1}{200}$, $\beta_1 = 0.4167$ (*or* $\alpha = .25$), $K_p = 150$ and $K_d = 100$.

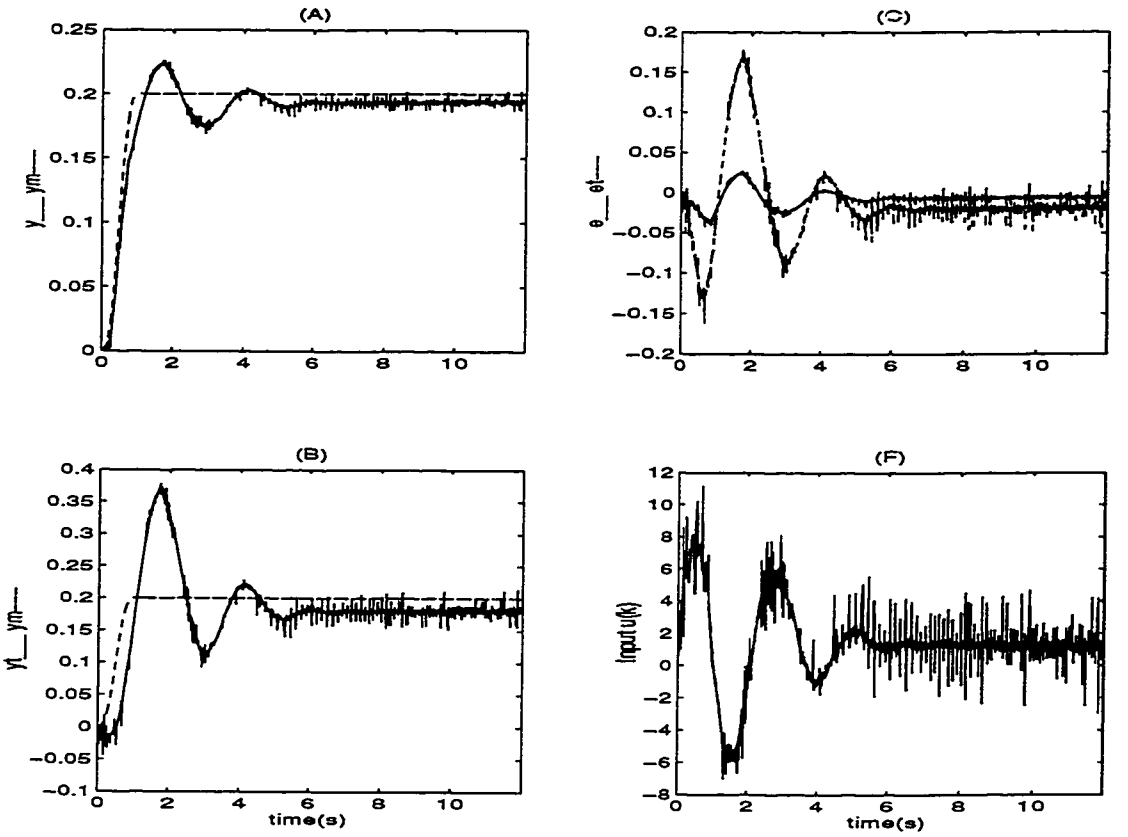

Figure 6.15: *Experimental Results* PD controller for a single-link flexible manipulator. (A) re-defined output $y(k)$ ___ and desired trajectory $y_m(k)$ $- -$, (B) tip position $y_t(k)$ ___ and desired trajectory $y_m(k)$ $- -$, (C) tracking errors $e(k) = y(k) - y_m(k)$ ___ and $e_t(k) = y_t(k) - y_m(k)$ $- -$, (E) input torque $\tau(k) = u(k)$ $- -$, for $M_L = 0.55$, $T = \frac{1}{200}$, $\beta_1 = 0.4167$ (*or* $\alpha = .25$), $K_p = 200$ and $K_d = 50$.

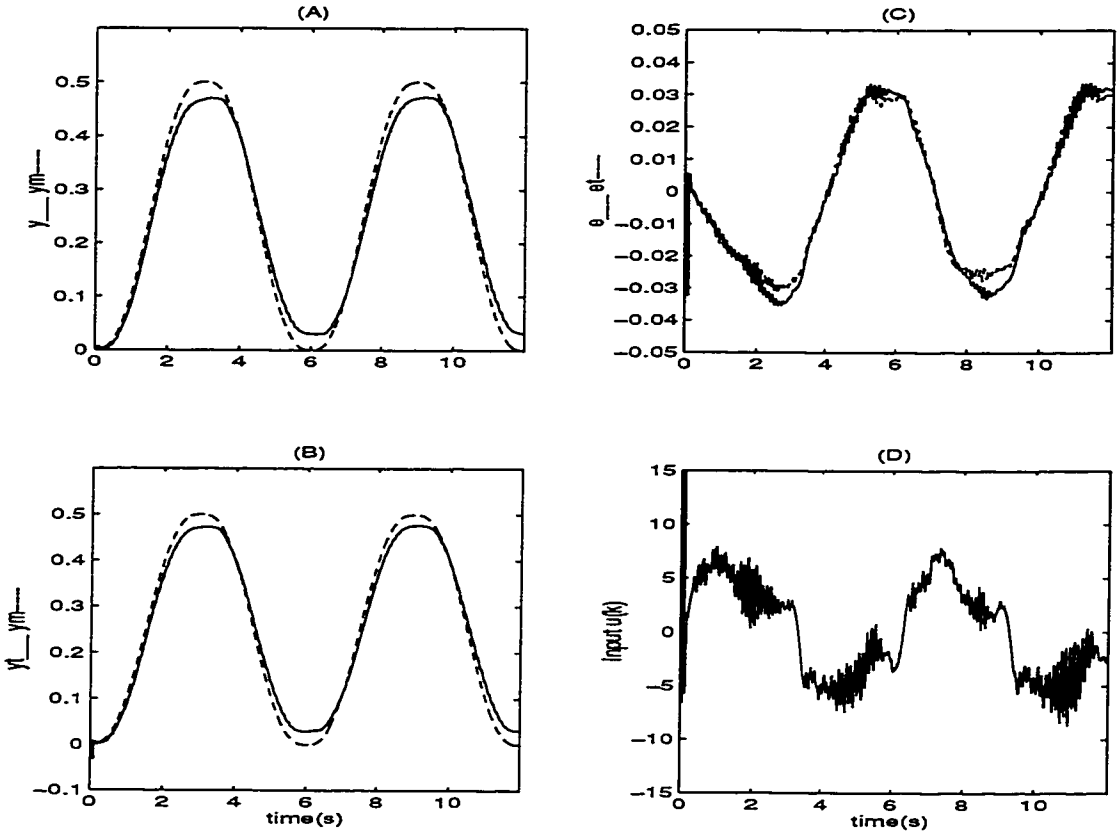

Figure 6.16: *Experimental Results* PD controller for a single-link flexible manipulator when desired trajectory is four quintic functions. (A) re-defined output $y(k)$ __ and desired trajectory $y_m(k)$ $--$, (B) tip position $y_t(k)$ __ and desired trajectory $y_m(k)$ $--$, (C) tracking errors $e(k) = y(k) - y_m(k)$ __ and $e_t(k) = y_t(k) - y_m(k)$ $--$, (D) input torque $\tau(k) = u(k)$ $--$, for $M_L = 0.55$, $T = \frac{1}{200}$, $\beta_1 = 0.4167$ (*or* $\alpha = .25$), $K_p = 150$ and $K_d = 100$.

Chapter 7

Concluding Remarks and Suggestions for Future Research

This dissertation aimed at addressing two major issues: adaptive control of nonlinear discrete-time systems and the application of the proposed method to tracking control of a single-link flexible manipulator. For the first part, the plant is a discrete-time system represented in the state-space form which could be either fully or partially feedback linearizable. The objective is to have the output $y(k)$ track a reference trajectory $y_m(k)$ as k goes to infinity despite the parametric uncertainties that are present. Towards this end, a local diffeomorphism for the change of coordinates and a nonlinear feedback control law are obtained such that the original nonlinear system is rendered input to output equivalent into a linear system. The resulting linear system is then used to solve the output tracking control problem using conventional linear control theory. The *multi-output Recursive-Least-Square (RLS)* algorithm is employed to identify the unknown parameters of the system. Based upon a certainty equivalence principle, the estimated parameters are then utilized in the controller. By using Lyapunov technique the adaptively controlled closed-loop system is shown to be stable. The main contributions here are the proof of stability of the closed-loop system and the application of the multi-output RLS identification algorithm

to indirect feedback linearization of discrete-time nonlinear systems. In contradistinction to continuous-time systems where the Lie derivatives are linear operators in the unknown parameters, for discrete-time systems this linear parameterization is not preserved by the composition operators. Consequently, the control problem is considerably more complicated. This problem is resolved by overparametrization and overrepresentation of the error dynamics in the proof of the stability.

In recent years output re-definition methods for *continuous model* of flexible-link manipulators have received a great deal of attention, however currently there is no work in the literature on the applicability of this concept to *discrete-time* models of flexible-link manipulators. Therefore, the aim of the second part of this dissertation is to apply the nonlinear adaptive control scheme proposed in the first part to a single-link flexible manipulator. The proposed adaptive control strategy further was implemented and tested on an experimental single-link flexible manipulator that had been constructed in the laboratory. This system is both nonlinear and nonminimum phase, that make the control design particularly difficult. The discrete-time model of the flexible-link manipulator is derived using two methods: forward difference method (Euler approximation) and a new method that enjoys the properties of both the forward difference and the step-invariance schemes. It is shown that both methods result in a similar discrete-time model with only a slight difference in forward dynamics and zero dynamics. The output re-definition scheme is used so that the resulting zero dynamics is exponentially stable. Finally, the proposed indirect adaptive feedback linearization and tracking controller is physically implemented where the *payload mass* is assumed to be unknown. Based on the experience gained during the course of this research, the following issues may be investigated in future.

The first issue to investigate is the development of indirect adaptive control strategies proposed in Chapters 2 and 3 by using output feedback. The proposed control

laws in Chapters 2 and 3 assume that all the states are measurable and available for feedback. In many practical systems it is physically or economically impractical to install all the necessary transducers and sensors to measure the states. Therefore, the study of observer structures and observer-based nonlinear adaptive controllers in the discrete-time domain is an important problem.

The other issue that needs to be investigated deals with the effects of the sampling period and the discretization strategy on the performance of the feedback linearizing control scheme. This is due to the fact that in designing discrete-time controllers based on sampled-data models of continuous-time systems (a subject that has been addressed by Guillaume *et al.* [22, 23]) these issues have a profound impact on the success of a proposed control strategy.

Since input-output models do not have the problems associated with state measurements, therefore development of direct and indirect adaptive controllers based on input-output models is envisaged to be very promising. In Chapter 5, we have considered a class of nonlinear discrete-time systems. However, this class is not a general input-output model. Note that, Narendra and Parthasarathy [57] have proposed other models that are more suitable and attractive for neural network-based control and identification applications. Therefore, another issue for future research will be to investigate the applicability of the above models (or possibly other models) to adaptive control of discrete-time nonlinear systems.

Finally, it would be of great interest to investigate adaptive control of multi-link flexible manipulators based on discrete-time models. This problem should be more challenging as multi-link flexible manipulators are significantly more nonlinear in nature.

Appendix A

Internal Dynamics Construction

In this Appendix a systematic procedure for finding the internal dynamics of the system discussed in Chapter 3 which is associated with the states η_k is presented. The problem may be stated as follow. Consider the SISO discrete-time nonlinear system

$$x_{k+1} = f(x_k, \theta) + g(x_k, \theta)u_k \tag{A.1}$$

where $x_k \in M$, $u_k \in U_u$ and $\theta \in \Re^p$ and M and U_u are the submanifolds of $\Re^n$ and $\Re$, respectively. The problem is to find $n - \gamma$ outputs $\eta_{i,k}$, $i = 1, \cdots, n - \gamma$ such that the relative degree of (A.1) with respect to each such output is at least 2, where γ is the relative degree of system (A.1). It is possible to show that the above problem may be reduced to that of finding only a single output. Suppose we can find a fictitious output $\lambda(x_k)$ such that the relative degree of (A.1) with respect to it is $\gamma' \triangleq n - \gamma + 1$. Therefore, the $n - \gamma$ desired outputs $\eta_{i,k}$, $i = 1, \cdots, n - \gamma$ may be selected as

$$\begin{aligned} \eta_{1,k} &= \lambda(x_k) \\ \eta_{2,k} &= \lambda(x_k) \circ f_o(x_k, \theta) \\ &\vdots \\ \eta_{n-\gamma,k} &= \lambda(x_k) \circ f_o^{n-\gamma-1}(x_k, \theta) \end{aligned} \tag{A.2}$$

Note that the relative degree of (A.1) with respect to $\eta_{i,k},\ i = 1, \cdots, n-\gamma$ is $\gamma' - i + 1$. The problem may now be reformulated as simply finding a single function $\lambda(x_k)$. In the following, by referring to the results of Jayaraman & Chizeck (1993), the necessary and sufficient conditions for constructing such a function are given briefly using the geometric approach.

Given system (A.1), in local coordinates (x_k, u_k) the canonical projection $\pi_M : M \times U \to M$ and $\pi_U : M \times U \to U$, satisfy $\pi_M(x_k, u_k) = x_k$ and $\pi_U(x_k, u_k) = u_k$. The input u_k is treated as an additional state in Jayaraman & Chizeck (1993) and is augmented to (A.1) to define the extended system

$$\begin{bmatrix} x_{k+1} \\ w_{k+1} \end{bmatrix} = \begin{bmatrix} f(x_k) + g(x_k)w_k \\ 0 \end{bmatrix} + \begin{bmatrix} 0 \\ 1 \end{bmatrix} u_k$$

or in compact representation $X_{k+1} = F_1(X_k) + g_1(X_k)u_k$ where $X_k = [x_k^T \ \ u_k]^T$ and

$$F_1(X_k) = \begin{bmatrix} f(x_k) + g(x_k)w_k \\ 0 \end{bmatrix} \ , \ g_1(X_k) = \begin{bmatrix} 0 \\ 1 \end{bmatrix}$$

Define the vector field $D^s_{F_1} g_1$ by utilizing the following algorithm:

step 0 : Set $s = 0$.

step 1 : Define the vector field $D^0_{F_1} g_1 = g_1$ that belongs to $ker(\pi_M)_*$ and the distribution $G_0 = span\{g_1\}$.

step 2 : Set $s = s + 1$.

step 3 : Given the vector field $D^s_{F_1} g_1$ and the tangent mapping of F_1 as $F_{1*} : T(M \times U) \to TM$, if $[D^s_{F_1} g_1 \ , \ ker F_{1*}] \in ker F_{1*}$, then define a unique vector field $D^{s+1}_{F_1} g_1 \in T(M \times U)$ such that $D^{s+1}_{F_1} g_1 \subset ker(\pi_U)_*$ and satisfies $(\pi_M)_* D^{s+1}_{F_1} g_1 = F_{1*} D^s_{F_1} g_1$. The distribution G_{k+1} can be defined as

$$G_{k+1} = span\{g_1, \cdots, D^{s+1}_{F_1} g_1\}$$

However, if $[D^s_{F_1} g_1 \ , \ ker F_{1*}] \notin ker F_{1*}$ then stop.

step 4 : Go to step 2.

Using the above algorithm, it can be shown that there exists a function $\lambda : M \times U \rightarrow R$ such that for $0 \leq s \leq \gamma'$,

$$< d\lambda, D^s_{F_1} g_1 >= 0 \tag{A.3}$$

in a neighborhood of equilibrium (x^0, u^0) and

$$< d\lambda, D^{\gamma'+1}_{F_1} g_1 > (x^0, u^0) \neq 0 \tag{A.4}$$

if and only if the distributions G_1, $G_2, \cdots, G_{\gamma'+1}$ are all involutive and constant dimension in a neighborhood of (x^0, u^0), where $d\lambda \in T^*(M, U)$ is an exact one-form. Finally, the function λ may be obtained by simultaneously solving the set of differential equations (A.3) and the condition (A.4).

Appendix B

Stability Proof

This Appendix provides the stability proof of Theorem 4.1. For the sake of notational simplicity k is used as a subscript. Using Assumption (4.1) and the results of Chen & khalil [7] where it was shown that the *Converse Lyapunov Theorem* is also applicable to discrete-time systems, we conclude that for zero dynamics (4.44) there exists a Lyapunov function $W(\eta_k)$ such that on any compact set we have

$$\begin{aligned} k_1 \parallel \eta_k \parallel^2 &\leq W(\eta_k) \leq k_2 \parallel \eta_k \parallel^2 \\ \triangle W_{k+1}^{\eta} &\triangleq W(\eta_{k+1}) - W(\eta_k) = W \circ q_0(\eta_k) - W(\eta_k) \leq -k_3 \parallel \eta_k \parallel^2 \\ \parallel \frac{\partial W(\eta_k)}{\partial \eta_k} \parallel &\leq k_4 \parallel \eta_k \parallel \end{aligned} \tag{B.1}$$

where $k_1 - k_4$ are positive constants. Using Assumption (4.2) yields

$$\parallel q(\xi_{2k}, \eta_{2k}) - q(\xi_{1k}, \eta_{1,k}) \parallel \leq L_2(\parallel \xi_{2k} - \xi_{1k} \parallel + \parallel \eta_{2k} - \eta_{1k} \parallel) \tag{B.2}$$

for all $\xi_k \in \Omega_1$ and $\eta_k \in \Omega$ with Lipschitz constant $L_2 > 0$. To prove the stability of the closed-loop system a Lyapunov function candidate is selected as

$$\begin{aligned} U(e_k, \eta_k, \tilde{\theta}_k) &\triangleq V_1(e_k) + W(\eta_k) + V_2(\tilde{\theta}_k) \\ &= \ln(1 + \mu e_k^T \Lambda e_k) + W(\eta_k) + V_2(\tilde{\theta}_k) \end{aligned} \tag{B.3}$$

where $\mu > 0$ and Λ is the positive definite solution of $H^T \Lambda H - \Lambda + I = -Q$ for an arbitrary positive definite symmetric matrix Q. As shown in [65, 70] and chapter

3, $\triangle V^e_{k+1} + \triangle V^{\tilde{\theta}}_{k+1} \triangleq V_1(e_{k+1}) - V_1(e_k) + V_2(\tilde{\theta}_{k+1}) - V_2(\tilde{\theta}_k)$ satisfies the following inequality

$$\triangle V^e_{k+1} + \triangle V^{\tilde{\theta}}_{k+1} \leq \mu(\frac{-e_k^T Q e_k + c^2 G_k^T \Lambda G_k}{1 + \mu e_k^T \Lambda e_k}) \tag{B.4}$$

where $c^2 = 1 + \lambda_{max}(A^T \Lambda A)$ with G defined in (4.45). Furthermore, using (B.1) it follows that

$$\begin{aligned} \triangle W^{\eta}_{k+1} &\triangleq W \circ q(\xi_k, \eta_k) - W(\eta_k) \\ &= [W \circ q_0(\eta_k) - W(\eta_k)] + [W \circ q(\xi_k, \eta_k) - W \circ q_0(\eta_k)] \\ &\leq -k_3 \parallel \eta_k \parallel^2 + W \circ q(\xi_k, \eta_k) - W \circ q_0(\eta_k) \end{aligned} \tag{B.5}$$

In view of (B.2) and by using the results in [69], one may then express $q(\xi_k, \eta_k)$ and $q_0(\eta_k)$ according to

$$\begin{aligned} \parallel q(\xi_k, \eta_k) \parallel &\leq L_2(\parallel \xi_k \parallel + \parallel \eta_k \parallel) \\ \parallel q_0(\eta_k) \parallel &\leq L_2(\parallel \eta_k \parallel) \ , \ \forall \, \xi_k \in \Omega_1 \ , \ \eta_k \in \Omega \end{aligned} \tag{B.6}$$

Also since $W(\eta_k)$ is decrescent, $W \circ q = W(q) \leq k_2 \parallel q \parallel^2$ and $W \circ q_0 = W(q_0) \leq k_2 \parallel q_0 \parallel^2$. Therefore, by substituting (B.6) into (B.5), it yields

$$\triangle W^{\eta}_{k+1} \leq -k_3 \parallel \eta_k \parallel^2 + k_2 L_2(\parallel \xi_k \parallel + \parallel \eta_k \parallel)^2 - k_2 L_2 \parallel \eta_k \parallel^2 \tag{B.7}$$

In conclusion, using (B.3), (B.4) and (B.7), $\triangle U_{k+1}$ satisfies

$$\begin{aligned} \triangle U_{k+1} &= U(e_{k+1}, \eta_{k+1}, \tilde{\theta}_{k+1}) - U(e_k, \eta_k, \tilde{\theta}_k) \\ &= \triangle V^e_{k+1} + \triangle V^{\tilde{\theta}}_{k+1} + \triangle W^{\eta}_{k+1} \\ &\leq \mu(\frac{-e_k^T Q e_k + c^2 G_k^T \Lambda G_k}{1 + \mu e_k^T \Lambda e_k}) - k_3 \parallel \eta_k \parallel^2 + k_2 L_2(\parallel \xi_k \parallel + \parallel \eta_k \parallel)^2 - k_2 L_2 \parallel \eta_k \parallel^2 \end{aligned} \tag{B.8}$$

Using Assumptions (4.1) to (4.4) and the fact that x_k is a local diffeomorphism in ξ_k and η_k, we get

$$\begin{aligned} \parallel \xi_k \parallel &\leq \parallel e_k \parallel + b_1, \\ \parallel x_k \parallel &\leq l_x(\parallel \xi_k \parallel + \parallel \eta_k \parallel) \leq l_x(\parallel e_k \parallel + \parallel \eta_k \parallel + b_1) \\ \parallel \Xi(x, \hat{u}(k)) \parallel &\leq l_z(\parallel x_k \parallel + |\hat{\theta}_k|) \leq l_x l_z(\parallel e_k \parallel + \parallel \eta_k \parallel + b_1) + l_z|\hat{\theta}_k| \end{aligned} \tag{B.9}$$

where $l_x > 0$, $l_z > 0$, $\xi_k \in \Omega_1$, $\eta_k \in \Omega$ and $\hat{\theta}_k \in \Omega_{\hat{\theta}}$. Therefore, by using (B.9) in (B.8) and the fact that $1 \leq |1 + \mu e_k^T \Lambda e_k| \leq 1 + \mu \parallel e_k \parallel^2 \parallel \Lambda \parallel$ it may be shown that

$$\begin{aligned} \Delta U_{k+1} &\leq \frac{-\mu \lambda_{min}(Q) \parallel e_k \parallel^2}{1 + \mu \parallel \Lambda \parallel e_k \parallel} - k_3 \parallel \eta_k \parallel^2 \\ &+ \mu c^2 \parallel \Lambda \parallel |\tau_k|^2 + k_2 L_2 \parallel \xi_k \parallel^2 + 2k_2 L_2 \parallel \xi_k \parallel \parallel \eta_k \parallel \end{aligned} \tag{B.10}$$

Furthermore, according to (4.42), $|\tau_k| = \parallel \beta \parallel T^2 (\parallel M^{-1} - \hat{M}_k^{-1} \parallel) \parallel \Xi_k \parallel$. Now since matrix M has a special structure, we can find the upper bound of $\parallel M^{-1} - \hat{M}_k^{-1} \parallel$. First note that

$$\parallel M^{-1} - \hat{M}_k^{-1} \parallel \leq \parallel M^{-1} \parallel + \parallel \hat{M}_k^{-1} \parallel \tag{B.11}$$

Therefore, in the following our goal is to find the upper bound of $\parallel M^{-1} \parallel$ and $\parallel \hat{M}_k^{-1} \parallel$. Since $M^{-1} = \frac{Adj(M)}{\Delta}$, where $Adj(M)$ and Δ are adjoint matrix and determinant of mass matrix M, respectively, one can conclude that

$$\parallel M^{-1} \parallel \leq \frac{\parallel Adj(M) \parallel}{\Delta_{min}} \tag{B.12}$$

where Δ_{min} is the minimum of Δ. Now let's examine the structure of mass matrix M with entries (cf. Appendix C for more details)

$$\begin{aligned} m_{11} &= I_0 + J_0 + J_p + \rho A \boldsymbol{\delta}^T \boldsymbol{\delta} + L^2 M_L + M_L (\Phi^T(L) \boldsymbol{\delta})^2 \\ m_{ij} &= a_{ij} + M_L b_{ij} \quad \textit{for the remaining entries} \end{aligned} \tag{B.13}$$

where $\theta = M_L$ is payload mass and all other parameters are known. It can be shown that since M is a positive definite matrix that is a function of space vectors $X_1(k)$, $X_2(k)$ and payload M_L, Δ_{min} may be calculated when $X_1(k)$, $X_2(k)$ and M_L are set to zero, namely,

$$\Delta_{min} = \Delta|_{X_1 = X_2 = 0,\, M_L = 0}$$

To prove this, note that M is a positive definite matrix if and only if its successive principal minors are all positive. This in turn shows that all the diagonal entries

must be positive. Consequently, for example consider the 1×1 and the 2×2 matrices in the upper left-hand corner of matrix M as follow

$$A \triangleq m_{11} \ , \quad B \triangleq \begin{bmatrix} m_{11} & m_{12} \\ m_{12} & m_{22} \end{bmatrix}$$

Since $\| A \| > 0$ and $\| B \| > 0$, all the eigenvalues of A and B are positive and in addition we have

$$\lambda_1(B) \leq \lambda(A) \leq \lambda_2(B) \tag{B.14}$$

Therefore, one can conclude that $(\lambda_1(B))_{min} \leq (\lambda(A))_{min} \leq (\lambda_2(B))_{min}$. Now since the minimum of $\lambda(A) = m_{11}$ occurs when $X_1 = X_2 = 0$ and $M_L = 0$, we can conclude that this is case for $\lambda_1(B)$ and $\lambda_2(B)$ as well. As a result, the determinant of $B = \lambda_1(B).\lambda_2(B)$ is also minimum when $X_1 = X_2 = 0$ and $M_L = 0$. If we keep increasing the dimension of matrices A and B, it is clear that at the end matrix B becomes mass matrix M and as a result Δ reaches to its minimum with the same condition.

To find the upper bound of $\| Adj(M) \|$ in terms of $\| x \|$ and $|M_L|$, note that we have

$$Adj(M) = \begin{bmatrix} M_{11} & M_{12} & \cdots & M_{1,m+1} \\ M_{12} & M_{22} & \cdots & M_{2,m+1} \\ \vdots & \vdots & \vdots & \vdots \\ M_{1,m+11} & M_{2,m+1} & \cdots & M_{m+1,m+1} \end{bmatrix} \tag{B.15}$$

where $M_{1j} \ , \ \ j = 1, 2, \cdots, m+1$ are polynomials of order m in M_L and the other entities have the structure $m_{11}\gamma_{ij}^2 + \gamma_{ij}^3$ where m_{11} is given in (B.13) and γ_{ij}^2 and γ_{ij}^3 are polynomials of order $m-1$ in M_L. Now using (B.12), (B.13) and (B.15), and after some algebraic manipulations it can be shown that

$$\| M^{-1} \| \leq \frac{1}{\Delta_{min}} \| Adj(M) \| \leq \frac{1}{\Delta_{min}} (\gamma^1 + \gamma^0 \| X_{1,k} \|^2) \tag{B.16}$$

where γ^0 and γ^1 are polynomials of order m in $|M_L|$. To summarize, using (B.11) and (B.16) one can conclude that

$$\| M^{-1} - \hat{M}_k^{-1} \| \leq S_1(|\hat{\theta}_k|) + S_2(|\hat{\theta}_k|) \| X_{1,k} \|^2 \tag{B.17}$$

where $S_1 \triangleq \frac{1}{\Delta_{min}}(\gamma^1 + \hat{\gamma}^1)$ and $S_2 \triangleq \frac{1}{\Delta_{min}}(\gamma^0 + \hat{\gamma}^0)$ and $\hat{\gamma}^0$ and $\hat{\gamma}^1$ are γ^0 and γ^1, respectively where M_L is replaced with $\hat{M}_L$. Note that since it is assumed that the upper bound of M_L is known, $|M_L|$ is a known quantity and as a result S_1 and S_2 are polynomials of order m in $|\hat{M}_L| = |\hat{\theta}_k|$. Now to guarantee the stability of the closed-loop system a bounded region for $|\hat{\theta}_k|$ should be determined such that $\triangle U_{k+1} \leq 0$. Towards this end, by substituting (B.17) and $|\tau_k|$ into (B.10) and after some algebraic manipulations we get

$$N(|\hat{\theta}_k|) \leq \frac{1}{d_2^6}[\frac{\mu\lambda_{min}(Q) \| e_k \|^2}{1 + \mu \| \Lambda \| \| e_k \|^2} + k_3 \| \eta \|^2] - \frac{3k_2 L_2}{d_2^4} \tag{B.18}$$

where

$$\begin{aligned} N(|\hat{\theta}_k|) &\triangleq d_1(S_1(|\hat{\theta}_k|) + l_x^2 S_2(|\hat{\theta}_k|))^2(l_x + |\hat{\theta}_k|)^2 \\ d_1 &\triangleq \mu \| \Lambda \| (cT^2 l_z \| \beta \|)^2 \\ d_2(\| e_k \|, \| \eta_k \|) &\triangleq \| e_k \| + \| \eta_k \| + b_1 \end{aligned} \tag{B.19}$$

Therefore, inequality (B.18) characterizes a bounded region $\Omega_{\hat{\theta}}$ for $\hat{\theta}_k$ such that the closed-loop system (4.45) is stable (since $\triangle U_{k+1} \leq 0$). Consequently, we may conclude that e_k and x_k remain locally bounded and system (4.45) is a locally stable system. In addition, if the parameter estimation error tends to zero, then $\tau \to 0$ and the tracking error for the re-defined output in (4.45) converges to zero given the fact that H is a Hurwitz matrix.

In summary, provided that the estimate of the payload is ensured to satisfy (B.18) one gets $\triangle U_{k+1} \leq 0$. Given the fact that the Lyapunov candidate $U(e_k, \eta_k, \tilde{\theta}_k)$

is a function of $\tilde{\theta}_k$ we need to express it as a function of $\hat{\theta}_k$ in order to characterize the region of stability. Observe that $U(e_k, \eta_k, \tilde{\theta}_k) = V_1 + W + V_2$ where $V_2 = \| P_k^{-1} \| |\tilde{\theta}_k|^2 \leq \| P_k^{-1} \| (|\hat{\theta}_k|^2 + 2\delta|\hat{\theta}_k| + \delta^2)$ with δ representing the upper bound of the parameter θ, i.e., $|\theta| \leq \delta$. Therefore, defining U_n as a new function of $\hat{\theta}_k$ instead of $\tilde{\theta}_k$ we get $U_n(e_k, \eta_k, \hat{\theta}_k) \triangleq V_1 + W + \| P_k^{-1} \| (|\hat{\theta}_k|^2 + 2\delta|\hat{\theta}_k| + \delta^2)$ so that $U \leq U_n \leq c$, $c > 0$ and $U_n = c$ is the largest level set contained in $\triangle U_{k+1} \leq 0$. Consequently, for all $(e_k, \eta_k, \hat{\theta}_k) \in \Omega_c$ the closed-loop system is stable, where $\Omega_c \triangleq \{(e_k, \eta_k, \hat{\theta}_k) | U_n(e_k, \eta_k, \hat{\theta}_k) \leq c\}$, $c > 0$ and $U_n(e_k, \eta_k, \hat{\theta}_k) = c$ is the largest level set contained in $\triangle U_{k+1} \leq 0$.

Note that throughout Chapter 4, $y_m(k)$ is taken as the reference trajectory of the normalized re-defined output tip and the re-defined error is defined as $e_1(k) = y(k) - y_m(k)$. However, we are more concerned with the tracking characteristics of the normalized tip position. Thus, to find the bound for the tracking error of the normalized tip position $e_t(k) \triangleq y_t(k) - y_m(k)$, we rewrite $e_1(k)$ as

$$e_1(k) = y(k) - y_m(k) = e_t(k) + (y(k) - y_t(k)) \tag{B.20}$$

Now using the definition of the normalized tip position output $y_t(k)$ and the re-defined output $y(k)$ given in (4.4), one may conclude that

$$|y(k) - y_t(k)| \leq m\frac{\phi_{max}}{L} \| X_1(k) \| (1 + \alpha_{max}) \tag{B.21}$$

where $\phi_{max} \triangleq \max\{|\phi_i|\}$ and $\alpha_{max} \triangleq \max\{|\alpha_i|\}$ for $i = 1, 2, \cdots, m$. Therefore, by taking the l_∞ norm of (B.20) and using (B.21) and in view of the fact that $e_1(k) \in l_\infty$ and $X_1(k) \in l_\infty$

$$|e_t(k)| \leq |e_1(k)| + m\frac{\phi_{max}}{L} \| X_1(k) \| (1 + \alpha_{max}) \in l_\infty$$

which proves the boundedness of the normalized tip position tracking error.

Appendix C

Modeling of a Single-Link Flexible Manipulator

Consider a uniform slender beam which is connected to a rigid hub and has a payload mass shown in Figure (C.1). The beam is assumed to be initially straight and to satisfy the assumption of Euler-Bernolli beam theory. It is assumed that the height of the beam is much greater than its width, all deflections of beam are assumed to be small and the shear deformation and rotary inertia effects are ignored. The parameters of the link are as follows:

L beam length $[m]$

ρ mass density $[\frac{kg}{m^3}]$

M_L payload mass $[kg]$

I_0 hub inertia $[kgm^2]$

J_0 beam inertia with respect to hub $[kgm^2]$

J_p payload inertia $[kgm^2]$

A beam cross-sectional area $[m^2]$

E Young's modulus $[Nm^2]$

I beam area moment of inertia about the neutral axis $[kgm^2]$

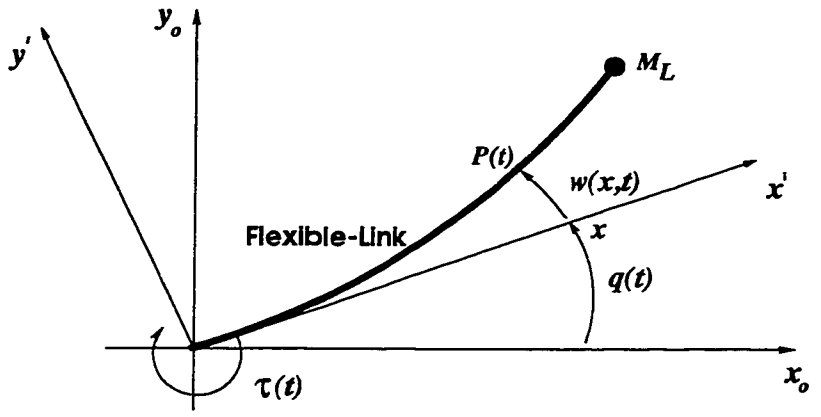

Figure C.1: Modeling of a single-link flexible manipulator

Each point on the beam has its position determined by the variable x which measures the distance of the point from the motor hub driving the beam. The elastic deformation at x is denoted by $w(x,t)$ while $y(x,t)$ is the net circumference movement of that point. In other words,

$$y(x,t) = w(x,t) + q(t)x$$

Therefore, the net deflection at x is the sum of a rigid body deflection and an elastic deformation. A frame $x' - y'$ is attached rigidly to the point where the beam is attached to the motor hub with x'—axis tangent to the beam. In other words, $x' - y'$ frame rotates such that the slope of the beam at $x = 0$ is zero. This implies that the boundary condition for $w(x,t)$ are clamped-free and that $w(x,t)$ can be expanded using the assumed modes approach as

$$w(x,t) = \sum_{i=1}^{m} \phi_i(x)\delta_i(t) = \Phi^T(x)\boldsymbol{\delta}(t) \tag{C.1}$$

where m is the number of modes considered, $\Phi(x) \triangleq [\phi_1(x) \ \cdots \ \phi_m(x)]^T$ is the eigenfunctions (mode shapes) vector and $\boldsymbol{\delta}(t) \triangleq [\delta_1(t) \ \cdots \ \delta_m(t)]^T$ is the vector of generalized coordinates. A state space model for the system can be derived using Euler-Lagrange method. The input is considered to be motor torque $\tau(t)$ while the

output is considered to be the net tip position deflection, namely,

$$y(L,t) = w(L,t) + q(t)L$$

Kinetic Energy

The position $P(x)$ of a point on the beam at a distance x from the hub in the inertial frame $x_0 - y_0$ is given by

$$P(x) = \begin{bmatrix} x\cos q - w\sin q \\ x\sin q + w\cos q \end{bmatrix}$$

Therefore, the total velocity $V(x)$ of x will be

$$V(x) \triangleq \dot{P}^T(x) = \begin{bmatrix} -x\dot{q}\sin q - \dot{w}\sin q - w\dot{q}\cos q \\ x\dot{q}\cos q + \dot{w}\cos q - w\dot{q}\sin q \end{bmatrix}$$

and

$$\| V(x) \|^2 = \dot{P}^T(x)\dot{P}(x) = (x^2 + w^2)\dot{q}^2 + \dot{w}^2 + 2x\dot{q}\dot{w} \tag{C.2}$$

The kinetic energy KE of the system can be written as

$$KE = \frac{1}{2}I_0\dot{q}^2 + \frac{1}{2}\int_0^L \dot{P}^T(x)\dot{P}(x)dm + \frac{1}{2}M_L\dot{P}^T(L)\dot{P}(L) + \frac{1}{2}J_p[\dot{q}(t) + \Phi'^T(L)\dot{\delta}(t)]^2 \tag{C.3}$$

where $\cdot$ denotes the derivative with respect to time and $'$ denotes the derivative with respect to x. The first term in (C.3) arises from the rotation of the hub. Since the hub is pinned there is no translational kinetic energy term due to this element. The second term is the kinetic energy due to the motion of the flexible link. The last two terms are the translational and rotational kinetic energy of the payload mass.

Now using (C.1), (C.2) and $dm = \rho A dx$, (C.3) can be written as

$$KE = \frac{1}{2}I_0\dot{q}^2 + \frac{1}{2}\int_0^L [(x^2 + (\Phi^T(L)\delta)^2)\dot{q}^2 + (\Phi^T(L)\dot{\delta})^2 + 2x\dot{q}(\Phi^T(L)\dot{\delta})]\rho A dx$$

$$+ \quad \frac{1}{2}M_L[(L^2 + (\Phi^T(L)\boldsymbol{\delta})^2)\dot{q}^2 + (\Phi^T(L)\dot{\boldsymbol{\delta}})^2 + 2x\dot{q}(\Phi^T(L)\dot{\boldsymbol{\delta}})]$$
$$+ \quad \frac{1}{2}J_p[\dot{q} + \Phi'^T(L)\dot{\boldsymbol{\delta}}]^2 \tag{C.4}$$

Thus, the three integrals involved in (C.4) can be simplified to

$$(i) \quad \frac{1}{2}\int_0^L (x^2 + (\Phi^T(L)\boldsymbol{\delta})^2)\dot{q}^2\rho A dx = \frac{1}{2}J_0\dot{q}^2 + \frac{1}{2}\rho A\dot{q}^2\boldsymbol{\delta}^T\boldsymbol{\delta}$$
$$(ii) \quad \frac{1}{2}\int_0^L (\Phi^T(L)\dot{\boldsymbol{\delta}})^2\rho A dx = \frac{1}{2}\rho A\dot{\boldsymbol{\delta}}^T\dot{\boldsymbol{\delta}}$$
$$(iii) \quad \frac{1}{2}\int_0^L 2x\dot{q}(\Phi^T(L)\dot{\boldsymbol{\delta}})\rho A dx = \dot{q}U^T\dot{\boldsymbol{\delta}}$$

where $J_0 \triangleq \rho A\int_0^L x^2 dx$ and $U^T(x) \triangleq \rho A\int_0^L x\Phi^T(x)dx$. Note that the *orthonormality* property of the mode shapes $\phi_i(t)$, $i = 1, \cdots, m$ is used in the above equations, namely,

$$\int_0^L \phi_i(x)\phi_j(x) = \begin{cases} 1\ , & i = j \\ 0\ , & otherwise \end{cases}$$

Consequently, the kinetic energy of the system becomes

$$\begin{aligned} KE &= \frac{1}{2}(I_0 + J_0)\dot{q}^2 + \frac{1}{2}\rho A\dot{q}^2\boldsymbol{\delta}^T\boldsymbol{\delta} + \frac{1}{2}\rho A\dot{\boldsymbol{\delta}}^T\dot{\boldsymbol{\delta}} + \dot{q}U^T\dot{\boldsymbol{\delta}} \\ &+ \frac{1}{2}M_L[(L^2 + (\Phi^T(L)\boldsymbol{\delta})^2)\dot{q}^2 + (\Phi^T(L)\dot{\boldsymbol{\delta}})^2 + 2x\dot{q}(\Phi^T(L)\dot{\boldsymbol{\delta}})] \\ &+ \frac{1}{2}J_p[\dot{q} + \Phi'^T(L)\dot{\boldsymbol{\delta}}]^2 \end{aligned} \tag{C.5}$$

Potential Energy

Assuming that the length of the link is an order of magnitude larger than its cross-sectional dimensions, shear effects and rotary inertia of the cross section can be neglected. In this case the only source of potential energy is the elastic stain energy of bending given by

$$PE = \frac{1}{2}EI\int_0^L y''(x,t)^2 dx = \int_0^L w''(x,t)^2 dx \tag{C.6}$$

Substituting for $w(x,t)$ into (C.6) from (C.1) gives

$$PE = \frac{1}{2}\boldsymbol{\delta}^T \mathbf{k}_2 \boldsymbol{\delta} \tag{C.7}$$

where $\mathbf{k}_2 \triangleq EI \int_0^L \Phi'' \Phi''^T dx$. Now the Lagrangian $L_g = KE - PE$ can be found as

$$\begin{aligned} L_g &= KE - PE \\ &= \frac{1}{2}(I_0 + J_0)\dot{q}^2 + \frac{1}{2}\rho A \dot{q}^2 \boldsymbol{\delta}^T \boldsymbol{\delta} + \frac{1}{2}\rho A \boldsymbol{\delta}^T \boldsymbol{\delta} + \dot{q} U^T \dot{\boldsymbol{\delta}} \\ &+ \frac{1}{2}[(L^2 + (\Phi^T(L)\boldsymbol{\delta})^2)\dot{q}^2 + (\Phi^T(L)\dot{\boldsymbol{\delta}})^2 + 2x\dot{q}(\Phi^T(L)\dot{\boldsymbol{\delta}})] \\ &+ \frac{1}{2} J_p [\dot{q} + \Phi'^T(L)\dot{\boldsymbol{\delta}}]^2 \\ &- \frac{1}{2}\boldsymbol{\delta}^T \mathbf{k}_2 \boldsymbol{\delta} \end{aligned} \tag{C.8}$$

Therefore, the Euler-Lagrange equations can now be applied to L_g to find the equations of motion given by

$$\begin{aligned} \frac{d}{dt}\left(\frac{\partial L_g}{\partial \dot{q}}\right) - \frac{\partial L_g}{\partial q} &= \tau(t) - D_1 \dot{q} - Fri(\dot{q}) \\ \frac{d}{dt}\left(\frac{\partial L_g}{\partial \dot{\boldsymbol{\delta}}}\right) - \frac{\partial L_g}{\partial \boldsymbol{\delta}} &= -\mathbf{D}_2 \dot{\boldsymbol{\delta}} \end{aligned} \tag{C.9}$$

where vector $\boldsymbol{\delta}$ can be considered as the generalized coordinates of the system, D_1 and $\mathbf{D}_2$ are the viscous and structural damping coefficients and $Fri(\dot{q})$ is the Coulomb friction torque. Now substituting (C.8) into (C.9) gives

$$\begin{aligned} [I_0 + J_0 + J_p + \rho A \boldsymbol{\delta}^T \boldsymbol{\delta} + L^2 M_L + M_L(\Phi^T(L)\boldsymbol{\delta})^2]\ddot{q} &+ \\ 2\rho A \dot{q} \boldsymbol{\delta}^T \dot{\boldsymbol{\delta}} + U^T \ddot{\boldsymbol{\delta}} + L M_L (\Phi^T(L)\ddot{\boldsymbol{\delta}}) &+ \\ 2M_L \dot{q}(\Phi^T(L)\boldsymbol{\delta})(\Phi^T(L)\dot{\boldsymbol{\delta}}) + J_p \Phi'^T(L)\ddot{\boldsymbol{\delta}} &= \tau(t) - D_1\dot{q} - Fri(\dot{q}) \\ \rho A \ddot{\boldsymbol{\delta}} + \ddot{q} U + M_L[\Phi(L)\Phi^T(L)\ddot{\boldsymbol{\delta}} + L\ddot{\boldsymbol{\delta}}\Phi(L)] &+ \\ J_P \Phi'[\ddot{q} + \Phi'^T(L)\ddot{\boldsymbol{\delta}}] + \mathbf{k}_2 \boldsymbol{\delta} &- \\ M_L \dot{q}^2 \Phi(L)\Phi^T(L)\boldsymbol{\delta} - \rho A \dot{q}^2 \boldsymbol{\delta} &= -\mathbf{D}_2 \dot{\boldsymbol{\delta}} \end{aligned} \tag{C.10}$$

Hence, the equations of motion of the link can be written in a matrix form as

$$M(\boldsymbol{\delta}) \begin{bmatrix} \ddot{q} \\ \ddot{\boldsymbol{\delta}} \end{bmatrix} + \begin{bmatrix} h_1(\dot{q}, \boldsymbol{\delta}, \dot{\boldsymbol{\delta}}) + Fri(\dot{q}) \\ \mathbf{h}_2(\dot{q}, \boldsymbol{\delta}) \end{bmatrix} + \begin{bmatrix} 0 & 0 \\ 0 & \mathbf{k}_2 \end{bmatrix} \begin{bmatrix} q \\ \boldsymbol{\delta} \end{bmatrix}$$

$$+\begin{bmatrix} D_1 & 0 \\ 0 & \mathbf{D_2} \end{bmatrix}\begin{bmatrix} \dot{q} \\ \dot{\boldsymbol{\delta}} \end{bmatrix} = \begin{bmatrix} \tau(t) \\ \mathbf{0} \end{bmatrix}$$

and the normalized tip position is given by

$$y(t) = [1 \quad \frac{\Phi^T(L)}{L}]\begin{bmatrix} q \\ \boldsymbol{\delta} \end{bmatrix}.$$

The entities for the mass matrix $M(\boldsymbol{\delta}) \triangleq \begin{bmatrix} m_{11} & \mathbf{m}_2^T \\ \mathbf{m}_2 & \mathbf{M}_3 \end{bmatrix}$ are

$$m_{11} = I_0 + J_0 + J_p + \rho A\boldsymbol{\delta}^T\boldsymbol{\delta} + L^2M_L + M_L(\Phi^T(L)\boldsymbol{\delta})^2$$
$$\mathbf{m}_2 = U + LM_L\Phi(L) + J_p\Phi'(L)$$
$$\mathbf{M}_3 = \rho A + M_L\Phi(L)\Phi^T(L) + J_P\Phi'(L)\Phi'^T(L)$$

and the nonlinear terms h_1 and $\mathbf{h}_2$ are given by

$$h_1(\dot{q}, \boldsymbol{\delta}, \dot{\boldsymbol{\delta}}) \triangleq 2M_L\dot{q}(\Phi^T(L)\boldsymbol{\delta})(\Phi^T(L)\dot{\boldsymbol{\delta}}) + 2\rho A\dot{q}\boldsymbol{\delta}^T\dot{\boldsymbol{\delta}}$$
$$\mathbf{h}_2(\dot{q}, \boldsymbol{\delta}) \triangleq -M_L\dot{q}^2\Phi(L)\Phi^T(L)\boldsymbol{\delta} - \rho A\dot{q}^2\boldsymbol{\delta}$$

where $q \in \Re$ is the joint angle, $\boldsymbol{\delta} = [\delta_1 \ \ \delta_2 \ \ \ldots \ \ \delta_m]^T \in \Re^m$ is the vector of flexible modes, M represents the inertia matrix, $h \triangleq [h_1 \ \ \mathbf{h}_2]^T$ represents the Coriolis and centrifugal forces, $Fri(\dot{q})$ is the Coulomb friction, $\mathbf{D} \triangleq \begin{bmatrix} D_1 & 0 \\ 0 & \mathbf{D_2} \end{bmatrix} \in \Re^{(m+1)\times(m+1)}$ represents the viscous and structural damping matrix, $\mathbf{k} \triangleq \begin{bmatrix} 0 & 0 \\ 0 & \mathbf{k}_2 \end{bmatrix} \in \Re^{(m+1)\times(m+1)}$ represents the stiffness matrix and $u(t) \triangleq \tau(t)$ is the input torque. Note that integer m represents the number of flexible modes (or equivalently the number of mode shape functions) considered in the model.

When for modeling of the link a single mode shape is considered (that is, $m = 1$), then the state vector becomes $[x_1 \;\; x_3 \;\; x_2 \;\; x_4]^T = [q \;\; \delta_1 \;\; \dot{q} \;\; \dot{\delta}_1]^T$ and mass matrix $M(\delta_1)$ and nonlinear terms h_1 and $\mathbf{h}_2$ become

$$M(\delta_1) = \begin{bmatrix} I_0 + J_0 + J_p + L^2 M_L + \rho A x_3^2 + M_L \phi^2(L) x_3^2 & U + L M_L \phi_1(L) + J_p \phi_1'(L) \\ U + L M_L \phi_1(L) + J_p \phi_1'(L) & \rho A + M_L \phi_1^2(L) + J_P \phi'(L)^2 \end{bmatrix}$$

$$h_1(x_2, x_3, x_4) = 2 M_L \phi^2 x_2 x_3 x_4 + 2 \rho A x_2 x_3 x_4$$

$$\mathbf{h}_2(x_2, x_3) = -M_L \phi^2(L) x_2^2 x_3 - \rho A x_2^2 x_3 \qquad \text{(C.11)}$$

The above model is employed for the all numerical simulations in Chapter 4.

To find the mode shape functions $\phi_1(x)$, $i = 1, \cdots, m$ the Euler-Bernoulli equation for constant EI is employed

$$EI \frac{\partial^4 w(x,t)}{\partial x^4} + m \frac{\partial^2 w(x,t)}{\partial t^2} = 0 \qquad \text{(C.12)}$$

Equation (C.12) can be solved by the separation of variables technique. Individual solution is expressed in the form

$$w(x,t) = \phi(x)\delta(t)$$

that after some algebraic manipulation yields

$$\frac{EI}{\rho A} \frac{d^4\phi(x)}{dx^4} \frac{1}{\phi(x)} = -\frac{\ddot{q}(t)}{q(t)} = \omega^2$$

where ω^2 is a positive constant. It is easily shown that the solution of $\phi(x)$ has the form

$$\phi(x) = A \sin x + B \cos x + C \sinh x + D \cosh x$$

To determine the unknown coefficient A to D, the following boundary condition should be used

$$w(0,1) = 0$$

$$\frac{\partial w(0,t)}{\partial x} = 0$$
$$\frac{\partial w^2(L,t)}{\partial x^2} = 0$$
$$\frac{\partial w^3(L,t)}{\partial x^3} = \frac{M_L}{EI}\frac{\partial w^2(L,t)}{\partial t^2}$$

Substituting these boundary conditions into $w(x,t) = \phi(x)\delta(t)$ yields the following expression for the mode shape functions

$$\phi(x) = D(\sinh kx - \sin kx - \frac{(\sin kL + \sinh kL)}{(\cos kL + \cosh kL)}(\cosh kx - \cos kx)) \qquad \text{(C.13)}$$

Each individual mode shape function $\phi(x)$ now may be found by substituting the value k determined from the following transcendental equation into (C.13)

$$\cosh kL \cos kL + 1 = 0$$

Finally D is selected such that each $\phi(x)$ is normalized, that is, $\int_0^L \phi^2(x)dx = 1$. Note that the natural frequency of vibration is given by $\omega^2 = \frac{k^4 EI}{\rho A}$.

Bibliography

[1] Barbot, J. P., Monaco S., Normand-Cyrot, D., and Pantalos, N. "Some Comments about Linearization Under Sampling". *Proceedings of the 32st Conference on Decision and Control*, pp. 2392-2397, Tucson, Arizona, December 1992.

[2] Book, W. J. "Recursive Lagrangian Dynamics of Flexible Manipulator Arms". *The International Journal of Robotics Research, Vol. 3, No. 3*, pp. 87-101, 1984.

[3] Byrnes, C. I., Lin, W., and Ghosh, B. K. "Stability of Discrete-Time Nonlinear Systems by Smooth State Feedback". *Systems and Control Letters 21*, pp. 255-263, 1993.

[4] Cannon, R. H. and Schmitz, E. "Initial Experiments on the End-point Control of a Flexible One-Link Robot". *International Journal of Robotics Research, Vol. 3, No. 3*, pp. 62-75, 1984.

[5] Centinkunt, S. and Wu, S. "Discrete-Time Tip position Control of a Flexible One Arm Robot". *Journal of Dynamic Systems, Measurement and Control, Vol. 114*, September pp. 428-435, 1992.

[6] Chen, F. and Khalil, H. K. "Adaptive Control of a Class of Nonlinear Discrete-Time Systems Using Neural Networks". *IEEE Transaction on Automatic Control , Vol. 40, No. 5*, pp. 791-801, May 1995.

[7] Chen, F. and Khalil, H. K. "Adaptive Control of Nonlinear Systems Using Neural Networks". *International Journal of Control, Vol. 55, No. 6*, pp. 1299-1317, 1992.

[8] Chen, F. and Khalil, H. K. "Adaptive Control of Nonlinear Systems Using Neural Networks - A Dead-Zone Approach". *Proceedings of American Control Conference*, pp. 667-672, 1991.

[9] Chen, F. and Tsao, W. "Adaptive Control of Linearizable Discrete-Time Systems". *Proceedings of American Control Conference*, pp. 880-881, Baltimore, Maryland, June 1994.

[10] Cook, P. A. "Direct Adaptive Control of Nonlinear Systems". *IFAC Nonlinear Control Systems Design, Capri, Italy*, pp. 235-238 1989.

[11] Copley Controls Corp. *"Servo Controllers Installation, Operation and Service Manual"*.

[12] Datta, A. "Robustness of Discrete-Time Adaptive Controllers: An Input-Ouput Approach". *IEEE Transactions on Automatic Control, Vol. 38, No. 12*, pp. 1852-1857, December 1993.

[13] De Luca, A. and Lanari, L. "Achieving Minimum Phase Behavior in a One-Link Flexible Arm". *Proceedings of the International Symposium on Intelligent Robotics*, pp. 224-235, Bangalore, India, 1991.

[14] De Luca, A. and Siciliano, B. "Trajectory Control of a Non-linear One-Link Flexible Arm". *International Journal of Control, Vol. 50, No. 5*, pp. 1966-1715, 1989.

[15] Donne, J. D. and Özgüner, Ü. "Neural control of A Flexible-Link Manipulator". *Proceedings of IEEE International Conference on Neural Networks*, pp. 2327-2332, 1994.

[16] Feliu, V., Rattan K. S., and Brown, H. B. "Adaptive Control of a Single-Link Flexible Manipulator". *IEEE Control Systems Magazine*, pp. 29-33, February 1990.

[17] Ganguly, S., Tarn, T. J., and Bejczy, A. K. "Control of Robots with Discrete Nonlinear Model: Theory and Experimentation". *Proceedings of the 1991 IEEE International Journal on Robotics and Automation*, Sacramento, California, pp. 528-533, April 1991.

[18] Geniele, H. *"Control of a flexible-link manipulator"*. M.A.Sc. Thesis, Concordia University, 1994.

[19] Geniele, H., Patel, R. V., and Khorasani, K. "Control of a Flexible-Link Manipulator". *Proceedings of IEEE International Conference on Robotics and Automation*, pp. 1217-1222, Nagoya, Japan, 1995.

[20] Goodwin, G. C. and Sin, K. S. *"Adaptive Filtering, Prediction, and Control"*. Prentice-Hall, 1984.

[21] Grizzle, J. W. *"Feedback Linearization of Discrete-Time Systems"*. Lecture Notes in Control and Information Sciences (83), Analysis and Optimization of Systems, Springer-Verlag, June 1986.

[22] Guillaume, A., Bastin, G., and Campion, G. "Discrete Time Adaptive Control for a Class of Nonlinear Continuous Systems". *IFAC Nonlinear Control Systems Design, Capri, Italy*, pp. 239-244, September 1989.

[23] Guillaume, A., Bastin, G., and Campion, G. "Sampled-Data Adaptive Control for a Class of Nonlinear Continuous Systems". *International Journal of Control, Vol. 60, No. 4*, pp. 569-594, 1994.

[24] Hashtrudi–Zaad, K. and Khorasani, K. Control of nonminimum phase singularly perturbed systems with applications to flexible link manipulators. *International Journal of Control Vol. 63, No. 4*, pp. 679-701, March 1996.

[25] Hashtrudi-Zaad, K. and Khorasani, K. "Control of Non-minimum Phase Singularly Perturbed Systems with Application to Flexible-Link manipulators". *International Journal of Control, Vol. 63, No. 4*, pp. 679-701, 1996.

[26] Isidori, A. *"Nonlinear Control Systems An Introduction"*. Springer Verlag, 1989.

[27] Jakubczyk, B. "Feedback Linearization of Discrete-Time Systems". *Systems and Control Letters 9*, pp. 411-416 1987.

[28] Jayaraman, G. and Chizeck, H. J. "Feedback Linearization of Discrete-Time Systems". *Proceedings of the 32th Conference on Decision and Control*, pp. 2972-2977, San Antonio, Texas, December 1993.

[29] Johansson, R. "Global Lyapunov Stability and Exponential Convergence of Direct Adaptive Control". *International Journal of Control, Vol. 50, No. 3*, 1pp. 859-869, 989.

[30] Kanellakopoulos, I. "A Discrete-Time Adaptive Nonlinear System". *IEEE Transaction on Automatic Control, Vol. 39, No. 11*, pp. 2362-2365, November 1994.

[31] Kanellakopoulos, I., Kokotovic, P. V., and Marino, R. "Adaptive Control Design of a Class of Nonlinear Systems". *Proceedings of the American Control Conference*, pp. 1713-1717.

[32] Kanellakopoulos, I., Kokotovic, P. V., and Middleton, R. H. "Indirect Adaptive Output-Feedback Control of a Class of Nonlinear Systems". *Proceedings of the*

29th Conference on Decision and Control, pp. 2714-2719, Honolulu, Hawaii, December 1990.

[33] Kanellakopoulos, I., Kokotovic, P. V., and Morse, A. S. "Systematic Design of Adaptive Controllers for Feedback Linearizable Systems". *IEEE Transaction on Automatic Control, Vol. 36, No. 11*, pp. 1241-1253, November 1991.

[34] Kanellakopoulos, I., Kokotovic, P. V., and Morse, A. S. "Adaptive Output-Feedback Control of Systems With Output Nonlinearities". *IEEE Transaction on Automatic Control, Vol. 37, No. 11*, pp. 1666-1681, November 1992.

[35] Kanellakopoulos, I., Krstic, M., and Kokotovic, P. V. "Interlaced Controller-Observer Design for Adaptive Nonlinear Control". *Proceedings of the American Control Conference*, pp. 1337-1342 1992.

[36] Khalil, H. K. *"Nonlinear systems"*. Macmillan, New York, 1992.

[37] Khorasani, K. Adaptive control of flexible-joint robots. *IEEE Trans. on Robotics and Automation*, pp. 250-267, April 1992.

[38] Khorasani, K. and Spong, M. W. "Invariant Manifolds and their Application to Robot Manipulators with Flexible Joints". *Proceedings of IEEE International Conference on Robotics and Automation*, pp. 978-983 1995.

[39] Kistic, M., Kanellakopoulos, I., and Kokotovic, P. V. "Adaptive Nonlinear Control Without Overparameterization". *Systems and Control Letters 19*, pp. 177-185 1992.

[40] Koivo, A. J. and Lee, K. S. "Self-Tuning Control of a planar Two-Link Manipulator With Non-Rigid Arm". *IEEE International Conference on Robotics and Automation, Scottsdale*, 1989.

[41] Krstic, M., Kokotovic, P. V., and Kanellakopoulos I. "Adaptive Nonlinear Output-Feedback Control with an Observer-Based Identifier". *Proceedings of*

the American Control Conference, pp. 2821-2825, San Francisco, California, June 1993.

[42] Kung, M. and Womack, B. "Stability Analysis of a Discrete-Time Adaptive Control Algorithm Having a Polynomial Input". *IEEE Transaction on Automatic Control , Vol. 28, No. 12*, pp. 1110-1112, December 1983.

[43] Lee, H. G., Arapostathis, A., and Marcus, S. I. "Linearization of Discrete-Time Systems". *International Journal of Control, Vol. 45, No. 5*, pp. 1803-1822, 1987.

[44] Lee, H. G. and Marcus, S. I. "On Input-Output Linearization of Discrete-Time Nonlinear Systems". *Systems and Control Letters 8*, pp. 249-259 1987.

[45] Lee, H. G. and Marcus, S. I. "Approximate and Local Linearizability of Non-Linear Discrete-Time Systems". *International Journal of Control, Vol. 44, No. 4*, pp. 1103-124, 1986.

[46] Lin, J. and Kanellakopoulos, I. "Adaptive Output-Feedback Nonlinear with Parameter Convergence". *Proceedings of the American Control Conference*, pp. 3029-3033, Seattle, Washington, June 1995.

[47] Lin, W. and Yong, J. "Direct Adaptive Control of a Class of MIMO Nonlinear Systems". *International Journal of Control, Vol. 56, No. 5*, pp. 1103-1120, 1992.

[48] Lucibello, P. and Bellezza, F. "Nonlinear Adaptive Control of a Two Link Flexible Robot Arm". *Proceedings of the 29th Conference on Decision and Control*, pp. 2545-2550, December 1990.

[49] Madhavan, S. K. and Singh, S. N. "Inverse Trajectory Control and Zero-Dynamics Sensitivity of an Elastic Manipulator". *International Journal of Robotics and Automation Vol. 6, N0. 4*, pp. 179-192, 1991.

[50] Mahmood, N. and Walcott, B. L. "Neural Network based Adaptive Control of a Flexible Link Manipulator". *Proceedings of the IEEE National Aerospace and Electronics Conference*, pp. 851-857, 1993.

[51] Moallem, M., Khorasani, K., and Patel, R. V. Tip position tracking of flexible multi-link manipulators: An integral manifold approach. In *Proceedings of the IEEE International Conference on Robotics and Automation*, pages 2432–2437, 1996.

[52] Moallem, M., Khorasani, K., and Patel, R. V. "An Integral Manifold Approach for Tip Position Tracking of Flexible Multi-Link Manipulators". *to appear in IEEE Transactions on Robotics and Automation*, 1997.

[53] Moallem, M., Patel, R. V., and Khorasani, K. An inverse dynamics control strategy for tip position tracking of flexible multi-link manipulators. In *Proceedings of the 13th IFAC World Congress*, pages 85–90, 1996.

[54] Monaco, S. and Normand-Cyrot, D. "Minimum-Phase Nonlinear Discrete-Time Systems and Feedback Stabilization". *Proceedings of the 26th Conference on Decision and Control*, pp. 979-986, Los Angeles, California, December 1987.

[55] Nam, K. "Linearization of Discrete-Time Nonlinear Systems and a Canonical Structure". *IEEE Transaction on Automatic Control, Vol. 34, No. 1*, pp. 119-122, January 1989.

[56] Nam, K. and Arapostathis, A. "A Model Reference Adaptive Control Scheme for Pure-Feedback Nonlinear Systems". *IEEE Transaction on Automatic Control, Vol. 33, No. 9*, pp. 803-811, September 1988.

[57] Narendra, K. S. and Parthasarathy, K. "Identification and Control of Dynamical Systems Using Neural Network". *IEEE Transactions on Neural Networks, Vol. 1, No. 1*, pages 444–466, March 1990.

[58] Nicosia, S., Tomei, P., and Tornambe, A. "Discrete-Time Modeling of Flexible Robots". *Proceedings of the Conference on Decision and Control*, pp. 539-544, Honolulu, Hawaii, December 1990.

[59] Nijmeijer, H. and Van der Shaft, A. *"Nonlinear Dynamical Control Systems"*. Springer Verlag, 1990.

[60] Ossman, K. A. "Indirect Adaptive Control for Interconnected Systems". *IEEE Transaction on Automatic Control, Vol. 34, No. 8*, pp. 908-911, August 1989.

[61] Patel, R. V. and Misra, P. "Transmission Zero Assignment in Linear Multivariable Systems, Part II: The General Case". *Proceedings of American Control Conference*, pp. 1042-1047, Chicago, IL, 1992.

[62] Qian, W. T. and Ma, C. H. "A New Controller Design for a Flexible One-Link". *IEEE Transaction on Automatic Control, Vol. 37, No. 1*, pp. 132-137, January 1992.

[63] Recker, D. and Kokotovic, P. V. "Indirect Adaptive Nonlinear Control of Discrete-Time Systems Containing a Deadzone". *Proceedings of the 32th Conference on Decision and Control*, pp. 2647-2653, San Antonio, Texas, December 1993.

[64] Rokui, M. R. and Kalaycioglu, S. "Control Moment Gyro (CMG) Based Spacecraft Attitude Control using Feedback Linearization Control Technique". *Proceedings of AAS/AIAA Astrodynamics Specialist Conference*, Sun Valley, Idaho, August 1997.

[65] Rokui, M. R. and Khorasani, K. "An Indirect Adaptive Control for Fully Feedback Linearizable Discrete-Time Nonlinear Systems". *To appear in International Journal of Adaptive Control and Signal Processing*, 1997.

[66] Rokui, M. R. and Khorasani, K. "Adaptive Tracking Control of a Flexible Link Manipulator Based on the Discrete-time Nonlinear Model". *Proceedings of American Control Conference*, Albuquerque, New Mexico, June 1997.

[67] Rokui, M. R. and Khorasani, K. "Discrete-Time Nonlinear Adaptive Tracking Control of a Flexible Link Manipulator With Unknown Payload". *Submitted to IEEE Transactions on Control Systems Technology*, April 1997.

[68] Rokui, M. R. and Khorasani, K. "Adaptive Tracking Control of Partially Linearizable Discrete-Time Nonlinear Systems". *Submitted to Automatica*, March 1997.

[69] Rokui, M. R. and Khorasani, K. "Adaptive Tracking Control of Partially Linearizable Discrete-Time Nonlinear Systems". *Proceedings of the IEEE International Conference on Control Applications*, pp. 1025-1030, Dearborn, Michigan, September 1996.

[70] Rokui, M. R. and Khorasani, K. "An Indirect Adaptive Feedback Linearization Control for Discrete-Time Nonlinear Systems". *Proceedings of the 13th World Congress of IFAC 1996*, pp. 13-18, San Francisco, California, June 1996.

[71] Rokui, M. R. and Khorasani, K. "Direct Adaptive Control of Discrete-Time Nonlinear Systems Using Input-Output Model". *Proceedings of the 35th IEEE Conference on Decision and Control*, pp. 857-862, Kobe, Japan, December 1996.

[72] Rudin. *"Nonlinear systems"*. Macmillan, New York, 1976.

[73] Sastry, S. S. and Isidori, A. "Adaptive Control of Linearizable Systems". *IEEE Transaction on Automatic Control, Vol. 34, No. 11*, pp. 1123-1131, November 1989.

[74] Siciliano, B., W. J. Book, and G. De Maria. An integral manifold approach to control of a one-link flexible arm. In *Proceedings of the 25th IEEE Conference on Decision and Control*, 1986.

[75] Siciliano, B. and Book W. "A Singular Perturbation Approach to Control of Lightweight Flexible Manipulator". *The International Journal of Robotics Research, Vol. 7, N0. 4*, pp. 79-89, August 1988.

[76] Siciliano, B., Yuan, B. S., and Book, W. J. "Model Reference Adaptive Control of a One Link Flexible Arm". *Proceedings of the 25th Conference on Decision and Control, Athens*, December 1986.

[77] Song, Y. and Grizzle, J. W. "Adaptive Output-Feedback of a Class of Discrete-time Nonlinear Systems". *Proceedings of the American Control Conference*, pp. 1359-1364, June 1993.

[78] Spong, M. W., Khorasani, K., and Kokotovic, P. V. An integral manifold approach to the feedback control of flexible joint robots. *IEEE J. of Robotics and Automation*, pp. 291-300, August 1987.

[79] Stubbs, D. and Svoronos, S. "A Simple Controller via Feedback Linearization and its Use in Adaptive Control". *Proceedings of the American Control Conference*, pp. 1857-1862 1989.

[80] Teel, A., Kadiyala, R., Kokotovic, P., and Sastry, S. "Indirect Techniques for Adaptive Input Output Linearization of Nonlinear Systems". *Proceedings of American Control Conference*, pp. 79-80.

[81] Teel, A., Kadiyala, R., Kokotovic, P., and Sastry, S. "Indirect Techniques for Adaptive Input-Output Linearization of Non-Linear Systems". *International Journal of Control, Vol. 53, No. 1*, pp. 193-222, 1991.

[82] United Detector Technology. *"The Guide to Position Sensing".*

[83] Wang, D. and Vidyasagar, M. "Transfer Function for a Single Flexible Link". *Proceedings of IEEE International Conference on Robotics and Automation*, pp. 1042-1047, 1989.

[84] Warshaw, G. D. and Schwartz, H. M. "Sampled-Data Robot Adaptive Control with Stabilizing Compensation". *Proceedings of America Control Conference*, Baltimore, Maryland, pp. 602-608, June 1994.

[85] Warshaw, G. D. and Schwartz, H. M. "Sampled-Data Robot Adaptive Control with Stabilizing Compensation". *The International Journal of Robotics Research, Vol. 15, No. 1*, pp. 78-91, February 1996.

[86] Wen, C. and Hill, D. J. "Nonsingular And Stable Adaptive Control of Discrete-Time Bilinear Systems". *IFAC Nonlinear Control Systems Design, Capri, Italy*, pp. 229-234 1989.

[87] Yang, S., Woo P., and Wang R. "Discrete-Time Model Reference Adaptive Controller Designs for Robotic Manipulators". *The International Journal of Robotics Research, Vol. 15, No. 3*, pp. 280-289, June 1996.

[88] Yang, Y. P. and Gibson, J. S. "Adaptive Control of a Manipulator With a Flexible-Link". *Journal of Robotic Systems, Vol. 6, No. 3*, 1989.

[89] Yeh, P. and Kokotovic, P. "Adaptive Output-Feedback Design for a Class of Nonlinear Discrete-Time Systems". *IEEE Transaction on Automatic Control , Vol. 40, No. 9*, pp. 1663-1668, September, 1995.

[90] Yeh, P. and Kokotovic, P. "Adaptive Control of a Class of Nonlinear Discrete-Time Systems". *International Journal of Control, Vol. 62, No. 2*, pp. 303-324, 1995.

[91] Yu, J. S. and Müller, P. C. "Indirect Adaptive Control for Interconnected Systems with Linear and Nonlinear Parts". *Proceedings of the American Control Conference*, pp. 1606-1610 1992.

[92] Yuh, J. "Application of Discrete-Time Model Reference Adaptive Control to a Single-Link Flexible Robot Arm". *Journal of Robotic Systems, Vol. 4, No. 5*, 1987.

[93] Yurkovich, S. and Pacheco F. E. "On Controller Tuning For a Flexible-Link Manipulator With Varying Payload". *Journal of Robotic Systems, Vol. 6, No. 3*, 1989.

[94] Zhao, J. and Kanellakopoulos, I. "Adaptive Control of Discrete-Time Strict-Feedback Nonlinear Systems". *Proceedings of the American Control Conference*, June 1997.